Tran-SET

Transportation Consortium of South-Central States

Solving Emerging Transportation Resiliency, Sustainability, and Economic Challenges through the Use of Innovative Materials and Construction Methods: From Research to Implementation

Expanding the Concept of Comprehensive Area Ratio Parameter to the South-Central States: Towards Simplifying the Structural Evaluation of Flexible Pavements at the Network Level

Project No. 20PUTSA34

Lead University: University of Texas at Tyler

Collaborative Universities: University of Texas at San Antonio

Final Report

December 2021

Disclaimer

The contents of this report reflect the views of the authors, who are responsible for the facts and the accuracy of the information presented herein. This document is disseminated in the interest of information exchange. The report is funded, partially or entirely, by a grant from the U.S. Department of Transportation's University Transportation Centers Program. However, the U.S. Government assumes no liability for the contents or use thereof.

Acknowledgements

The authors would like to acknowledge the support and direction of the Project Review Committee (PRC) who provided valuable feedback to this project. The PRC members are Michael Elwardany, Bryan Rossman, and Cameroon Williams.

TECHNICAL DOCUMENTATION PAGE

1. Project No.	2. Government Accession No.	3. Recipient's Catalog No.
20PUTSA34		

4. Title and Subtitle	5. Report Date
Expanding the Concept of Comprehensive Area Ratio Parameter to the South-Central States: Towards Simplifying the Structural Evaluation of Flexible Pavements at the Network Level	Dec. 2021
	6. Performing Organization Code
7. Author(s)	**8. Performing Organization Report No.**
PI: Dr. Mena I. Souliman https://orcid.org/0000-0001-6204-7857 PI: Dr. Samer Dessouky https:/orcid.org/0000-0002-6799-6805 GRA: Nitish R. Bastola https://orcid.org/0000-0002-0999-9127	
9. Performing Organization Name and Address	**10. Work Unit No. (TRAIS)**
University of Texas at Tyler, University Blvd, Tyler, TX 75701 University of Texas at San Antonio, One UTSA Circle, San Antonio, TX 78249	
	11. Contract or Grant No. 69A3551747106
12. Sponsoring Agency Name and Address	**13. Type of Report and Period Covered**
United States of America Department of Transportation Research and Innovative Technology Administration	Final Research Report August 2020 – December 2021
	14. Sponsoring Agency Code

15. Supplementary Notes

Report uploaded and accessible at Tran-SET's website (http://transet.lsu.edu/).

16. Abstract

The surface deflection bowl data collected through falling weight deflectometer (FWD) test is utilized by highway agencies in assessing the performance of the flexible pavement. However, a robust method to evaluate pavement sections utilizing FWD data from all the sensors is seldom developed. There is always a need for DOTs and highway agencies to have a simplified procedure, which can be directly implemented in agencies' databases. This study focuses on expanding and validating the concept of previously developed area ratio parameters towards the pavement section of South-Central States (Arkansas, Louisiana, New Mexico, Oklahoma, and Texas) in effectively analyzing the pavement performances. Simulation-based deflections are utilized to develop enhanced deflection-based parameters and to reduce the need for extensive FWD testing in the field. Ninety-seven pavement sections in these states are considered to implement and validate simplified procedures that will be readily available to various transportation agencies to evaluate their pavement conditions at the network level. Due to this purpose, a pavement ranking chart is proposed for the five South-Central states, which categorizes the pavement section into very good, good, fair, and poor pavement sections. Eventually, load-induced effects concerning developed parameters are effectively analyzed to predict the remaining service life of the flexible pavement structures. The developed methodologies will be helpful for DOTs and highway agencies to carry out the rehabilitation and maintenance work in time and estimate the budget required in these procedures.

17. Key Words	18. Distribution Statement
Pavement structural health, deflection bowl and deflection parameters; pavement categorization; remaining service life, software simulations	No restrictions. This document is available through the National Technical Information Service, Springfield, VA 22161.

19. Security Classif. (of this report)	20. Security Classif. (of this page)	21. No. of Pages	22. Price
Unclassified	Unclassified	210	

Form DOT F 1700.7 (8-72) **Reproduction of completed page authorized.**

SI* (MODERN METRIC) CONVERSION FACTORS

APPROXIMATE CONVERSIONS TO SI UNITS

Symbol	When You Know	Multiply By	To Find	Symbol
		LENGTH		
in	inches	25.4	millimeters	mm
ft	feet	0.305	meters	m
yd	yards	0.914	meters	m
mi	miles	1.61	kilometers	km
		AREA		
in^2	square inches	645.2	square millimeters	mm^2
ft^2	square feet	0.093	square meters	m^2
yd^2	square yard	0.836	square meters	m^2
ac	acres	0.405	hectares	ha
mi^2	square miles	2.59	square kilometers	km^2
		VOLUME		
fl oz	fluid ounces	29.57	milliliters	mL
gal	gallons	3.785	liters	L
ft^3	cubic feet	0.028	cubic meters	m^3
yd^3	cubic yards	0.765	cubic meters	m^3
		NOTE: volumes greater than 1000 L shall be shown in m^3		
		MASS		
oz	ounces	28.35	grams	g
lb	pounds	0.454	kilograms	kg
T	short tons (2000 lb)	0.907	megagrams (or "metric ton")	Mg (or "t")
		TEMPERATURE (exact degrees)		
^oF	Fahrenheit	5 (F-32)/9 or (F-32)/1.8	Celsius	^oC
		ILLUMINATION		
fc	foot-candles	10.76	lux	lx
fl	foot-Lamberts	3.426	candela/m^2	cd/m^2
		FORCE and PRESSURE or STRESS		
lbf	poundforce	4.45	newtons	N
lbf/in^2	poundforce per square inch	6.89	kilopascals	kPa

APPROXIMATE CONVERSIONS FROM SI UNITS

Symbol	When You Know	Multiply By	To Find	Symbol
		LENGTH		
mm	millimeters	0.039	inches	in
m	meters	3.28	feet	ft
m	meters	1.09	yards	yd
km	kilometers	0.621	miles	mi
		AREA		
mm^2	square millimeters	0.0016	square inches	in^2
m^2	square meters	10.764	square feet	ft^2
m^2	square meters	1.195	square yards	yd^2
ha	hectares	2.47	acres	ac
km^2	square kilometers	0.386	square miles	mi^2
		VOLUME		
mL	milliliters	0.034	fluid ounces	fl oz
L	liters	0.264	gallons	gal
m^3	cubic meters	35.314	cubic feet	ft^3
m^3	cubic meters	1.307	cubic yards	yd^3
		MASS		
g	grams	0.035	ounces	oz
kg	kilograms	2.202	pounds	lb
Mg (or "t")	megagrams (or "metric ton")	1.103	short tons (2000 lb)	T
		TEMPERATURE (exact degrees)		
^oC	Celsius	1.8C+32	Fahrenheit	^oF
		ILLUMINATION		
lx	lux	0.0929	foot-candles	fc
cd/m^2	candela/m^2	0.2919	foot-Lamberts	fl
		FORCE and PRESSURE or STRESS		
N	newtons	0.225	poundforce	lbf
kPa	kilopascals	0.145	poundforce per square inch	lbf/in^2

TABLE OF CONTENTS

LIST OF FIGURES

LIST OF TABLES

ACRONYMS, ABBREVIATIONS, AND SYMBOLS

ANSYS	Analysis and Simulation
A_r	Area Ratio
CAPP	Comprehensive Area under Pavement Profile
$CA_{r'}$	Comprehensive Area Ratio
$CA_{r'}$	Normalized Comprehensive Area Ratio
CD_r	Comprehensive Deflection Ratio
$CD_{r'}$	Normalized Comprehensive Deflection Ratio
D_0	Central Deflection
DOT	Department of Transportation
D_r	Deflection Ratio
FEM	Finite Element Modeling
FWD	Falling Weight Deflectometer
HMA	Hot Mix Asphalt
LTPP	Long Term Pavement Performance
NDT	Non-Destructive Testing
PMS	Pavement Management System

EXECUTIVE SUMMARY

The surface deflection bowl data collected through Non-Destructive Testing (NDT) has been widely utilized by various Department of Transportation (DOTs) in the South-Central States and other places. The primary purpose of using deflection-based NDTs in network-level assessment is to identify a weak pavement section that requires further analysis at the project level. The falling weight deflectometer (FWD) test is one of the common NDT based tests utilized by highway agencies in assessing the performance of the flexible pavement. However, a robust method to evaluate pavement sections utilizing FWD data from all the sensors are seldom developed. There is always a need for DOTs and highway agencies to have a simplified procedure, which can be directly implemented in agencies' databases.

This study focuses on expanding the concept of previously developed area ratio parameters towards the pavement section of South-Central States (Arkansas, Louisiana, New Mexico, Oklahoma, and Texas) in effectively analyzing the pavement performances. Simulation-based deflections are utilized to develop enhanced deflection-based parameters. The need for extensive FWD testing at the field will be reduced with software-based simulations. 3D-MoveAnalysis and Analysis and Simulation (ANSYS) were utilized to simulate the surface deflection obtained from FWD test. Deflection values obtained through the software simulations were highly correlated with the field test results. Furthermore, ninety-seven pavement sections in these states are considered to implement and validate simplified procedures that will be readily available to various transportation agencies to evaluate their pavement conditions at the network level. Area ratio parameters developed in the study are reliable enough to consider the effect of different drop loads and various pavement sections across the South-Central States.

Additionally, a pavement ranking chart is proposed for the five South-Central states, which categorizes the pavement section to very good, good, fair, and poor pavement sections. The chart will be helpful for DOTs and highway agencies to carry out the rehabilitation and maintenance work in time and estimate the budget required in these procedures. Similarly, the remaining fatigue life of the pavement section can be easily predicted utilizing the newly developed relationship based on comprehensive area ratio parameters and number of cycles to fatigue failure.

1. INTRODUCTION

Asphalt pavement structures are the most common form of roadways in the entire United States. The performance of the pavement structures is the primary concern for most of the transportation agencies. With its age and the increased traffic loading, the performance of a pavement structure gradually decreases. Various non-destructive techniques (NDT) are performed for assessing the routine performance of the pavement structures. One of the famous NDT tests practiced in the United States and the whole world is the Falling Weight Deflectometer (FWD) test. Being simple and based on the actual field conditions, the FWD test is one of the most preferred form of tests in pavement structural evaluations *(1)*. In the United States, FWD testing has a long history, and it is usual to find the abundant data stored in the country's dominant database-Long Term Pavement Performance (LTPP) database. Various studies related to performance monitoring of pavement structures have been performed with the utilization of the FWD data *(2)*. However, in most transportation agencies, FWD data are often analyzed with back-calculations, which are very tedious and time consuming**.** The simplified procedures to utilize the FWD data in assessing the pavement performance are not available in network level analysis which is a broader perspective of pavement management system (PMS) and utilizes the entire network for prioritization and maintenance *(3)*. Project 17PUTA02, entitled Simplified Approach for Structural Evaluation of Flexible Pavements at the Network Level, provided simplified procedures to assess the flexile pavement structures at the network *(2)*. Under this project, various parameters encompassing a wider area of the deflection bowls were developed, and the study focused on the pavement sections in Texas. This study is the foundation for assessing the pavement conditions in all South-Central States: Arkansas, Louisiana, New Mexico, Oklahoma, and Texas.

In this research study, various LTPP sections in the states of Arkansas, Louisiana, New Mexico, Oklahoma, and Texas are analyzed concerning their fatigue performance to assess the pavement structural conditions. Ninety-seven sections are utilized and verified to go through the procedure of formulating the deflection area parameters and their utilization in the network level of pavement management system (PMS) database. An extensive categorization of each one of the pavement sections is made eventually for simplifying the performance prediction tasks for engineers and researchers so that the maintenance and rehabilitation tasks can be carried out at the optimum time.

Additionally, the deflection from the FWD tests is simulated through two software packages namely the 3D-Move Analysis and Analysis System (ANSYS). The need to utilize the simulation is to reduce the number of field FWD tests performed at the pavement sections and analyze the structural conditions of pavement. The categorization is made at various rankings starting from “very good towards the good, fair, and poor sections”. And it is evident that the pavement structures in very good and good categories are less damaged, and they do not require immediate maintenance and rehabilitation.

2. OBJECTIVES

The study aims to achieve the following objectives-

a. Implement and validate a simple analysis method for determining the structural conditions of pavement at the network level.

b. Simulate the entire deflection bowl from the FWD test with 3D-Move Analysis Software, leading to the reduction of extensive field based FWD tests at the network level.

c. Utilize another software platform such as ANSYS in simulating the FWD testing.

d. Develop a simplified pavement health categorization chart for the South-Central States for assessing the pavement conditions.

e. Estimate the remaining service life of the flexible pavement based on the developed deflection area ratio parameters.

3. LITERATURE REVIEW

3.1. Deflection-Based Measurement Devices

Varieties of NDT are practiced for monitoring the performance of any flexible pavement structures. NDT's significant advantage is that it will not affect the structure intactness, unlike the previously followed procedures, such as taking field cores. Various NDT analyses are practiced in the pavement engineering field, and some of the notable ones are Benkelman Beam, La Croix deflect graph, falling weight deflectometer (FWD), Dynaflect, the Road rater system, and the dynamic deflection device *(4)*. Among them, FWD is referred to as the oldest and most popular form of NDT related tests practiced throughout the world. Application of load at a pavement surface and recording the deflection at specific locations is the fundamental principle in FWD testing. Similarly, the load applied at different drop heights results in deflection values noted by geophone sensors placed at specified offsets from the load plate. The following figure shows the loading plate's location and sensors offset in an FWD device *(5)*.

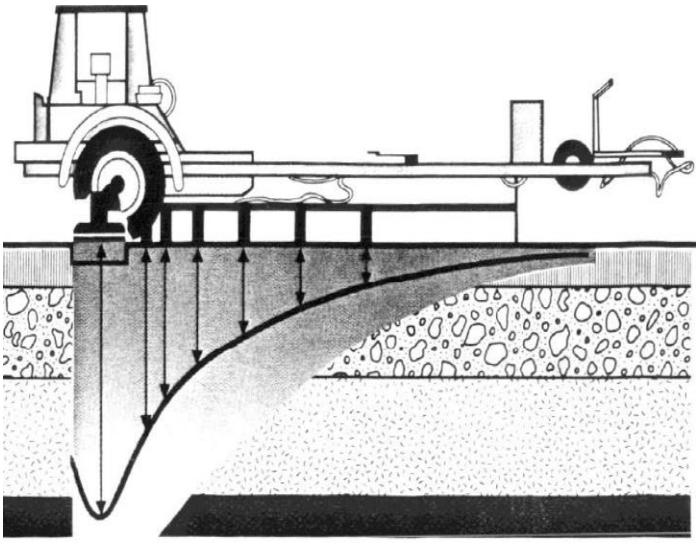

Figure 1. FWD device and sensors *(5)*

Notably, in the United States, the FWD test has been one of the main the pavement monitoring tools for decades. Although being practiced for decades, FWD measurement is processed with time-consuming procedures of back-calculation to predict the dynamic modulus of pavement layers. A simplified system to be utilized by the transportation agencies not readily available, and many researchers are working on developing a streamlined version through the development of deflection bowl-based parameters.

Table 1 presents a summary of relevant practices performed by various agencies with the utilization of FWD in network-level analyses of pavement structures *(6)*.

Table 1. Summary of useful practices of FWD in network-level analyses *(5)*

Agency and Publication	Test Point Spacing	FWD Test Frequency	FWD Sensor Positions	Limiting Factors	Basic Details of the PMS Approach
South Africa. Benchmarking the Structural Condition of Flexible Pavements with Deflection Bowl Parameters	0.2 km	N/A	300 mm typical	Flexible pavements only	Pavement is divided into three zones based on depth. Uses basin parameters to characterize base, mid-depth, and subgrade structural condition such as sound, warning or severe.
Alaska Department of Transportation (AkDOT); Modeling Flexible Pavement Response and Performance	0.1 mi	After repaving	SHRP positions	No limits	Deflections are converted to layer moduli, which are then used to obtain stress/strain values under a standard equivalent single axle load (ESAL). Transfer functions relate stress/strain to cracking in bound layers and permanent deformation in unbound layers.
Texas Department of Transportation (TxDOT); Incorporating a Structural Strength Index into the Texas Pavement Evaluation System (FHWA/TX-88/409-3F)	0.5 mi	One recommended per year	1 ft	Flexible pavements less than 5.5 inches AC thickness	Structural strength index (SSI) varies from zero to 100 (weak to strong). Based on normalized basin parameters, such as outer deflections, surface curvature index (SCI), and center deflection under a 9,000-lb load. Can characterize subgrades and pavement structure independently in terms of relative stiffness. System based on statistical valuation of deflections statewide.

3.2 FWD Test-Based Parameters

Hossain and Zaniewski in 1991 performed a characterization of falling weight deflectometer deflection basin *(7)*. In this study, various parameters were developed for describing the structural characteristics of a pavement structure. The development was based on the non-destructive testing device. A curve in an exponential form Y=A *eBX was developed to fit the field deflections and the back-calculated deflections. Y is the surface deflection, and X is the offset distance of the center, while A and B denote the structural characteristics of the pavement. A higher value of A represents the stiffer layer at the top. In contrast, the stiff subgrade is represented by a higher value of B. The developed procedure and fitting were utilized in judging the suitability of back-calculation in predicting the layer moduli, which is a time-consuming process *(7)*.

Similarly, Haas et al. *(8)* developed the structural adequacy index (SAI) with the utilization of the Benkelman beam test. The index was formulated with a single deflection value being susceptible to a minor error. However, in another study conducted by Haas et al., an abounded scale of 1 to 10 was provided for SAI *(9)*. The pavement characteristics and the number of expected equivalent single axle loads (ESALs) were utilized in calculating the maximum tolerable deflection (MTD). MTD values were 1 for a weak pavement section, while for a strong pavement section, the MTD value was assigned 10. The limitation of the system was that the scale was not fixed, and it needed changes whenever it was applied to different transportation agencies.

Wimsatt also presented a direct method of utilizing falling weight deflectometer data, which was divided into 72 inches away from the load plate, and the surface deflection was related to the ratio of the pavement modulus and the subgrade modulus in a two-layer system *(10)*. Similarly, the effect of stiffness of the base is also correlated with the pavement structure. These procedures are eventually evaluated utilizing the MODULUS software package developed at Texas Transportation Institute (TTI). The deflection ratio was analyzed to fit the best scenarios of the pavement structures by relating the pavement surface deflections with the stiffness of base materials.

Also, in a report prepared under the North Carolina Department of Transportation, a utilization of falling weight deflectometer multi-load data was accessed to estimate pavement strength *(11)*. The mechanistic-empirical method was developed to assess pavement layer conditions utilizing a finite element program that incorporates the stress-dependent soil model. The procedures for evaluating the performance of flexible pavement concerning fatigue cracking and rutting was also developed. The research team concluded that the utilization of load data is crucial to get the actual pavement conditions.

Zhang et al. 's research focused on developing a structural condition index for maintenance and rehabilitation of pavement structures at the network level. Structural strength index (StSI) was developed to address how the pavement conditions deteriorate with the structural deformation of layers and subgrades. Various falling weight deflectometer data has been collected and stored in the database of the Pavement Information Management System (PMIS) at the Texas Department of Transportation. Pavement's modulus and structural numbers were utilized as the structural stimators, and eventually, the evaluation was based on the sensitivity of the structural estimators to pavement structure deterioration parameters. The developed index was calibrated for utilization in maintenance and rehabilitation analysis at the network level *(12)*. Eventually, it was detected that the developed index StSI was unable to capture the pavement performance based on the

accumulated distress. Moreover, the index was developed based on a single deflection value at 18 inches from the loading plate.

Scullion *(13)* introduced a new structural strength index to the pavement evaluation system (PES) utilized in Texas. Present Serviceability Index (PSI) and visual distresses were the prime factors in rating the pavement condition following this system. The utilization of deflection bowl parameters and mechanistic approach in the calculation process of the developed system made this index more promising to estimate the remaining service life of pavement sections at the project level. The conclusion was made under the report that under a load level of 9000 lbs, the structural strength index might be utilized to assess pavement structure at the network-level.

Horal and Emery presented the practice and basis for utilizing deflection bowl parameters to obtain the entire deflection bowl's elastic response. Nine different parameters were developed to assess the pavement response under this study (Table 2). Five parameters (maximum deflection (D0), Radius of Curvature (RoC), Base Layer Index (BLI), Middle Layer Index (MLI), and Lower Layer Index (LLI) had a good correlation with pavement structural conditions. Therefore, the parameters with good correlation were utilized to distinguish between structurally strong, warning, and severe damaged pavements sections. However, the parameters were determined based on the deflection obtained from only four different offsets of 200, 300, 600, and 900 mm from the load plate.

Table 2. Collection of parameters and their formulae *(14)*

Parameter	Formula	Structural indicator
Maximum deflection	D_0 as measured	Gives an indication of all structural layers with about 70 % contribution by the subgrade
Radius of Curvature (RoC)	$RoC = (L)^2 / 2\ D_0\ (1 - D_0/D_{200})$ where L=127mm in the Dehlen curvature meter and 200mm for the FWD	Gives an indication of the structural condition of the surfacing and the base condition
Base Layer Index (BLI)	$BLI=D_0-D_{300}$	Gives an indication of primarily the base layer structural condition
Middle Layer Index (MLI)	$MLI=D_{300}-D_{600}$	Gives an indication of primarily the subbase and probably selected layer structural condition
Lower Layer Index (LLI)	$LLI=D_{600}-D_{900}$	Gives an indication of the lower structural layers like the selected and the subgrade layers
Spreadability, S	$S = \{[(D_0 + D_1 + D_2 + D_3)/5] * 100\} / D_0$ where D1, D2, D3 spaced at 300 mm.	Supposed to reflect the structural response of the whole pavement structure, but with weak correlations
Area, A	$A = 6\ [1 + 2(D_1/D_0) + 2(D_2/D_0) + D_3/D_0]$	The same as above
Shape factors	$F_1=(D_0-D_2)/D_1$ $F_2=(D_1-D_3)/D_2$	The F2 shape factor seemed to give better correlations with subgrade moduli while F1 gave weak correlations
Slope of Deflection	$SD = \tan^{-1} (D_0 - D_{600})/600$	Weak correlations observed

A study in similar to Horal and Emery, Aavik, and Talvik utilized a falling weight deflectometer for the pavement structural evaluation and repair design with the introduction of more advance pavement deflection bowl parameters *(15)*. Various FWD deflection data have been used to create a deflection basin to characterize the test site's pavement conditions. Different basin parameters were utilized for calculating equivalent pavement modulus, including surface curvature index, base

damage index, and base curvature index. The following **Error! Reference source not found.** presents the parameter developed and analyzed in the study. However, in this study, a deflection bowl of 1500mm offset was utilized in creating the parameters and indices.

Table 3. Deflection Basin Parameters *(15)*

Deflection basin parameter	**Equation**	**Unit**	**Parameter's objective**
Surface Curvature Index	SCI= d_0- d_{300} SCI= d_0- d_r (used also r ϵ [450, 600])	µm, mm	Characterizing condition of bound layers
Base Damage Index	BDI= d_{300}-d_{600}	µm, mm	Characterizing condition of base layers
Base Curvature Index	BCI= d_{600}-d_{900} (used in USA) BCI= d_{900}-d_{1200} (used in Finland) BCI= d_{1200}-d_{1500} (used in Estonia)	µm, mm	Characterizing condition of subbase or subgrade
Area Under Pavement Profile	AUPP= $(5d_0+2d_{300}+2d_{600}+d_{900})/d_0$	-	Characterizing conditions of the pavement upper layers
Shape Factors	F1= $(d_0-d_{600})/d_{300}$	-	Determination of condition of the layer at the equivalent depth
	F2= $(d_{300}-d_{900})/d_{600}$		
Deflection Ratio	DR= d_{600}/d_0	-	Determination of condition of the layer at the equivalent depth
d_o, d_{300}, d_{600}, d_{900}, d_{1200}, d_{1500}- measured deformations at the distance of 0, 300, 600, 900, 1200, 1500 mm from the center of the loading plate : D_o, D_1, D_2, D_3- measured deformations at the distance of 0ft, 1ft (305mm) , 2ft (610mm), 3ft (914mm) from the center of the load plate.			

Similarly, research by Kavussi et al. was also focused on the development of a new method to determine maintenance and repair activities at the network level of pavement management utilizing FWD *(16)*. FWD data were being used in developing appropriate maintenance and repair methods. Two regression models were developed based on the FWD deflection data for calculating the effective structural number (SNeff) and resilient modulus (Mr) of the subgrades. A strong correlation was observed between surface deflection of 60cm from the load plate (D60), SNeff, and Mr, respectively, with the utilization of deflection data. Furthermore, the determination of

appropriate maintenance and repair technology can be implemented at a network-level pavement management system (PMS) utilizing SNeff and Mr derived from the study.

Researchers developed Regression-based equations from Kansas State University and Kansas Department of Transportation (KDOT) utilizing central deflection under a 40-kN (9,000-lb) load *(17)*. The primary objective of the study was to estimate the remaining service life (RSL) of a pavement section utilizing the central deflection. The calibration of RSL equations with the information from non-interstate routes showed a good correlation with serviceability based on remaining life predictions. Likewise, Gedafa et al *(18)* utilized the KDOT pavement management system (PMS) data to develop Effective Structural Number (SNeff). Unlike the AASHTO procedure for SNeff, including effective pavement modulus of all layers above subgrade and the thickness of pavement layers, the developed method incorporated various properties of a pavement section such as central deflection and fatigue. Twelve different regression models for 12 different road categories were developed under this study. The developed model was positively correlated with the AASHTO procedure; however, the developed model was highly sensitive to central deflection resulting in a higher susceptibility towards measurement errors.

Flora *(19)* developed the basis for the structural strength indicator (SSI) as a comprehensive index utilizing FWD values. Cumulative distribution of deflections from a group of pavement section was utilized for SSI. The deflection in a pavement section was compared with the deflection in the group of pavements within the network. The scale of 0 to 100 was utilized in ranking a pavement section. The value of 0 was for a poor SSI, and the value of 100 was for a perfect SSI.

Similarly, Bryce et al. defined the structural conditions of the pavement in terms of the structural requirements of the pavement structure. The distress data and FWD measurements were utilized to develop decision approaches and indices in this study. The study was based on the state of Virginia. Furthermore, numerous sensitivity analyses were performed, which revealed the in-situ conditions were the prime factors influencing a flexible pavement structure *(20)*. Statistical correlation of central deflection and functional indicators such as Pavement Condition Rating (PCR) and International Roughness Index (IRI) was significantly less; however, a new structural-based condition index was developed for central deflection as presented in equation (1).

$$SSI = 100\ (1\text{-}1.0069e^{\frac{-1071.8}{d_1^{3.9622}}}) \quad [1]$$

where:

d_1 = the FWD central deflection; and

SSI = the structural strength indicator

Chang et al. study was also focused on evaluating the structural strength of the flexible pavement structure with FWD data. The study was based on the numerous test sections in the freeways of Taiwan *(21)*. A temperature correction equation, structural strength index (SSI), and structural evaluation system were developed for the reliable assessment of pavement conditions. 1176 FWD tests were performed at two specific built test sections for obtaining the temperature correction factors. Traffic loads, as well as its effect, were eliminated from the analysis. The study concluded that the original and temperature corrected model differed by 13%. Additionally, SSI was also established for identifying a pavement section as good and poor; however, the developed system did not account for the full deflection bowls.

Apart from temperature correction, another study by Aavik et al. *(22)* was focused on moisture and its effects when assessing the pavement structural index by FWD. Cobb- Douglas equation was utilized in taking into account of the unlimited numbers of factors influencing the pavement structural conditions. The month at which the FWD measurements were taken and the road embankment height were different correction factors acknowledged in this study.

Similarly, in a study by Romanoschi and Metcalf, a simple approach for estimating the pavement structural capacity is determined *(23).* This system excludes the process of a cumber-some back-calculation procedure by relating FWD deflections to structural numbers. Two different relationships were developed based on flexible and semi-rigid pavements. Normalizations and temperature correction were provided for the FWD deflections, and the relationship developed was in the acceptable reliability level. The thickness of overlay required in the pavement maintenance and repair procedures can be easily determined following the presented analysis and methods utilizing the structural layer coefficients. In addition, the study also concluded that the structural function must be assigned in accordance with laboratory-derived modulus rather than the back-calculated values.

A study by Nazzal et al. was based on evaluating lightweight falling weight deflectometer (LWFD) in the measurement of in-situ elastic modulus of pavement layers and sub-grades *(24).* Various highway sections in the state of Louisiana have been utilized in this study. FWD, plate load test (PLT), and Dynamic Cone Penetrometer (DPT) were used in conjunctions to LWFD. Various linear regressions were conducted in between these tests, and it was found that LWFD can be utilized in predicting the FWD and PLT moduli at a significant confidence level. However, soil properties played a substantial role in improving the performance of pavement moduli .

Significant utilization of falling weight deflectometer has been presented by Alland et al. in their study to interpret FWD *(25).* Summarization of data analysis and testing procedures are made in three different sections of the report. The first section beholds the testing protocol required in FWD data collection, while the second section shows the proposed change in PennDOT guidelines, including the mechanistic-empirical pavement design guide (MEPDG). The third section is the appendix. The study has been very beneficial in maintaining proper procedures to evaluate the pavement structures with FWD.

Besides Allen, a study performed by Smith et al. was also based on utilizing FWD data in the mechanistic and empirical design analysis of the pavement structures. Rehabilitation procedures for the flexible pavement structures with FWD data are extensively discussed in this report along with the review of pre-existing systems followed by the various transportation agencies. The back-calculation procedure for flexible and composite pavement structures are also reviewed. The whole of the study was found to be equally crucial for the researchers and agencies practicing the rehabilitation and management of pavement structures *(1).*

Advance utilization of the FWD test integrated with Ground Penetrating Radar (GPR) is performed by Plati et al. *(26)*. The principal objective of this study was to utilize thickness data provided by GPR and deflection data FWD in obtaining a relationship with the pavement layer thickness. An integrated regression analysis was performed considering both GPR and FWD data to develop a relationship with FWD deflection indexes and GPR-estimated AC thicknesses. The relationship was calibrated with GPR, core thicknesses and validated with errors of about 10%. It was evident from this study that deflection data through FWD can equally be valuable in obtaining a pavement section thickness. Another modern utilization of FWD is performed by Al-Khoury et al. *(27)* with

the dynamic interpretation of FWD test results. Spectral analysis is explored as a tool to assess the impact of FWD on pavement surfaces. Layered Media Dynamic Analysis (LAMDA) is utilized in simulating the FWD load pulse and pavement structure. A similar principle as the finite element method is followed in this study. Computational requirements are reduced with larger mesh in multiple layers. Back calculation related analysis is significantly simplified with the use of LAMDA.

Elbagalati et al. *(28)* performed a study to develop a prediction model for pavement structure capacity at an interval of 0.16km (0.1mi) based on the Rolling Wheel Deflectometer (RWD) measurements. In most early research studies, functional parameters such as ride quality and surface distress were utilized to assess the pavement conditions. After that, the structural condition index (SCI) of a pavement section is determined by dividing the effective structural number (SN_{eff}) with the required structural number (SN_{req}). SCI was found to very sensitive over pavement deterioration when sensitivity analysis was performed over TXDOT PMS data. According to SCI value, it was clear that few sections are in very good condition compared to the predicted section, which had asphalt stripping and material deterioration problems. A coefficient of determination (R2) value of 0.80 showed an acceptable accuracy. However, the model needed to be recalibrated before the use by other agencies. The study also compared the deflection measurements between RWD and FWD and found that the mean central deflection varied between these two tests.

The effective pavement number (PN_{eff}) was described by Horak et al. Equivalent layer thickness and surface modulus were utilized to get the value of PN_{eff} *(29)*. The whole of the deflection bowl was being used in obtaining the Equivalent Long-Term Stiffness (ELTS) for the calculation of PN_{eff}. The study accounted for a more massive database of pavement layer structures. However, the distresses related issues were not pointed out.

The utilization of deflectograph has been obsolete in most countries. Notably, highway agency in the United Kingdom discontinued the use of deflectograph from the early 2000s itself *(30)*. Lane closure, excessively expensive, and time consumption were significant issues with the devices. Instead, a traffic speed deflectometer (TSD) was introduced. Utilization of the laser at offsets was the main objective of the study, and it was only limited to routine network-level assessment. The laser-based system successfully captured the pavement response for a 30m section, although installing an accelerometer into the asphalt pavement layer was required for measuring reliable deflection bowls seemed time and resources consuming.

Also, utilization of FWD test data for the sectionalizing project is performed by Ganji et al *(31)*. In this methodology, the pavement in roadway and airfields were divided into sections where each section will have a similar pavement condition. Weaker pavement sections and more robust pavement sections were distinguished. The FWD testing was performed before and after a Superpave resurfacing program to know the effectiveness of the sectionalizing concept. FWD test results indicated that the median effective structural number (SN_{eff}) had increased by 1.6(i.e., 16 years increase in the pavement life) with necessary milling and resurfacing. However, the weaker section had a lower SN_{eff} signifying that they will require more rehabilitation effort.

Moreover, more refined parameters for assessing the pavement structural capacity were developed by Saleh et al. *(32- 34)*Deflection ratio (D_r) was normalized and expressed as normalized deflection ($CD_{r'}$) and is given by equation (2).

$$CD_{r'} = D_r / D_{250} \quad [2]$$

where:

$D_r = D_{250} / D_0$ and D_{250} – deflection measured at 250 mm from the load plate (micrometers (µm)),
D_0 = deflection below the load plate (micrometers (µm))

A normalized area ratio was developed utilizing 140 pavement sections with variable modulus and layer thicknesses. For that purpose, the area under the deflection bowl was obtained utilizing the following equation (3).

$$AREA = (50 / D_0) / \{((D_0 + D900) / 2) + \sum_{i=50}^{850} Di \ \} \quad [3]$$

where:

D_{900}= deflection at offset 900 mm from the load
D_i = deflection at offset i (mm) from the load.

Furthermore, the developed area was compared to an extremely stiff pavement where no displacement was observed. The area of the stiff pavement deflection bowl was obtained as the equation (4).

$$AREA = (50 / D_0) / \{ ((D_0 + D_0) / 2) + 17 * D0 \ \} = 900 \text{ mm2/mm.} \quad [4]$$

The area under the deflection bowl was eventually related to the area of rigid pavement section with the development of area ratio parameter Ar (5). Ar was further normalized for central deflection, as shown in equation (6).

$$Ar = (50 / D_0 * 900) / \{ ((D_0 + D_{900}) / 2) + \sum_{i=50}^{850} Di \ \} = AREA / 900 \quad [5]$$

$$Ar' = (50 / D_0 * 900) / \{ ((D0 + D_{900}) / 2) + \sum_{i=50}^{850} Di \ \} = A_r/D_0 \quad [6]$$

The newly developed area ratio parameter was useful in categorizing a pavement section from weak to strong. A pavement section having the value near to 1 was a strong section, and a pavement section having the area ratio value near to zero was referred to as a weak section. This study proved to be a backbone in the development of area-based parameters which can include full deflection bowls. However, utilization of the deflection bowl till 900mm was a slight demerit in the system.

Unlike Saleh et al., a study by Souliman et al. considered wider deflection bowls of 1524 mm offsets to develop area-based deflection parameters for the state of Texas *(2)*. Simulated deflection bowls were utilized in developing the area-based parameters. Deflection and the newly developed area ratio parameter correlated significantly, proving the reliable functioning of the newly developed parameter. Equation 7 shows the normalized comprehensive area ratio (CAr') developed under this study.

$$CAr' = \left(\frac{1}{D0*D0}\right) * \{203*\left(\frac{D0+D203}{2}\right) + 102*\left(\frac{D203+D305}{2}\right) + 152*\left(\frac{D305+D457}{2}\right) + 153*\left(\frac{D457+D610}{2}\right) + 304*\left(\frac{D610+D914}{2}\right) + 610*\left(\frac{D914+D1524}{2}\right)\} / 1524 \quad [7]$$

where:

D_0, D_{203}, D_{305}, D_{457}, D_{610}, D_{914}, and D_{1524} = deflections measured at the center of the plate, 203, 305, 457, 610, 914, and 1524 mm from the center of the load plate, respectively.

Various advanced studies related to pavement structural capacity assessments were also performed based on the study. The utilization of area ratio parameters to obtain the remaining service life of pavement structures and ranking the pavement sections based on the distress conditions were the two significant findings from the *(35-36)*. However, the project only focused on the pavement sections in the state of Texas.

3.3 Software simulations of FWD test

Various software packages had been utilized in the simulation of the FWD test as a simplified approach to determine the performance of the pavement structures. Software simulations are equally significant in bypassing the need to perform the extensive FWD tests on the field. Various researchers have utilized software simulations for the prediction of the deflections. Software such as 3D Move, BISAR, JULEA has been widely used for decades *(37)*. Furthermore, in recent days advance finite element modeling (FEM) software packages are utilized. Namely, Analysis System (ANSYS) and ABAQUS are the noted FEM software packages in the group. They are preferred due to their multi-task and multi-function capabilities.

The simulation of FWD through the help of finite element modeling software has a significantly lesser history. Airport pavements had been evaluated by Tarefdar et al. with the modeling of the FWD deflection basin *(38)*. Depths of the deflection basin were measured from the center of the FWD device and the respective offsets. Back calculation was proceeded after the deflection was carried out. In the later stage, the finite element model was evaluated to simulate the pavement's exact field conditions focusing on elastoplastic behavior. Numerous dynamic and static analyses were performed, but only the static studies showed promising results since the FWD test is static.

In another study by Fernandes et al., the FWD test application for the evaluation of the railway sub-way structure was made simultaneously with FEM *(39)*. A proper railway maintenance policy for evaluating the conditions of the existing sub-structure was the study's main agenda. Various non-destructive loading tests were performed for granular ballast sub-structures and bituminous ballast sub-structures. The deflection related data were utilized to develop and calibrate the numerical models. Different 2D and 3D models were developed and studied to understand FWD's dynamic impact on railway structures.

Hamim et al. had a study related to the utilization of static and dynamic FEM for predicting deflections on flexible pavement structures, intending to simulate FWD *(40)*. The analysis was performed in the ANSYS software package. Various parametric conditions were established by utilizing the variable sizes of model geometry with different element types and sizes to judge the model's effectiveness. 5000 x 5000 mm model geometry was being used in the simulations. It was found that the resulting accuracy from FEM associated with FWD is the function of appropriate material selection, loading, and boundary conditions, as well as the type and size of the elements.

Tutumluer et al. report NEXTRANS Project No. 010/Y01 was also based on the non-destructive pavement evaluation utilizing finite element analysis *(41)*. An innovative methodology developed as Soft Computing Based Pavement and Geomaterial System Analyzer (SOFT SYS) is used to bypass the need for core cutting. Core cutting was previously performed to obtain the pavement layer thickness and the stiffness of the materials. In this study, the finite element (FE) program ILLI-PAVE is utilized along with an artificial neural network model for predicting pavement deflection under FWD loadings. Field validation was performed for the result obtained, and it was satisfactory.

Similarly, Li and Wang had a prediction study related to FWD and soft computing. In this study, various finite element models were developed and validated, considering the viscoelastic properties of the unbound layer and the asphalt layer *(42)*. A database was developed incorporating different pavement structures, temperature profiles, material properties, and loading levels for surface deflections and strain responses in asphalt layers. Eventually, a genetic algorithm-based Artificial Neural Network is utilized for training and verifying the database. It had been observed that the model developed with the ANN system provides better accuracy than the older way of multivariable regression. FEM and ANN with a genetic algorithm proved to be an influencing tool in assessing the pavement's existing conditions without the tedious back-calculation procedures.

3.4 Summary on the conducted literature review

It is observed that FWD testing results in lane closures, excessive time consumption, and safety issues. Similarly, FWD data are most often assessed with back-calculation procedures, and simplified tools to evaluate the pavement structure conditions utilizing FWD data have not been used by many researchers. Most of the studies require extensive data collection procedures through field FWD testing, resulting in lane closures during the test periods. Hence, numerous simulation-based analyses can be an efficient method for obtaining pavement structures' performance without consuming resources and time. The utilization of finite element modeling and generation of FWD test simulations have been well understood with the research works. Various new technologies are being performed in pavement engineering to simplify the structural assessment. The majority of studies are concerned with pavement rehabilitation and maintenance associated with single-point FWD measured deflection, which could not represent the actual pavement structure conditions. The extensive literature review under this chapter facilitates an easy understanding of the utilization of FWD data in developing pavement evaluation parameters and pavement categorization charts; however, it is observed that the utilization of single deflection points and lesser deflection bowl area were the major drawbacks in the previously accomplished studies. Therefore, in this study, deficiencies of the previously followed procedures are overcome following the comprehensive area ratio (CAr') procedure *(2)*. CAr' is developed, validated, and implemented utilizing surface deflection bowl simulations through different software packages (3D Move Analysis and ANSYS). Eventually, CAr' is validated utilizing numerous pavement sections in the South-Central States and further processed to categorize pavement structures under their structural performance.

4. METHODOLOGY

4.1. Data Collection Procedure

Initiated in the year 1987, Long Term Pavement Performance (LTPP) database has always been the largest pavement database under the Strategic Highway Research Program (SHRP) [43]. The Transportation research board (TRB), with the cooperation of the American Association of State Highway and Officials (AASHTO) and the sponsorship from Federal Highway Administration (FHWA), undertook Strategic Transportation Research Study (STRS) for national bridge and highway infrastructure systems and LTPP was one of the branches of the recommended strategic research. LTPP databases hold more than 2500 numbers of pavement sections all over the USA and Canada. LTPP sections are categorized as General Pavement Studies (GPS) and Specific Pavement Studies (SPS) based on the series of studies of in-service pavement sections and specific variables, including new construction practices, maintenance, and rehabilitation practices, respectively. In general, both studies have a 152m long pavement sections and Figure 2 shows the section layout of both types *(43)*.

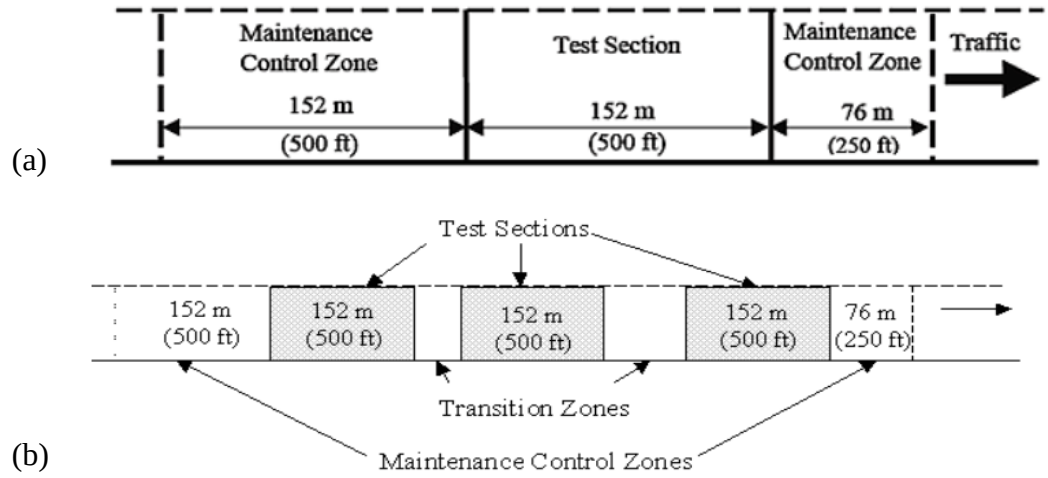

Figure 2 Layout of (a) GPS test section and (b) SPS test section *(43)*

This study included five South-Central States in the United States for evaluating the proposed Comprehensive Area Ratio parameter that was develop under the project 17PUTA02 for effective utilization by various transportation engineers and officials in the early estimation of proper pavement rehabilitation and maintenance strategies. The following Figure 3 shows the South-Central States and the pavement sections considered in the study. The name of the sections and the state-wise location will be described extensively in the proceeding paragraphs.

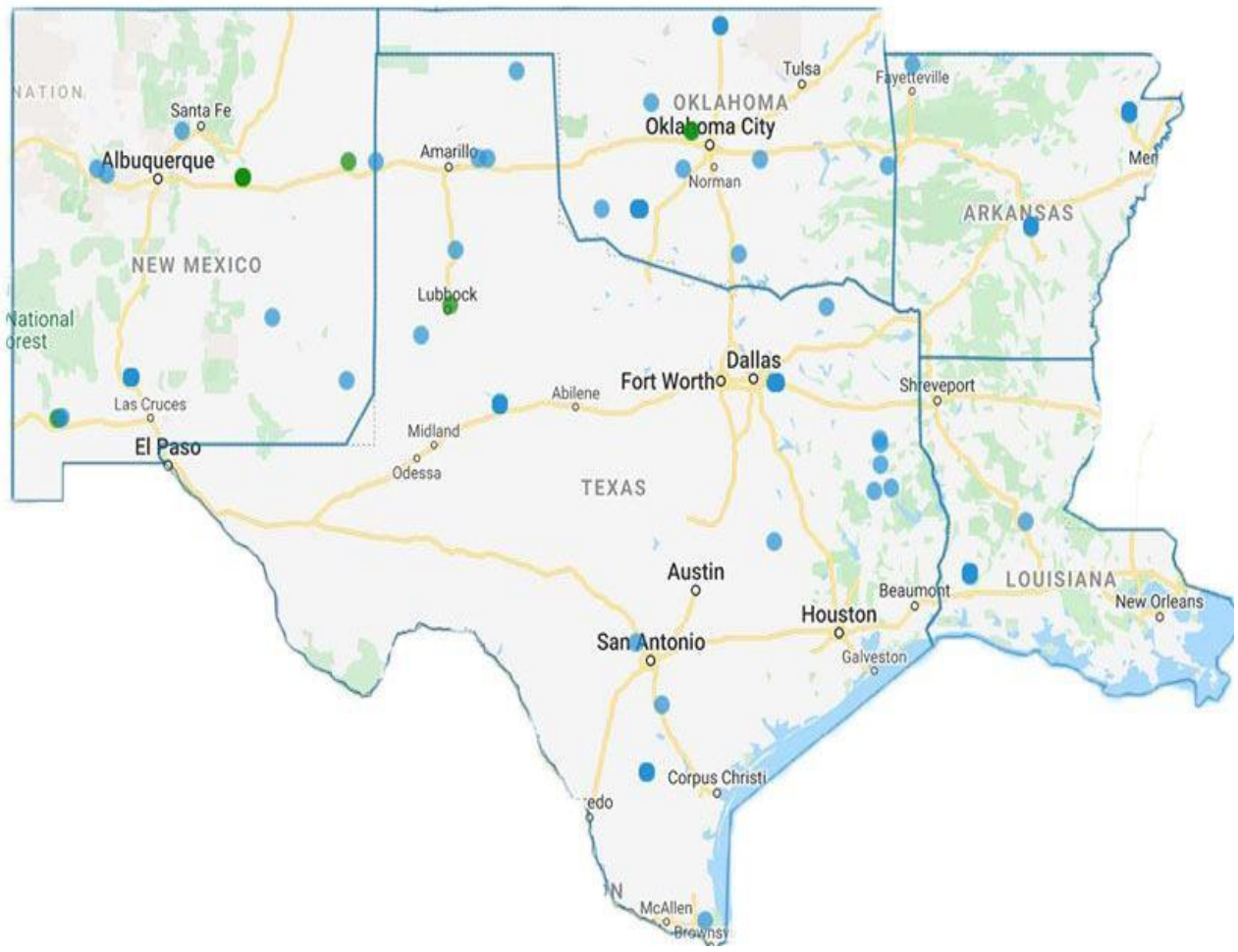

Figure 3. South-Central States and Pavement Sections considered in the study

4.1.1 Locations and Layer Properties of Selected LTPP Pavement Sections

The definition of the location of the pavement section is identified based on the latitude and longitude of the sections under consideration. The location of the sections in the South-Central states (Arkansas, Louisiana, New Mexico, Oklahoma, and Texas) can be easily extracted from the LTPP database. The location of all the five states sections based on the Global Positioning System considered under the interest of the study is provided in appendix A. Table 4 presents the number of sections considered for each one of the five South-Central states. The sections are chosen to represent the whole of the area of the given states and with respect to the availability of FWD and fatigue cracking at the same date.

Table 4. Number of sections in each state for the study

State	No. of Pavement Sections
Arkansas	11
Louisiana	11
New Mexico	18
Oklahoma	22
Texas	35

Error! Reference source not found. a, b, c, and d present the number of sections considered in this study. Active sections (green) and the out of study section (blue) were utilized. Out of study sections also represent valuable historical data which can be utilized in assessing the pavement conditions during certain time frame. The primary purpose for the utilization of both types of sections is creating the vast database of the pavement section to generate a state inclusive classification chart. Furthermore, the data utilized in this study is the data associated with pavement deflection through FWD testing performed over the ranges of time; therefore, both section types can be fruitful for fulfilling the sole purpose of this study.

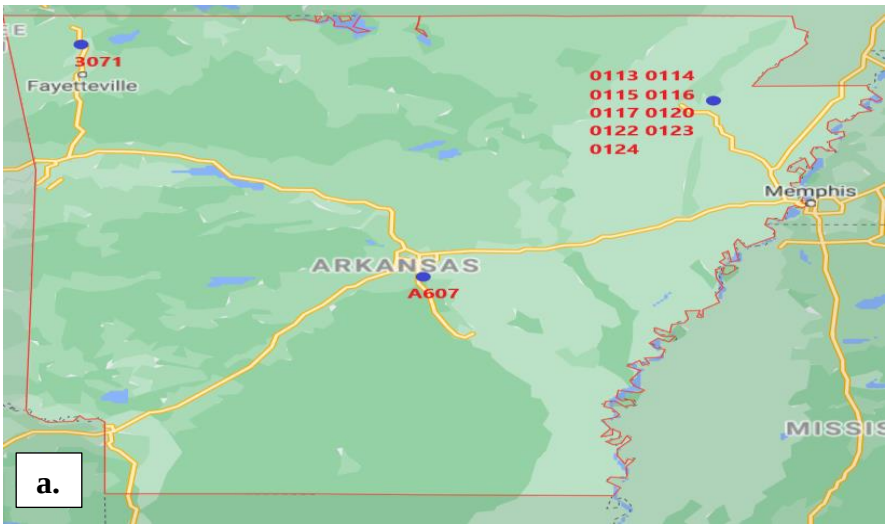

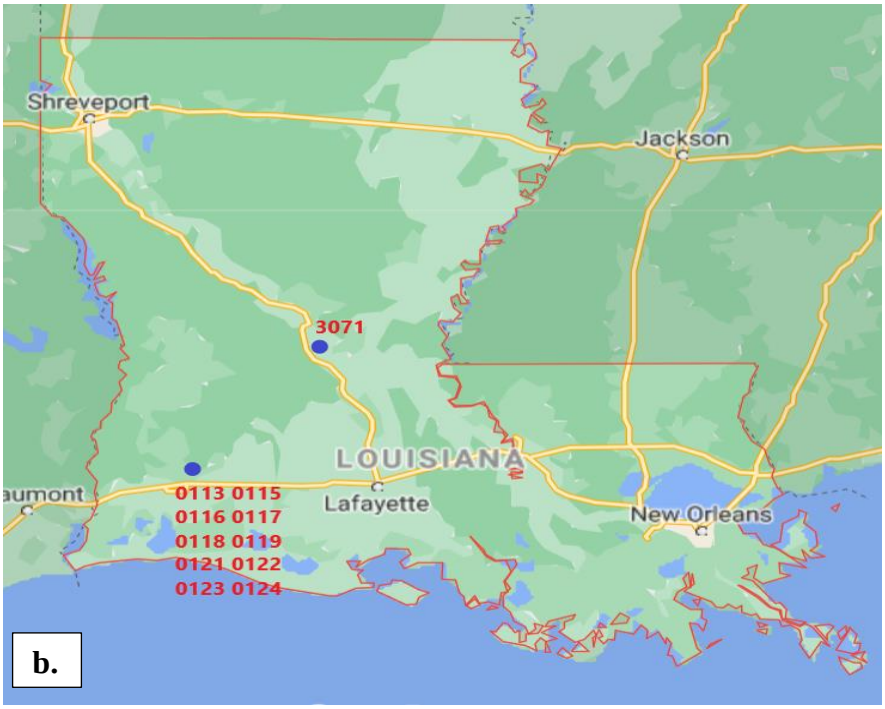

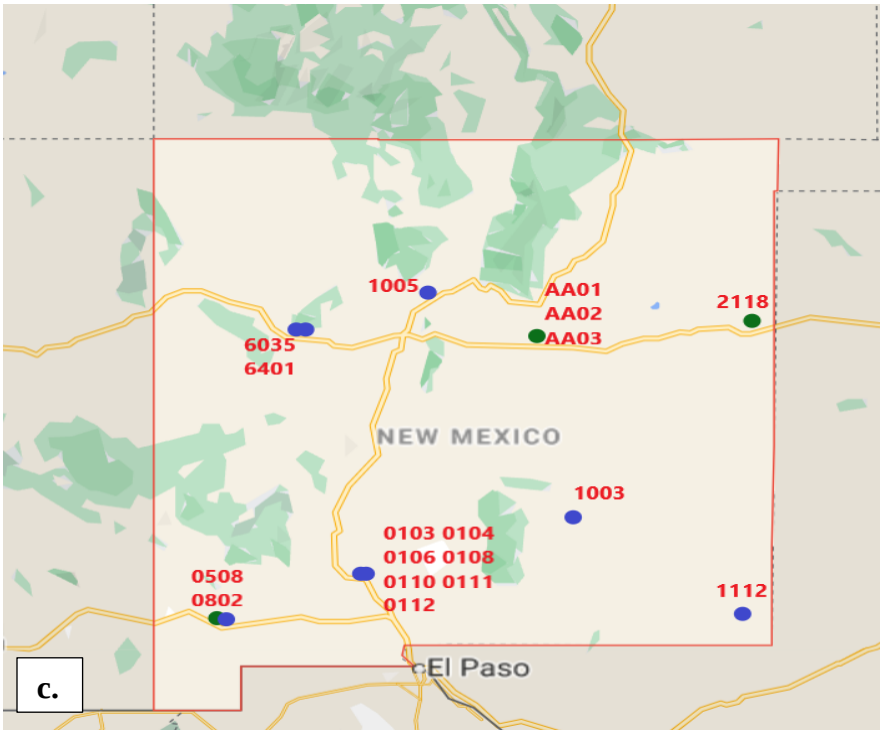
1005
AA01
AA02
AA03
2118
6035
6401
NEW MEXICO
1003
0103 0104
0106 0108
0110 0111
0112
0508
0802
1112
El Paso
c.

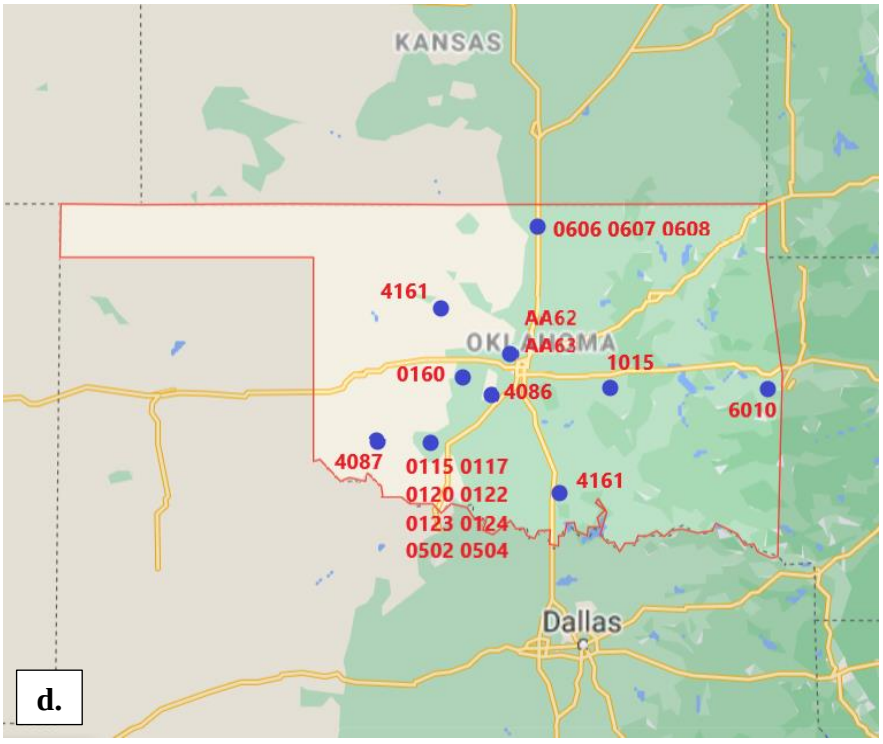
KANSAS
0606 0607 0608
4161
AA62
AA63
OKLAHOMA
1015
0160
4086
6010
4087
0115 0117
0120 0122
0123 0124
0502 0504
4161
Dallas
d.

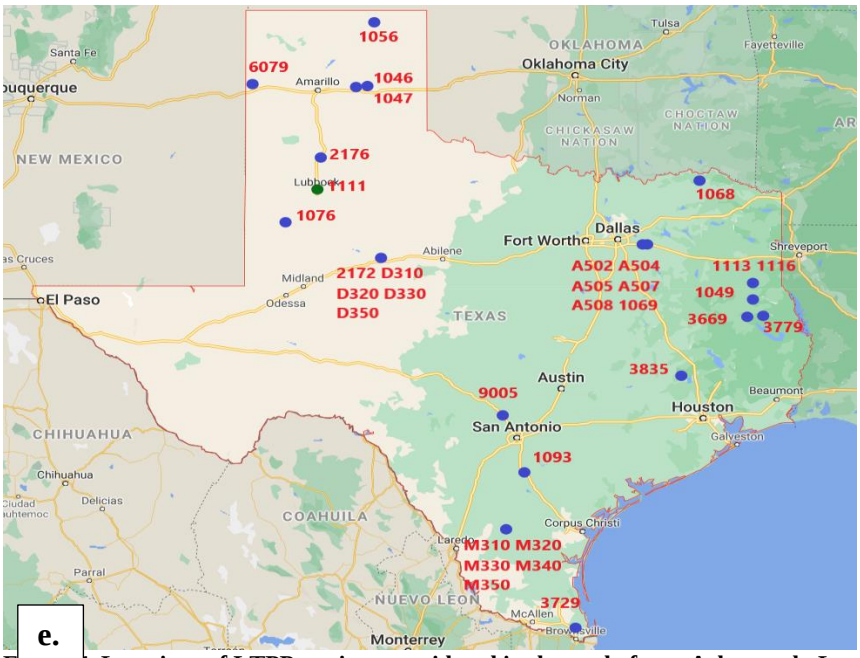

Figure 4. Locations of LTPP sections considered in the study for a. Arkansas b. Louisiana, c. New Mexico, d. Oklahoma and e) Texas (cont.)

Each of the pavement sections in the LTPP database is characterized by their distinguished section numbers. For example, in **Error! Reference source not found.**c, the state of New Mexico with 0103 refers to the section number considered in the study and can be easily matched with the database in the LTPP website. Similarly, as mentioned earlier, the primary database for this study is LTPP; hence, it has been utilized for obtaining the layer modulus as well as layer thickness. ANNACAP software had been used in getting the HMA elastic modulus. The approximation has been carried out to match the age of pavement sections during the time of FWD testing. Soil classification data, as presented under the material properties, were utilized to get the properties of the base, sub-base, and sub-grade layers. Table 5, Table 6, Table 7, Table 8 and Table 9 refer to the modulus values of the sections of Arkansas, Louisiana, New Mexico, and Oklahoma, respectively.

Table 5. Elastic Modulus Values for Pavement Section in Arkansas (psi)

Sections	Asphalt Layer 1	Asphalt Layer 2	Base (T)	Base (UT)	Subgrade
0113	1380000	1100000		32000	28000
0114	978000	964000		23000	28000
0115	1390000	1100000	100000		37500
0116	1800000	1630000	400000		35500
0117	959000	796000	100000	35000	28000
0120	1080000	1080000	200000	37400	28000
0122	1660000	1660000	400000	50000	37500
0123	1440000	1100000	400000	55000	35500
0124	1300000	903000	300000	52000	35500
A607	759100	759100	346500	83000	24000
3074	2088100	1802800	500000		24000

Note: T is treated, and UT is untreated base and subbases.

Table 6. Elastic Modulus Values for Pavement Section in Louisiana (psi)

Sections	Asphalt Layer 1	Asphalt Layer 2	Asphalt Layer 3	Base (T)	Base (UT)	Subbase (T)	Subbase (UT)	Subgrade
0113	1050000	1050000		30000		21700	28000	24000
0115	1411000	1411000		500000		250000	45000	24000
0116	1310000	1310000		500000		180000	45000	24000
0117	1310000			500000	45000	50000	29000	37500
0118	1193000			500000	55000	75000	29000	35500
0119	1405400			120000	28000	50000	75000	24000
0121	991300			86000	28000	60000	29000	24000
0122	430000			500000	45000	90000	35000	24000
0123	1350000			500000	50000	90000	29000	33500
0124	1480000			500000	80000	75000	29000	42000
3056	1344000	659160	543000		45000			37500
Note: T is treated, and UT is untreated base and subbases.								

Table 7. Elastic Modulus Values for Pavement Section in New Mexico (psi)

Sections	Asphalt Layer 1	Asphalt Layer 2	Base (T)	Base (UT)	Subbase (T)	Subbase (UT)	Subgrade
0103	691000		283000			37200	29000
0104	700000		265800			42000	29000
0106	1300000		200000	45000		32000	29000
0108	1140000		180000	35000		32000	21500
0110	1010000		290500	180000		45000	24000
0111	1610000		350000	50000		50000	24000
0112	1010000		300000	120000		24000	24000
0508	617000	617000		18000			13500
0802	501000			22000			13500
1003	1139000			26000			24000
1005	1020500			30100			24000
1112	1773000			91500			24000
2118	440300			89000		8000	21500
6035	1320000			84000		15200	21500
6401	529520	529520		8900	75000		21500
AA01	983000	983000		18000			29000
AA02	1001000	1001000		15000			29000
AA03	960000	960000		12000			24000
Note: T is treated, and UT is untreated base and subbases.							

Table 8. Elastic Modulus Values for Pavement Section in Oklahoma (psi)

Sections	Asphalt Layer 1	Asphalt Layer 2	Asphalt Layer 3	Base (T)	Base (UT)	Subbase (UT)	Subgrade
0115	1430000	1650000		600000		75000	13500
0116	1413900	1484596		623200	55000	13500	13500
0117	1164000	1390000		498700	22000	35000	8000
0120	1164000	1390000		498700	22000	35000	10000
0122	1835000	1835000		573000	150000	45800	13500
0123	657000	657000		457000	75000	18250	13500
0124	957600	1149120		515400	100000	15000	13500
0160	1413900	1484596		623200	55000	150000	13500
0504	1398000	139800		300000			13500
0505	483200	483200			75000		21500
0507	750400	750400			80000		21500
0606	329360			2504000	30000		13500
0607	300000			2100000	13500		13500
0608	322400			3000000	34100		13500
1015	1172320			400000			21500
4086	925400	925400		226800			29000
4087	571400	571400		300000		14100	21500
4161	557600	557600		414000			21500
4163	2122700	2122700		500000			24000
6010	498300	498300	498300				13500
AA62	100000	100000			5000		13500
AA63	100000	130000			8000		13500
Note: T is treated, and UT is untreated base and subbases.							

Table 9. Elastic Modulus Values for Pavement Section in Texas (psi)

Sections	Asphalt Layer 1	Asphalt Layer 2	Asphalt Layer 3	Base	Subbase	Sub-grade
1046	882000	798035		32000	26000	26000
1047	756000			32000	32000	24000
1049	1296000			400000	100000	26000
1056	12600			28000		13500
1068	324000	324000		32000	100000	8000
1069	648000			28000	17000	17000
1076	378000			26000		26000
1093	648000	504000		26000		17000
1111	630000			32000		26000
1113	486000			38000		32000
1116	486000			38000		17000
2172	1377000	1071000		26000	32000	17000
2176	693000			250000		26000
3669	648000			350000	100000	26000
3679	1620000			400000		29000
3729	1458000			32000	8000	8000
3835	1539000			40000	24000	24000
6079	1008000	1296000	1008000	32000		24000
9005	1340603	1134000		26000		17000
A502	1134000			28000	100000	17000
A504	504000	648000		28000	17000	17000
A505	756000	972000		28000	17000	17000
A507	1134000			28000	100000	17000
A508	1296000			28000	100000	17000
B310	972000			28000	100000	17000
B320	648000			28000	100000	17000
D310	1296000	1008000		26000	32000	17000
D320	1260000	1620000	1620000	28000	17000	17000
D330	1620000			40000	20000	20000
D350	1053000	819000		26000	32000	17000
M310	48600	37800		32000	15000	5000
M320	63000			32000	40000	6000
M330	37800			24000	40000	6000
M340	63000			32000	20000	8000
M350	37800			32000	20000	8000

The pavement sections utilized in the study had different layers. Some were typical four-layer systems, while others had numerous layers such as asphalt layer, treated base, untreated base, treated subbase, untreated subbase, and subgrade. Thickness concerning the layer systems is presented in

Table *10*, Table 11, Table 12, Table 13, and Table 14.

Table 10. Layer thickness for Pavement Section in Arkansas (inches)

Sections	Asphalt Layer 1	Asphalt Layer 2	Base (T)	Base (UT)	Subgrade
0113	1.5	2.5		8	240
0114	1.39	5.5		11	240
0115	2	5	7.4		240
0116	1.5	2.6	11.8		240
0117	1.7	5.2	3.8	4.2	240
0120	1.4	2.9	3.2	8.1	240
0122	1.8	2.6	4.1	3.5	240
0123	1.7	5.5	8.2	3.2	240
0124	1.6	5.3	11.1	3.7	240
A607	2.45	4.4	10	6	240
3074	1.5	3.9	10.5		240
Note: T is treated, and UT is untreated base and subbases.					

Table 11. Layer thickness for Pavement Section in Louisiana (inches)

Sections	Asphalt Layer 1	Asphalt Layer 2	Asphalt Layer 3	Base (T)	Base (UT)	Subbase (T)	Subbase (UT)	Subgrade
0113	1.5	3.4		8		6	12	240
0115	1.5	5.4		8.8		6	9	240
0116	1.9	2.8		10.9		6	12	240
0117	7			3.9	5.3	6	12	240
0118	4.4			6.9	4.1	6	12	240
0119	6.9			3.6	4.4	6	12	240
0121	4.2			3.9	3.2	6	12.6	240
0122	4.6			3.5	3.7	6	12.6	240
0123	6.8			7.3	4.2	6	12	240
0124	7.2			10.6	3.8	6	12	240
3056	1.5	7.1	1.6		7.9			240
Note: T is treated, and UT is untreated base and subbases.								

Table 12. Layer thickness for Pavement Section in New Mexico (inches)

Sections	Asphalt Layer 1	Asphalt Layer 2	Base (T)	Base (UT)	Subbase (T)	Subbase (UT)	Subgrade
0103	5.3		7			6	240
0104	8.4		11			6	240
0106	7.8		8.1	2.9		6	240
0108	7.8		4.6	7.7		6	240
0110	8		4.6	3.5		6	240
0111	4.9		7.6	3.7		6	240
0112	5.4		11.7	3.2		6	240
0508	11.5	3.3		12			240
0802	7			12.7			240

1003	7.3			6.5			240
1005	8.7			8.3			240
1112	6.2			6.4			240
2118	4.7			6.4		19	240
6035	7.9			6		9.2	240
6401	4.2	4		5.9	6		240
AA01	8.7	2.1		12			240
AA02	8	4		12			240
AA03	3.3	9.2		12			240
Note: T is treated, and UT is untreated base and subbases.							

Table 13. Layer thickness for Pavement Section in New Mexico (inches)

Sections	Asphalt Layer 1	Asphalt Layer 2	Asphalt Layer 3	Base (T)	Base (UT)	Subbase (UT)	Subgrade
0115	2	5.6		9		8	144
0116	1.5	6.5		4	5.4	8	240
0117	1.9	5.9		4.14		8	72
0120	1.6	3.1		4.8	7.9	9	108
0122	1.8	2.6		3.9	4.8	8	30
0123	1.6	5.5		8.6	4.4	8	36
0124	1.9	5.4		10.9	4.5	6	204
0160	1.5	6.5		4	5.4	8	240
0504	6.5	4.3		7.3			240
0505	3.9	4.3			9		240
0507	1.7	4			9.4		240
0606	4.4			9.1	14.8		240
0607	5.2			9	16		240
0608	11			5.8	12.5		240
1015	1.4			8.1			240
4086	3.4	4.3		7.9			240
4087	2.9	2		7.8		4.1	240
4161	0.8	2		7.6			240
4163	1.6	0.9		8.5			240
6010	1.9	1.5	10				192
AA62	1.9	8.7			10		192
AA63	1.8	9			12		240
Note: T is treated, and UT is untreated base and subbases.							

Table 14. Layer thickness for Pavement Section in Texas (inches)

Sections	Asphalt Layer 1	Asphalt Layer 2	Asphalt Layer 3	Base	Subbase	Subgrade
1046	10	2.4		8.4	5.1	240
1047	10			15.3	14.4	240
1049	4.6			11.2	7.8	240
1056	1.8			14.4		240
1068	2.1	7.8		6	8	240
1069	9.5			15.2	6.5	240
1076	5.4			8.4		240
1093	1.9	2.4		17.2		240
1111	9.5			8.4		240
1113	4.2			11.5		240
1116	4.6			10.9		240
2172	0.9	10		6.8	8.8	240
2176	2.3			9.4		240
3669	4.2			8	7.9	240
3679	1.6			8.4		240
3729	11.6			10.5	5.4	240
3835	8.5			13	6	240
6079	2.6	1.6	5.2	5		240
9005	1.9	1.2		9.4		240
A502	9.3			14.6	8	240
A504	5	8.9		10	8	240
A505	2.1	9.4		15	10.4	240
A507	8.8			15	8.3	240
A508	9.5			14	8	240
B310	9.9			15.2	6.5	240
B320	9.7			15.2	6.5	240
D310	1.9	9.9		6.8	8.8	240
D320	2.2	1.9	7.3	15	10.4	240
D330	3.1			15.6	8.4	240
D350	0.8	10.1		6.8	8.8	240
M310	0.6	1.6		8.1	8.8	240
M320	1.7			8.1	8.8	240
M330	1.9			8.1	8.8	240
M340	1.7			8.1	8.8	240
M350	1.6			8.1	8.8	240

4.1.2 Falling Weight Deflectometer Data

Structural performances of flexible pavement sections are in many cases assessed by Non-Destructive Techniques (NDT). Among various utilized methods of NDT in pavement technology, FWD is referred to as one of the simple and easily applicable technologies *(27)*. A significant amount of data had been obtained over time through FWD tests performed in pavement sections in the United States. These data are housed at LTPP info pave website for utilizing in research investigation and pavement performance monitoring purposes. MON_DEFL named tables are being used in obtaining the surface deflection data. A typical FWD deflection data in the LTPP website is either based on seven offsets geophones or nine offsets geophones. The following are the significant elements of the FWD data:

1) Peak drop load,
2) Drop height,
3) Sensors offset distances from the load point, and
4) Peak deflection values [44].

Peak drop load and drop height are considered simultaneously in any FWD testing. The dropped load is highly dependent on drop height. Four different drop height tests are conducted, which have their respective loadings. For any load range being acceptable in FWD testing, the load must lie between 90 and 110 percent of the targeted load. Table 15 presents the drop height, target loads, and an acceptable range of loads for any typical FWD testing procedure *(44)*.

Table 15. Drop Height and Associated Load Levels *(44)*

Drop Height	Targeted Load, kN (kips)	Acceptable Range, kN (kips)
1	26.7 (6.0)	24.0 to 29.4 (5.4 to 6.6)
2	40.0 (9.0)	36.0 to 44.0 (8.1 to 9.9)
3	53.4 (12.0)	48.1 to 58.7 (10.8 to 13.2)
4	71.2 (16.0)	64.1 to 78.3 (14.4 to 17.6)

Four deflection replicates were recorded for each drop height for the FWD test in LTPP. FWD tests were conducted at a different location in each section along the length of 152m to account for capturing the performance of the whole section. A location has its own four drop loads, and respective pavement deflections captured. Therefore, to account for the accuracy and covering the whole of the pavement sections, this study utilizes the average of the deflection for all locations of section.

Table 16 presents the examples of the FWD data collected in four different areas of Tran-SET South-Central States. For the other sections, the data are shown in the appendix B. Similarly, a simplified illustration is followed in Figure 4, associated with the location of sensors and the points of the FWD test in 152m pavement sections. With the application of FWD loading, a deflection bowl is obtained as shown in the following figure.

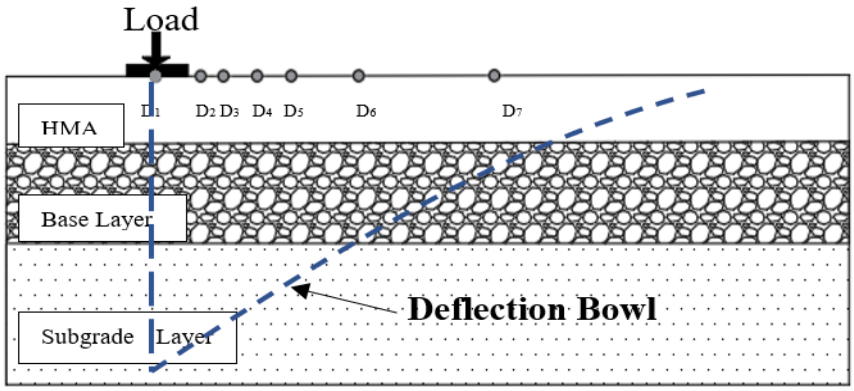

Figure 4. Location of Sensors and Load in FWD testing

Table 16. Surface Deflection Bowl Data Sample for the South-Central States

State/ Section	Drop Height	Drop Load, kPa	Average Peak Deflection of all points, micrometers						
			D1	D2	D3	D4	D5	D6	D7
AK 0113	1	375.8	165.7	127.4	99.0	71.9	57.4	41.5	34.5
	2	563.0	232.3	185.5	146.0	109.9	89.5	64.1	52.5
	3	769.5	307.9	246.1	197.0	150.4	122.8	90.1	71.5
	4	944.6	358.1	286.9	228.4	177.3	146.3	106.7	84.6
LA 0113	1	384.1	171.3	139.9	120.3	95.9	78.8	56.9	42.3
	2	598.3	257.4	213.6	185.3	149.8	124.4	90.6	67.4
	3	796.0	330.9	275.9	240.3	196.0	163.4	119.3	88.4
	4	1036.5	409.3	345.9	302.5	248.2	206.8	150.5	112.2
NM 0103	1	385.2	85.5	73.9	68.0	61.0	54.2	42.8	33.1
	2	577.8	129.0	111.5	102.6	92.2	82.1	64.4	49.9
	3	761.7	172.6	149.4	138.1	123.3	110.0	86.4	67.2
	4	998.6	228.9	198.4	182.8	164.0	146.2	114.5	89.1
OK 0115	1	413.9	66.1	51.7	44.4	38.7	32.1	24.1	17.8
	2	608.8	98.0	77.2	66.9	57.8	48.4	36.4	26.9
	3	815.3	134.9	106.2	92.6	79.3	67.1	50.2	37.7
	4	1065.0	181.1	142.7	124.0	107.0	91.0	68.3	51.2
TX 1046	1	406.7	102.2	87.3	80.2	69.0	62.2	49.8	32.3
	2	618.9	160.8	136.8	125.8	109.0	98.0	78.6	49.9
	3	841.8	223.2	192.9	177.7	154.7	139.1	111.3	70.1
	4	1030.9	276.8	237.7	219.5	191.4	172.1	137.7	86.6

4.1.3 Distress Conditions Data

A single section of pavement experiences various distresses such as fatigue cracking, rutting, and many other distresses. Fatigue cracking is one of the common forms of distress accounted to pavement structures. Therefore, to assess and categorize the pavement with the fatigue cracking occurrence, the fatigue-related distress data are collected from LTPP databases. The primary basis for selecting distress data was through the LTPP distress identification manual *(45)*. Fatigue cracking data obtained were reported in terms of area of occurrences, expressed in m2. Some of the sections had less fatigue, while some sections showed an excessive amount of fatigue. Furthermore, the fatigue data collected for each of the sections where in the same time frame when the FWD tests were conducted. Table 17 presents fatigue observed in a different section of the pavement in Arkansas, Louisiana, New Mexico, Oklahoma, and Texas.

Table 17. Distress Data for the South-Central States

AK		LA		NM		OK		TX	
Sections	**Fatigue %**	**Sections**	**Fatigue %**	**Sections**	**Fatigue %**	**Sections**	**Fatigue %**	**Sections**	**Fatigue %**
0113	6.16	0113	2.82	0103	0.05	0115	3.88	1046	0.00
0114	14.12	0115	0.24	0104	0.05	0117	5.28	1047	0.23
0115	4.39	0116	0.17	0106	0.00	0120	12.12	1049	2.37
0116	3.44	0117	0.00	0108	0.00	0122	2.03	1056	34.18
0117	7.25	0118	0.29	0110	0.00	0123	1.64	1068	16.78
0120	10.63	0119	0.72	0111	0.00	0124	0.34	1069	8.71
0122	3.23	0121	2.28	0112	0.00	0160	0.00	1076	11.31
0123	1.74	0122	0.95	0508	0.00	0502	0.00	1093	24.38
0124	3.01	0123	0.20	1003	0.00	0504	0.00	1111	0.16
3071	0.00	0124	0.15	1005	0.00	0505	0.02	1113	16.83
A607	4.98	3056	2.40	1112	0.00	0507	0.03	1116	24.80
				2118	4.03	0606	0.38	2172	0.00
				6035	7.18	0608	6.45	2176	16.69
				6401	6.61	0607	6.71	3669	3.57
				0802	15.04	1015	3.24	3679	0.00
				AA01	0.00	4086	1.83	3729	1.85
				AA02	0.00	4087	5.88	3835	2.15
				AA03	0.00	4161	9.83	6079	0.81
						4163	1.59	9005	8.80
						6010	2.21	A502	0.00
						AA62	36.66	A504	0.00
						AA63	25.93	A505	0.00
								A507	0.17
								A508	0.48
								B310	0.73
								B320	12.10
								D310	0.00
								D320	0.00
								D330	0.00
								D350	0.00
								M310	30.58
								M320	25.92
								M330	32.87
								M340	29.68
								M350	19.78

4.2 Computer Simulation for FWD for the most Common Flexible Pavement Structures

FWD tests are conducted utilizing a lot of resources and time; therefore, there is always a need for capturing the behavior of flexible pavement structures without the requirement to perform significant amount of FWD testing, especially at the network level. Various software packages become handy in predicting the performance of pavement structures as well as replicating FWD testing. In this study, two different software programs are explored for effectively simulating the deflection bowls under FWD plate loadings: 3D- Move Analysis software package and Analysis System (ANSYS) are the two software packages utilized in this study. The 3D- Move Analysis software package is one of the widely used software packages in the analysis of flexible pavements. At the same time, ANSYS is a modern and advanced finite element-based software package in pavement engineering and design. The proceeding sub-sections will describe more about these software packages and their utilization in simulating the field measured deflection bowls.

4.2.1 Utilization of 3D-Move Analysis Software Packages in simulating deflection bowls

The 3D Move Software package is one of the most distinguished software packages in the analysis of flexible pavement structures. The open-source software developed and released by the University of Reno under the cooperative agreement with Federal Highway Administration (FHWA) is distinguished by its ability to encounter variable loading conditions. Continuum based finite element approach is utilized in the development of the software along with the Fourier transformation technique. Various advantages of using 3D- Move Analysis software package are handling complex surface loadings and non-uniform tire pressures *(46)*. Some other advanced applications of the software are the estimation of pavement performance at the intersection and under the off-road farm vehicles. The applications of the 3D-Move software package are not limited to a few of these functions. Furthermore, the software package can be utilized in an adjustable loading configuration in analyzing non generic tire and axle configuration. Similarly, modeling of 3D surface stresses, the effect of braking, and viscoelastic systems are other advanced applications of the 3D- Move Software Package.

Figure 5 represents the 3D-Move software welcome screen and its various applications.

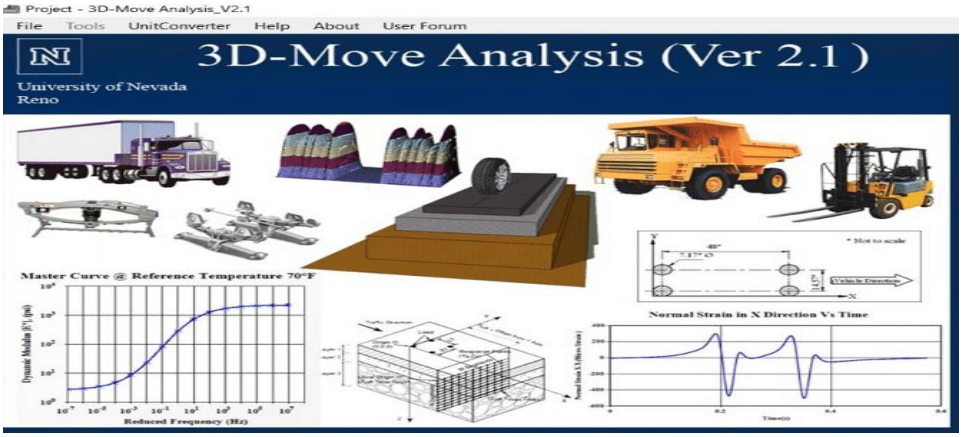

Figure 5. 3D- Move software and its application

Details of the Analysis Approach followed

In this sub-section, the detailed analysis procedure followed in the 3D-Move Analysis software package is described. The stepwise methods for accurately estimating the FWD testing through a software package are presented in this section. Additionally, a static analysis approach is followed to simulate field FWD testing. The following steps are required for simulating the field measured FWD deflection bowl utilizing the 3D-Move Software package.

Project Identification and Type of Analysis

The first task in analyzing any pavement structure in the 3D-Move Software package is assigning the project location for easy identification of the pavement sections encountered. Project location, milepost, and traffic directions are the specific input in this section. Furthermore, types of analysis (Static/Dynamic) are also provided in this section. In this study, for a better simulation of the FWD testing device, static analysis is selected to simulate the FWD plate loading condition.

Pavement structure and pavement layer properties

Pavement sections are characterized by their distinct structures and thickness of each layer. Furthermore, the material properties of the pavement at the layer systems play a vital role in the performance of the pavement. The number of layers, along with their corresponding thicknesses, are input in this section. Other materials related to properties such as modulus values and Poisson's ratio are input following their respective layers. For the sake of uniformity, asphalt layers, base layers, subbase layers, and subgrade layers had been provided the Poisson's ratio of 0.35, 0.4, 0.4, and 0.45, respectively *(2)*.

Load input and contact pressure distribution

This section is one of the vital sections in any 3D-Move analysis procedures. The required load for running the analysis is provided in this section. The software offers six different options (A to F) for assigning the configuration of tires in any analysis. In this study, configuration type B was deemed most suitable for the analysis since this type is based on the single load type, and the FWD test matches with such setup. The definition of the contact area and the application of the loads is made simultaneously in this section. Each of the load is associated with the respective drop heights. Therefore, every section had four different analyses due to the prevalence of four types of load. The stress utilized in the FWD testing and the area of the load plate (300 mm in diameter) resulted in the required load for the analysis. Eventually, a circular contact area was considered to match the load plate in field FWD devices.

Response points

An FWD test device is characterized by numerous offsets from the central location of the load plate towards the entire test sections. Therefore, the software simulations also require the exact offset of the sensor to analyze and predict the FWD test successfully and accurately. Different coordinates of interest are input as the response point for analysis through the 3D-Move3D-Movesoftware package. The response points resembling the actual FWD test are presented in Table 18. Z- oordinate was made constant as the point of interest of the deflection was the pavement surface.

Table 18. Sensors Offsets in 3D-Move

Sensors	Location (mm)		
	X	**y**	**Z**
1	0	0	0.001
2	203	0	0.001
3	305	0	0.001
4	457	0	0.001
5	610	0	0.001
6	913	0	0.001
7	1524	0	0.001

3D-Move Software Outputs

Various outputs can be obtained from 3D-Move software such as strain, stress, and displacement at any given point in the pavement layers. However, as a fundamental goal of this research study, displacement values are utilized to develop and simulate FWD the deflection bowls. Table 19 presents the deflection of a pavement section of Arkansas, Louisiana, New Mexico, Oklahoma, and Texas. Distinct deflection-based results are provided in appendix C for each of the states studied.

Table 19. Example of Deflection Output in 3D-Move

Sensor Offsets, mm	**Deflection output through 3D Move, micrometers**				
	AK 0113	**LA 0113**	**NM 0103**	**OK 0115**	**TX M310**
0	117.34	177.70	318.26	396.11	277.21
203	96.08	143.36	222.69	286.99	181.71
305	82.72	118.54	171.28	235.59	100.25
457	65.62	87.36	114.77	176.37	77.60
610	51.52	63.97	76.18	129.57	59.77
914	31.68	35.90	35.95	68.58	29.44
1524	12.19	14.00	12.53	20.22	21.31

Comparison of the 3D-Movesimulated deflection and actual FWD test deflection

As mentioned earlier, the LTPP database hosts the countless number of FWD test results as deflection bowls. A similar deflection bowl has been obtained through the simulation by the 3D-Move software package. A plot between the LTPP deflection bowls and the software simulated bowl has been presented to facilitate the easy comparisons. It is observed that similar deflection related performances have been obtained through software. Figure 6 illustrates the field measured FWD deflection bowl as compared to the simulated FWD using 3D-Move Analysis software package.

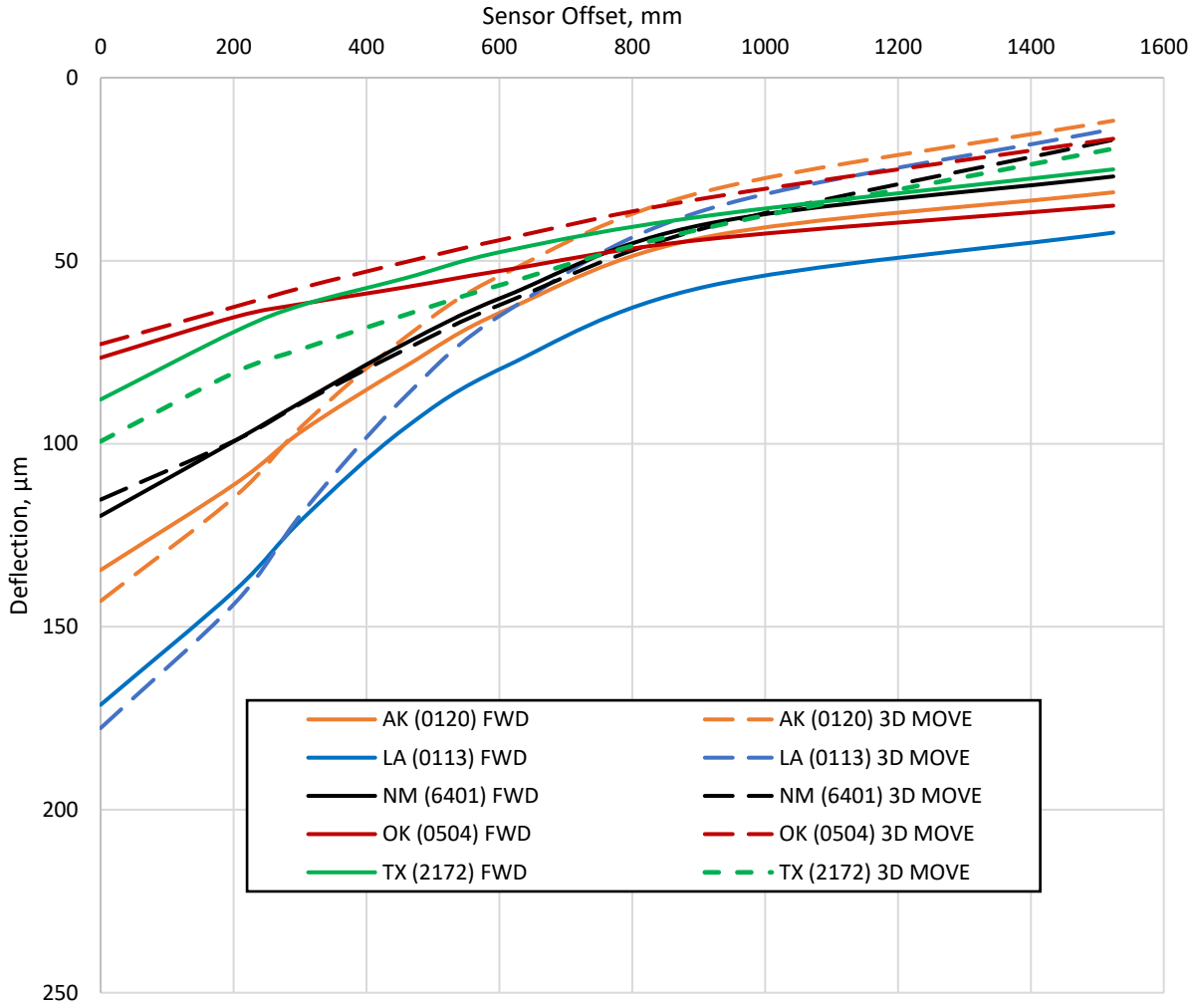

Figure 6. Comparison of Deflection observed for different state based on 3D-Move and FWD

The presented observations suggest that 3D-Move can be utilized in FWD based deflection prediction on varieties of pavement structures. Replications of pavement with software and original FWD tests were very much alike and provided a similar result; therefore, 3D- Move can be utilized by pavement engineers who are interested in finding deflection induced impacts. Furthermore, all sections FWD and software simulated comparisons are shown in the appendix C.

Comparison between simulated and field-based deflection bowls

It is well known that surface deflection values play a significant role in pavement structural evaluation. An FWD test deflection values are measured at different offsets, which can be utilized in the early condition assessment of flexible pavement structures. More importantly, the deflection value at the center of the load plate has a better role in acknowledging the conditions of the pavement. This is due to the reason that deflection is maximum under the center of load plates and fades being away from the plate. Deflection under the load plates is defined as central deflection and represented as D_0. D_0 must resemble the actual D_0 from the FWD testing. Therefore, the

comparison had been provided for simulated and actual D_0 of all the states (Arkansas, Louisiana, New Mexico, Oklahoma, and Texas) in Figure 7 to Figure 11. Similarly, all deflection bowls obtained from 3D-Move are also compared with the actual FWD test, as presented in Figure 12 to Figure 16.

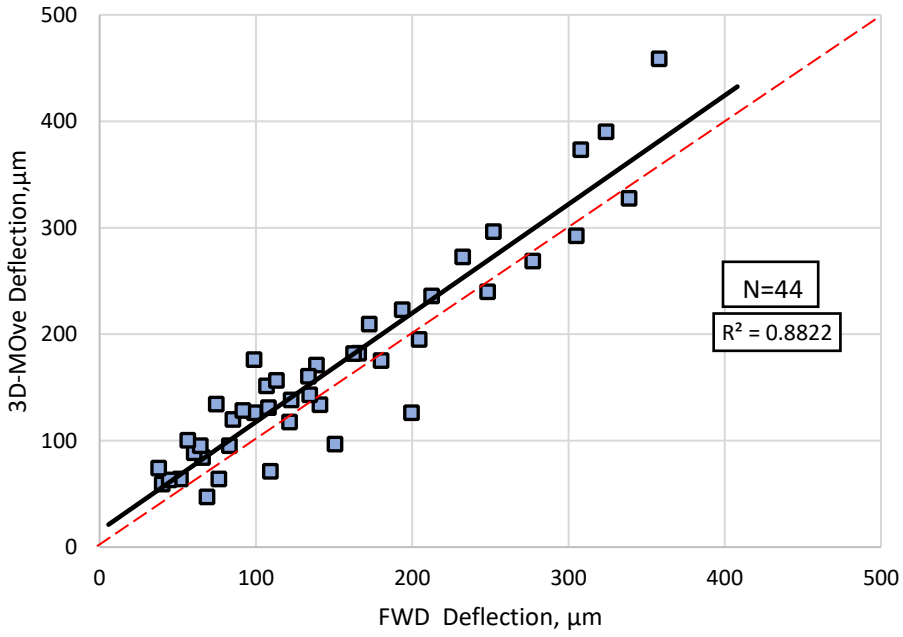

Figure 7. Comparison of Central Deflection (Do) for 3D-Move and FWD (Arkansas)

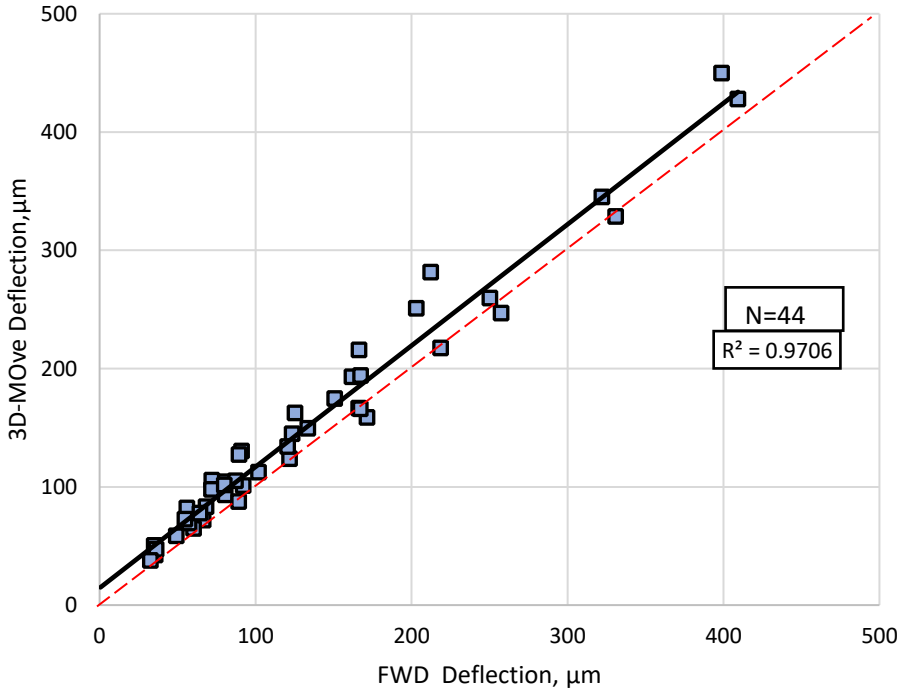

Figure 8. Comparison of Central Deflection (Do) for 3D-Move and FWD (Louisiana)

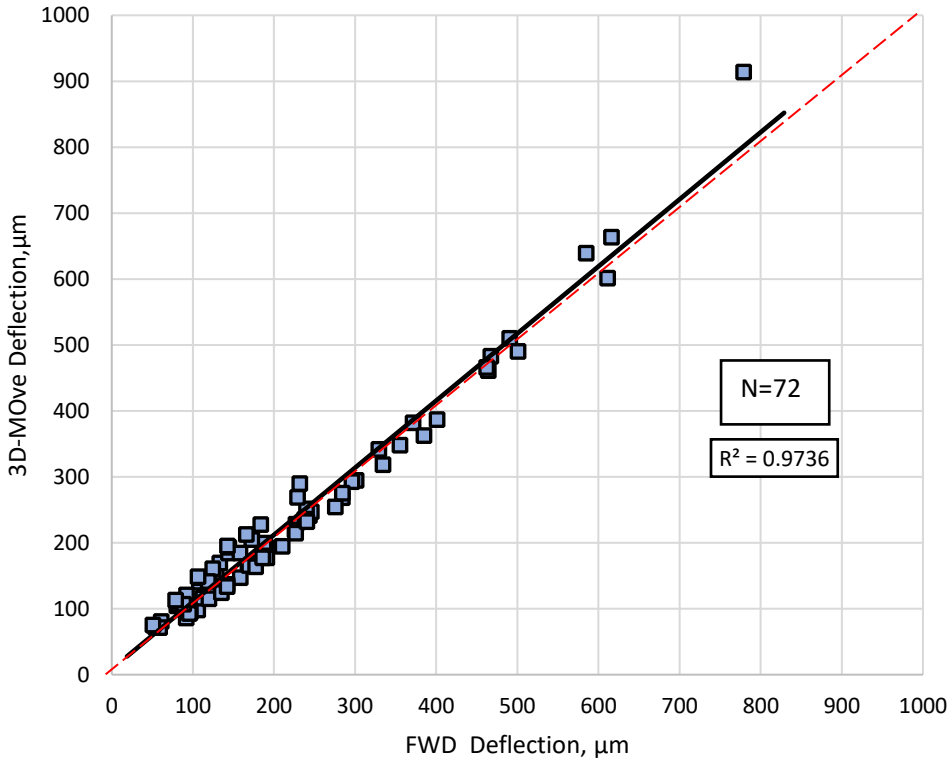

Figure 9. Comparison of Central Deflection (Do) for 3D-Move and FWD (New Mexico)

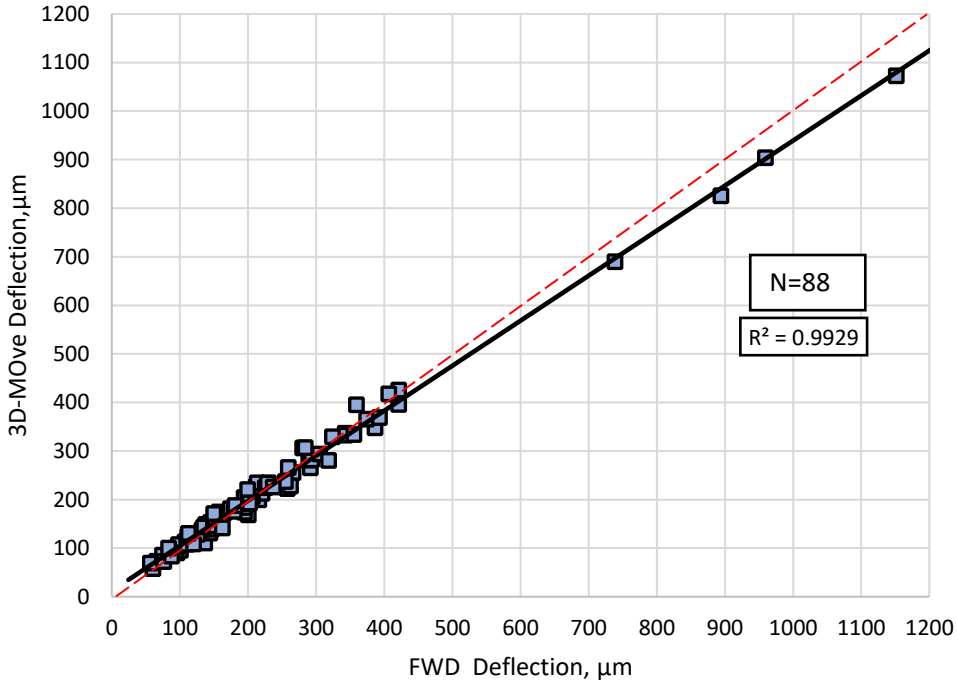

Figure 10. Comparison of Central Deflection (Do) for 3D-Move and FWD (Oklahoma)

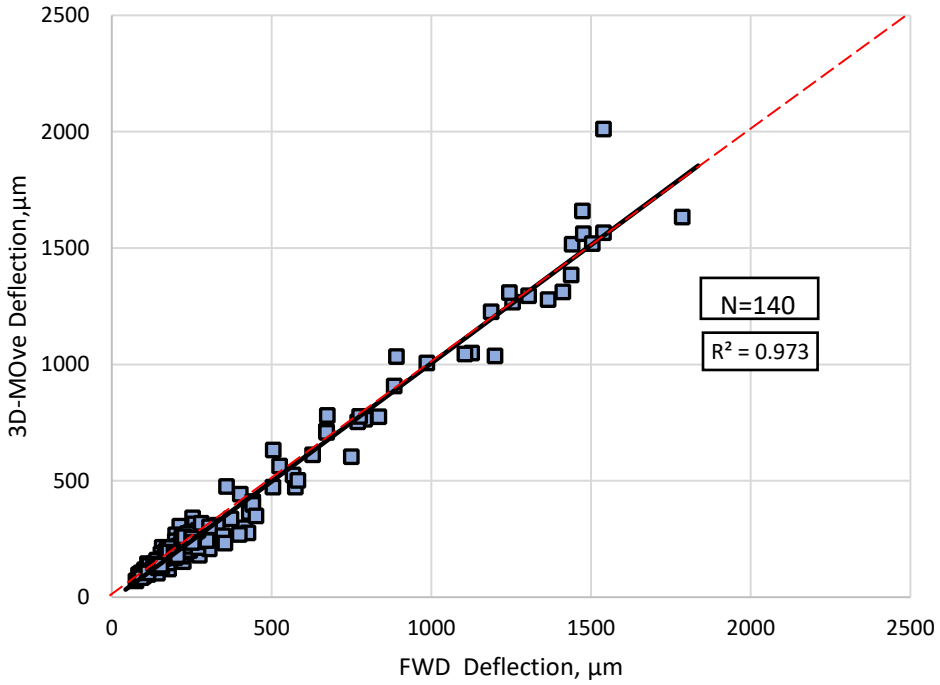

Figure 11. Comparison of Central Deflection (Do) for 3D-Move and FWD (Texas)

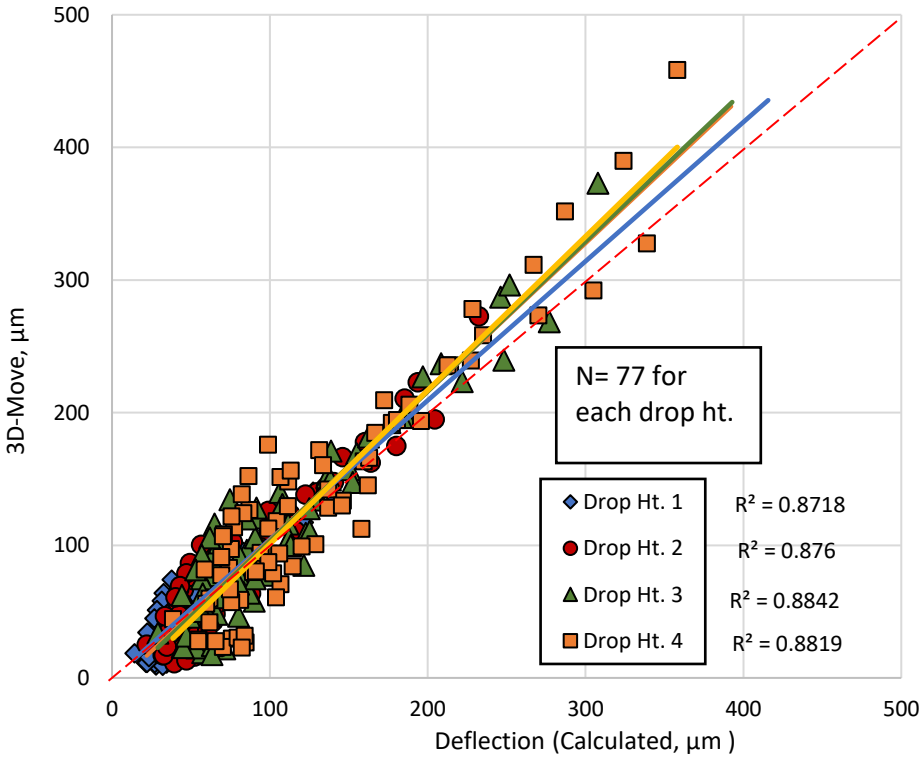

Figure 12. Comparison of All Deflection for 3D-Move and FWD (Arkansas)

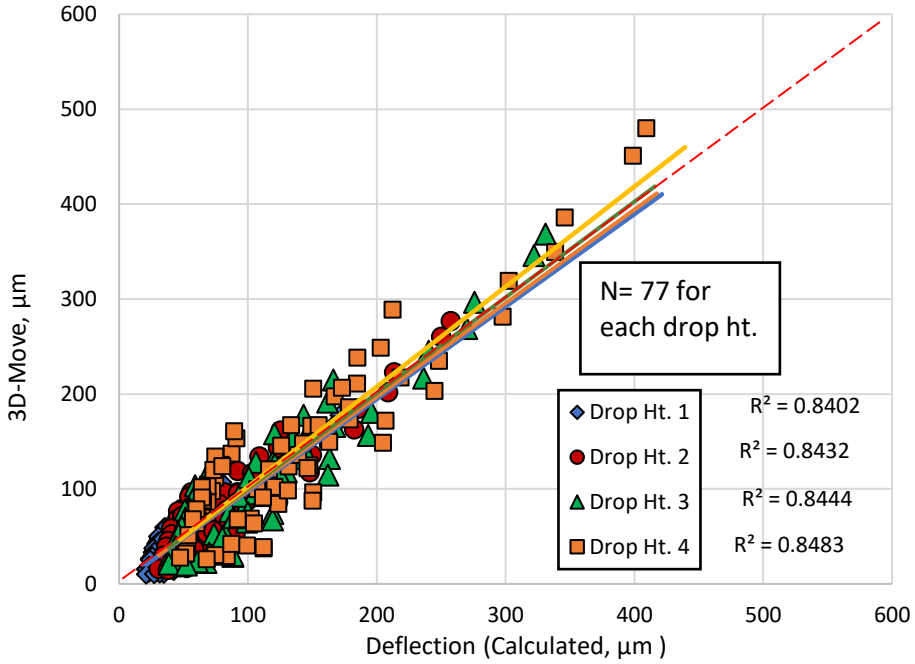

Figure 13. Comparison of All Deflection for 3D-Move and FWD (Louisiana)

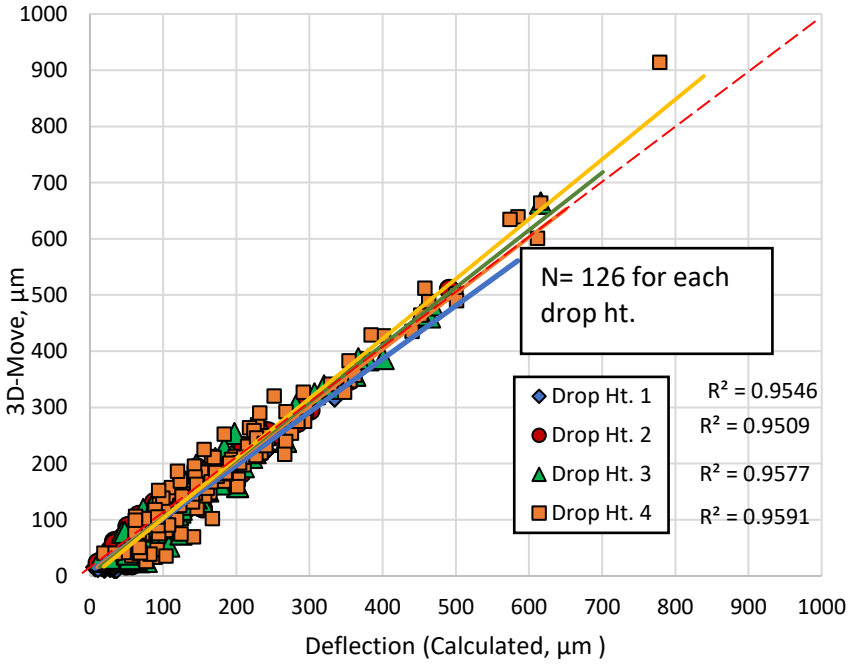

Figure 14. Comparison of All Deflection for 3D-Move and FWD (New Mexico)

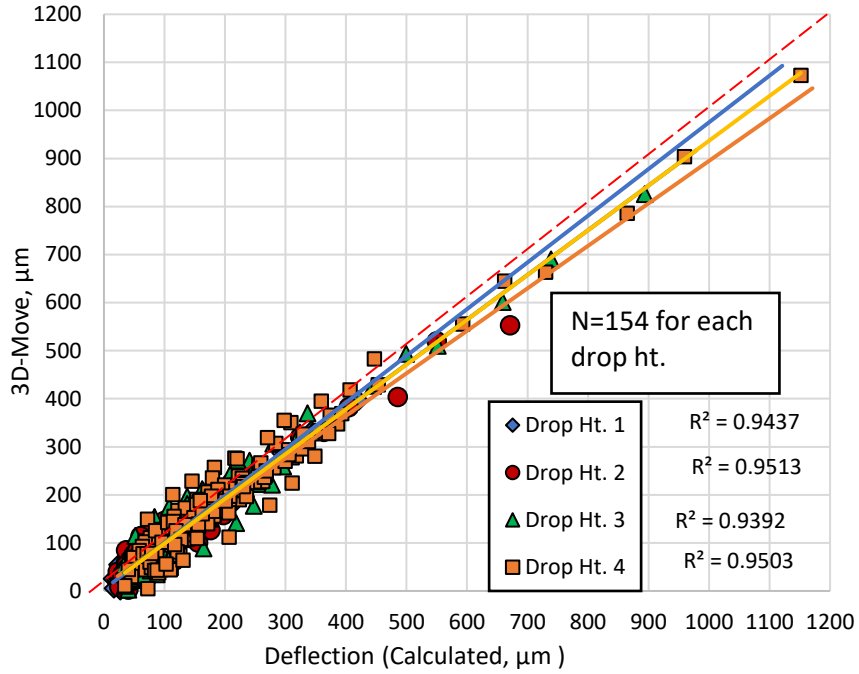

Figure 15. Comparison of All Deflection for 3D-Move and FWD (Oklahoma)

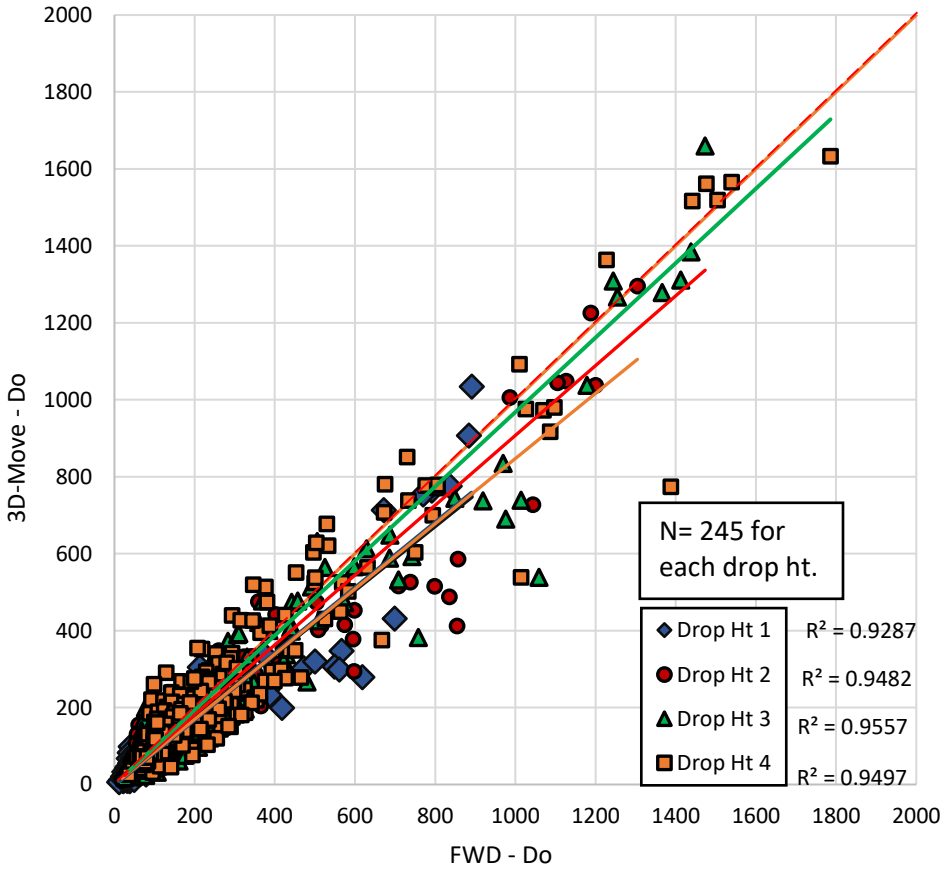

Figure 16. Comparison of All Deflection for 3D-Move and FWD (Texas)

It is observed that the deflection obtained from 3D-MoveAnalysis was highly correlated with the deflection from the field measured FWD test. The comparison of Do have a higher coefficient of determination (R2) than the comparison between the entire deflection bowls. These higher degrees of determination show the reliability of the 3D-Movesoftware package in predicting and replicating the deflection and simulation of deflection bowls. Figure 17 and Figure 18 present all the South-Central States actual versus predicted deflection in terms of central deflection and the entire deflection bowl data points. A higher coefficient of determination is observed in both cases.

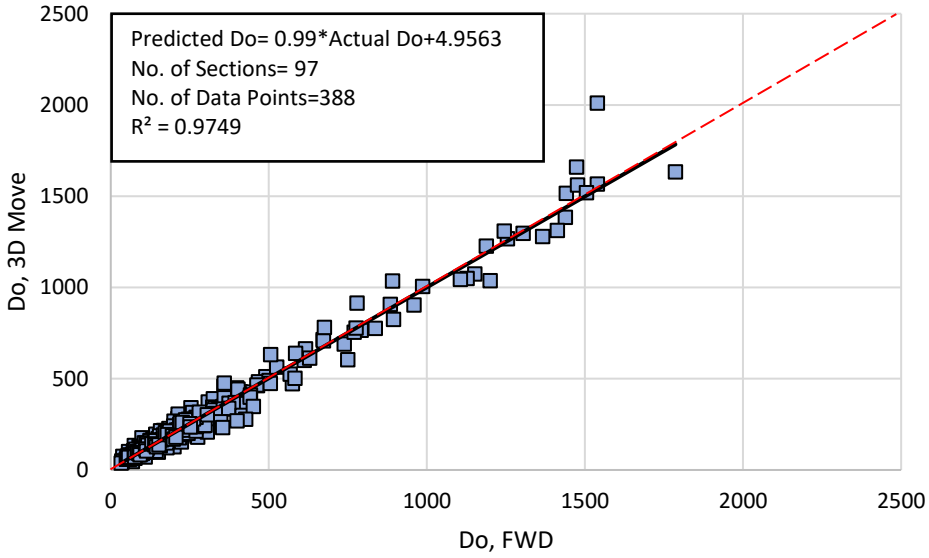

Figure 17. Measured FWD versus simulated 3D-Move central deflections for South-Central States

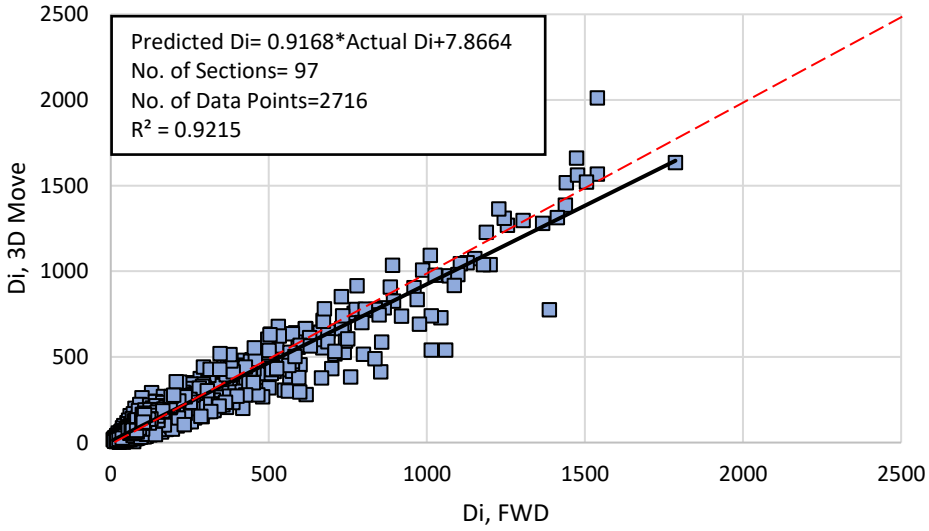

Figure 18. Measured FWD versus simulated 3D-Move all point deflections for South-Central States

4.2.2 Utilization of ANSYS software package in simulating deflection bowls

FWD is the common non-destructive technique practiced throughout the world. The deflection captured by any FWD measuring device can be utilized in monitoring the conditions of the flexible pavement structure. The FWD test uses a lot of resources and time, and in some cases, blockades of the roads are normal. Therefore, there is a need for developing models to simulate the tests as it is done in the field. Various analytical and numerical models have been presented to simulate the FWD testing to overcome the disadvantages of actual field tests. Finite element modeling software such as ABAQUS and ANSYS are extensively utilized to model flexible pavement structures by various researchers *(38-39)*. Dynamic and static analyses were done in previous studies. Although, there has been a mixed ideology in utilizing the appropriate analysis form of the FWD test in FEM. Some of the researchers found static analysis as a favorable and accurate way of modeling an FWD test *(42)*. Therefore, as a preliminary explorative study, a static analysis procedure is utilized in this study to understand FWD related phenomena. Deflection characteristics of various sections were being utilized in obtaining the deflection bowls in an attempt to be implemented in further studies.

The utilization of ANSYS FEA was completed with seven pavement sections from each of the South-Central States. The seven pavement sections were chosen in such a way that the analysis incorporates different pavement structures. Structural differences in pavement structures were obtained by selecting a three-layer system, a four-layer system, a five-layer system, and a six-layer system. Figure 19 shows the different pavement layer systems utilized in the study.

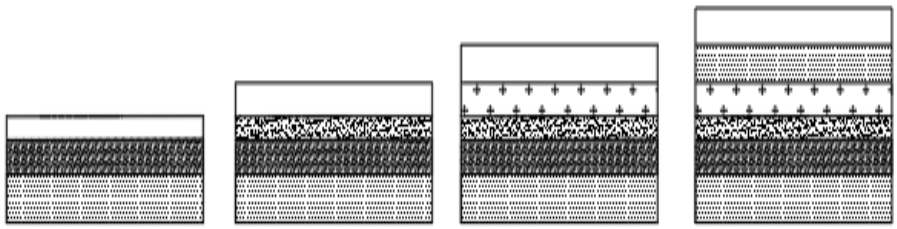

Figure 19. A 3-layer, 4-layer, 5-layer, and 6-layer pavement sections considered in the analysis

The modeled pavement structures were varied following the field conditions. As mentioned earlier, numerous pavement sections were modeled from the state of Arkansas, Louisiana, New Mexico, Oklahoma, and Texas. The pavement performance was monitored concerning the deflection obtained from the finite element analysis.

Developing a finite element model

A finite element model is developed following the stepwise procedures as 1) selecting model geometry, 2) Providing layer properties, 3) meshing the model, 4) defining the boundary conditions, and 5) assigning the load conditions. A multilayered flexible pavement structure is provided for the analysis. The response of the pavement structure, including surface deflection, was analyzed after developing the model.

Model Geometry

A crucial step in any FEM is defining the model geometry. Setup for the FWD test is presented in this section. A geometry that can simulate the field conditions is determined through a literature review and is optimized per the need of the study *(40)*.

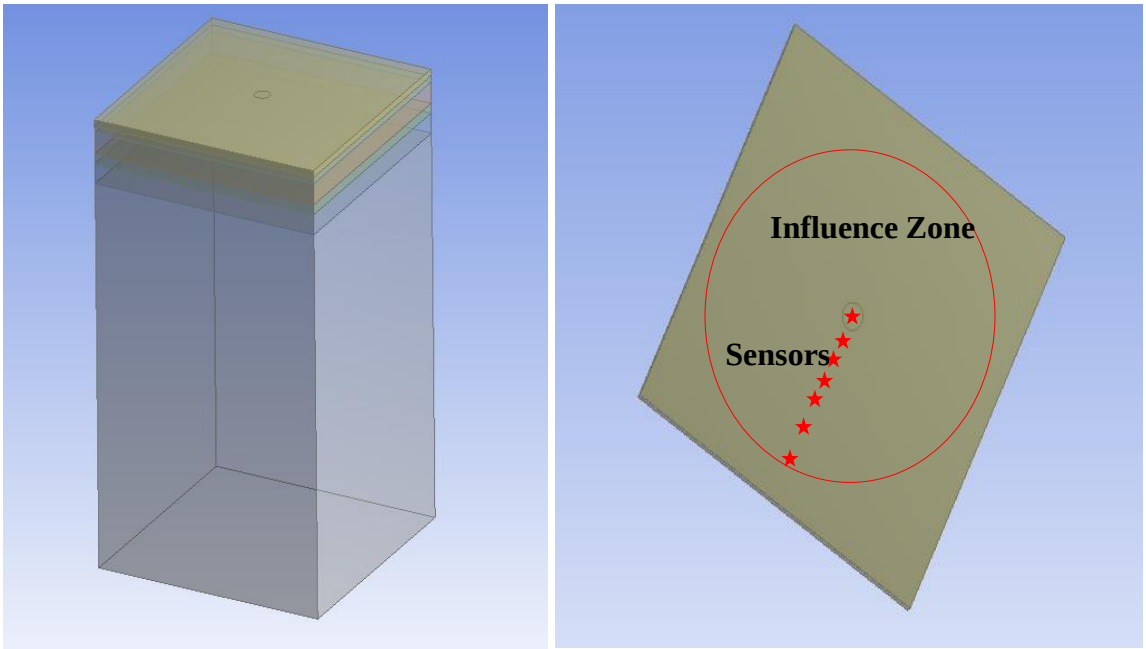

Figure 20. Pavement Geometry, Loading Plate and Sensors

Figure 20 shows the pavement layers and the respective region in the FWD test. Sensors, as in the actual FWD tests, are placed at 0, 203, 305, 457, 610, 913, and 1524 mm apart. A static loading was applied on the surface of the pavement to get the deflection output. Deflection is equal in all radial directions, and the radial zone is more often referred to as an influence zone *(40)*. A 3D-model is utilized in this study to simulate the field measured FWD test. The geometry of the model was selected in a way that all sensors fall under the area of influence. In this study, the model geometry of 168x168 inches is utilized for providing enough provision to fit all the sensors, therefore, the geometry is successful in capturing the effect of FWD loading towards the entire sensors.

Layer Properties

Layer properties predefine the pavement structure conditions. In a flexible pavement structure, each layer has a complex property that is not easily definable. Therefore, the utilization of layer theory is made for simplifying the FE modeling of pavement structures *(47)*. Homogenous, isotropic, and linear elastic model is presented in this study with the characterization of Young's Modulus and Poisson's Ratio. Modulus values and layer thickness are presented in the table 3-6 and 7-10, respectively, for each of the studied sections. Table 20 shows the density and Poisson's ratio for different pavement layers. The ranges of utilized Poisson’s ratio effectively captured the pavement performance *(2)*.

Table 20. Pavement Section Properties Layer wise *[48]*

Pavement Section Layers	Density (lb./ft3)	Poisson's ratio
Asphalt Layer	140	0.35
Base Layer (T)	137	0.40
Base Layer (UT)	99.85	0.40
Subbase Layer (T)	103	0.40
Subbase Layer (UT)	103	0.40
Subgrade Layer	137	0.45

The meshing of the model

Another step in utilizing the FEM is the meshing of the model. Meshing is much more related to the accuracy of the model. Various meshing associated functions can be implemented in ANSYS, such as linear and quadratic. The choice of the meshing function depends on the accuracy required *(49)*. In this study, quadratic functions are provided for the circular load plate and top of the pavements, while the linear function is provided at the other faces of the pavement surface. Figure 21(a) shows the meshing arrangement for load plates and pavement structures.

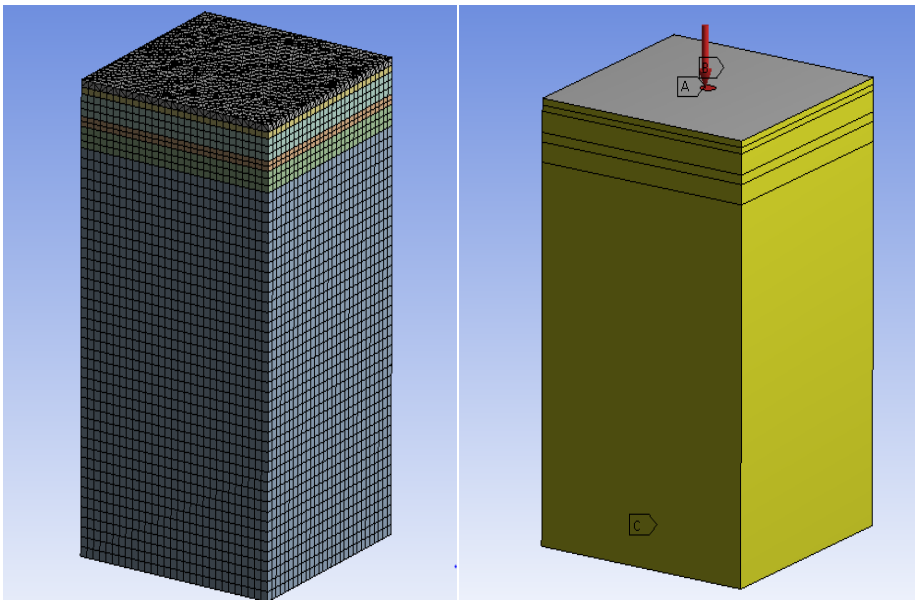

Figure 21. Finite Element Modeling a) Meshing b) Boundary Conditions and Loads

Boundary Conditions

Boundary conditions are necessities in FEM, and boundary conditions act as a support in any pavement structure. Mostly utilized support conditions are roller, hinge, and fixed. In this study,

all the four faces of the three-dimensional pavement model are provided with roller support to restrain the horizontal movement *(40)*. Furthermore, fixed support is assigned at the bottom of the subgrade. This way, both the horizontal and vertical movements are controlled. The pavement system is a multi-layer system; therefore, the connection between the layers is fully bonded with no gap in between *(42)*. Figure 21(b) shows the boundary conditions provided in ANSYS.

Loading Conditions

To replicate the actual FWD testing device, this study utilized the static loading conditions. Static load related data were derived from the field measured FWD test. Each of the sections under different drop heights has their respective loads as an input. Therefore, a section had four runs in total. The loading is based on the target load level, as presented in Chapter 3. Each of the loadings utilized in the research are obtained from LTPP database.

Finite Element Analysis and Results

A pavement system has several responses when loaded with FWD plate load. In this study, the response related to displacement is investigated utilizing the FE model. The surface deflection was considered to get the shape of the deflection bowl in ANSYS. Figure 22 shows a typical 5-layer section and its displacement due to FWD consideration in the analysis.

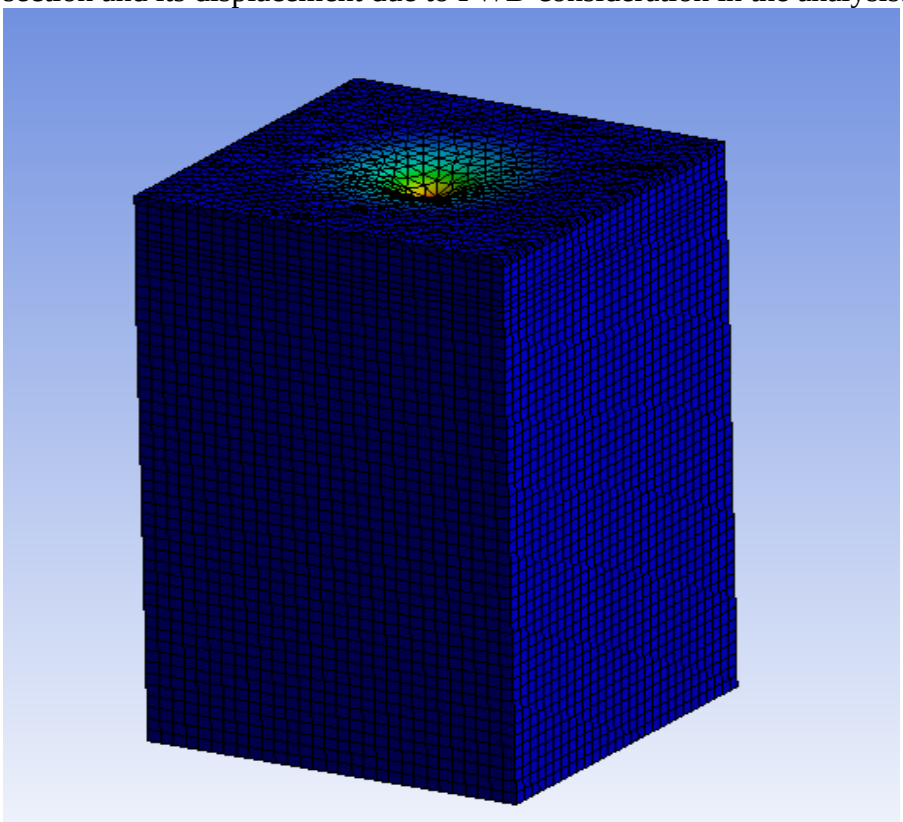

Figure 22. Deflection observed in a typical pavement section loaded with FWD

A total of 35 sections were analyzed in this study resulting in the 140 runs (35 sections times 4 drop loads). Each of the drop height recorded a different type of response. Displacement responses

for each of the sections at drop height one obtained through the 3D-Move, ANSYS, and FWD are compared in Figure 23 for a section from each of the South-Central States.

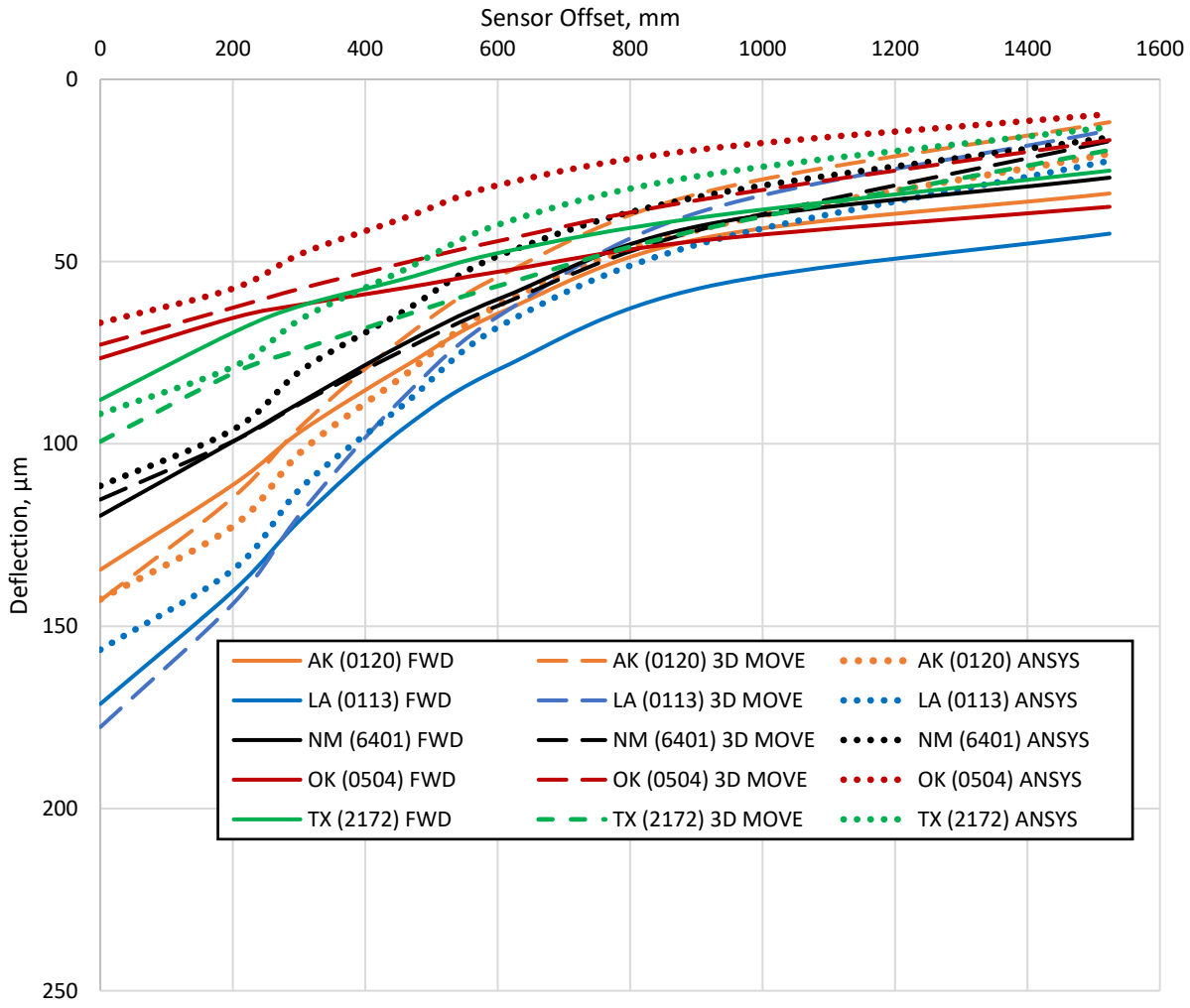

Figure 23. Deflection Comparison for FWD, 3D-Move, and ANSYS

It is observed that the deflection produced by the software packages ANSYS, and 3D-Move Analysis are similar to field measured FWD deflection bowl-which suggests that the utilization of ANSYS and 3D-Move Analysis software packages can be an appropriate tool to replicate the field measured FWD deflection bowl.

Comparison of simulated deflection: FWD Vs. ANSYS & 3D-Move Vs. ANSYS

In the previous section, it was well observed that the deflection obtained on all the analysis, including FWD tests, were similar. However, the results presented were only based on a single section comparison. This section compares the deflection obtained from FWD, ANSYS, and 3D-Moveutilizing all the 35 pavement sections. Figure 24 to Figure 28 shows the comparison of deflection obtained from FWD and ANSYS software package for different states. A highly correlated value was observed between the field measured and software simulated deflection.

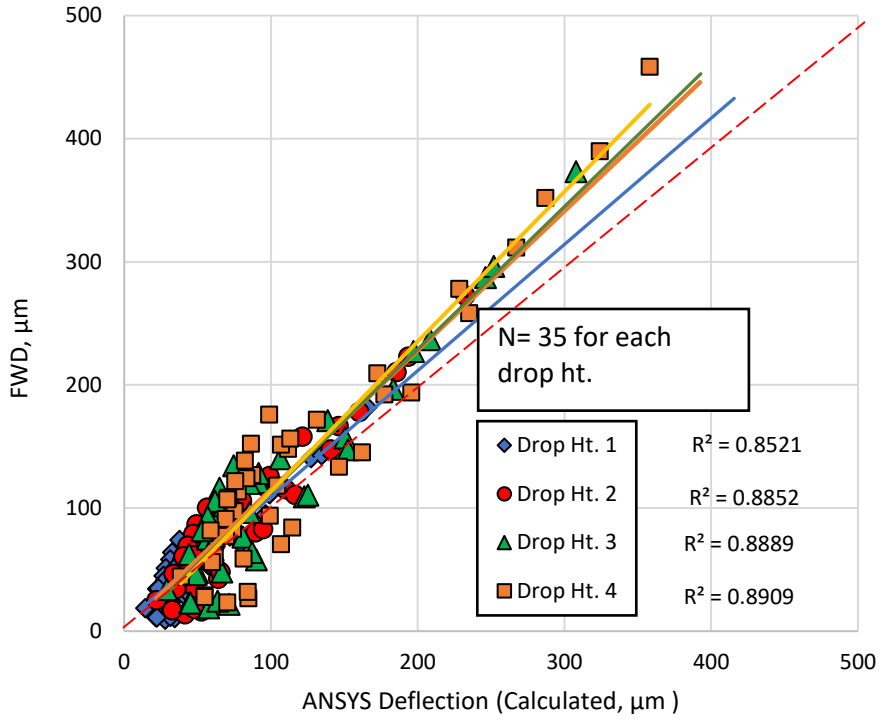

Figure 24. Comparison of All Deflection for ANSYS and FWD (Arkansas)

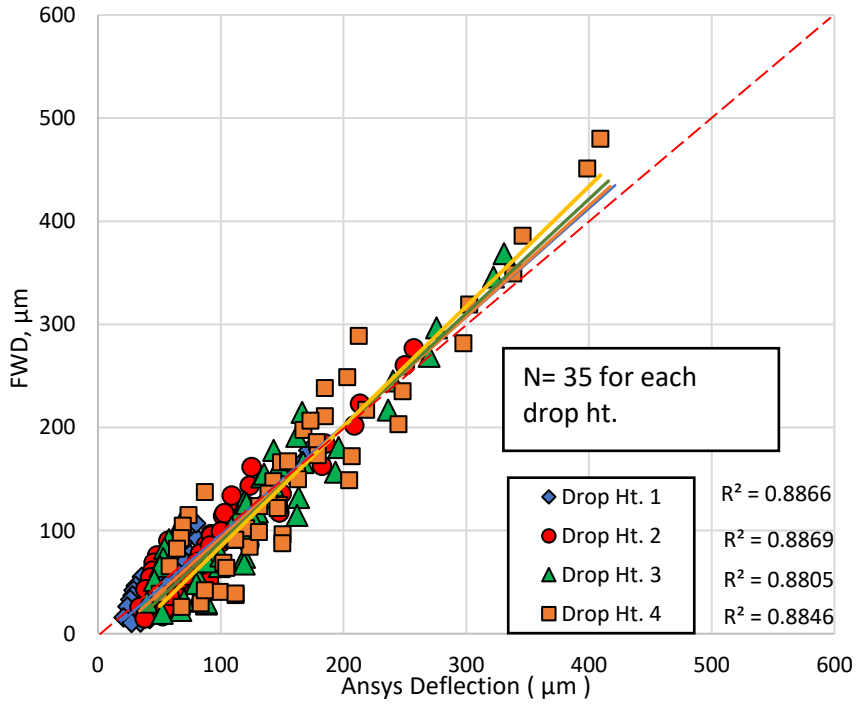

Figure 25. Comparison of All Deflection for ANSYS and FWD (Louisiana)

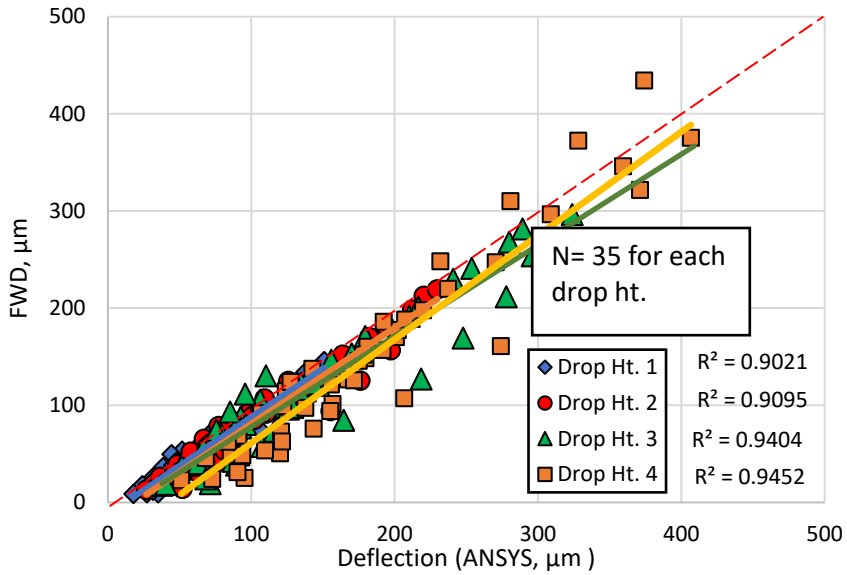

Figure 26. Comparison of All Deflection for ANSYS and FWD (New Mexico)

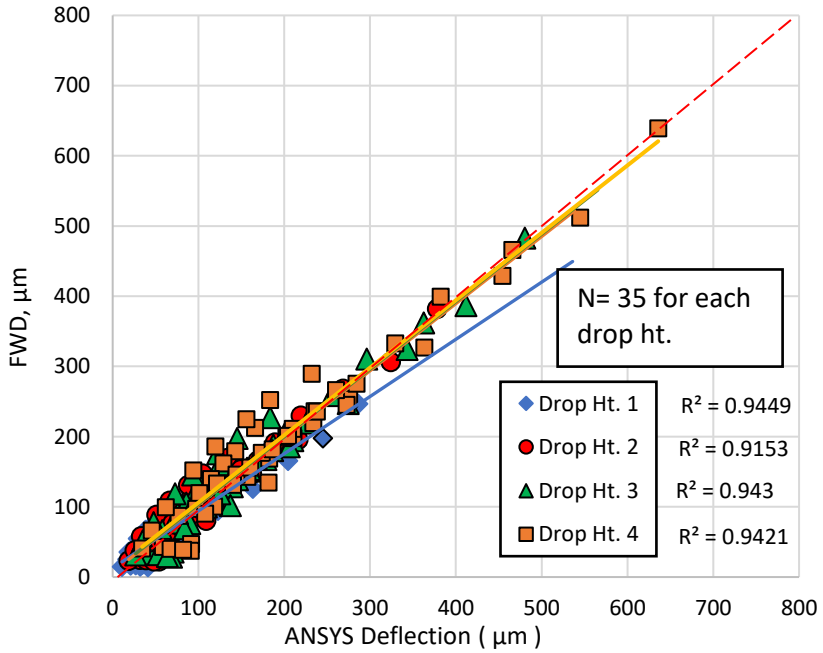

Figure 27. Comparison of All Deflection for ANSYS and FWD (Oklahoma)

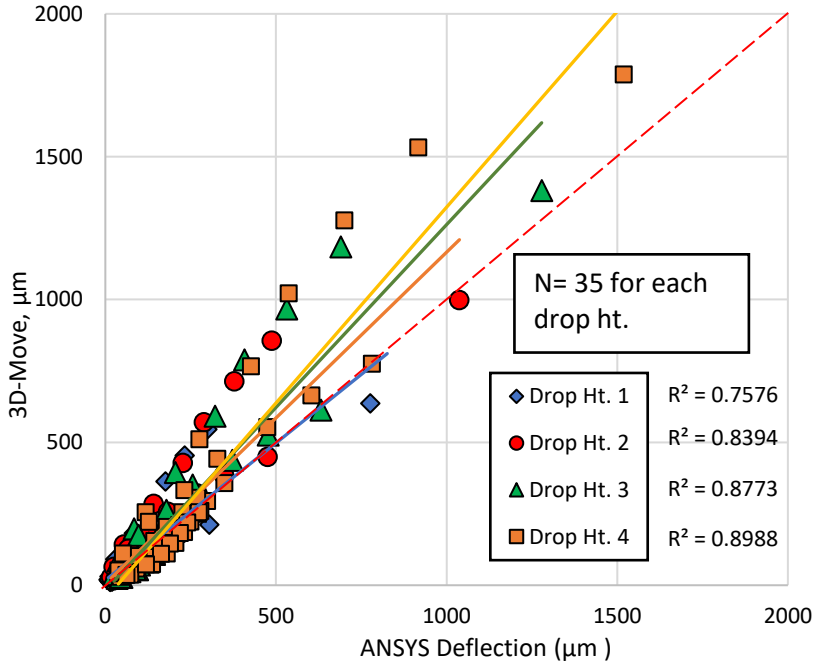

Figure 28. Comparison of All Deflection for ANSYS and FWD (Texas)

Furthermore, to judge the suitability of software ANSYS and 3D-Move, a regression analysis is performed. Figure 29 to Figure 33 show the comparison of deflection obtained from 3D-Move and ANSYS software packages for different states. Thirty-five data points are utilized in each of the drop heights, and a highly correlated value between the deflection obtained suggests that either of the software can be utilized in simulating the deflection bowls.

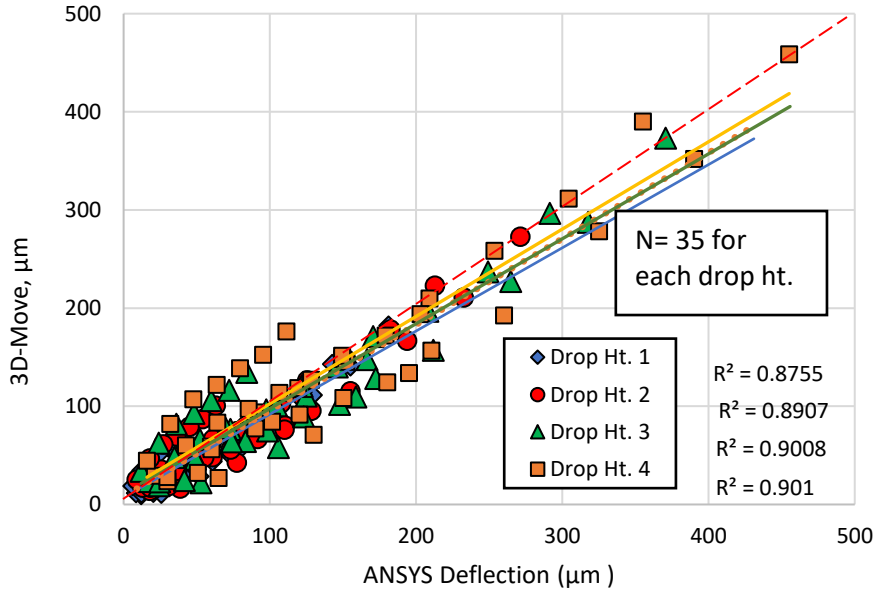

Figure 29. Comparison of All Deflection for ANSYS and 3D-Move (Arkansas)

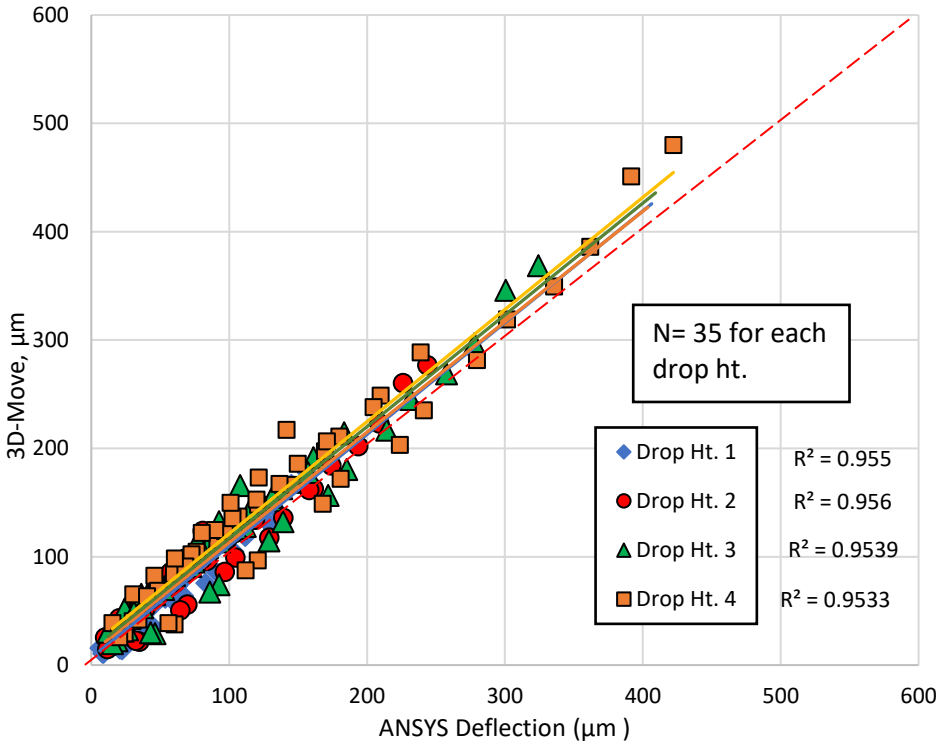

Figure 30. Comparison of All Deflection for ANSYS and 3D-Move (Louisiana)

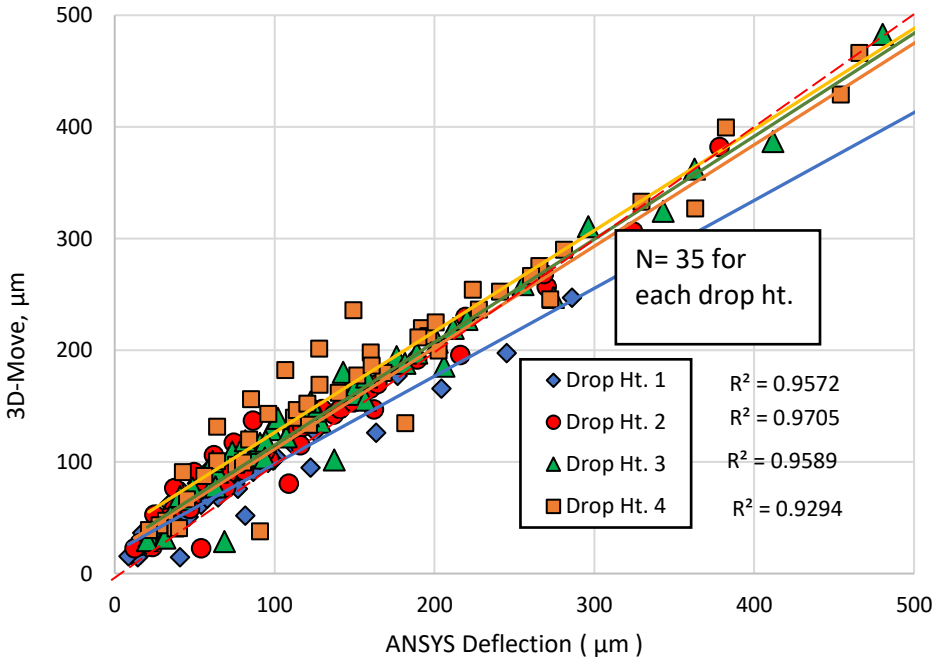

Figure 31. Comparison of All Deflection for ANSYS and 3D-Move (New Mexico)

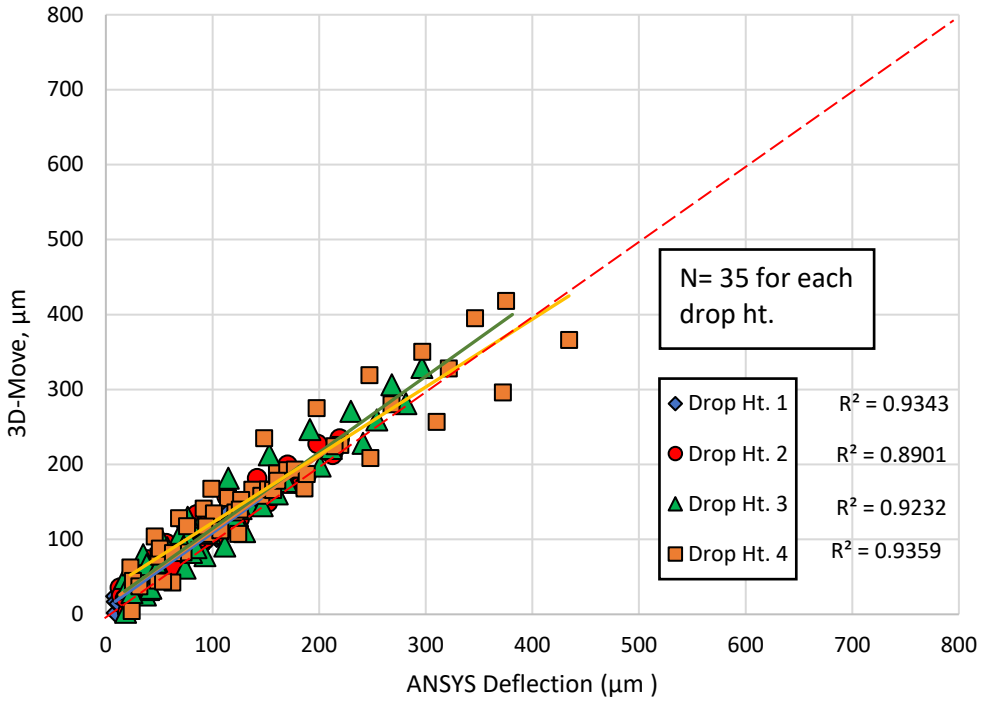

Figure 32. Comparison of All Deflection for ANSYS and 3D-Move (Oklahoma)

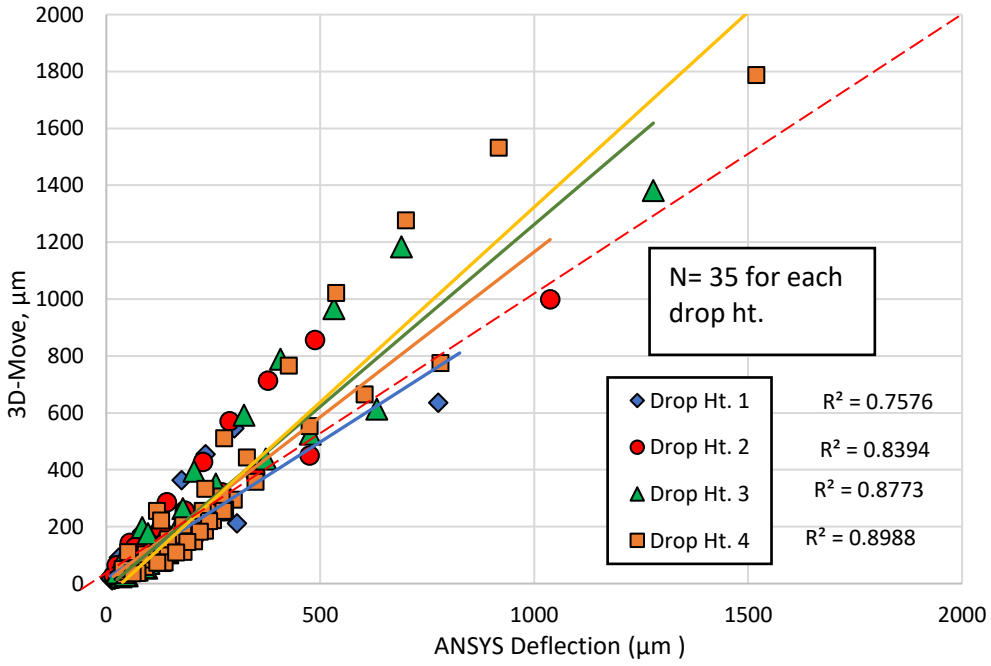

Figure 33. Comparison of All Deflection for ANSYS and 3D-Move (Texas)

Previously, it is mentioned 97x4 analyses were performed with the 3D-Move Analysis software package due to its quick and simplified nature. On the other hand, the analytical study through the ANSYS software package requires higher computational power and comparatively higher time for analysis. Therefore, only the preliminary explorative analysis is made with the ANSYS software package, as it offers more flexibility on different loading options and material databases. However, further analyses are followed with the surface deflection bowl obtained through 3D-Move Analysis as all the sections considered in the study are analyzed through the 3D-Move Analysis Software Package.

5. ANALYSIS AND FINDINGS

5.1 Evaluation of Deflection Parameters

In the previous chapter, it is observed that simulated deflections from both 3D-Move and ANSYS were highly correlated with an actual FWD field test result. These two different software packages were utilized in developing the deflection bowls, and both provided promising results. Ninety-seven sections were analyzed using 3D-Move software package, out of which 35 sections were analyzed using ANSYS. Due to the fact that the entire 97 sections were completed using 3D-Move software package, the simulated values from it are utilized in generating the deflection parameters for the South-Central States. Utilizing the various properties of pavement, such as, moduli value and thickness, 3D-Move software results were further implemented in this chapter.

Varieties of deflection value were obtained in different sections. Some sections had a relatively high central deflection, while some sections had a lower central deflection value. The primary reason for the differing deflection value was the thickness and stiffness of the pavement layer system. Some of the pavement sections had a thick surface layer resulted in a lower central defection. In contrast, some pavement had treated bases, and the stiff underlying subgrade resulting in deflection of low order. The resulting deflections are often assessed by various parameters as central deflection alone cannot provide the desired relationships. Therefore, entire area under the deflection bowls are utilized to capture the overall structural health of pavement layer systems. It is well observed that the central deflection provides the characteristic of the asphalt layer. In contrast, the deflection far from the plate denotes the characteristic effect of base and subbase layers.

5.1.1 Comprehensive Deflection Ratio (CDr)

The deflection ratio (D_r) has been widely utilized by various transportation agencies as it is a simple tool and takes into account of the deflection at 250 mm, given as equation 8.

$$D_r = D_{250}/D_o \quad [8]$$

where:

D_{250}=deflection at 250 mm offset.

However, such parameter does not cover the entire deflection bowl and provides a similar results to the central deflection. To overcome this shortcoming, a parameter referred to as the Comprehensive deflection ratio (CDr) was developed [2] [34]. Furthermore, the parameter is generated from the deflection at 600mm, and it takes into account the effect of the base and subbase layer. Equation 9 represents CDr.

$$CDr = D_{600}/D_0 \quad [9]$$

where:

D_{600}= deflection at 600mm offset

Various sections were examined with the newly developed CDr and Dr. It was found that Dr remains almost the same for the sections with varying central deflection, although fatigue cracking percentage was different between different pavement sections. Except in the case of CDr, the

values were different, and it indicates that CDr can be applied for any of the sections having a lower deflection values.

Figure 34 shows the comparison of the Dr and CDr for two sections (0124 & 0113) in the state of Arkansas. Sections are chosen in such a way that the materialistic properties of the pavement sections are similar. Similarly, the deflection is presented for the drop height 1(target load of 27 kN).

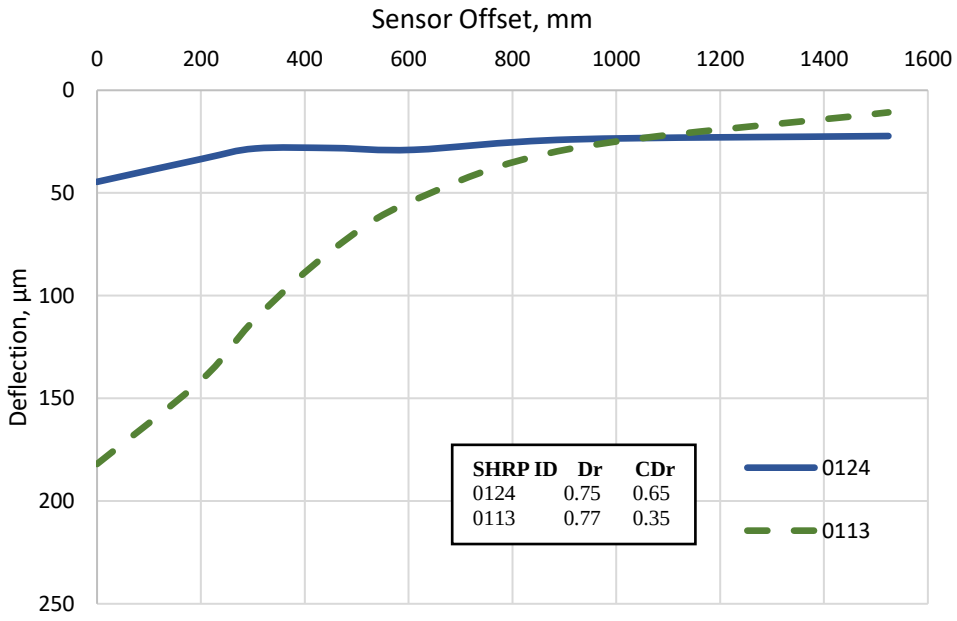

Figure 34. Comparison between Dr and CDr

The stiff pavement structures must have a higher deflection ratio, but on the contrary, both types of pavement structures had a similar Dr value, which is not valid. On the other hand, CDr showed a matching performance concerning the pavement types, which indicates the effectiveness of CDr in assessing the pavement conditions. Additionally, Figure 35 presents the plot between Do and CDr for the South-Central States, where a higher coefficient of determination is observed. The higher central deflection values resulted in a lesser CDr, while the lower deflection values resulted in higher CDr. The utilization of central deflection may be misleading for some sections. Therefore, it can be concluded that CDr can be a better tool to assess the pavement conditions than Do and Dr.

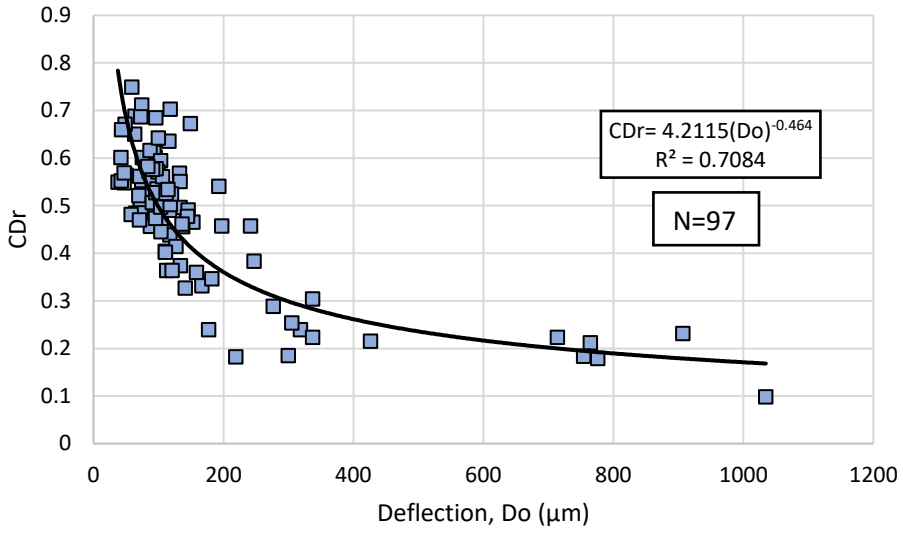

Figure 35. Relationship between Do and CDr for the South-Central State

5.1.2 Normalized Comprehensive Deflection Ratio (CDr')

CDr was calculated for all the sections of the South-Central States at all four drop heights under different drop loads (27 kN, 40kN, 53kN, and 70kN). 3D-Movesimulated deflection bowls are plotted for a section 0115 of Arkansas (Figure 36). It is observed that the slope of the deflection bowl was changing for different drop loads, moving far away from the center of the load plate, but the calculated CDr was the same for all the drop loads. However, variable drop loads must provide a different CDr values. Therefore, Normalized Comprehensive Deflection Ratio (CDr') was implemented for obtaining the effect of load change. The normalized deflection ratios for the same section were plotted, and it was found that a gradual shift occurred with the normalization of the central deflection ratio. CDr' had a strong correlation with the central deflection (Do), as presented in Figure 37. SHRP Section 0115 of Arkansas is reported to show the interpretation based on different target loads, as illustrated in Figure 38. The plots show a good relationship between all the three factors- Drop loads, Central Deflection, and Normalized Comprehensive Deflection Ratio (CDr'). Hence, CDr' can be considered as a more refined deflection-based parameter for assessing the structural condition of any pavement section.

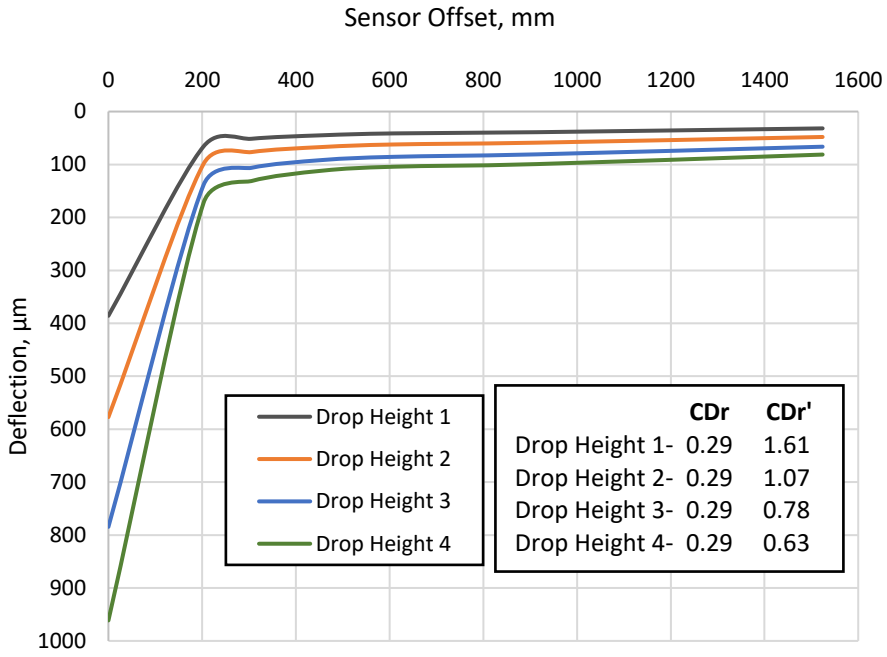

Figure 36. An illustration of the importance of CDr and CDr' based on AK SHRP 0115

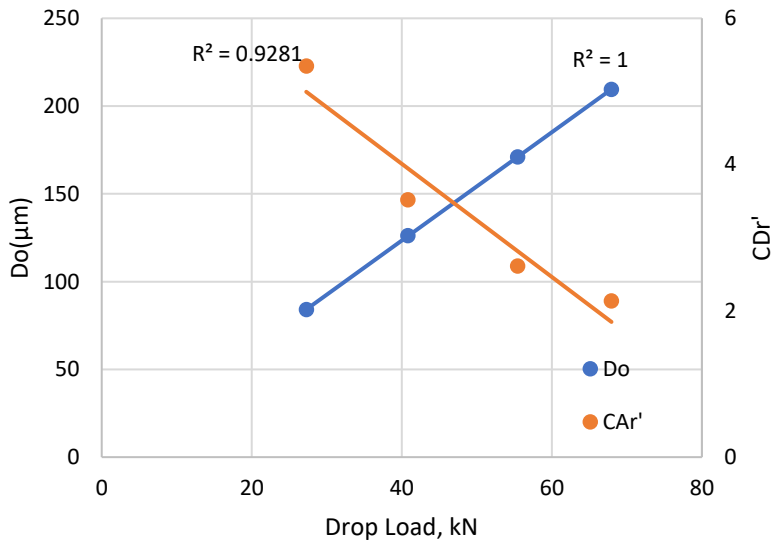

Figure 37. Sensitivity between Do, CDr' and Drop Load for AK SHRP section 0115

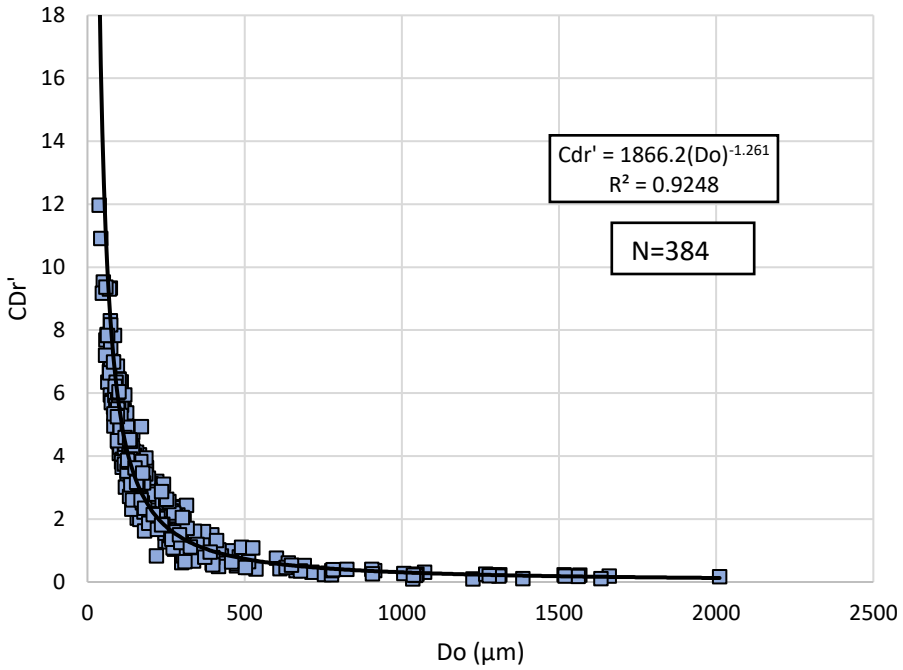

Figure 38. Relationship between normalized comprehensive deflection ratio (CDr') and central deflection (D0)

5.1.3 Comprehensive Area under Pavement Profile (CAPP)

It is observed from the previous section that CDr can be utilized, preferably in assessing the pavement conditions, but it only uses two deflection points. The data gathered from other offsets are never utilized. Therefore, to utilize all of the pavement deflection bowl data points, the area ratio concept was defined *(2)*, which was later updated for including deflections at regular intervals throughout the 900m length of the deflection sensors. Various deflections obtained from different offsets were combined with central deflection to provide important information on pavement structural capacity. And eventually, the area ratio parameter was updated to Comprehensive Area under Pavement Profile (CAPP) for representing the structural condition of pavement sections. Furthermore, this parameter was enhanced to cover the full pavement profile of 1500mm.

5.1.4 Comprehensive Area Ratio

A stiff pavement section is observed to have a minimum deflection. Likewise, deflection at a sensor far away from the center of the load plate will also have a minimum deflection. But in the case of a too stiff pavement section, deflection at all the sensors will be the same throughout the profile, and this assumption is equally crucial in determining the strength of the pavement. In this procedure, the area under the deflection bowl is divided into numerous subdivisions, where each subdivision will have an area as represented by the equation presented below. The trapezoidal area under the deflection bowl is considered in the analysis, as shown in equation 10.

$$CAPP = \left(\frac{1}{D0}\right) * \{203*\left(\frac{D0+D203}{2}\right) + 102*\left(\frac{D203+D305}{2}\right) + 152*\left(\frac{D305+D457}{2}\right) + 153*\left(\frac{D457+D610}{2}\right) + 304*\left(\frac{D610+D914}{2}\right) + 610*\left(\frac{D914+D1524}{2}\right)\} \quad [10]$$

Similarly, deflections for a strong pavement section measured at different sensor offsets would differ in minimum magnitude compared to the deflection at the center of the plate. A constant deflection is provided throughout the length (i.e., $D_0 = D_{203} = D_{305} = \ldots. = D_{1524}$) for a stiff pavement section. Equation 11 presents the Comprehensive Area under Pavement Profile CAPP of an imaginary pavement section deflection bowl. Figure 39 illustrates the difference between a rigid imaginary, strong and weak pavement sections based on CAr.

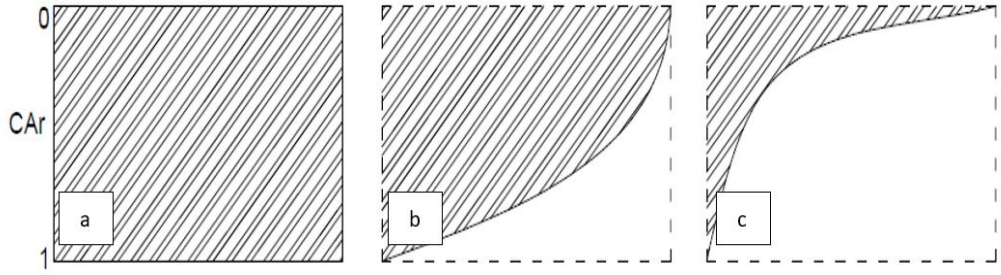

Figure 39. Pavement Section based on CAr: a) Imaginary Stiff Section, b) Strong Section, and c) Weak Section

$$CAPP = \left(\frac{1}{D0}\right) * \{203*\left(\frac{D0+D0}{2}\right) + 102*\left(\frac{D0+D0}{2}\right) + 152*\left(\frac{D0+D0}{2}\right) + 153*\left(\frac{D0+D0}{2}\right) + 304*\left(\frac{D0+D0}{2}\right) + 610*\left(\frac{D0+D0}{2}\right)\}$$

$$= 1524 \text{ mm}^2/\text{mm}. \quad [11]$$

Hence, a comprehensive area ratio (CAr) is developed, dividing the CAPP of the pavement section by the CAPP of imaginary pavement. Equation 12 represents the simplified formula for CAr. A strong section will have a bigger area than a weak section, and CAr will be less for a weak section. The weaker section could exhibit a CAr value of 0.1, while a strong section has this value of nearly 1.0.

$$CAr = \left(\frac{1}{D0}\right) * \{203*\left(\frac{D0+D203}{2}\right) + 102*\left(\frac{D203+D305}{2}\right) + 152*\left(\frac{D305+D457}{2}\right) + 153*\left(\frac{D457+D610}{2}\right) + 304*\left(\frac{D610+D914}{2}\right) + 610*\left(\frac{D914+D1524}{2}\right)\} / 1524 \quad [12]$$

Two SHRP pavement sections (0114 and 3071) of the state Arkansas were compared, as presented in Figure 40. It was observed that the imaginary rigid pavement area covered by SHRP section 0114 was less than the SHRP section 0115, and due to this reason, Car of 0.18 and 0.67 was found for section 0114 and 3071, respectively.

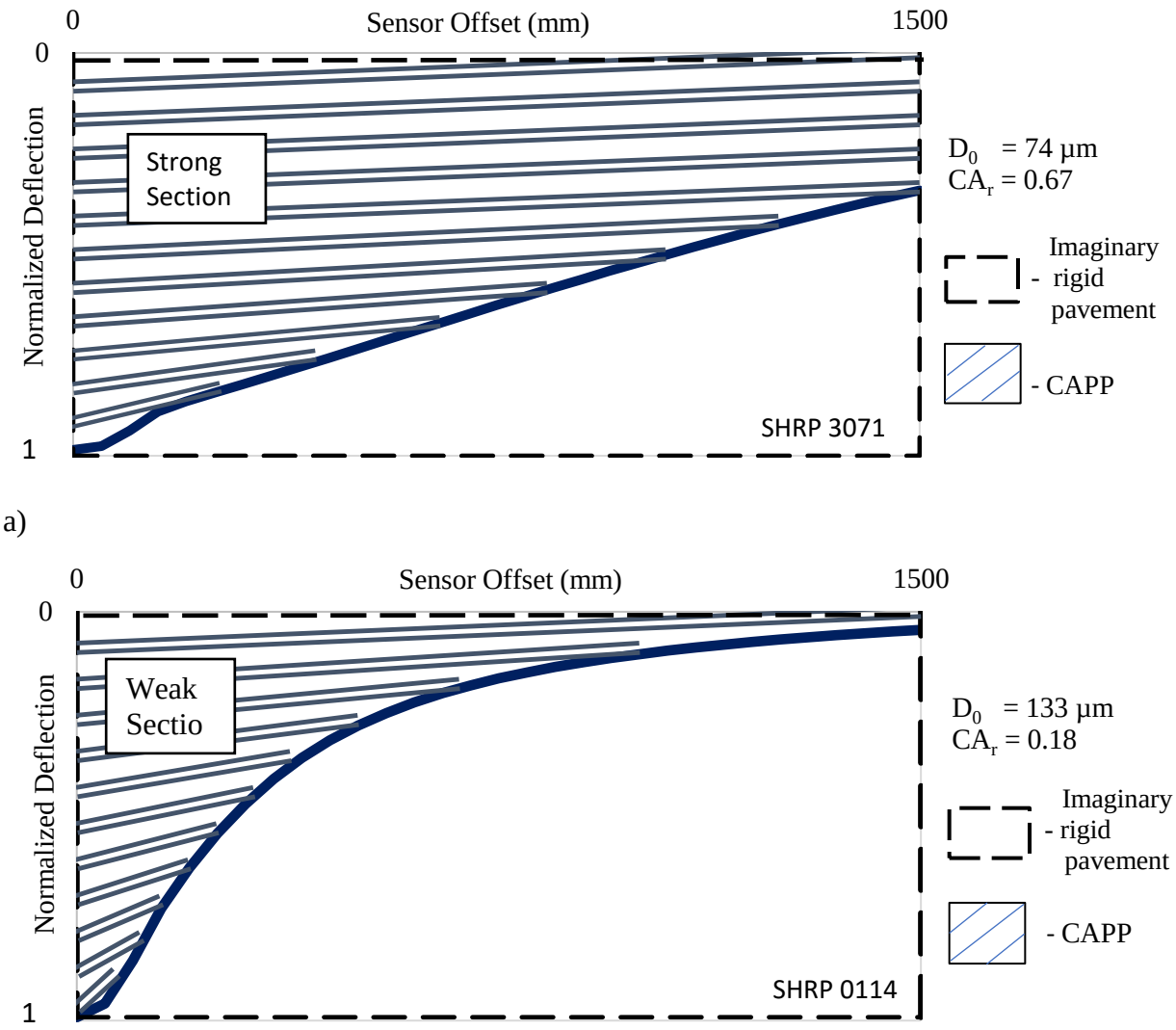

Figure 40. Normalized area of deflection profiles for SHRP sections: (a) 3071 and (b) 0114

5.1.5 Normalized Comprehensive Area Ratio (CAr')

The area ratio parameter provided a better approach for pavement structural assessment, although this parameter is does not take into account the different target load. Therefore, a combination of area ratio and central deflection is provided in an account to have the effect of different target loads reflected. The parameter was normalized by dividing the area ratio parameter by central deflection, and it was found that this procedure was very useful in assessing the structural capacity of flexible pavements (equation 13).

$$CAr' = \left(\frac{1}{D0*D0}\right) * \{203*\left(\frac{D0+D203}{2}\right) + 102*\left(\frac{D203+D305}{2}\right) + 152*\left(\frac{D305+D457}{2}\right) + 153*\left(\frac{D457+D610}{2}\right) + 304*\left(\frac{D610+D914}{2}\right) + 610*\left(\frac{D914+D1524}{2}\right)\} / 1524 \quad [13]$$

The area ratio could not effectively consider the effect of load changes. Different target load level was observed to be too minimum for differentiating the structural property of the pavement

sections. Figure 41 represents the deflection bowl observed for a section 0115 in Arkansas. A non-varying CAr was observed irrespective of the load levels, although variations in deflection were observed. The values suggest that the pavement was poor in structural performance.

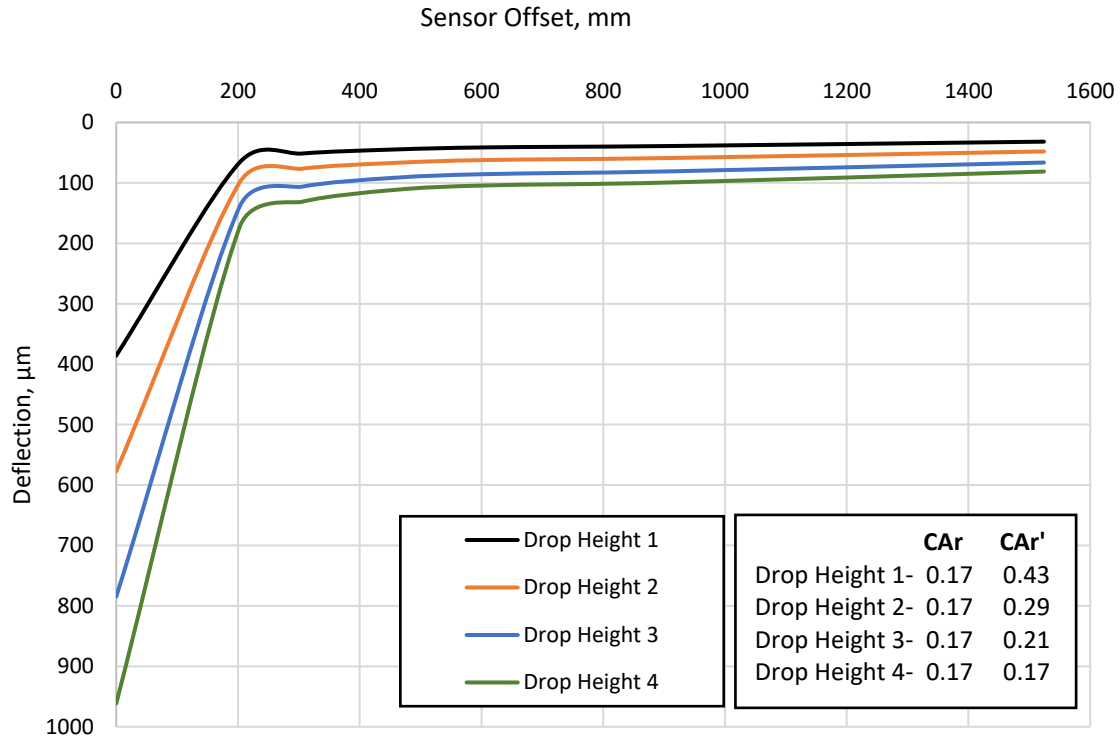

Figure 41. An illustration of the importance of CAr and CAr' based on AK SHRP 0115

It is evident that with different drop load levels, a pavement section must show a different response, but this was not done using CAr. However, the newly developed parameter Car' could account for the change in the pavement section as well as drop heights. It can be observed for section 0115 of Arkansas, CAr' varies from 0.43 to 0.17.

5.1.6 Relationship Between Comprehensive Area Ratio CAr' and Central Deflection Do

Central Deflection has always been the first parameter utilized while observing any response with FWD. Furthermore, it is vital to have a better relationship between CAr' and Do. A plot has been presented to illustrate the relationship between CAr' and Do. It is observed that there is a good relationship between CAr' and Do, which indicates that CAr' can be utilized as a parameter to assess the structural health condition of a pavement sections. The comprehensive area ratio parameter (CAr) does not account for the change in loading levels, although the central deflection was varied. Therefore, normalizing area ratio parameter via dividing CAr by Do prove to be effective with the change in loading level, and CAr' for different load levels can be plotted in a single graph (Figure 42).

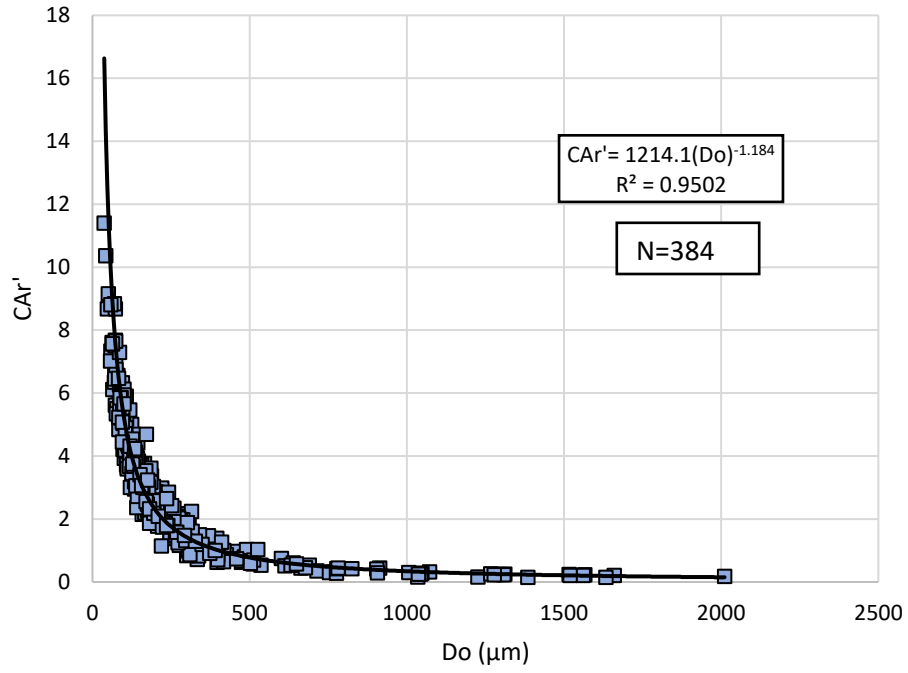

Figure 42. Relationship between CAr' and Do

Similarly, the variation between the CAr' and Do is plotted to obtain the relationship under four target load levels. Also, the structure of pavement sections remains the same in all the cases, but a variation was observed between all the target loads. SHRP Section 0115 of Arkansas is reported to show the interpretation based on different target loads, as presented in Figure 43. The plots show a good relationship between all the three factors- Drop loads, Central Deflection, and Comprehensive Area Ratio. Furthermore, the obtained relationships prove that the utilization of CAr' can be made at any drop load to assess the pavement performance. The load can be associated with the need of the users, which set forth the newly developed concept in generalizing the other load cases.

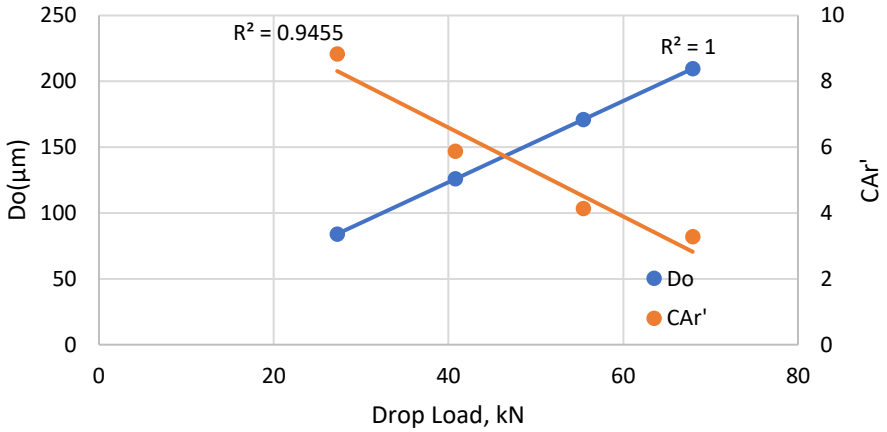

Figure 43. Sensitivity between Do, CAr' and Drop Load for AK SHRP 0115

It is observed that the parameter was sensitive to detect to the change in target load as similar to CAr'. Additionally, CAr' was compared to CDr' and both are well related (Figure 44), signifying that CDr' can represent the normalized comprehensive area ratio parameter. Hence, CDr' and CAr' can be considered as overall parameters for assessing the structural condition of any pavement section.

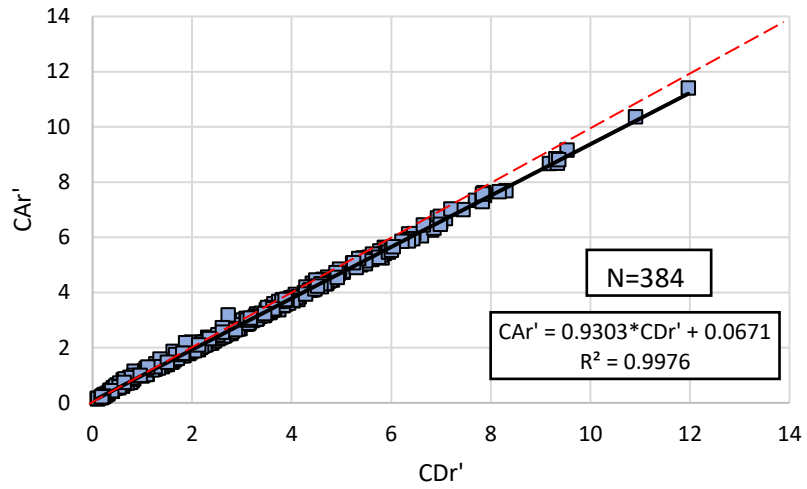

Figure 44. Relationship between normalized comprehensive deflection ratio (CDr') and normalized comprehensive area ratio (CAr')

5.1.7 Sensitivity of Normalized Comprehensive Area Ratio (CAr') and Normalized Comprehensive Deflection Ratio (CDr') to Asphalt Layer Thickness

Different pavement sections accounted for in this study had different asphalt layer thicknesses. The thickness ranged from 1.4 to 14.8 inches and the average thickness observed for all the 97 sections was 7 inches. Therefore, based on the average thickness, pavement sections were categorized into two groups. The first group has an average pavement section thickness greater than 7 inches while the second group beholds the pavement section less than 7 inches. The effect of thickness on the newly developed parameter was considered utilizing the 97 sections. Fifty pavement sections have a thickness greater than 7 inches, and they have the average Car' value of 3.32. On the other side, the relatively thin pavement sections have a lower value of Car' as 2.65. A similar trend was observed for the CDr' on the analyzed pavement section. A higher average Cdr' value of 3.53 was observed for the thicker pavement sections and a lower average CDr' value for the thinner pavement sections. The following charts (Figure 46) present the comparison following the thickness and developed parameters.

Car' and CDr' effectively account for the thickness of the HMA layer, which plays a significant role in the efficient performance of any pavement sections. It is important to note that the thinner section might not be weak, as the pavement weakness is mostly governed by the accumulated distresses. A categorization chart is developed concerning existing pavement conditions and discussed in the preceding chapters.

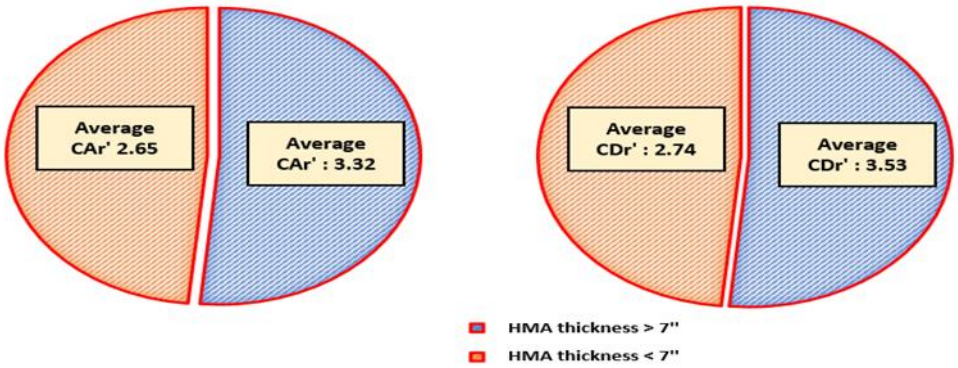

Figure 45. Average values of normalized comprehensive area ratio normalized comprehensive deflection ratio (CDr') based on asphalt layer thickness

5.2 Development of a Categorization Scale to Classify the Structural Capacity of Different Pavement Sections

5.2.1 Development of Normalized Comprehensive Area Ratio (CAr') scale based on observed Field Fatigue Cracking

Various deflection parameters were developed based on the simulated deflection bowls for 97 pavement sections of the South-Central States. Normalized Comprehensive Area Ratio (CAr') and Normalized Comprehensive Deflection Ratio (CDr') were effective and reliable parameters to assess the structural conditions of pavements structures. Furthermore, various distresses were compared to these newly developed parameters to develop a pavement overall health classification scale. Structural distresses, such as fatigue cracking, were thoroughly studied and correlated with such parameters. Fatigue cracking is the series of interconnected cracks developed due to the repeated traffic loadings and holds importance when the functioning of the pavement structure is studied. It was found that fatigue cracking, also referred to as alligator cracking, had a good sensitivity with the pavement performance *(50)*. Fatigue failure is often characterized as the area of occurrence in any pavement sections, and it is essential to know that the higher fatigue failure refers to a structurally weak section. Fatigue failure in one of the worst scenarios can lead to the reconstruction of a whole pavement section *(50)* and it is to the best interest to engineers to try to predict it.

The developed parameters were correlated with measured fatigue for categorizing and creating a scoring scale to rank the pavement sections. The relationship is shown in figure 47. Ninety-seven sections from the South-Central States were accounted for the generation of pavement ranking scale, and a coefficient of determination of greater than 0.7 was observed. The relationship between fatigue cracking and CAr' was found to be reliable as it encompasses different pavement structures throughout the South-Central states with a relatively high coefficient of determination. Furthermore, a pavement section with lesser CAr' exhibits a higher fatigue cracking extent as expected, proving the ability of the developed parameter to predict the conditions of the pavement structure effectively. Also, unlike the deflection ratio and pavement area ratio, the new scale distinguished the drop load effects, and the variations were observed based on different drop loads. An excellent pavement section concerning drop height 1 had the CAr' value of greater than 6, and a very good pavement section concerning drop height 4 has the CAr' of 2.4. This example signifies

that load-induced effects are accounted for in the newly developed scale. The following figure shows the newly developed scale based on the different drop heights. Each drop height and drop load can be easily matched with the traffic-induced pavement loading for the pavement performance prediction.

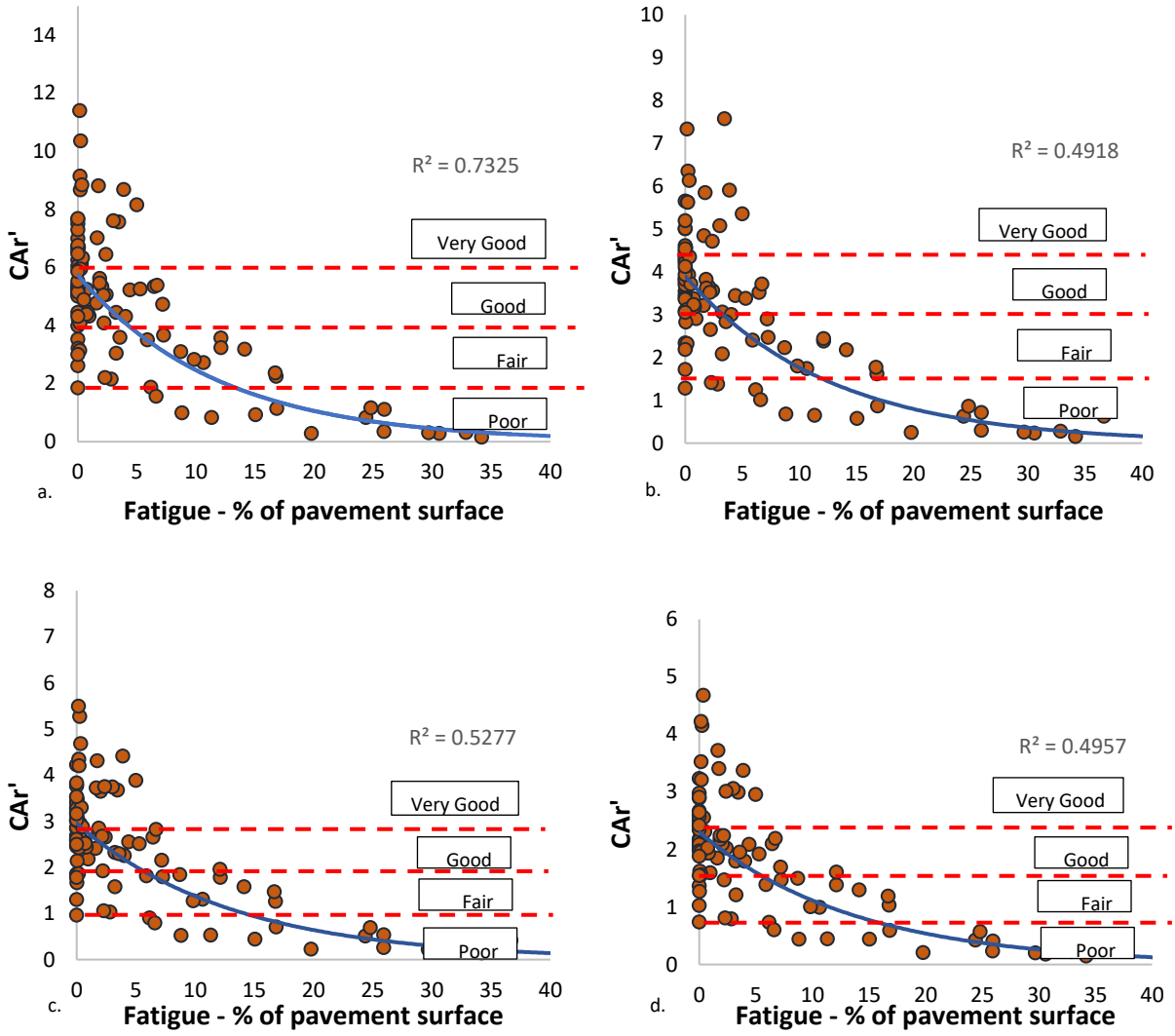

Figure 46. Pavement categorization scale based on fatigue cracking and comprehensive area ratio: a) Drop Height 1, b) Drop Height 2, c) Drop Height 3, and d) Drop Height 4

5.2.2 Classification of Pavement Sections based on Normalized Comprehensive Area Ratio (CAr')

A classification scale was developed based on the illustration in Figure 46 presented above, and the pavement sections are categorized into very good, good, fair, and poor pavement sections. The load levels at each drop height were utilized to generate the scale. An actual load in the pavement section can be matched with the target load level for effectively obtaining the resultant performance due to the prevalent traffic loadings. The developed scale is shown in the given Table 21.

Table 21. CAr' Range for different categories of the pavement structure

Drop Height	CAr' Range			
	Very Good	Good	Fair	Poor
27 kN (6,000 lbs)	>6.0	4.0-6.0	2.0-4.0	0-2.0
40 kN (9,000 lbs)	>4.5	3.0-4.5	1.5-3.0	0-1.5
53 kN (12,000 lbs)	>3.0	2.0-3.0	1.0-2.0	0-1.0
71 kN (16,000 lbs)	>2.4	1.6-2.4	0.8-1.6	0-0.8

The range of CAr' to be utilized in any flexible pavement is presented in the above table. The pavement section, which has CAr' values greater than six, is considered very good while the section having the CAr' in the range of 4-6, 2-4, and 0-2 can be categorized as good, fair, and poor section respectively under the target load of 27 KN. Each other target load has its own CAr' range. Furthermore, a validation can be presented utilizing the scale developed with four sections to compare the structural properties and pavement conditions. SHRP sections 0124, 0507, 4161, and AA63 of Oklahoma are being used in such comparisons. It is evident that section 0124 must be structurally sound due to its physical properties and lesser fatigue percentages. The following table compares different properties of the considered pavement sections in terms of elastic modulus, thickness, fatigue percentage, and CAr'. The differentiation is crucial as it provides basic knowledge in understanding the significance of developed pavement comprehensive area ratio categorization scales.

Table 22. Pavement sections comparison based on the new scale

Layers	SHRP Sections							
	0124		0507		4161		AA63	
	Elastic Modulus (Psi)	Thickness (inches)	Elastic Modulus (Psi)	Thickness (inches)	Elastic Modulus (Psi)	Thickness (inches)	Elastic Modulus (Psi)	Thickness (inches)
Asphalt Layer 1	957600	1.9	750400	1.7	557600	1.6	100000	1.8
Asphalt Layer 2	1149120	5.4	750400	8.4	557600	0.9	130000	9
Base (T)	515400	10.9			414000	7.6		
Base (UT)	100000	4.5	75000	9.4			8000	12
Subbase	15000	8						
Subgrade	13500	240	21500	240	21500	240	21500	240
Fatigue %	**0.34**		**6.45**		**9.83**		**25.93**	
CAr'	**8.84**		**5.92**		**2.82**		**2.11**	
Classification	**Very Good**		**Good**		**Fair**		**Poor**	

As presented in Table 22, it is observed that all the pavement systems are different due to its pavement structures. SHRP section 0124 comprises of 2 asphalt layers, treated and untreated base layers, with subbase and subgrade layers. Other sections 0507, 4161, and AA63 had two asphalt layers, base layers, and subgrade layers. Section 0124 has a lesser fatigue percentage, as well as higher stiffness modulus for all the layers leading to the categorization of the pavement in a very good class. The pavement sections 0507, 4161, and AA63 had a lower stiffness value with an increasing percentage of fatigue, and CAr' are reducing gradually. Therefore, the newly developed categorization scale is inclusive of the pavement sections properties as well as the fatigue distress occurrence. Hence, the developed classification scale is successful and reliable to include pavement practiced throughout.

Also, Figure 47 represents the classification of pavement in South-Central states with the newly developed scale and different colors represent different structural health conditions of the analyzed pavement structures.

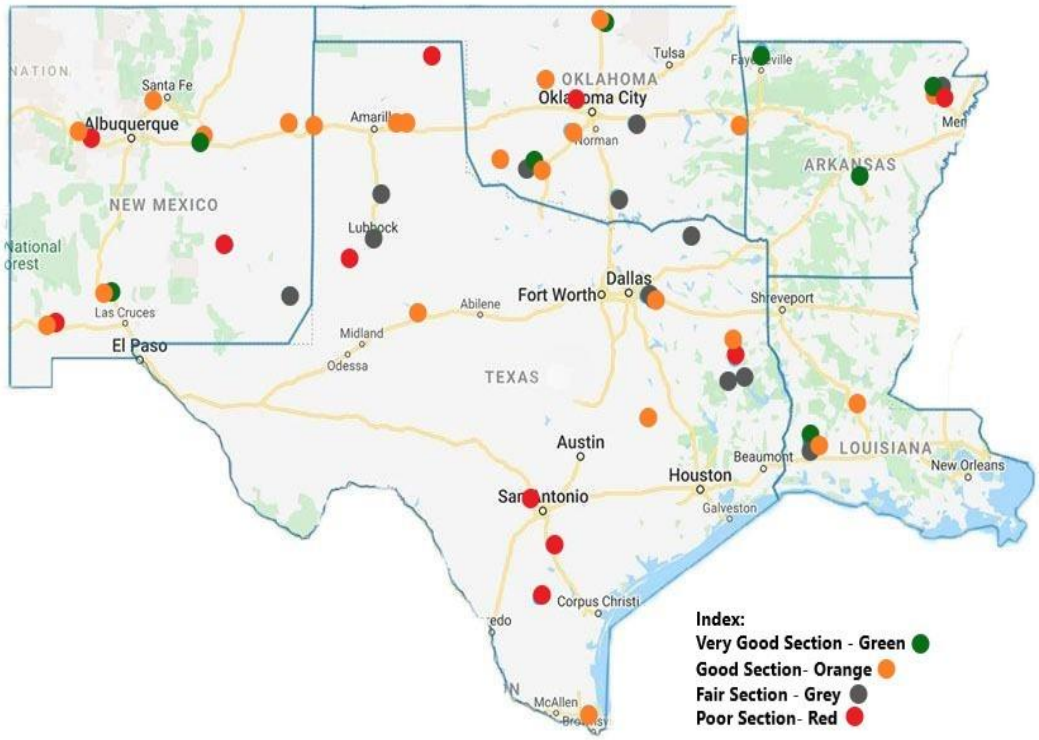

Figure 47. Classification of pavement structures with newly developed scale

A similar classification trend was observed for the developed CDr'. Each of the drop heights resulted in similar relationships as presented in CAr' vs. fatigue percentage. Figure 48 shows the relationship of CDr' with percentage fatigue of pavement surface at 27 kN targeted load. A higher coefficient of determination also suggests that both of the newly developed comprehensive deflection parameters can accurately assess the pavement conditions.

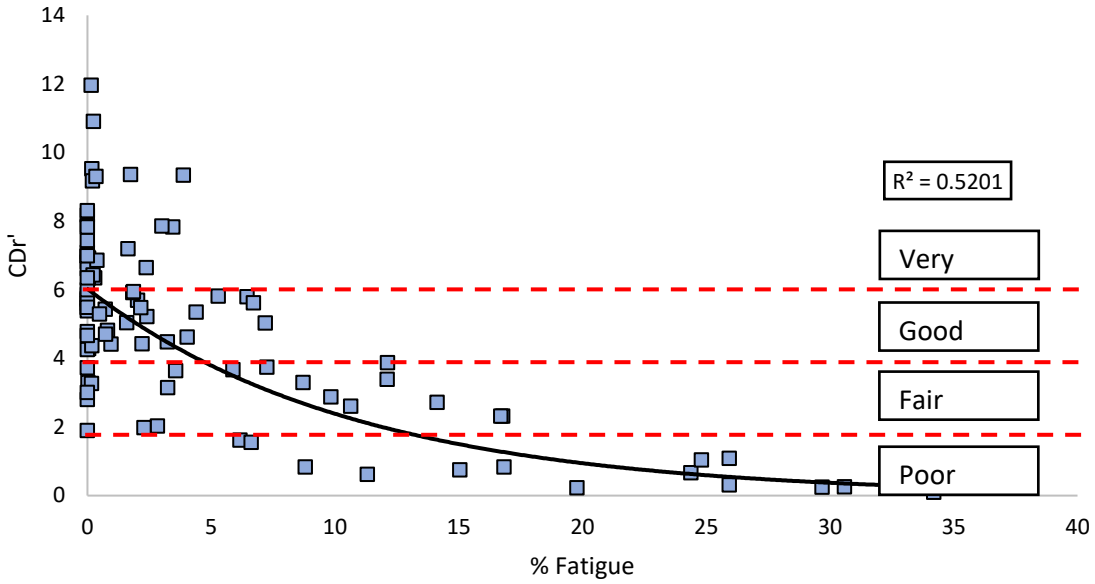

Figure 48. Categorization scale based on CDr' at drop height 1

Furthermore, some observations can be drawn from the newly developed scale regarding the classification of different pavement structures. Two pavement sections which are from the state of New Mexico (0106 and 1003) with zero fatigue percentage can be grouped into two ranking systems. This is since the newly developed classification system does not entirely look at the fatigue percentage and the various pavement structures. Section 0106 has a comparatively higher modulus of surface, base, subbase, and subgrade layer. On the other hand, lower moduli value and lower layer thickness were observed for the section 1003. This implies that CAr' and CDr' can assess the structural conditions of entire pavement sections as they are entirely based on pavement structural properties such as modulus. Additionally, different pavement structure categorization obtained despite having the same fatigue percentage can be explained concerning the tensile strain developed at the bottom of the asphalt layer. The 3D-Movesoftware package can predict tensile strain at the bottom of the HMA layer. The following Figure 49 shows the comparison of two sections and tensile strain developed for different drop loads.

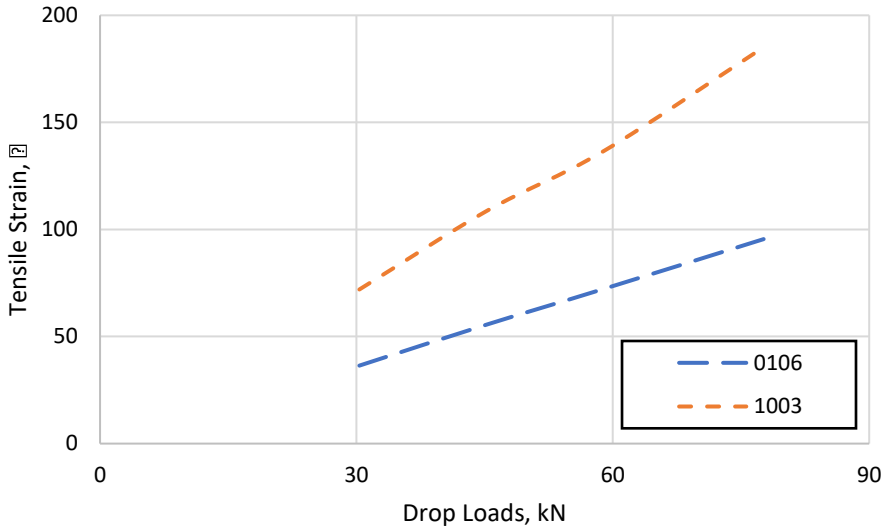

Figure 49. Strain comparison for two different sections based on drop loads

It is observed that the section, which has a higher tensile strain, developed falls under the poor pavement category. On other hand, the section with lesser developed tensile strain is assumed to have a higher performance and falls under the good pavement category. The stiffness of both asphalt and base layers can be directly related to the tensile strain developed at the bottom of the HMA layer. Therefore, the newly developed parameters (CAr' and CDr') and developed strain can be effectively utilized to assess the structural conditions of the pavement sections.

5.2.3 Relationship between tensile strain and developed comprehensive deflection ratio parameters

Bottom-up fatigue cracking in asphalt pavement structure is highly related to the developed tensile strain at the bottom of the HMA layer. Therefore, all the sections of the South-Central States were considered while developing the relationship between tensile strain and developed parameters. All four targeted loads were utilized in developing the relationship as well. A higher coefficient of determination was observed for the relationship between CAr,' and CDr' with the developed tensile strain. The relationships suggest a strong correlation between the developed parameter with the tensile strain at the bottom of the HMA layer. Figure 50, Figure 51 and equations 14 and 15 present the correlation between such factors.

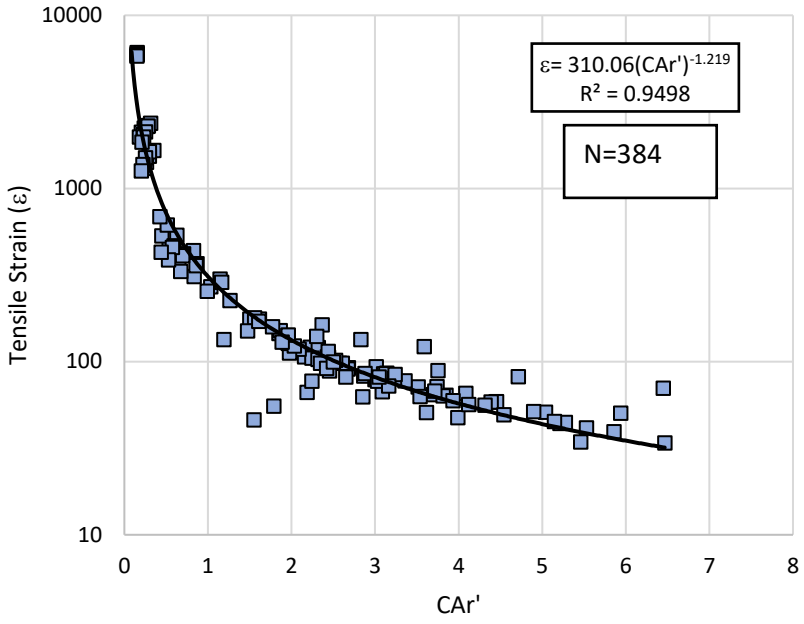

Figure 50. Relationship between tensile strain at the bottom of the HMA and Normalized Comprehensive Area Ratio (CAr')

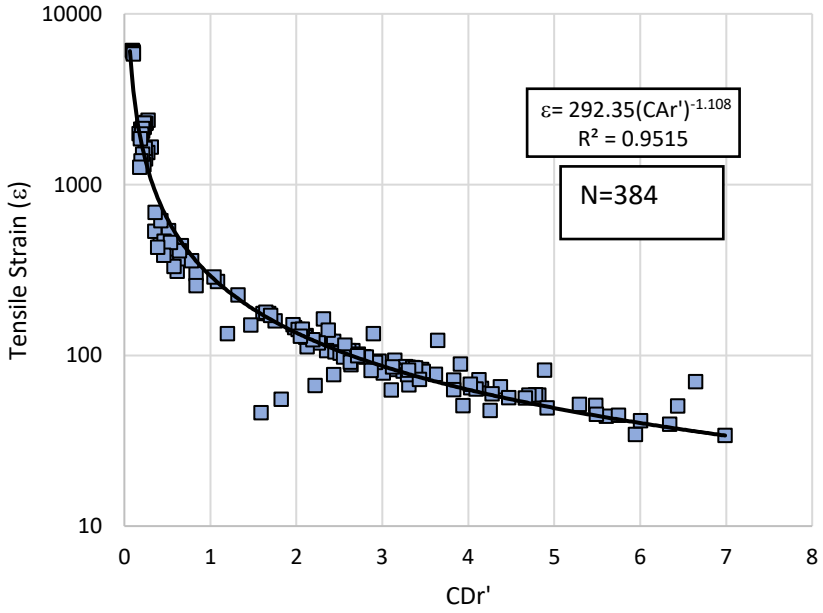

Figure 51. Relationship between tensile strain at the bottom of the HMA and Normalized Comprehensive Deflection Ratio (CDr')

$$\varepsilon = 310.06 * (CAr')^{-1.219} \quad [14]$$

$R^2 = 0.9498$

$$\varepsilon = 292.35 * (CDr')^{-1.108} \quad [15]$$

$R^2 = 0.9515$

where:

ε= tensile strain developed at the bottom of HMA layer
CAr' = Normalized Comprehensive Area Ratio
CDr'= Normalized Deflection Ratio

5.2.4 Prediction of remaining service life based on fatigue failure

In the previous section, it is observed that there is a strong correlation between the tensile strain at the bottom of the HMA layer and the developed comprehensive deflection ratio parameters. Prediction of the remaining service life of flexible pavement structure can be obtained utilizing the tensile strain developed based on the empirical pavement design fatigue model, which utilizes the strain and the stiffness of the asphalt layer as presented in equation 16 *(51)* . It is observed that the number of cycles to failure and tensile strain is inversely proportional; hence, higher strain results in a lower load cycle until failure. Load cycles to failure can be utilized in predicting the efficiency of pavement when loaded with repeated traffic loads.

$$N_f = 0.0795 * (1/\varepsilon)^{3.291} * (1/E)^{0.854} \quad [16]$$

where:

N_f = number of load repetitions to failure

ε = tensile strain developed at the bottom of HMA

E = modulus of the asphalt layer

Equation 9 can be utilized in calculating the Nf of all the considered sections, and it is observed that the number of cycles to failure was well related to CAr' and CDr.' The relationship presented in Figure 52 and Figure 53 provide a strong correlation between the developed CAr' and CDr' parameter and remaining fatigue life of the studied asphalt pavement structures. Furthermore, equations 17 and 18 are formulated to predict the remaining service life of flexible pavement based on CAr' and CDr'.

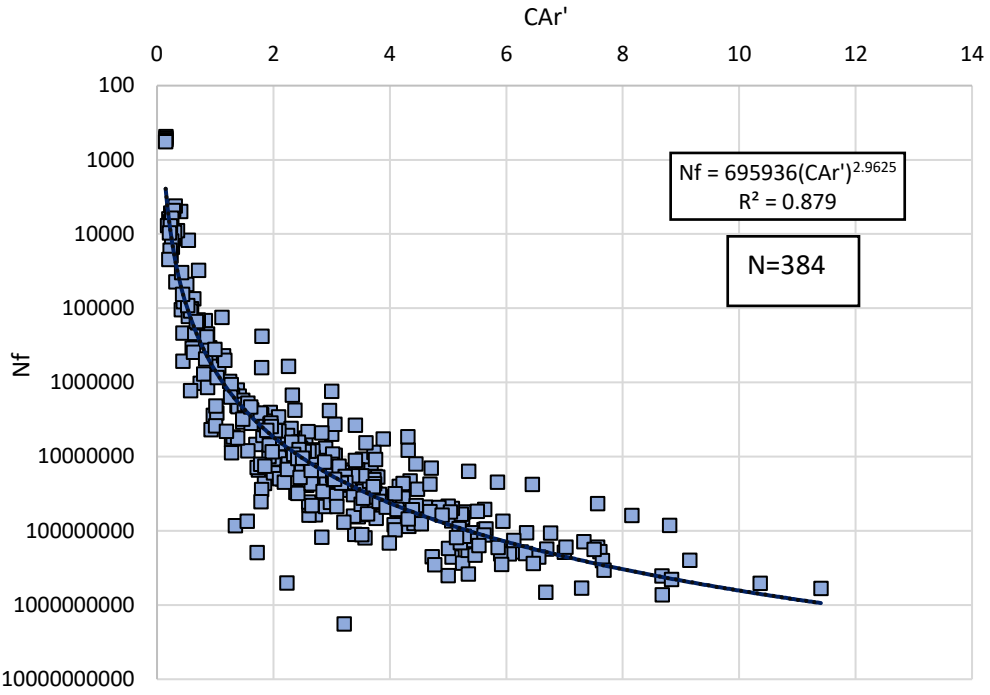

Figure 52. Relationship between Nf and Normalized Comprehensive Area Ratio (CAr')

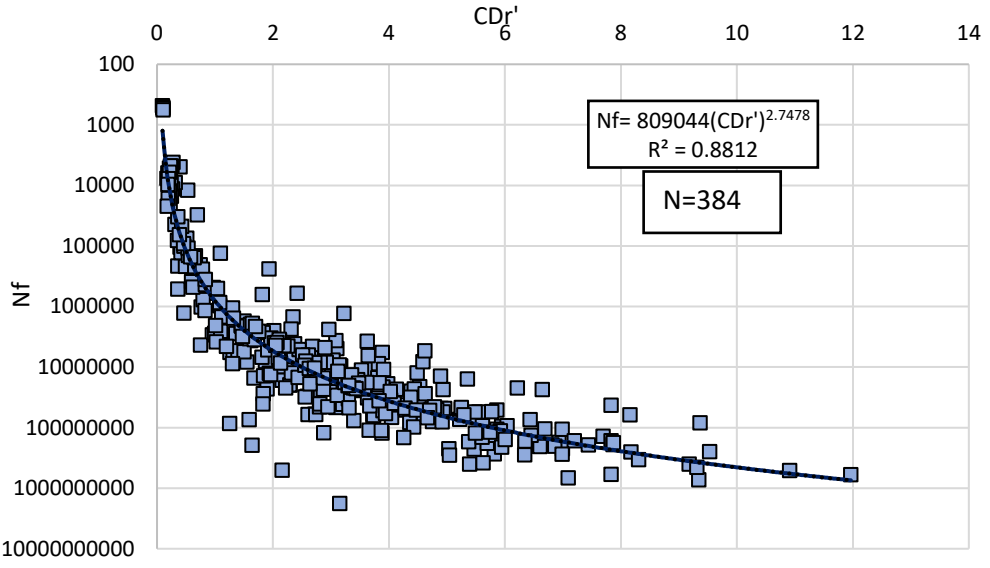

Figure 53. Relationship between Nf and Normalized Comprehensive Deflection Ratio (CDr')

$N_f = 695936 * CAr'^{(2.9625)}$ [17]
$R^2 = 0.879$

$N_f = 809044 * CDr'^{(2.7478)}$ [18]
$R^2 = 0.8812$

where:

N_f = number of load cycles to failure
CAr' = normalized comprehensive area ratio
CDr' = normalized comprehensive deflection ratio

Therefore, a significant relationship which can easily predict the remaining fatigue service life of a pavement section is developed. The predictive relationship will serve as an essential tool for assessing the pavement conditions by transportation agencies. The developed deflection bowl parameter (CAr' and CDr'), which can account for the whole of the deflection bowl, are more reliable than the previously followed parameter based on single deflection points.

6. CONCLUSIONS

The utilization of the FWD tests for assessing the pavement conditions has been practiced for decades. FWD surface deflection bowl data is often utilized to identify the structural condition of the flexible pavement sections. However, there are only a few simple procedures to identify the pavement sections utilizing the FWD data. The previously developed methods were based on the single deflection point measured at a certain distance from the load plate. For example, the comprehensive deflection ratio (CDr) was developed at 600mm from the center of the load plate and was correlated with central deflection (Do). The utilization of a single deflection may result in an erroneous evaluation as the entire deflection bowls are not considered. Therefore, in this study, 97 LTPP pavement sections and their respective simulated surface deflection bowl data are utilized to come across a simplified deflection-based method. ANSYS and 3D-MoveAnalysis software packages were utilized in simulating the actual FWD test. Both software packages provided similar deflection bowls results.

Then after utilizing simulated deflection bowls, an area ratio parameter was introduced for the evaluation of the entire pavement structure. The area ratio parameter is the function of the whole deflection bowl (up to 1500mm offsets). Imaginary stiff pavement having a uniform deflection is compared to the actual field measured deflection for calculating the area of deflection bowls. The respective area-based relationship is termed as a comprehensive area ratio (CAr). CAr' is a further normalization to reflect the response of pavement structures with different load variations. The normalization was achieved by dividing the CAr' by the central deflection (Do), referred to as normalized comprehensive area ratio (CAr'). Eventually, a classification scale is developed to categorize the pavement section in very good, good, fair, and weak pavement sections.

Similarly, a tensile strain (ε) developed at the bottom of the HMA layer strongly correlates with normalized comprehensive area ratio (CAr'). The following equation shows the relation of tensile strain with CAr'.

$$\varepsilon = 310.06 * (CAr')^{-1.219}$$
$$R^2 = 0.9498$$

Furthermore, the remaining service life of flexible pavement was calculated based on the MEPDG [51] fatigue failure model. The following equation presents a well-related relationship between Nf and CAr' for the entire studied South-Central States.

$$N_f = 695936 * CAr'^{(2.9625)}$$
$$R^2 = 0.879$$

Therefore, the pavement section's structural capacity at the South-Central States network level can be easily evaluated using the area ratio parameter (CAr'). The developed parameter can be a beneficial tool for transportation agencies to decide on pavement structural condition. The most suitable pavement maintenance and rehabilitation technique can be easily selected based on the developed procedure. The developed area ratio parameter can be an efficient tool for network-level analysis of flexible pavement structures based on FWD data. The parameter is created to utilize the abundant FWD surface deflection bowl data obtained by various DOTs and are processed as received. Temperature corrections and hard rock effect corrections may refine the correlation obtained with multiple factors. The utilization of these corrections is highly recommended for further study.

REFERENCES

1. Smith, K. D., J. E. Bruinsma, M. J. Wade , K. Chatti , J. M. Vandenbossche and H. T. Yu. Using Falling Weight Deflectometer Data with Mechanistic-Empirical Design and Analysis, Volume I: Final Report, Applied Pavement Technology Inc., Illinois, 2017.
2. Souliman, M., S. Romanoschi, S. Dessouky, K. Loganathan and M. Isied. Simplified Approach for Structural Evaluation of Flexible Pavements at the Network Level, Transportation Consortium of South-Central States (Tran-SET), 2018.
3. Pavement Interactive, Network Level Approach to Pavement Management. [Online]. Available: https://pavementinteractive.org/reference-desk/pavement-management/overview/network-level-approach-to-pavement-management/. [Accessed 11 2020].
4. Vij G. and P. Kumar. Non-Destructive Testing Methods in Highway Engineering. Indian Road Congress, 2004.
5. Wilke P. W. Network Level Structural Evaluation withRolling Wheel Deflectometer. 9th International Conference on Managing Pavement Assets, 2015.
6. Stubstad, R., R. Carvalho, R. Briggs, and Seleznev. Simplified Techniques for Evaluation and Interpretation of Pavement Deflections for Network-Level Analysis: Guide for Assessment of Pavement Structure Performance for PMS Applications, 2012.
7. Hossain, A. M. and J. P. Zaniewski. Characterization of Falling Weight Deflectometer Deflection Basin. Transportation Research Record 1293.
8. Haas, R., W. Hudson and J. Zaniewski, Modern pavement management, Malamar, Florida.: Krieger Press, 1994.
9. Haas, R., R. Hudson and S. Tighe. Maximizing customer benefits as the ultimate goal of pavement management," in 5th International Conference on Managing Pavements, Washington, 2001.
10. Wimsatt, A. J. Direct Analysis Methods for Falling Weight Deflectometer Deflection Data, Transportation Research Record 1655.
11. Kim Y. R. and H. Park, Use Of Falling Weight Deflectometer Multi-Load Data for Pavement Strength Estimation, North Carolina Department of Transportation, Raleigh, 2002.
12. Zhang, Z., G. Claros, L. Manuel and I. Damnjanovic. Development of Structural Condition Index to Support Pavement Maintenance and Rehabilitation Decisions at Network Level, Transportation Research Record 1827, no. 03-4278.
13. S. T., Incorporating a Structural Strength Index into the Texas Pavement Evaluation System, Research Report 409 – 3F, Texas Transportation Institute, 1988.
14. Horak, E. and S. Emery. Falling Weight Deflectometer Bowl Parameters as Analysis Tool for Pavement Structural Evaluations. 22nd Australian Road Research Board (ARRB) International conference, Brisbane, Australia, 2006.
15. Aavik, A. and O. Talvik. Use of Falling Weight Deflectometer (FWD) Measurement Data For Pavement Structural Evaluation And Repair Design. Faculty of Environmental Engineering Vilnius Gediminas Technical University - The 7th International Conference, Lithuania, 2008.
16. Kavussi, A., M. Abbasghorbani, F. M. Nejad and A. B. Ziksari. A new method to determine maintenance andrepair activities at network-level pavement management using falling weight

deflectometer. Journal of Civil Engineering and Management, vol. 23, no. 3, pp. 338-346, 2017.
17. Gedafa, D., A., M. Hossain, R. Miller and T. Van. Estimation of remaining service life of flexible pavements from surface deflections. *Journal of Transportation Engineering*, vol. 136, no. 4, pp. 342-352, 2010.
18. Gedafa, D., M. Hossain, R. Miller and T. Van. Network-level flexible pavement structural evaluation. *International Journal of Pavement Engineering*, vol. 15, no. 4, pp. 309-322, 2014.
19. Flora, W. Development of a structural index for pavement management: An exploratory analysis, M.S. thesis, Purdue University, 2009.
20. Bryce, J., G. Flintsch, S. Katicha and B. Diefenderfer. Developing a Network-Level Structural Capacity. *Journal of Transportation Engineering*, 2013.
21. Chang, J.-R., J.-D. Lin , W.-C. Chung and D.-H. Chen. Evaluating the Structural Strength of Flexible Pavements in Taiwan Using the Falling Weight Deflectometer. *International Journal of Pavement Engineering*, 2010.
22. Aavik, A., P. Paabo and T. Kaal. Assessment Of Pavement Structural Strength by the Falling Weight Deflectometer, *The Baltic Journal of Road And Bridge Engineering*, vol. 1, no. 4, pp. 193-199, 2006.
23. Romanoschi, S. and J. B. Metcalf. Simple Approach to Estimation of Pavement Structural Capacity. Transportation Research Record 1652.
24. Nazzal, M. D. M. Y. Abu-Farsakh, K. Alshibli and L. Mohammad. Evaluating the Light Falling Weight Deflectometer Device for In Situ Measurement of Elastic Modulus of Pavement Layers. Transportation Research Record: Journal of the Transportation Research Board, pp. 13-22, 2016.
25. Alland, K., N. Bech and J. M. Vandenbossche. Interpreting Falling Weight Deflectometer (FWD) Data (for Asphalt and Concrete Pavements). Pennsylvania Department of Transportation, 2018.
26. Plati, C., A. Loizos and K. Gkyrtis. Integration of non-destructive testing methods to assess asphalt pavement thickness. NDT and E International, 2020.
27. Al-Khoury, R., A. Scarpas, C. Kasbergen and J. Blaauwendraad. Dynamic Interpretation of Falling Weight Deflectometer Test Results Spectral Element Method.
28. Elbagalati, O., M. Elseif, K. M. A. Gaspard and Zha. Prediction of In-Service Pavement Structural-Capacity Based on Traffic-Speed Deflection Measurements. *Journal on Transportation Engineering*, 2016.
29. Horak, E., A. Hefer and J. Maina, Determination of Pavement Number for Flexible Pavements Using FWD Deflection Bowl Information. Proceedings of the 34th Southern African Transport Conference (SATC 2015), 2015.
30. Ferne, B., P. Langdale, N. Round and Fairc. Development of a calibration procedure for the U.K. Highways Agency Traffic-Speed Deflectometer. Transportation Research Board, 2009.
31. Ganji, V., K. Tabrizi and M. Frabizzio. Utilization of Falling Weight Deflectometer for Project Sectionalization. Applications of Advanced Technology in Transportation.
32. Saleh, M. Simplified Approach for Structural Capacity Evaluation of Flexible Pavements at the Network Level. *International Journal of Pavement Engineering*, 2014.

33. Saleh, M. Utilization of the Deflectograph Data to Evaluate Pavement Structural Condition of the Highway Network,2015.
34. Saleh, M. A Mechanistic Empirical Approach for the Evaluation of the Structural Capacity and Remaining Service Life of Flexible Pavements at the Network Level, NRC Research Press, 2016.
35. Loganathan, K., M. M. Isied, A. M. Coca, M. Souliman, S. Romanoschi and S. Dessouky, Development of comprehensive deflection parameters to evaluate the structural capacity of flexible pavements at the network level. International Journal of Pavement Research and Technology, pp. 1-9, 2019.
36. Loganathan, K., M. M. Isied, A. M. Coca, M. I. Souliman, S. Romanoschi and S. Dessouky, estimated remaining fatigue life of flexible pavements based on the normalized comprehensive area ratio deflection parameter, *Canadian Journal of Civil Engineering*, vol. 47, no. 5, pp. 546-555, 2020.
37. Ghanizadeh, A. R. and A. Ziaie. NonPAS: A Program for Nonlinear Analysis of Flexible Pavements. *International Journal of Integrated Engineering*, vol. 7, no. 1, pp. 21-28, 2015.
38. Tarefder, R. A., and M. U. Ahmed, Modeling of the FWD Deflection Basin to Evaluate Airport Pavements, International Journal of Geomechanics, 2014.
39. Fernandes, J., A. A. Paixão, S. Fontul and E. Fortu, The Falling Weight Deflectometer: Application to Railway Substructure Evaluation, Proceedings of the First International Conference on Railway Technology: Research, Development and Maintenance, 2012, Lisbon.
40. Hamim, A., N. I. M. Yusoff, H. Ceylan , S. A. P. Rosyidi and A. El-Shafie. Comparative study on using static and dynamic finite element models to develop FWD measurement on flexible pavement structures. *Construction and Building Materials*, vol. 176, pp. 583-592, 2018.
41. Tutumluer, E., O. Pekcan and J. Ghaboussi. Nondestructive Pavement Evaluation Using Finite Element Analysis Based Soft Computing Models, USDOT Region V Regional University Transportation Center, 2009.
42. Maoun L., and H. Wang. Prediction of Asphalt Pavement Responses from FWD Surface Deflections Using Soft Computing Methods. Journal of Transportation Engineering, vol. 144, no. 2, 2018.
43. Federal Highway Administration. Introduction to The LTPP Information Management System (IMS) June 2020. [Online]. Available: https://www.fhwa.dot.gov/publications/research/infrastructure/pavements/ltpp/reports/03088/01.cfm
44. Schmalzer, P. N. LTPP Manual for Falling Weight Deflectometer Measurements, Version 4.1, Federal Highway Administration, 2006.
45. Miller, J. and W. Bellinger, Distress Identification Manual for the Long-Term Pavement Performance Program, FHWA-HRT-13-092, USDOT, 2014.
46. Siddharthan, R. V., J. Yao and P. Sebaaly, Pavement strain from moving dynamic 3D load distribution, Journal of Transportation Engineering, 1998.
47. Liu, P., Q. Xing, Y. Dong , W. Dawei , M. Oeser and S. Yuan, Application of Finite Layer Method in Pavement Structural Analysis, Applied Sciences, 2017.

48. Huang, J., X. Pan, S. Dai and Y. Cai. FEM analysis of dynamic behavior of asphalt pavement structure weakened by grassroots with account of hydraulic and vehicle load coupling effects. 4th Global Conference on Materials Science and Engineering, 2015.
49. ANSYS, INC, Fundamental FEA Concepts- A Guidebook for the Use and Applicability of Workbench Simulation Tools.
50. Cui, P., Y. Xiao, M. Fang, Z. Chen, M. Yi and M. Li. Residual Fatigue Properties of Asphalt Pavement after Long-Term Field Service. Materials, vol. 11(6), no. 892, 2018.
51. Ara Inc., Eres Consultants Divisions. Guide for Mechanistic Pavement Design for New and Rehabilitated Pavement Structures (NCHRP 1-37A). National Co-operative Highway Research Program, 2004.

APPENDIX A: PAVEMENT SECTIONS AND THEIR GPS LOCATIONS

State of Arkansas

STATE_CODE	STATE_CODE_EXP	SHRP_ID	LATITUDE	LONGITUDE
5	Arkansas	0113	35.7447319	-90.57986
5	Arkansas	0114	35.74198914	-90.57984
5	Arkansas	0115	35.73757935	-90.57984
5	Arkansas	0116	35.73484039	-90.57979
5	Arkansas	0117	35.73950958	-90.57985
5	Arkansas	0120	35.71931076	-90.57971
5	Arkansas	0122	35.72439957	-90.57977
5	Arkansas	0123	35.72753906	-90.57977
5	Arkansas	0124	35.72945023	-90.57983
5	Arkansas	A607	34.43062973	-92.19396
5	Arkansas	3071	36.26721954	-94.15001

State of Louisiana

STATE_CODE	STATE_CODE_EXP	SHRP_ID	LATITUDE	LONGITUDE
22	Louisiana	0113	30.3668499	-93.20032
22	Louisiana	0115	30.36041069	-93.20024
22	Louisiana	0116	30.35848999	-93.2003
22	Louisiana	0117	30.36236954	-93.20026
22	Louisiana	0118	30.35545921	-93.20023
22	Louisiana	0119	30.33904076	-93.2001
22	Louisiana	0121	30.34358978	-93.20016
22	Louisiana	0122	30.34633064	-93.20016
22	Louisiana	0123	30.34845924	-93.20016
22	Louisiana	0124	30.35243988	-93.20019
22	Louisiana	3056	30.9751091	-92.29541

State of New Mexico

STATE_CODE	STATE_CODE_EXP	SHRP_ID	LATITUDE	LONGITUDE
35	New Mexico	0103	32.67758942	-107.07565
35	New Mexico	0104	32.67744064	-107.07774
35	New Mexico	0106	32.6771698	-107.08195
35	New Mexico	0108	32.67692184	-107.08607
35	New Mexico	0110	32.67644882	-107.0933
35	New Mexico	0111	32.67631149	-107.09541
35	New Mexico	0112	32.67610931	-107.09897
35	New Mexico	0508	32.20103836	-108.26075
35	New Mexico	0802	32.19353867	-108.29852
35	New Mexico	1003	33.38261032	-104.73346
35	New Mexico	1005	35.50965118	-106.2387
35	New Mexico	1112	32.63343811	-103.51941
35	New Mexico	2118	35.1728096	-103.48414
35	New Mexico	6035	35.0750618	-107.65322
35	New Mexico	6401	35.03593826	-107.48025
35	New Mexico	AA01	34.98873138	-105.23389
35	New Mexico	AA02	34.98892975	-105.23792
35	New Mexico	AA03	34.98931885	-105.24598

State of Oklahoma

STATE_CODE	STATE_CODE_EXP	SHRP_ID	LATITUDE	LONGITUDE
40	Oklahoma	0115	34.63367081	-98.69167
40	Oklahoma	0117	34.63404846	-98.68867
40	Oklahoma	0120	34.63599014	-98.67161
40	Oklahoma	0122	34.63476181	-98.68243
40	Oklahoma	0123	34.63690948	-98.664
40	Oklahoma	0124	34.63726044	-98.66103
40	Oklahoma	0160	34.6316185	-98.70947
40	Oklahoma	0502	34.6373291	-98.66239
40	Oklahoma	0504	34.63414001	-98.69014
40	Oklahoma	0505	34.63352966	-98.6953
40	Oklahoma	0507	34.63444901	-98.68716
40	Oklahoma	0606	36.7035408	-97.34597
40	Oklahoma	0607	36.70898056	-97.34588
40	Oklahoma	0608	36.70661926	-97.34595
40	Oklahoma	1015	35.19324112	-96.67488
40	Oklahoma	4086	35.07572174	-97.96171
40	Oklahoma	4087	34.63756943	-99.28864
40	Oklahoma	4161	34.11571121	-97.0396
40	Oklahoma	4163	35.84162903	-98.47516
40	Oklahoma	6010	35.12530899	-94.56988
40	Oklahoma	AA62	35.50799942	-97.81493
40	Oklahoma	AA63	35.5079689	-97.82235

State of Texas

STATE_CODE	STATE_CODE_EXP	SHRP_ID	LATITUDE	LONGITUDE
48	Texas	1046	35.20759964	-101.34516
48	Texas	1047	35.20766068	-101.17967
48	Texas	1049	31.65924072	-94.67828
48	Texas	1056	36.19438171	-100.70943
48	Texas	1068	33.50471878	-95.58941
48	Texas	1069	32.61717987	-96.42596
48	Texas	1076	33.16707993	-102.28275
48	Texas	1093	28.77722931	-98.30895
48	Texas	1111	33.53144073	-101.80471
48	Texas	1113	31.95767021	-94.7002
48	Texas	1116	31.89281082	-94.68111
48	Texas	2172	32.36639023	-100.99145
48	Texas	2176	34.16527176	-101.70905
48	Texas	3669	31.32793045	-94.78652
48	Texas	3679	31.37203979	-94.50556
48	Texas	3729	26.0866394	-97.5844
48	Texas	3835	30.73419952	-96.43423
48	Texas	6079	35.18151093	-103.03008
48	Texas	9005	29.51679993	-98.721
48	Texas	A502	32.61423111	-96.41357
48	Texas	A504	32.61339951	-96.40476
48	Texas	A505	32.61339951	-96.3972
48	Texas	A507	32.61339951	-96.40186
48	Texas	A508	32.61363983	-96.40928
48	Texas	B310	32.62041855	-96.43343
48	Texas	B320	32.61927032	-96.43085
48	Texas	D310	32.37173843	-100.9831
48	Texas	D320	32.37023163	-100.98542
48	Texas	D330	32.36431885	-100.99456
48	Texas	D350	32.36296082	-100.99666
48	Texas	M310	27.93181038	-98.55456
48	Texas	M320	27.93368912	-98.55273
48	Texas	M330	27.93512917	-98.55131
48	Texas	M340	27.93656921	-98.5499
48	Texas	M350	27.93839073	-98.54814

APPENDIX B: FWD TEST AND 3D-MOVEANALYSIS DEFLECTION BOWL SIMULATIONS

Note: Y-axis range is considered constant to distinguish the difference in deflection between four drop heights.

State of Arkansas

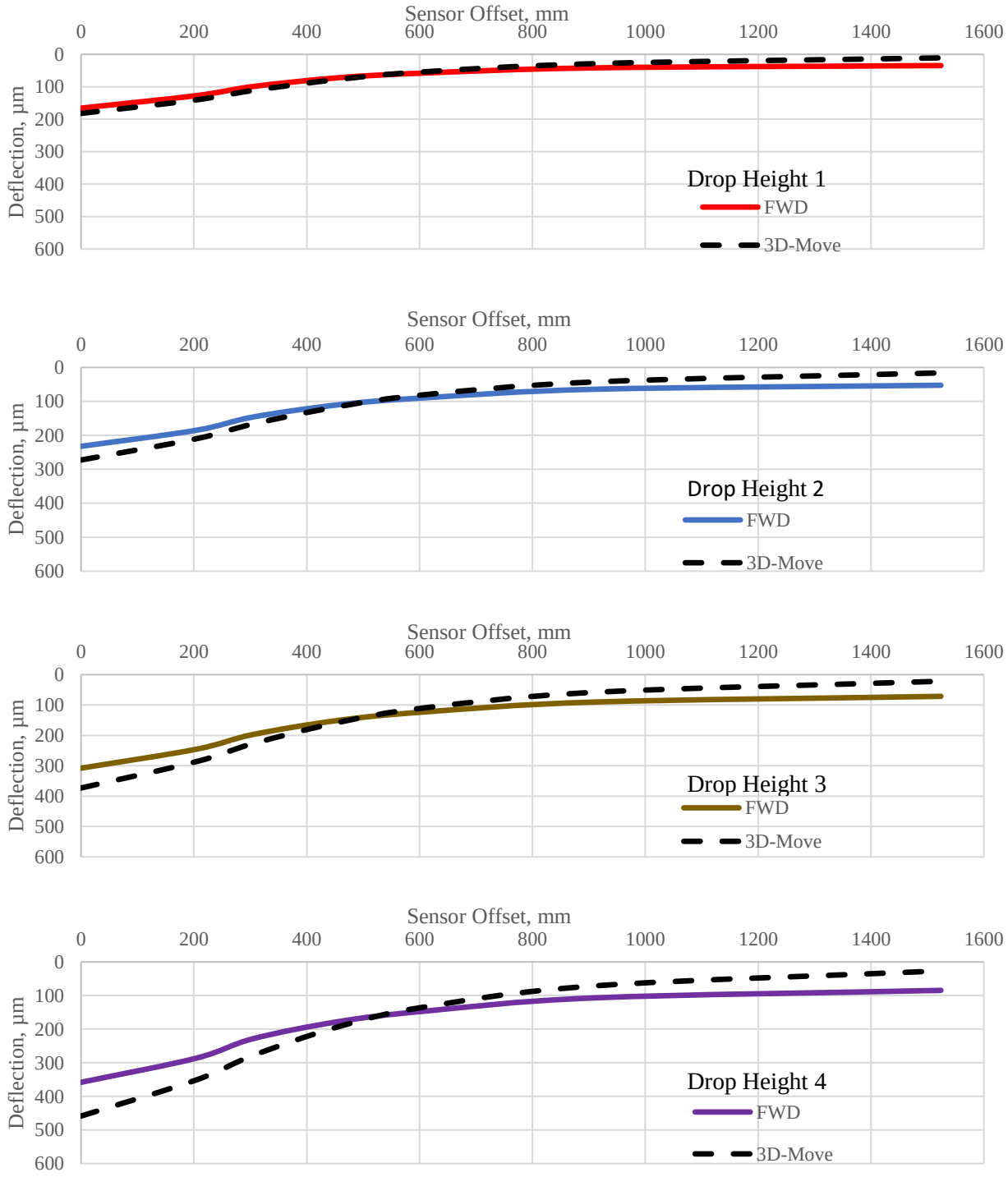

Figure C-1. Simulated Deflection Bowl for the SHRP section 0113.

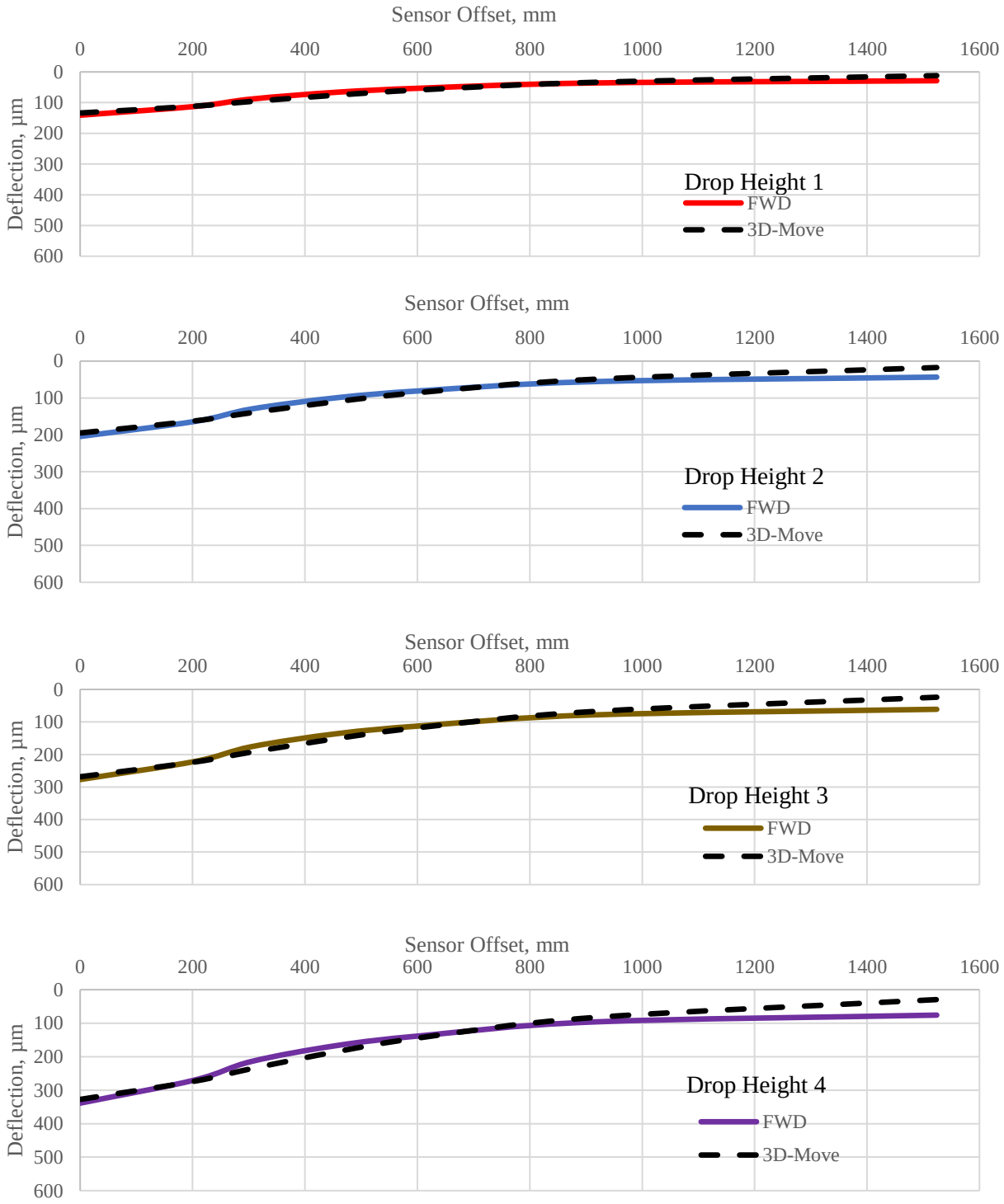

Figure C –2. Simulated Deflection Bowl for the SHRP section 0114.

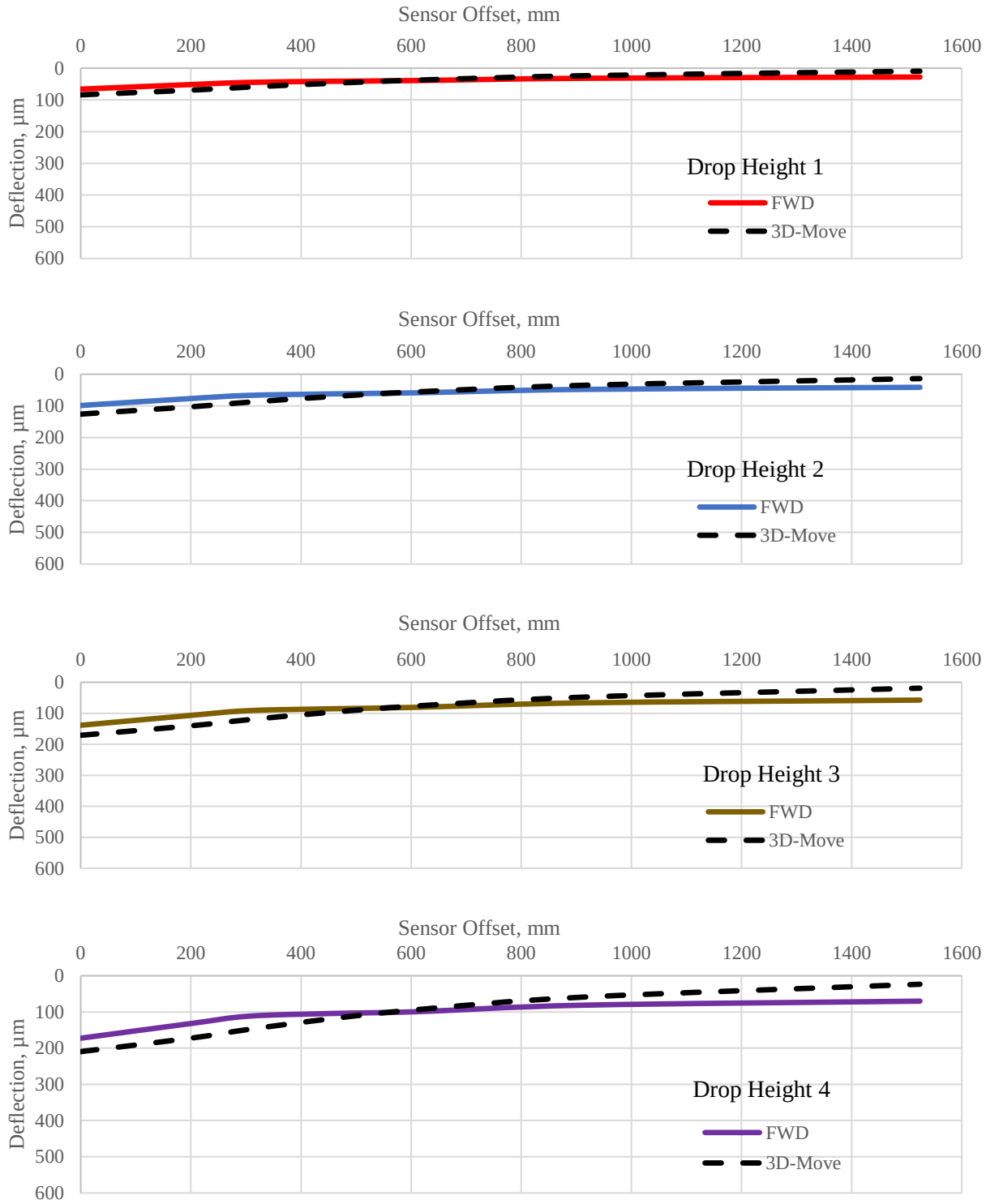

Figure C –3. Simulated Deflection Bowl for the SHRP section 0115.

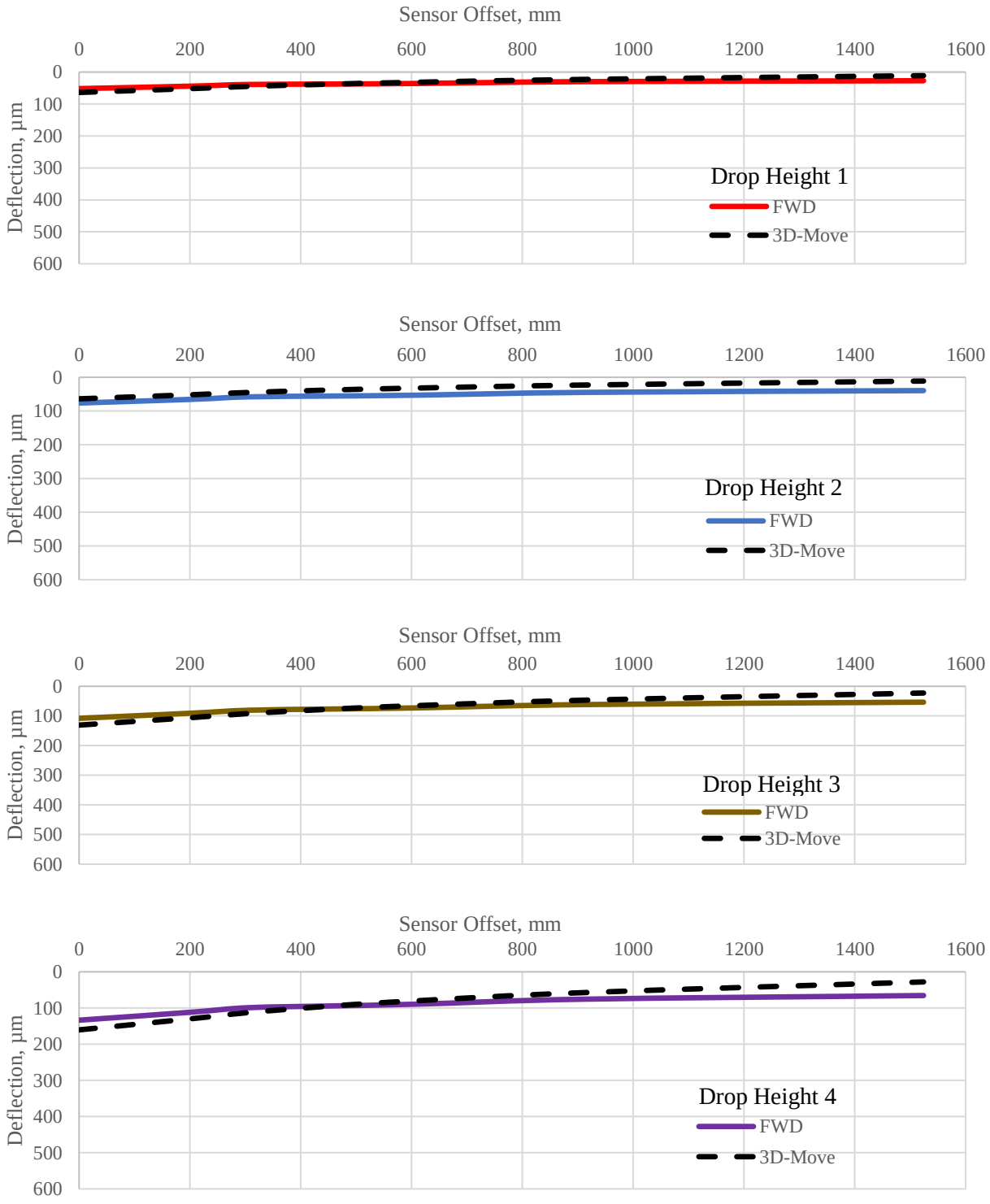

Figure C –4. Simulated Deflection Bowl for the SHRP section 0116.

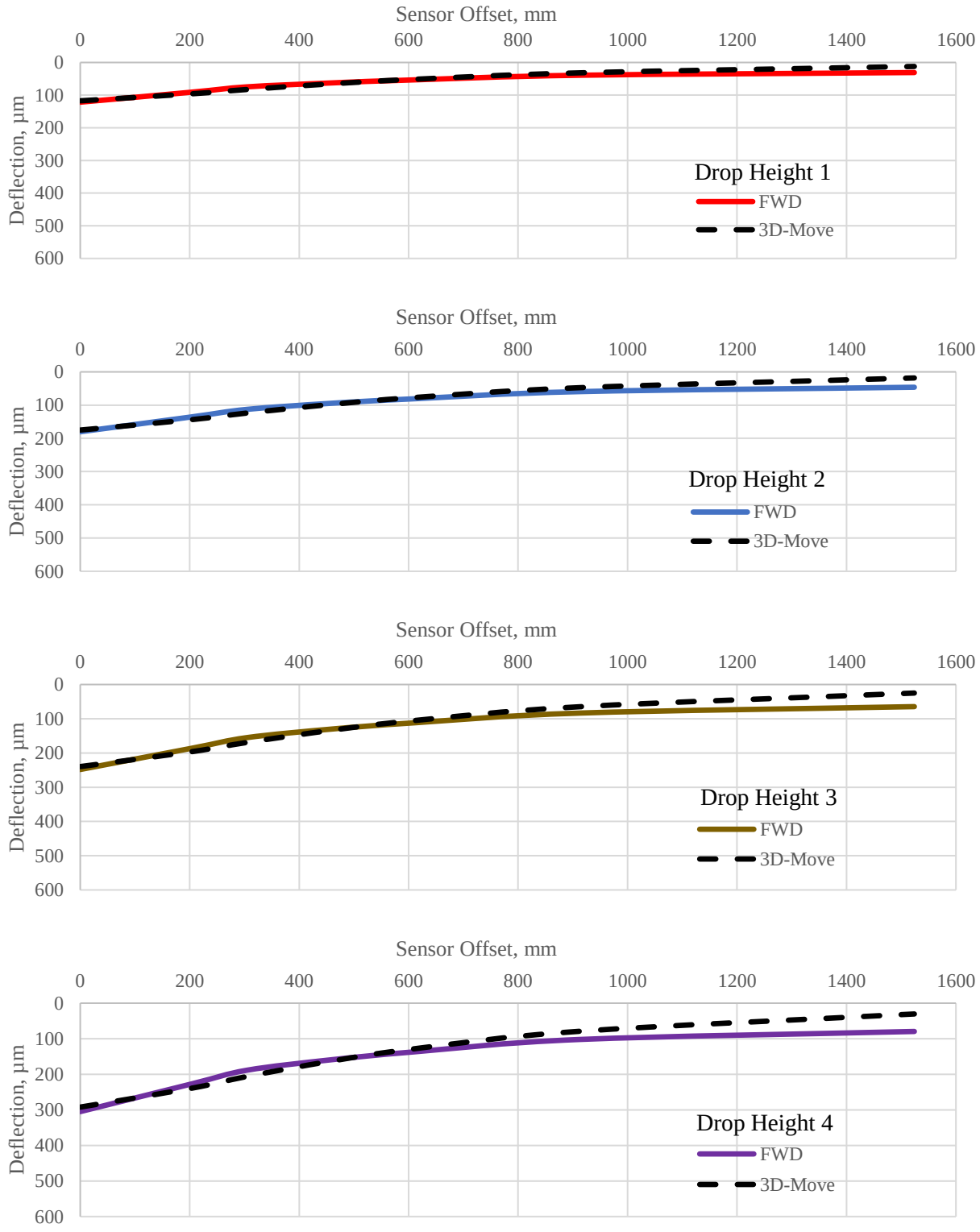

Figure C –5. Simulated Deflection Bowl for the SHRP section 0117.

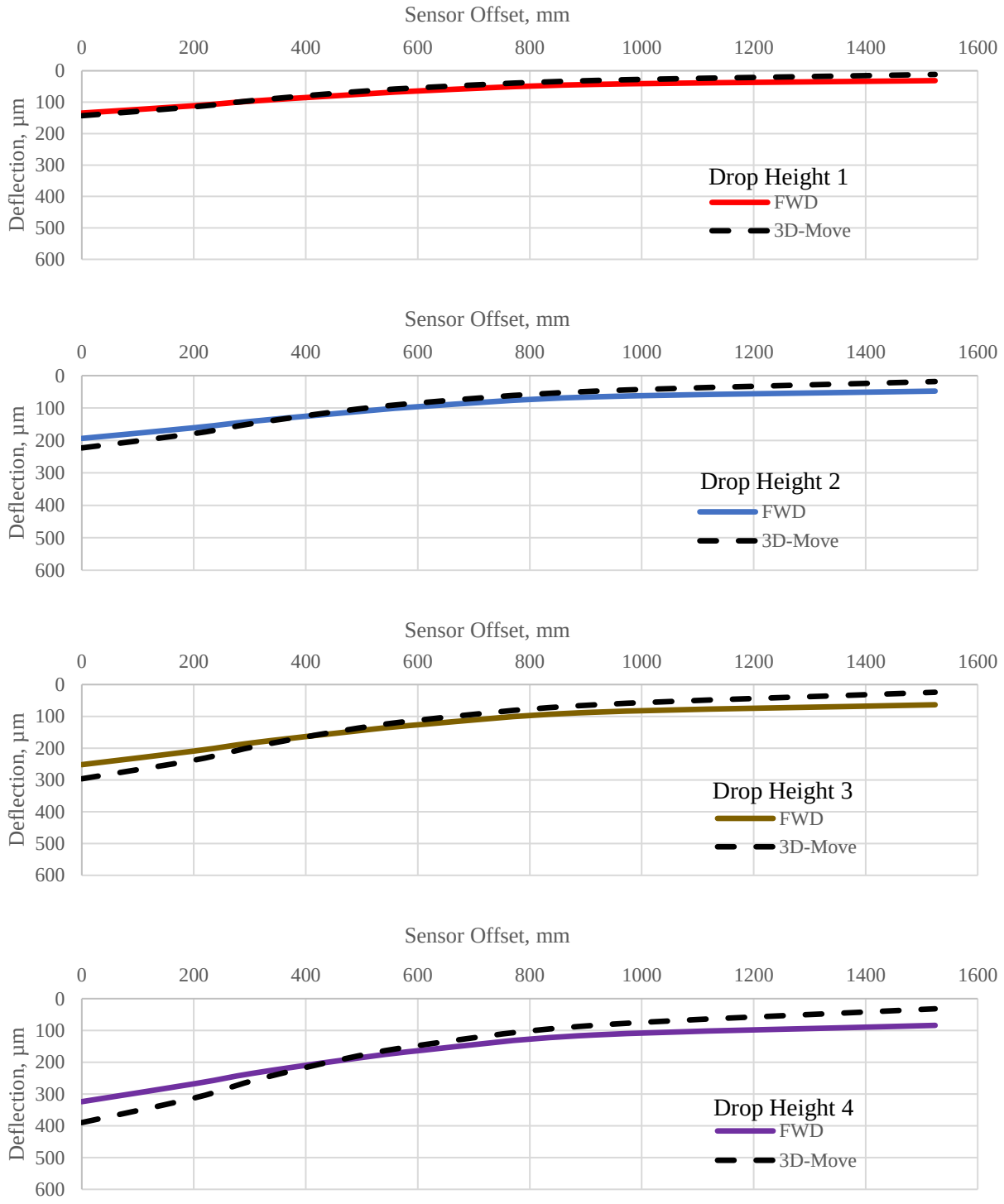

Figure C –6. Simulated Deflection Bowl for the SHRP section 0120.

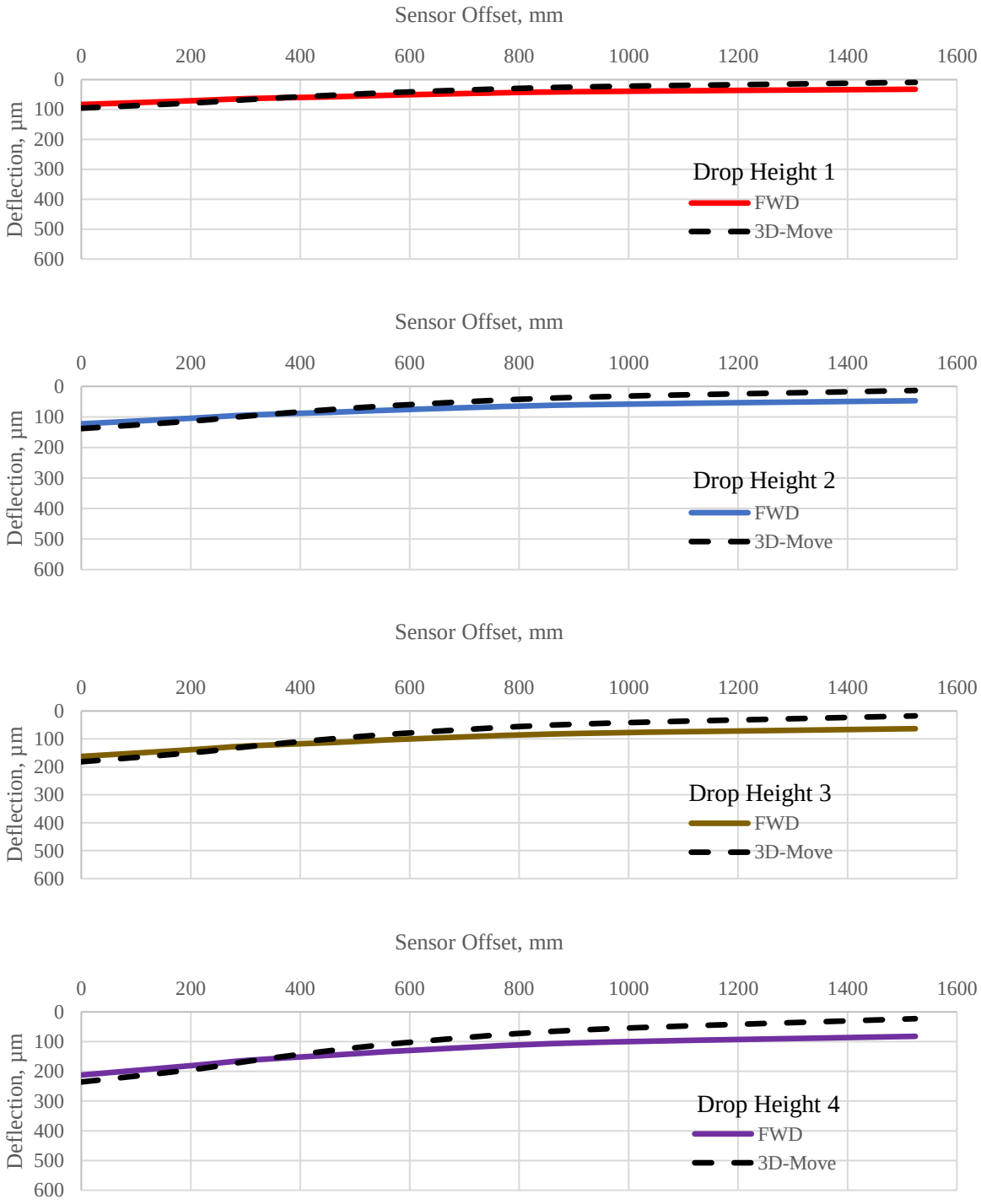

Figure C –7. Simulated Deflection Bowl for the SHRP section 0122.

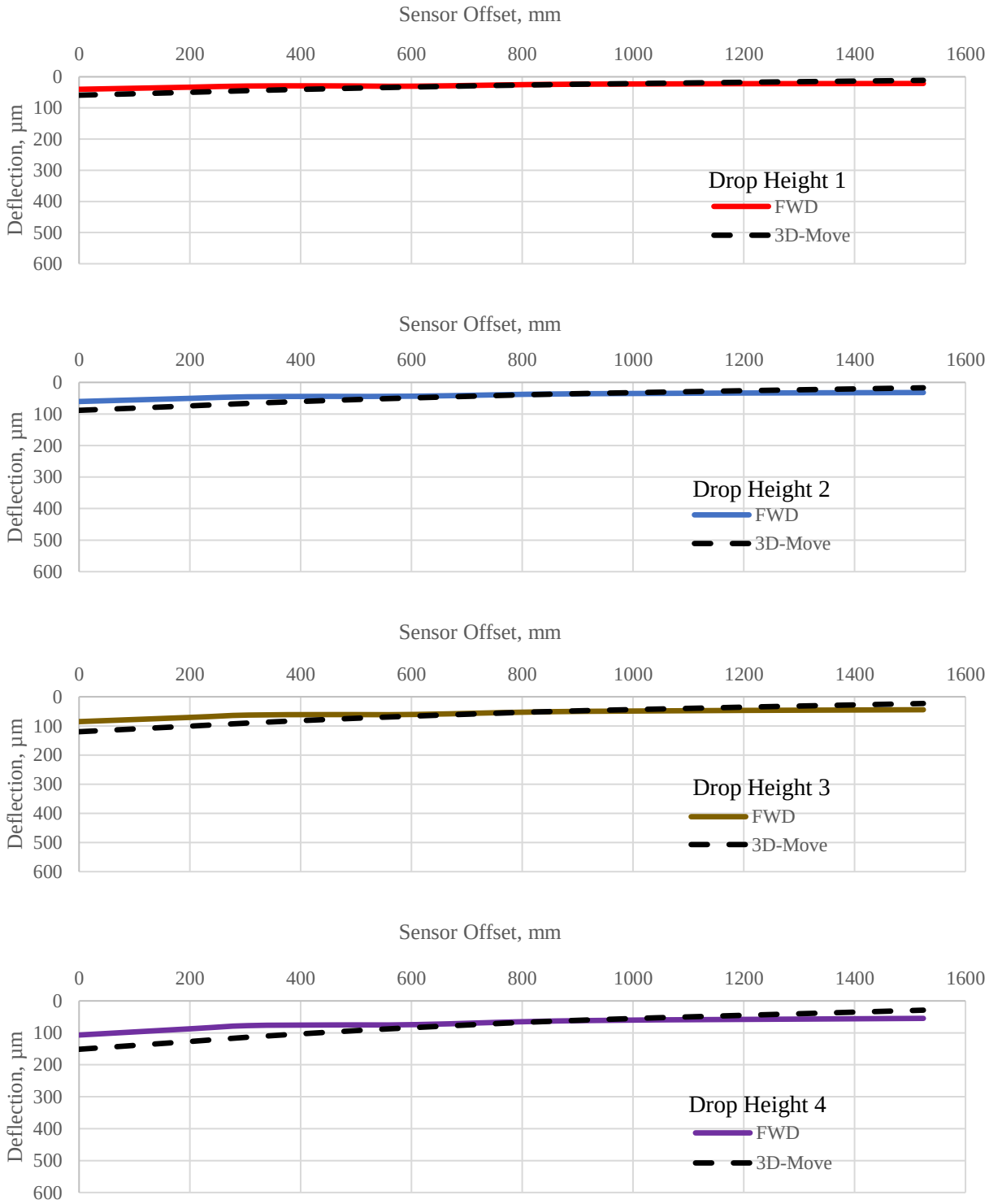

Figure C –8. Simulated Deflection Bowl for the SHRP section 0123.

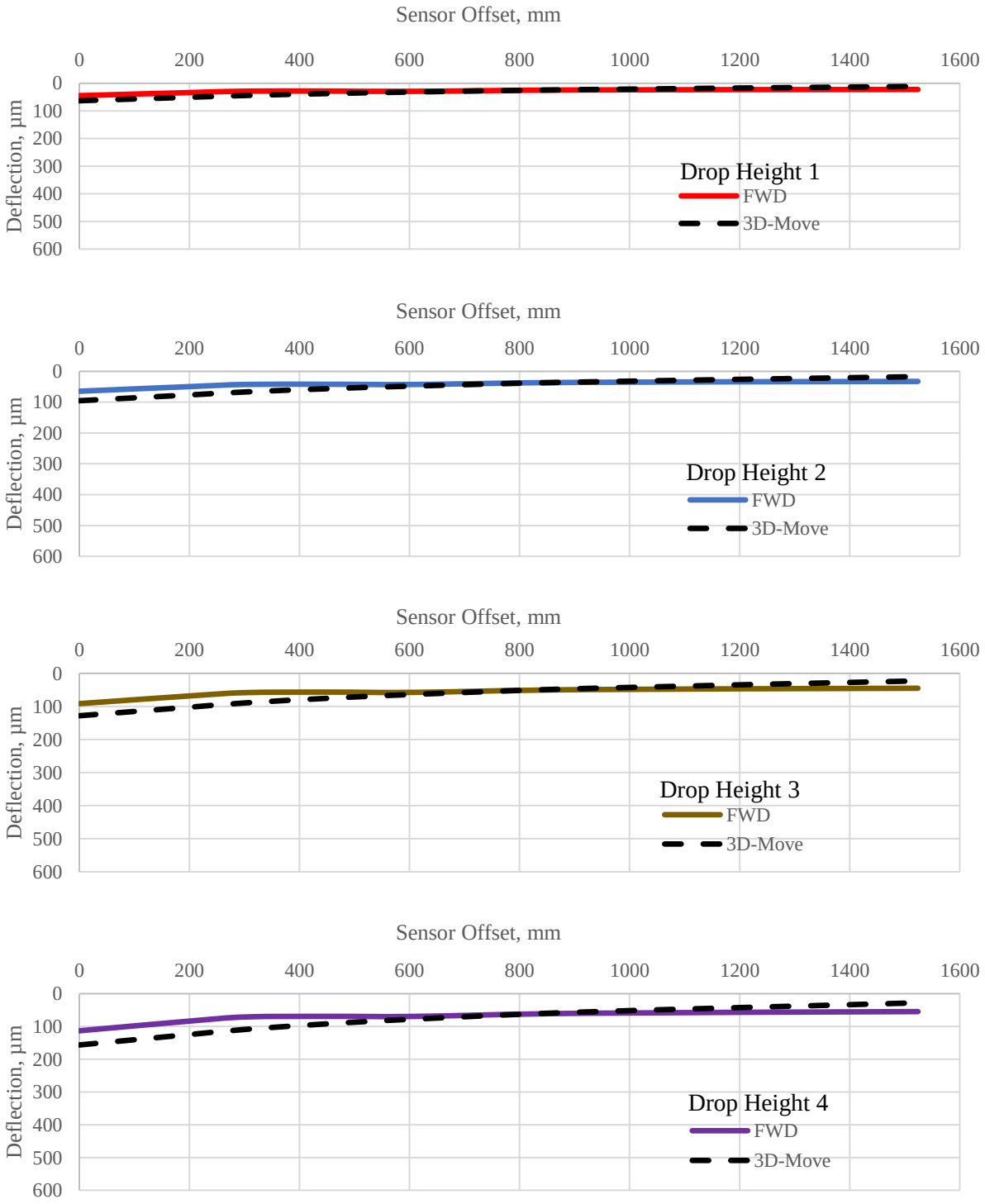

Figure C –9. Simulated Deflection Bowl for the SHRP section 0124.

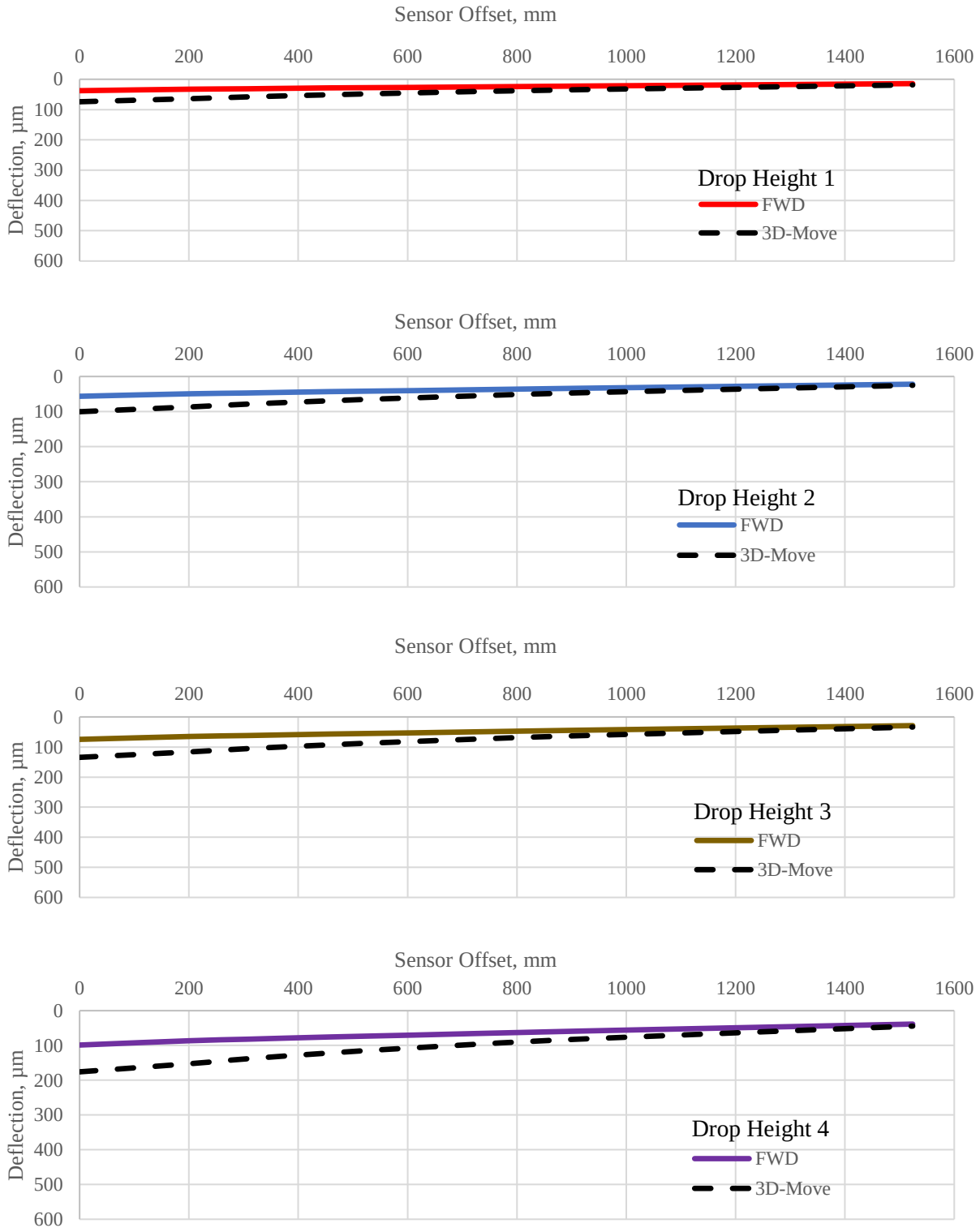

Figure C –10. Simulated Deflection Bowl for the SHRP section 3071.

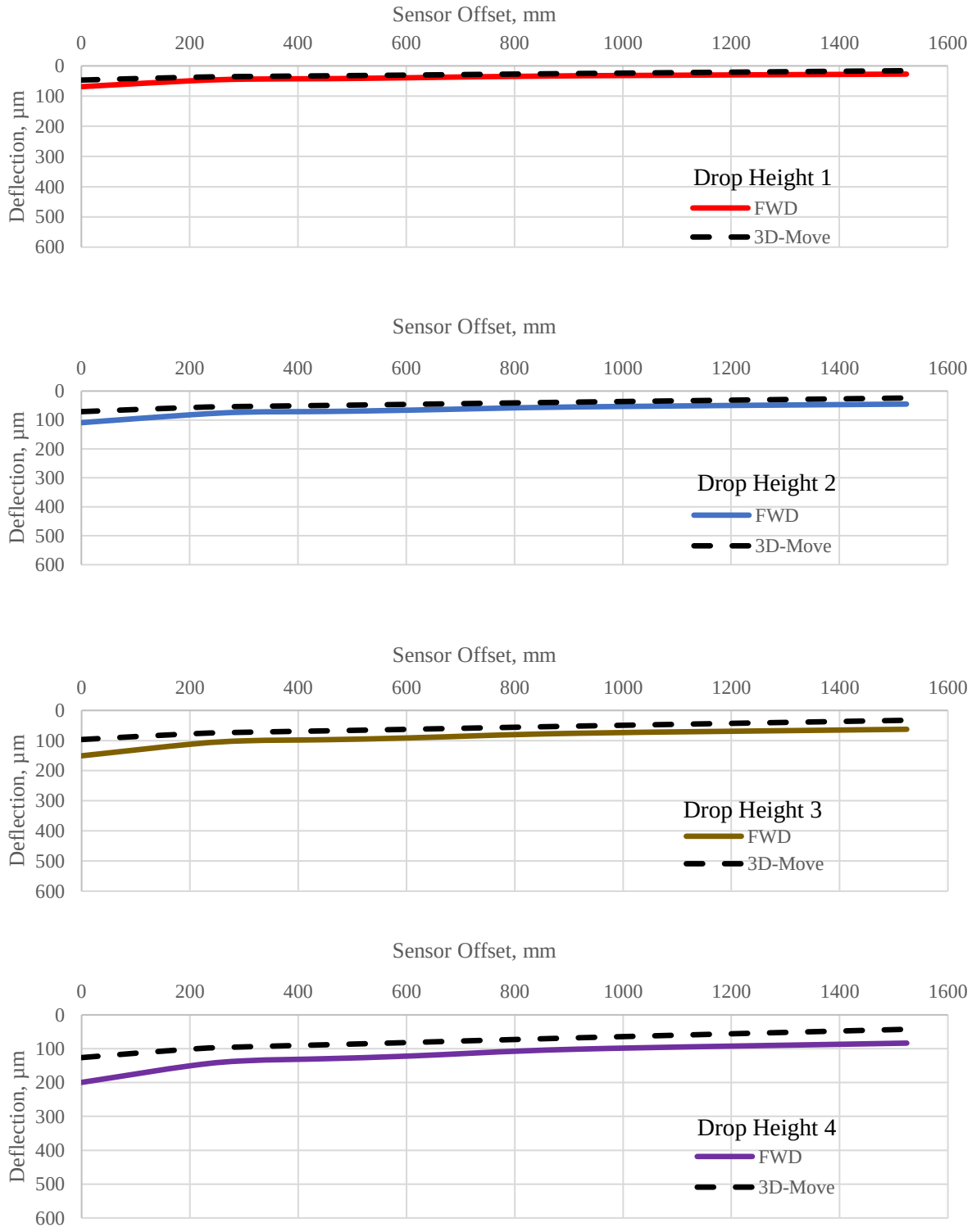

Figure C –11. Simulated Deflection Bowl for the SHRP section A607.

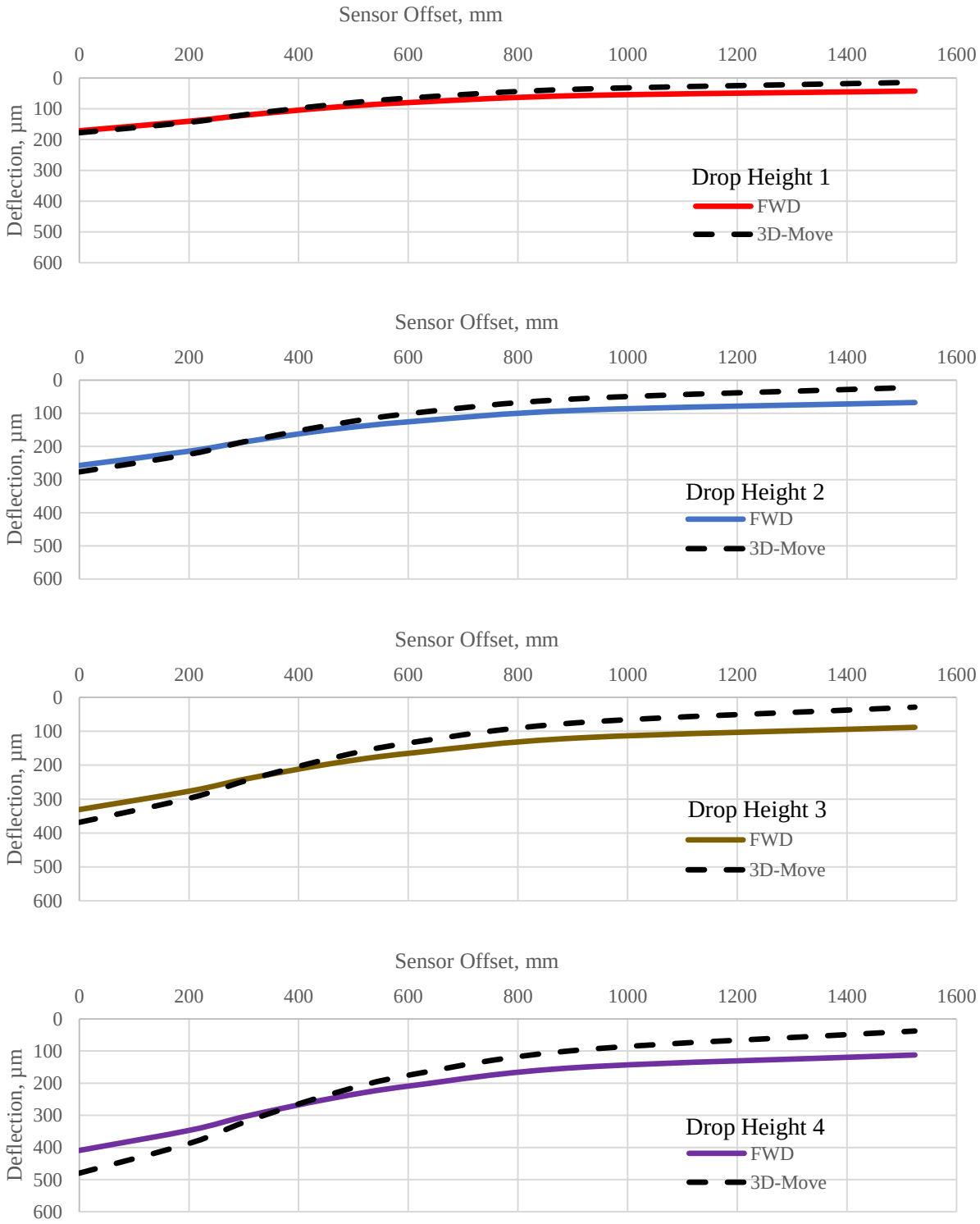

Figure C –12. Simulated Deflection Bowl for the SHRP section 0113.

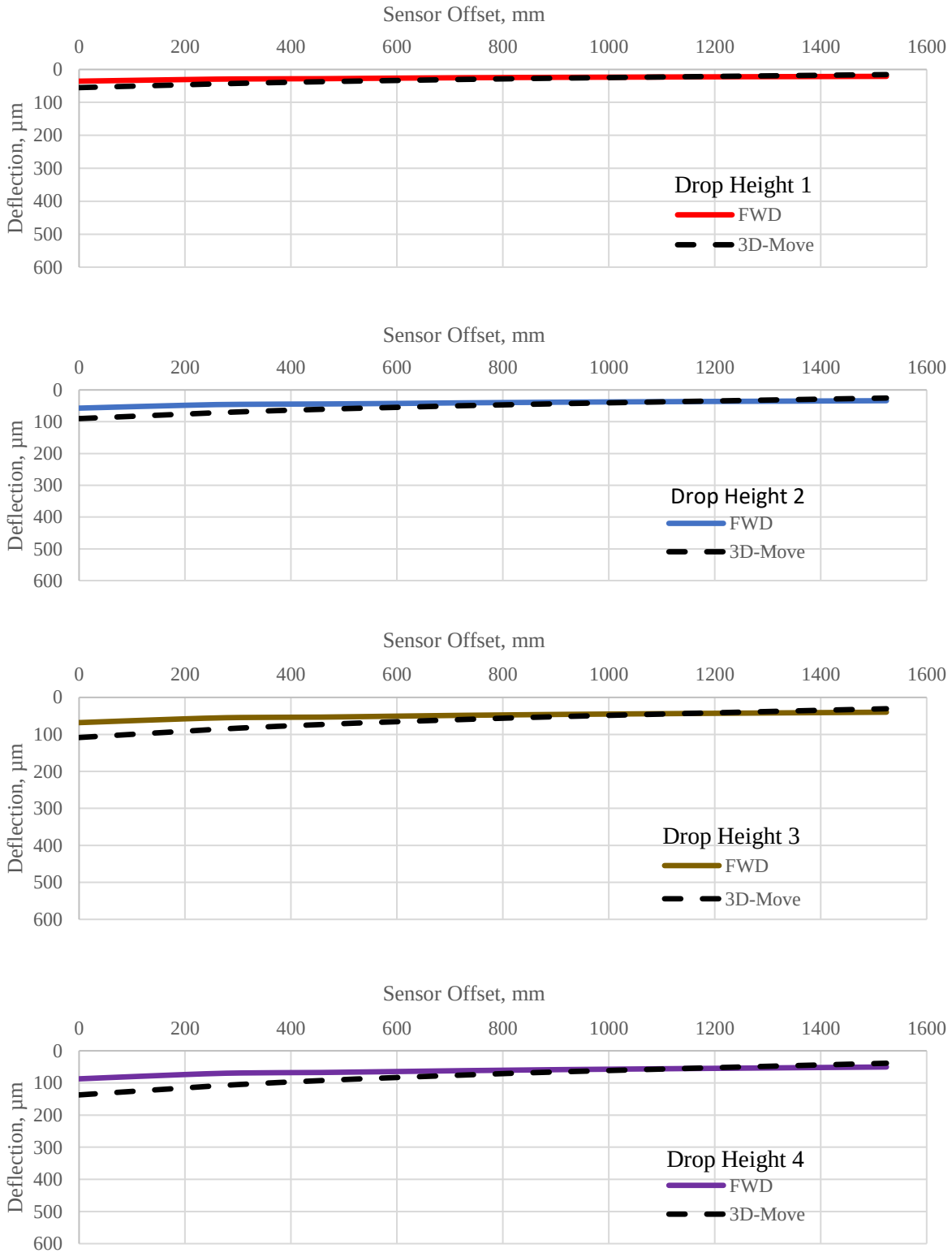

Figure C –13. Simulated Deflection Bowl for the SHRP section 0115.

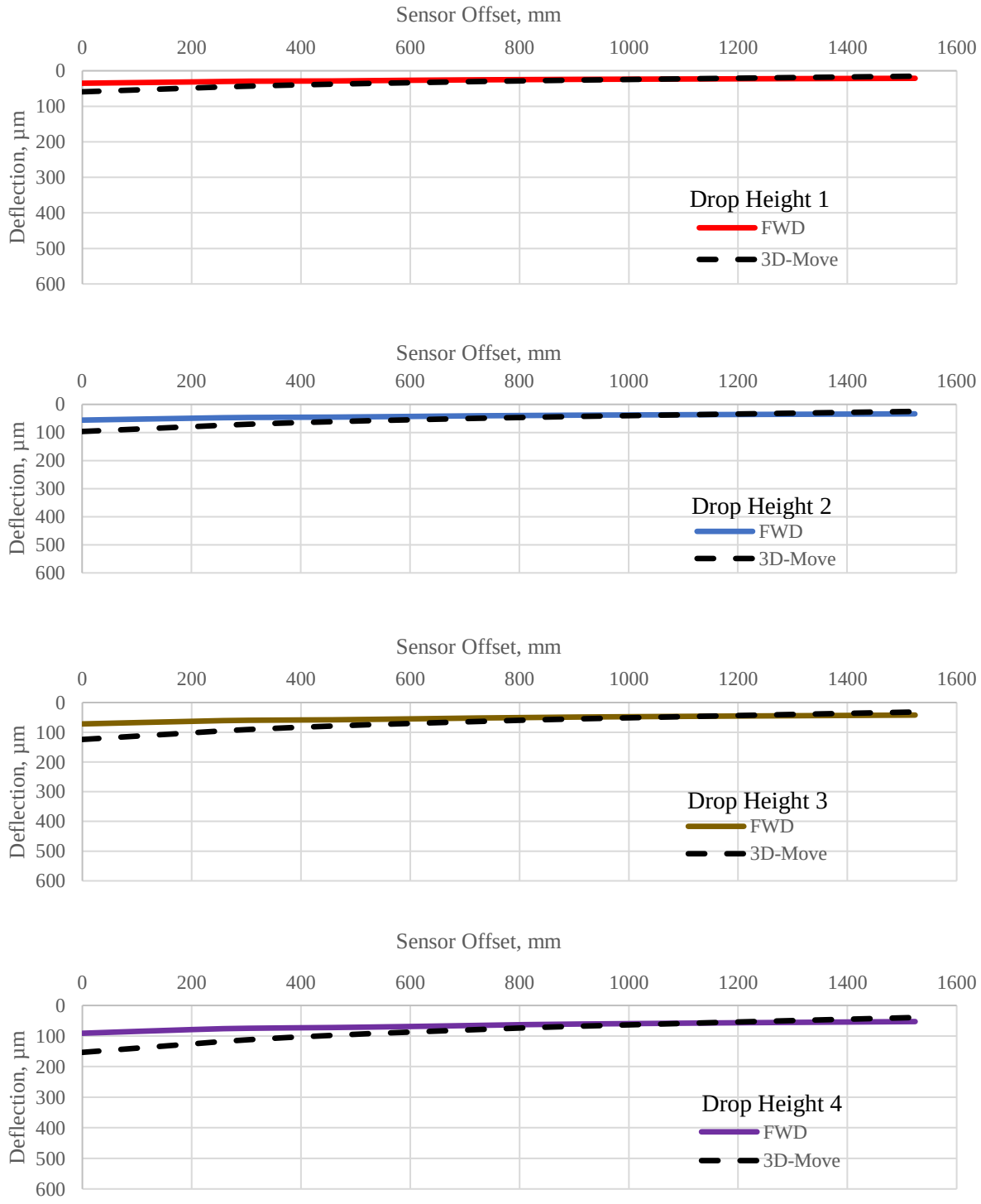

Figure C –14. Simulated Deflection Bowl for the SHRP section 0116.

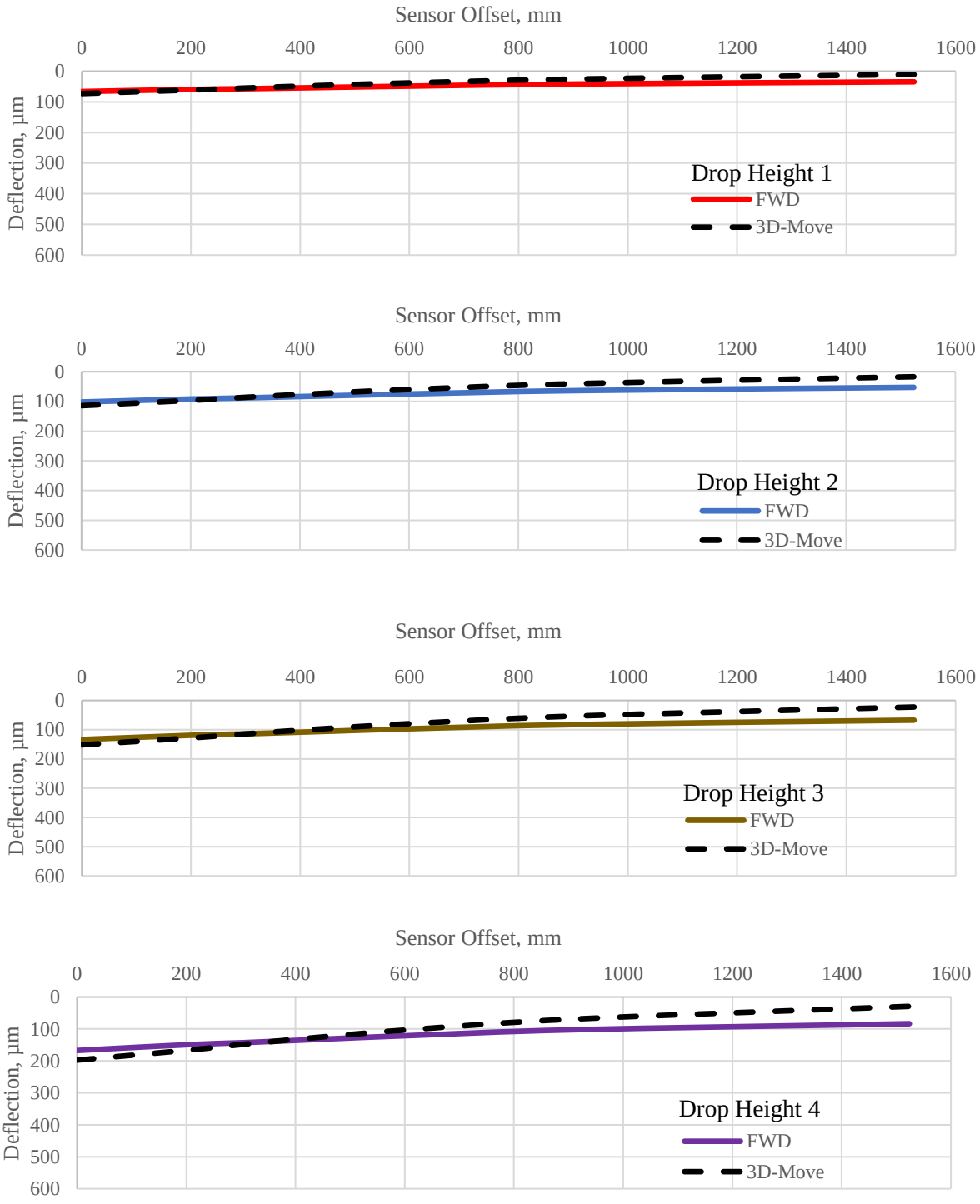

Figure C –15. Simulated Deflection Bowl for the SHRP section 0117.

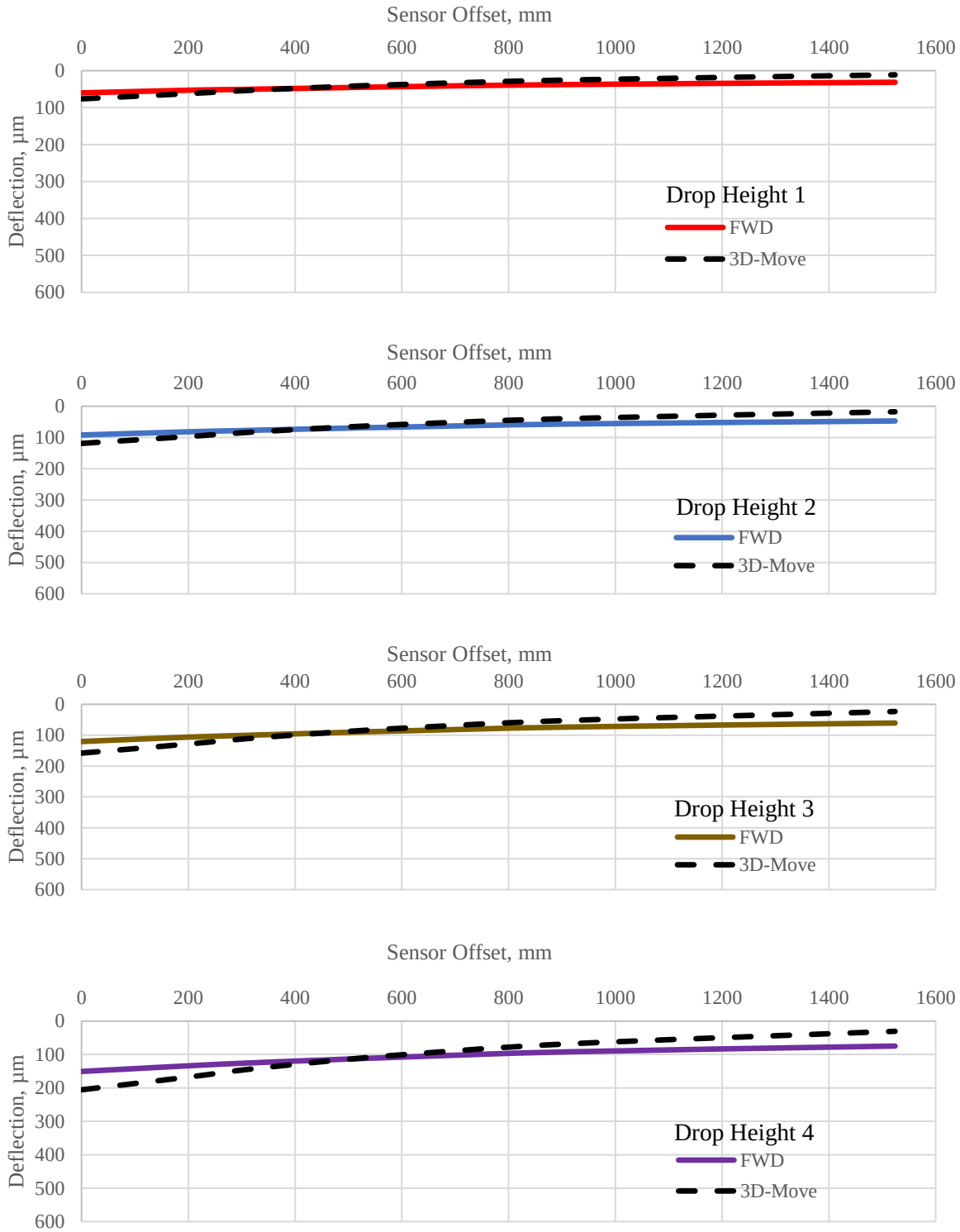

Figure C –16. Simulated Deflection Bowl for the SHRP section 0118.

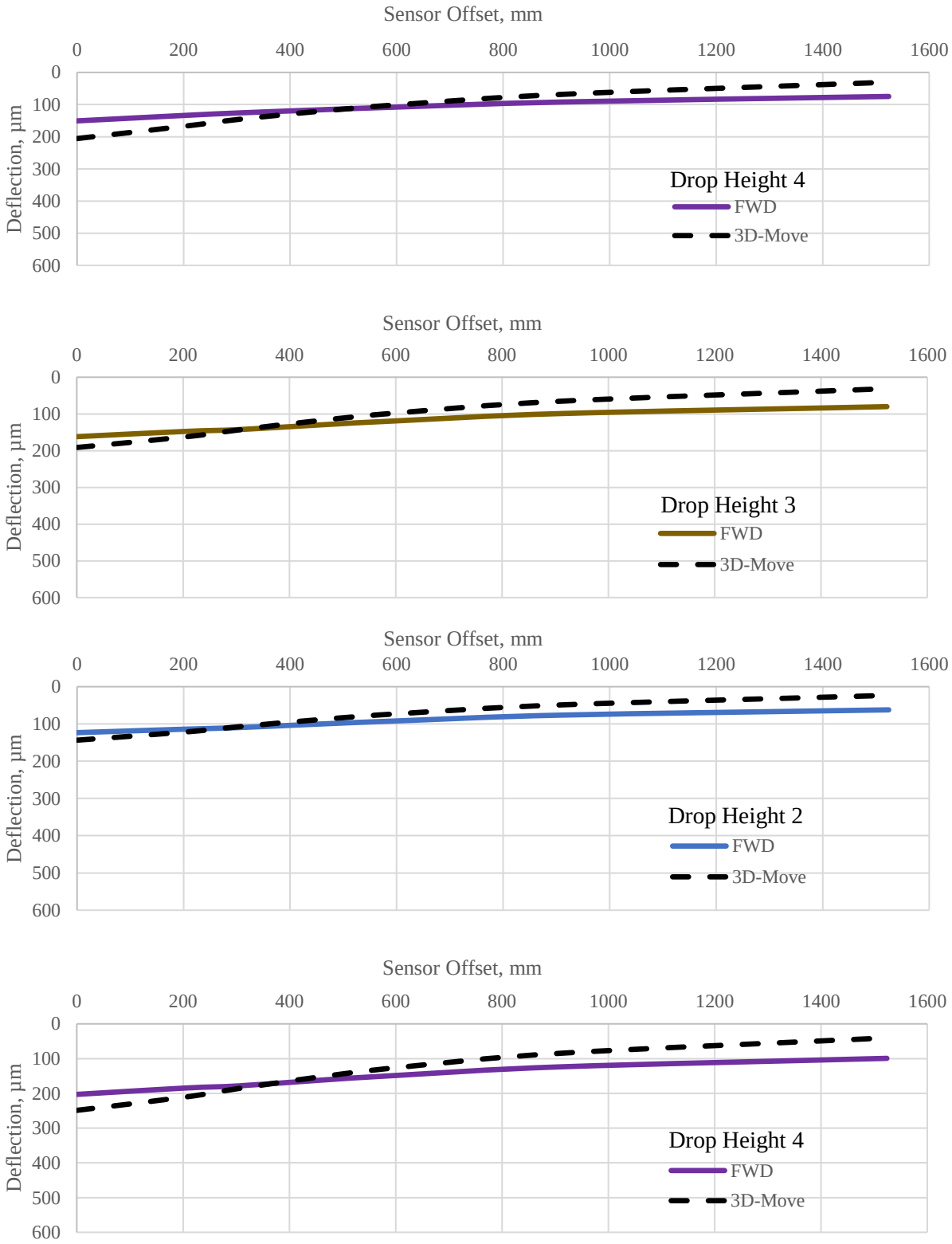

Figure C –17. Simulated Deflection Bowl for the SHRP section 0119.

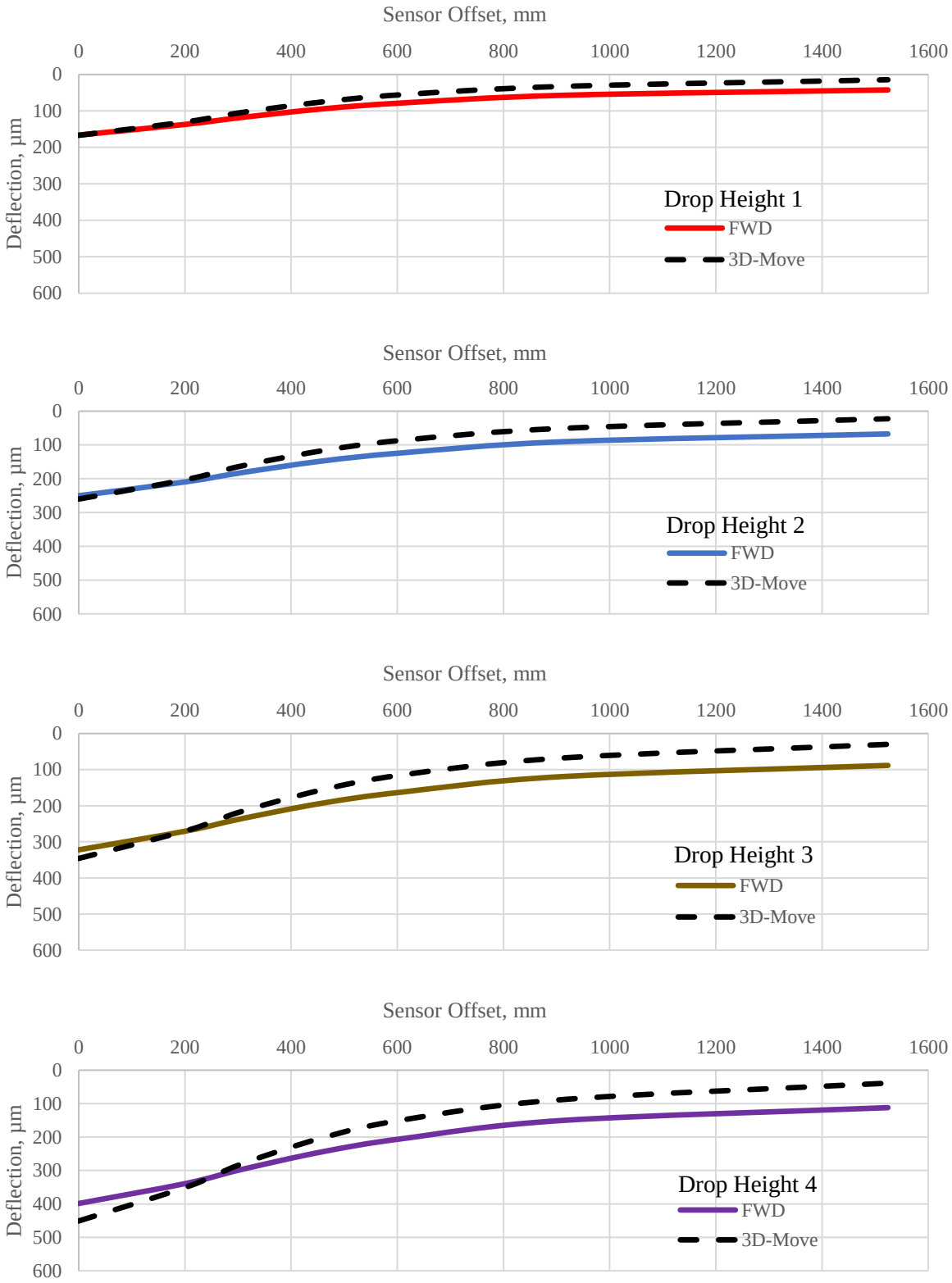

Figure C –18. Simulated Deflection Bowl for the SHRP section 0121.

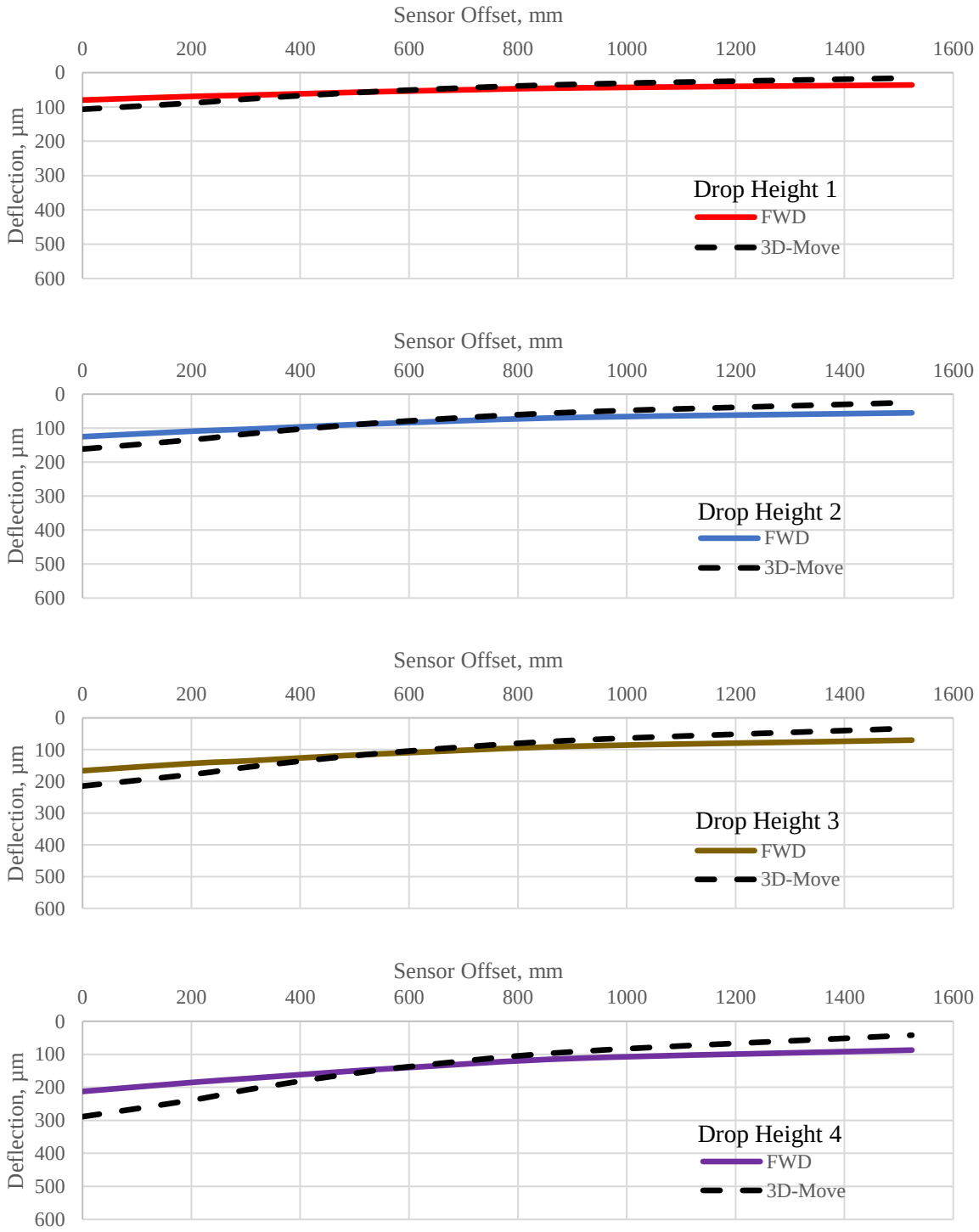

Figure C –19. Simulated Deflection Bowl for the SHRP section 0122.

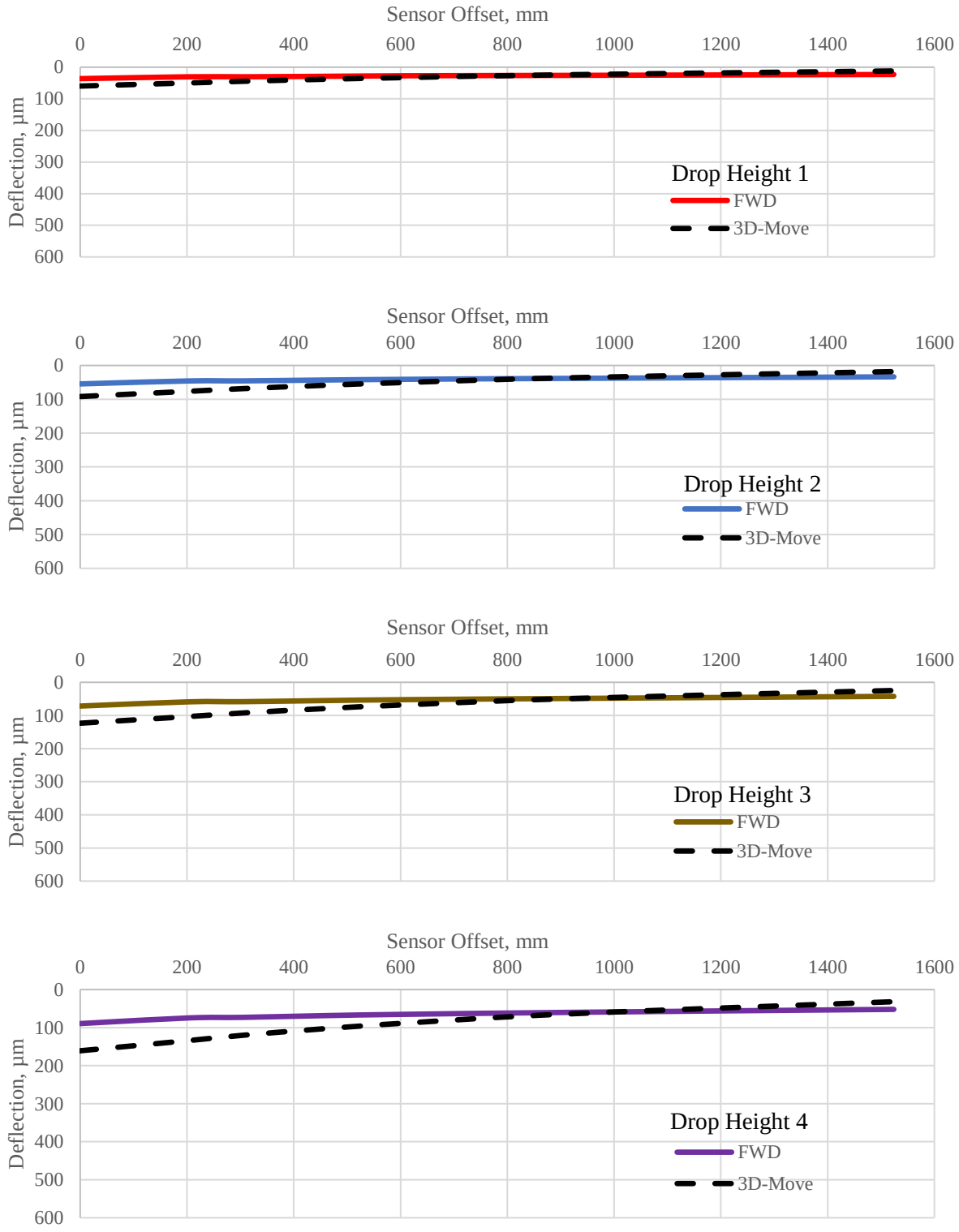

Figure C –20. Simulated Deflection Bowl for the SHRP section 0123.

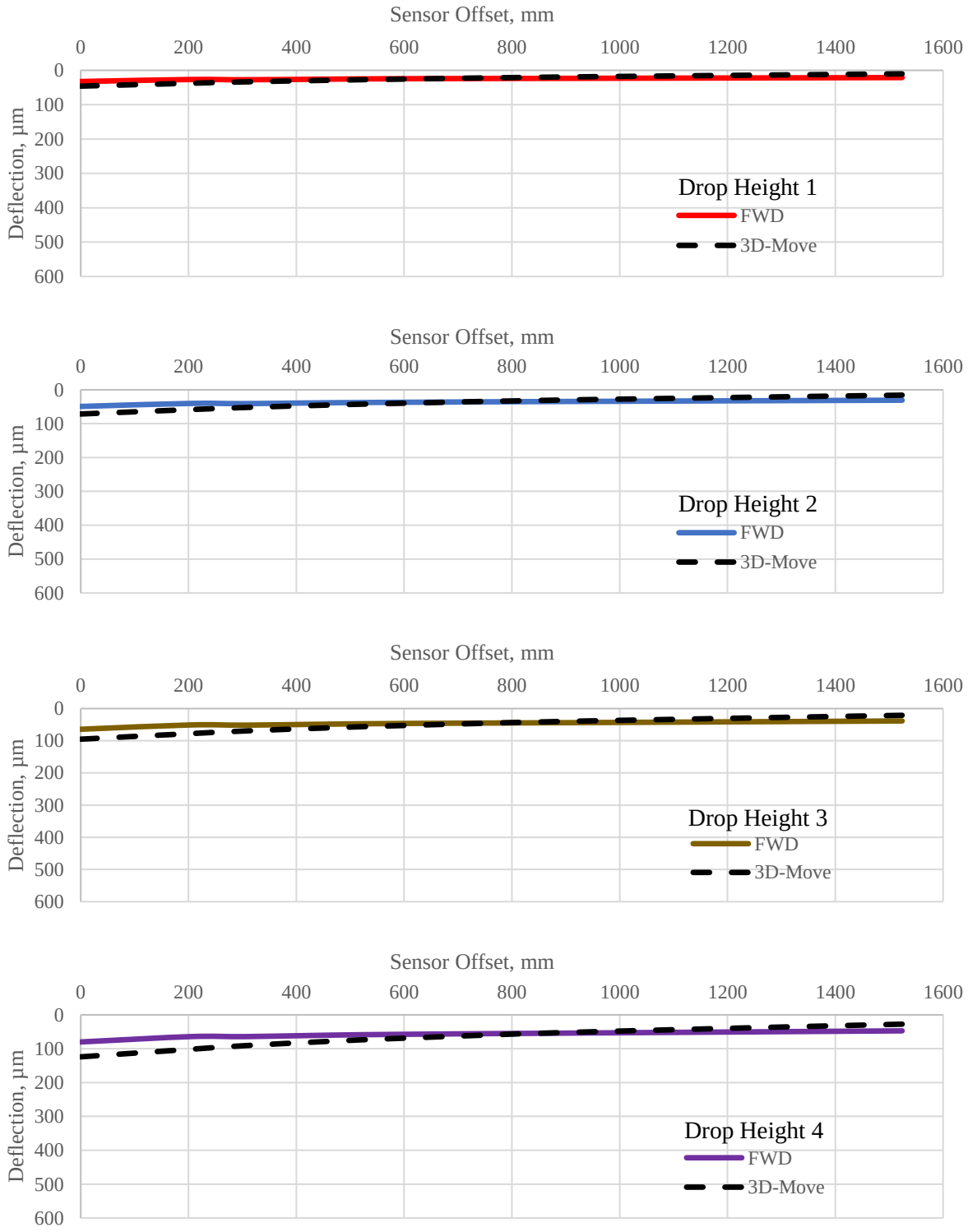

Figure C –21. Simulated Deflection Bowl for the SHRP section 0124.

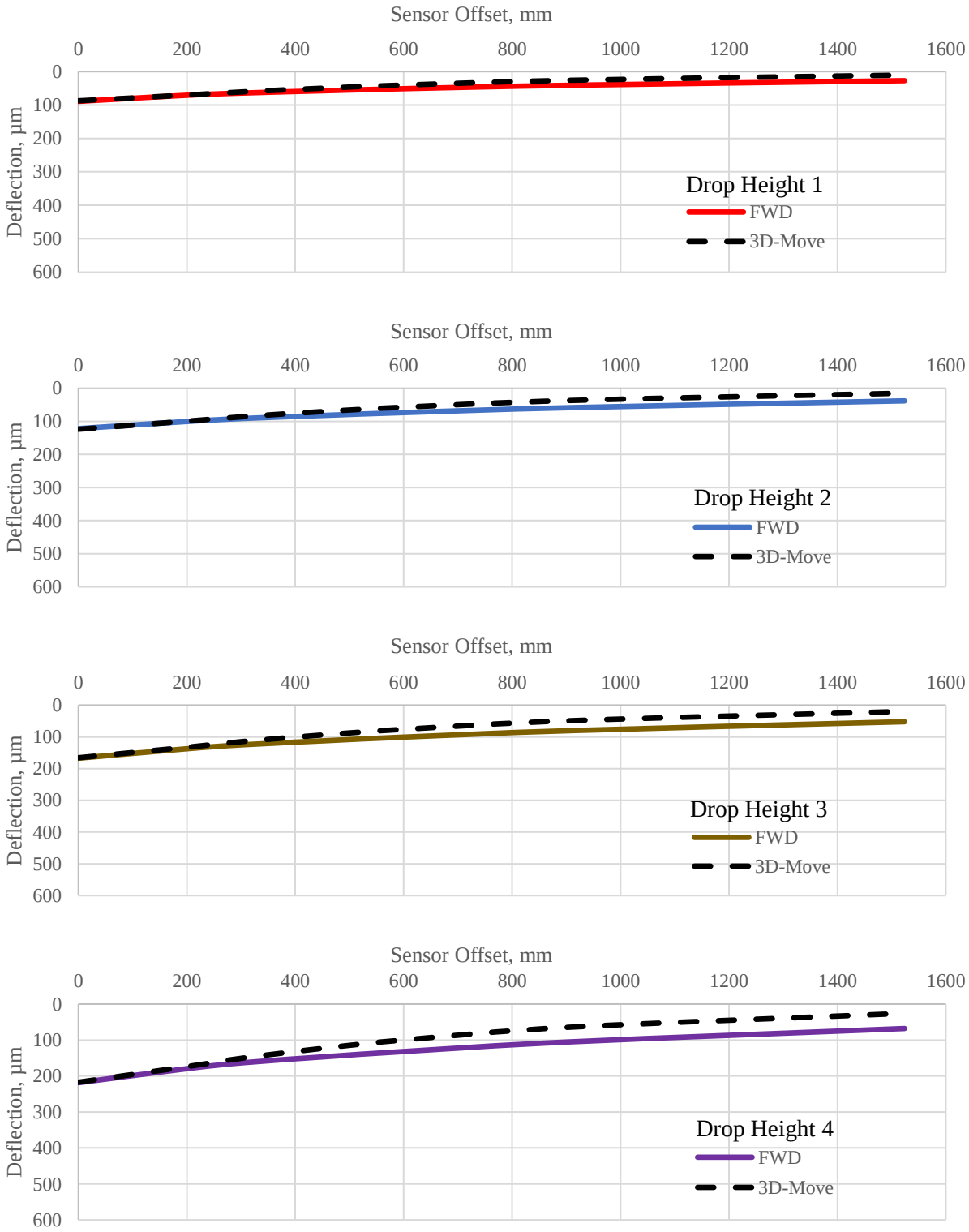

Figure C –22. Simulated Deflection Bowl for the SHRP section 3071.

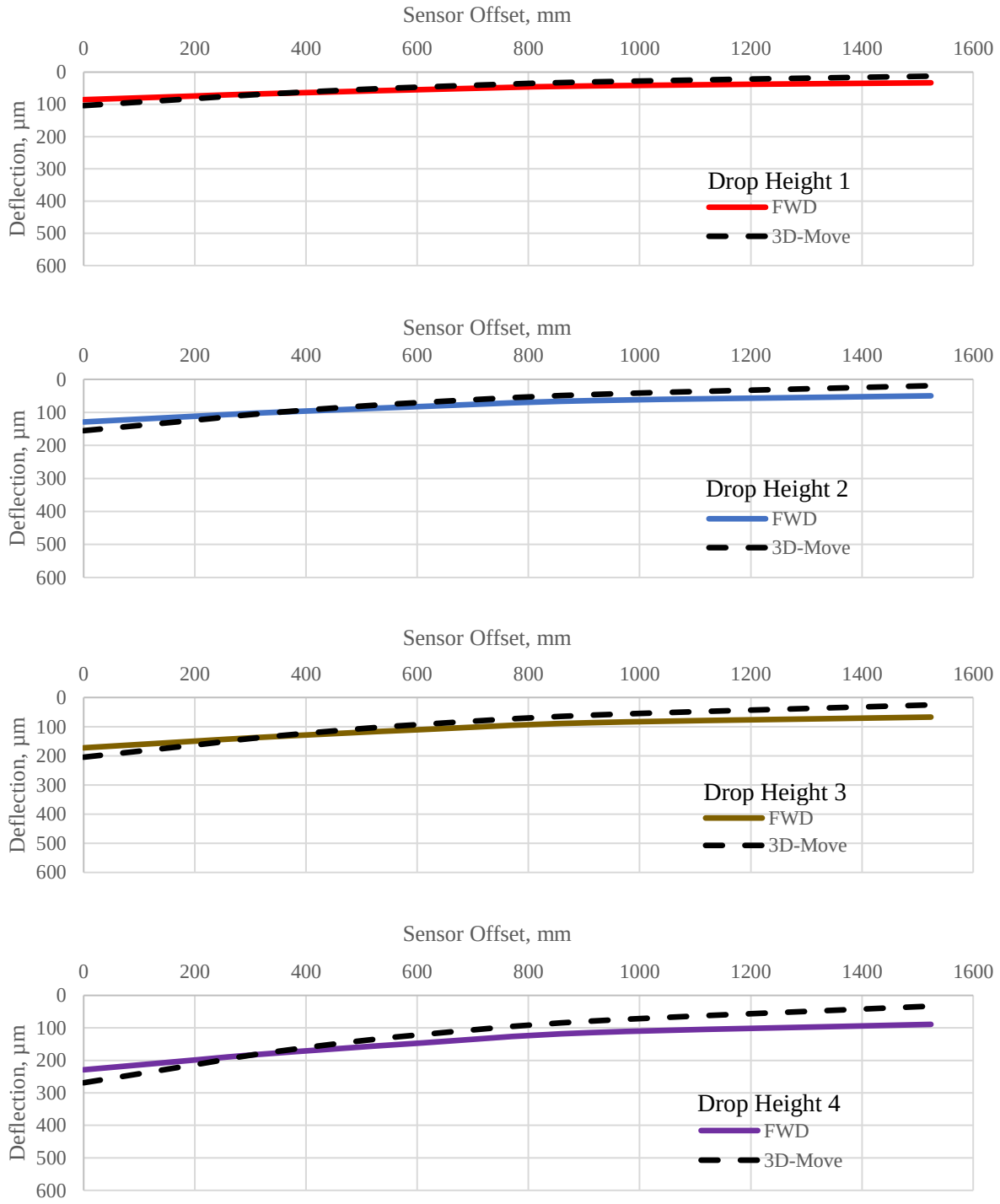

Figure C –23. Simulated Deflection Bowl for the SHRP section 0103.

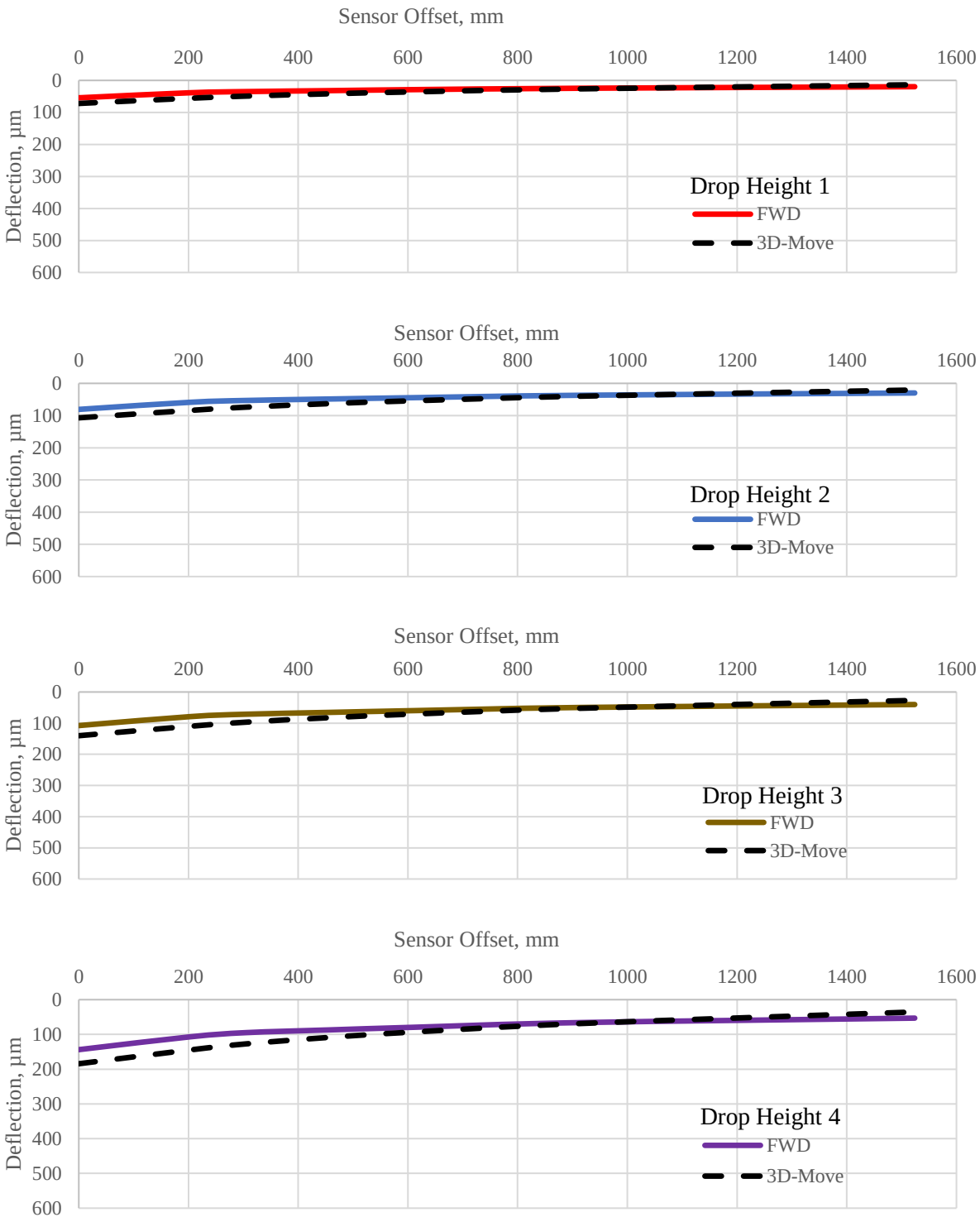

Figure C –24. Simulated Deflection Bowl for the SHRP section 0104.

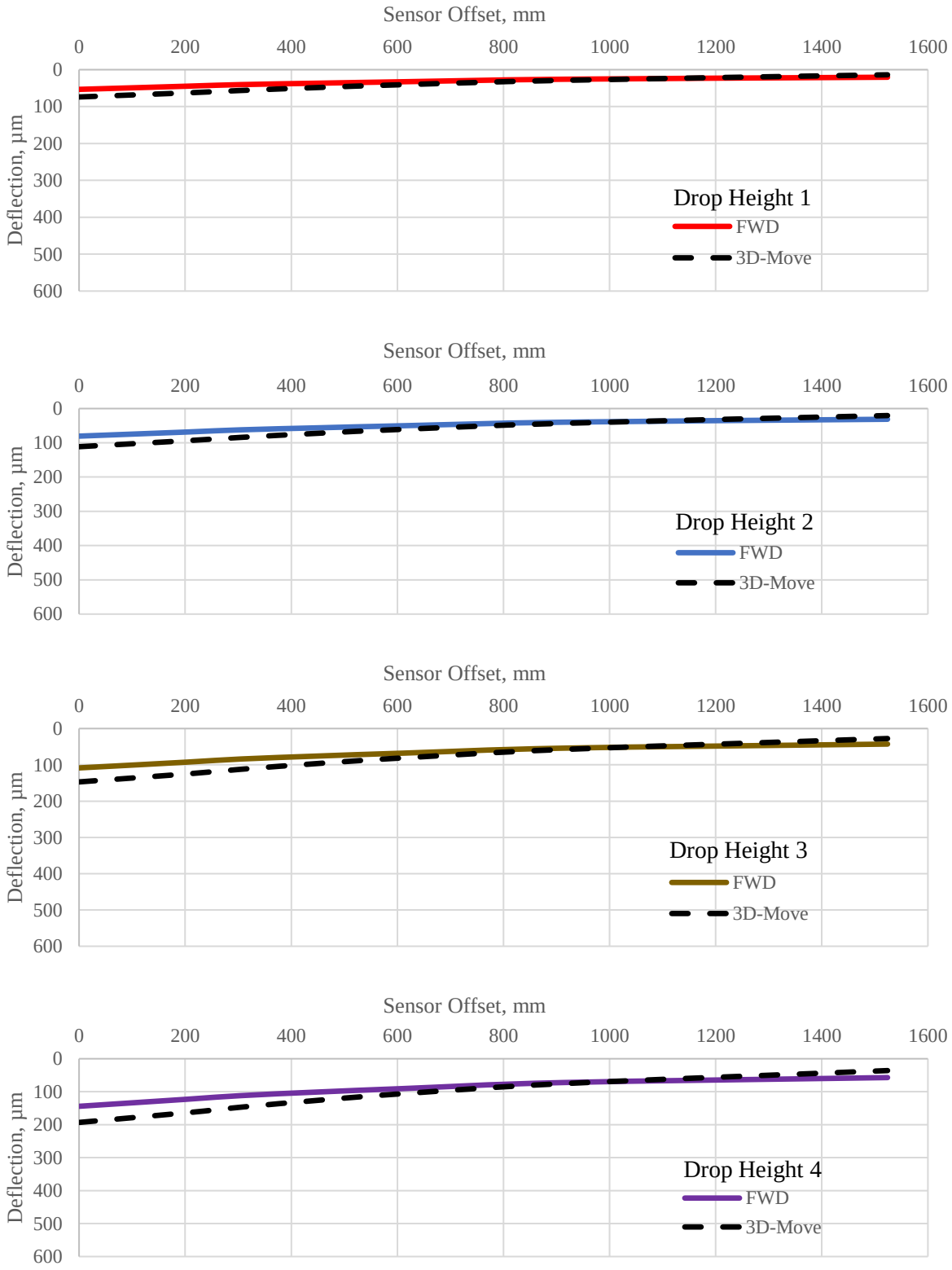

Figure C –25. Simulated Deflection Bowl for the SHRP section 0106.

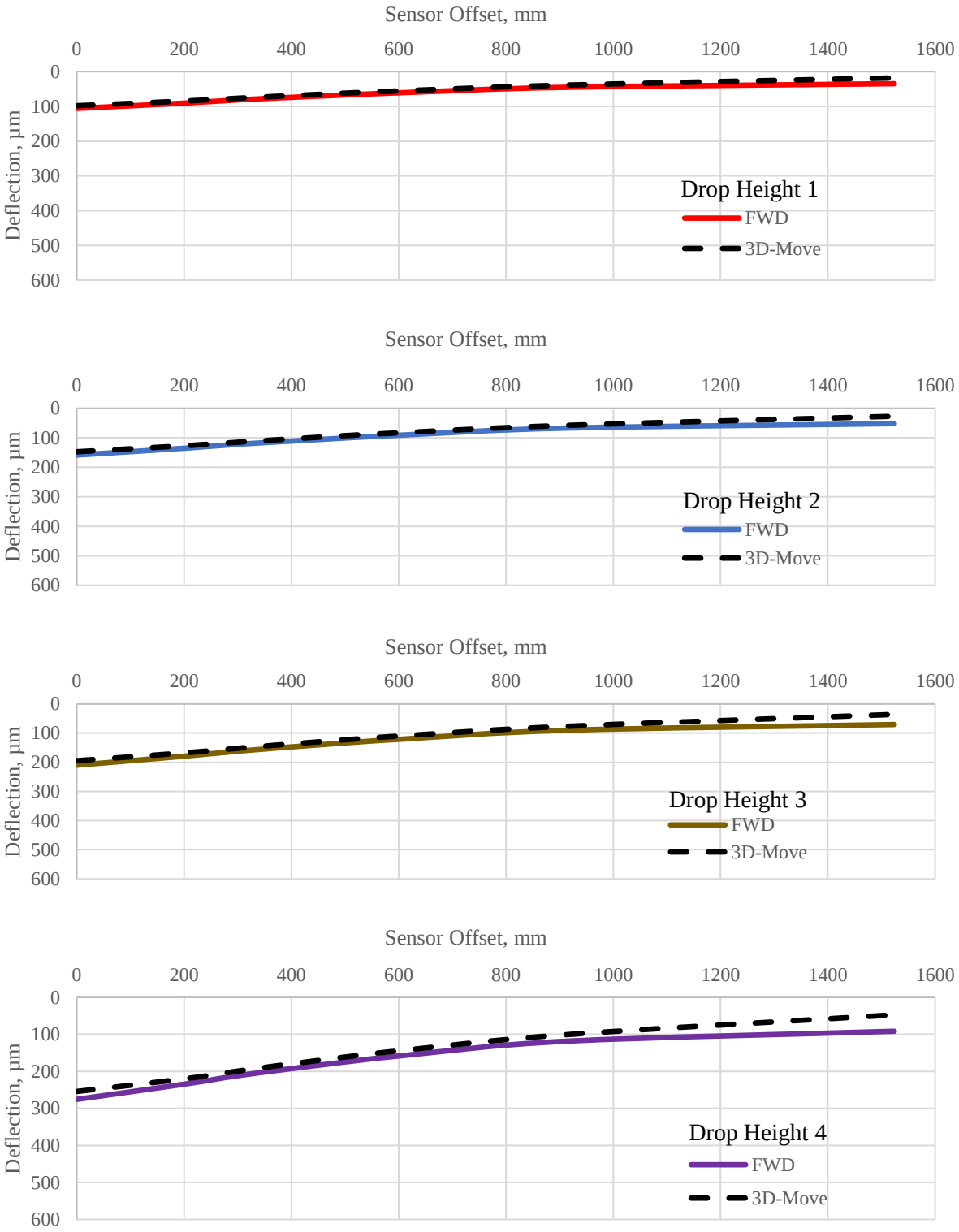

Figure C –26. Simulated Deflection Bowl for the SHRP section 0108.

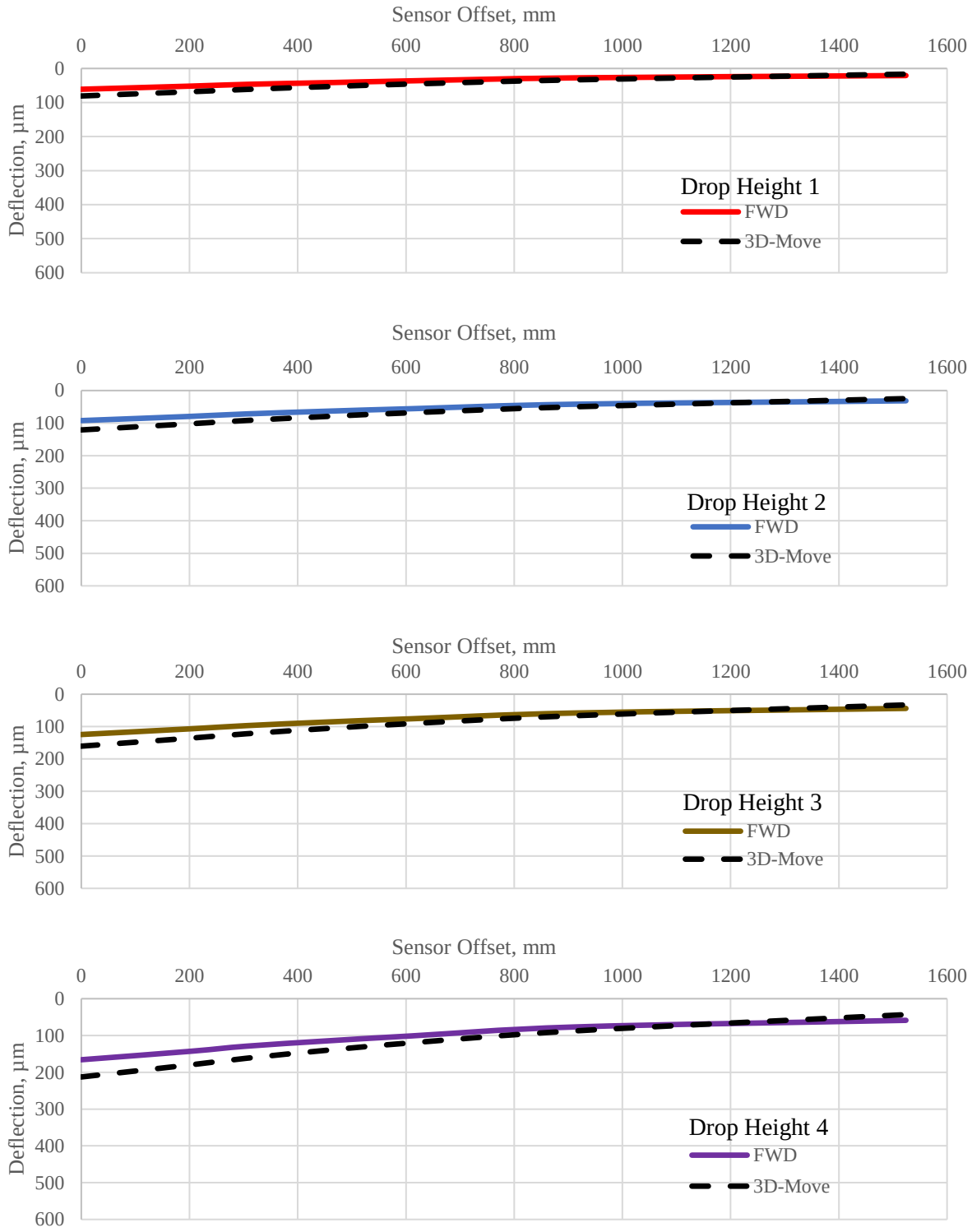

Figure C –27. Simulated Deflection Bowl for the SHRP section 0110.

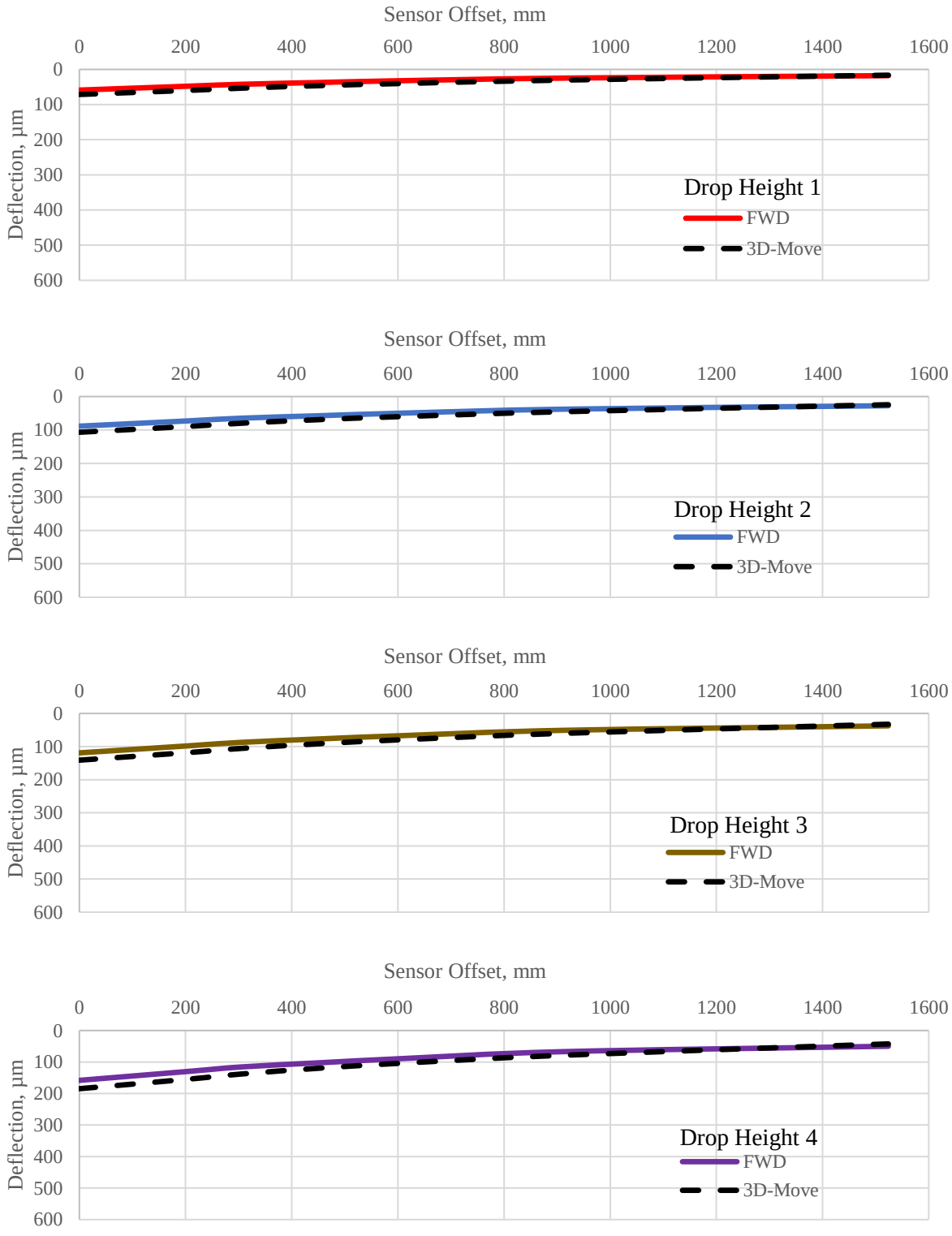

Figure C –28. Simulated Deflection Bowl for the SHRP section 0111.

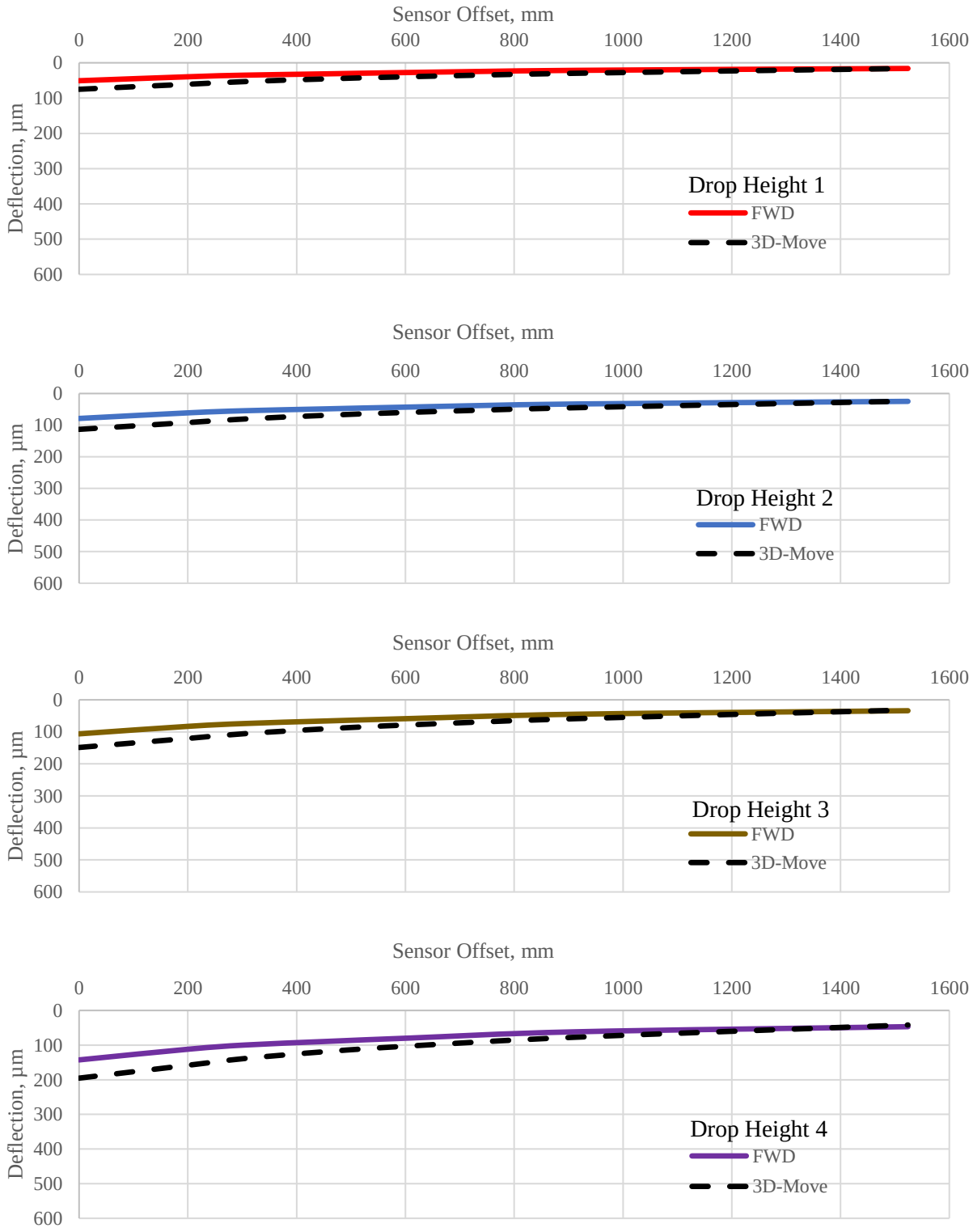

Figure C –29. Simulated Deflection Bowl for the SHRP section 0112.

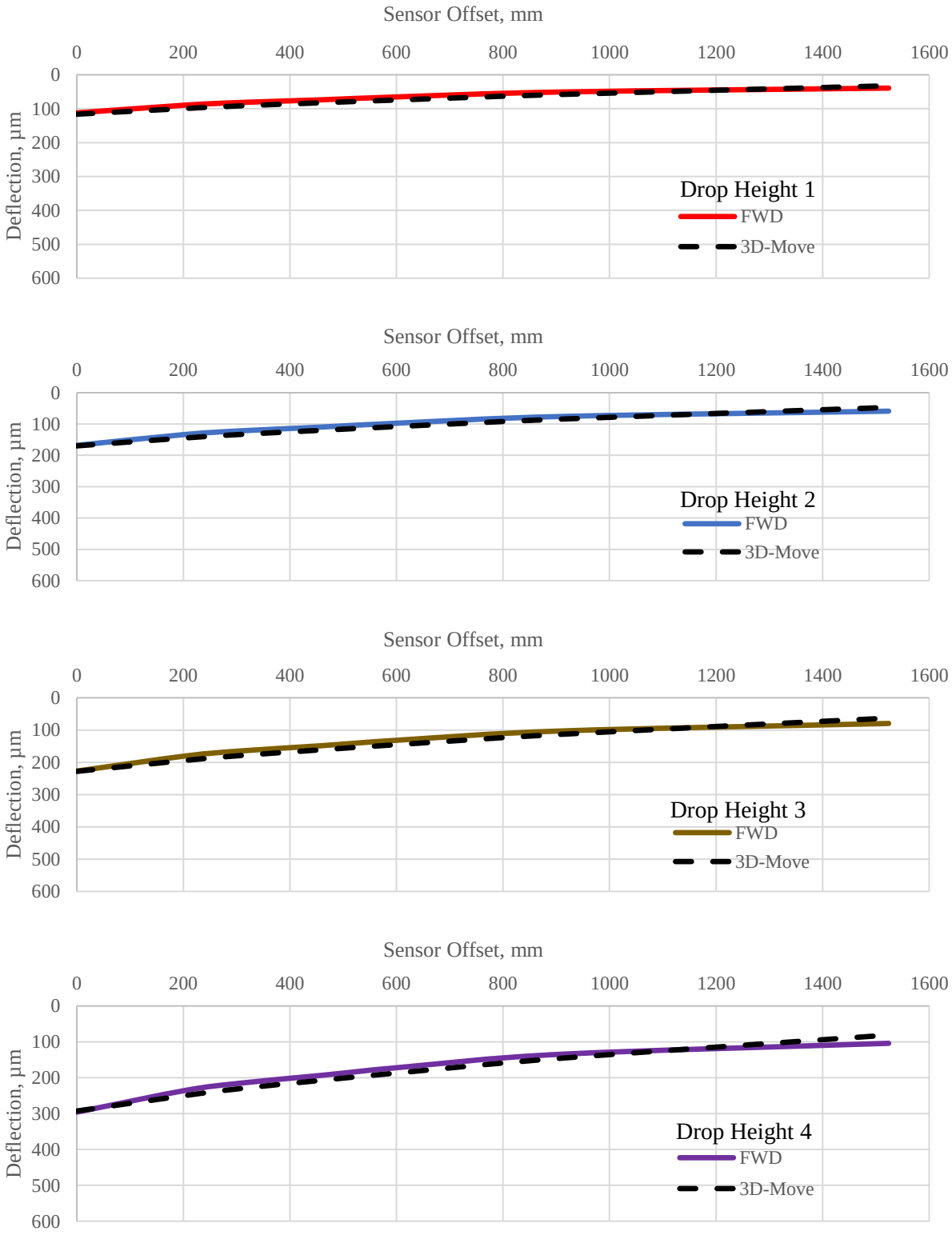

Figure C –30. Simulated Deflection Bowl for the SHRP section 0508.

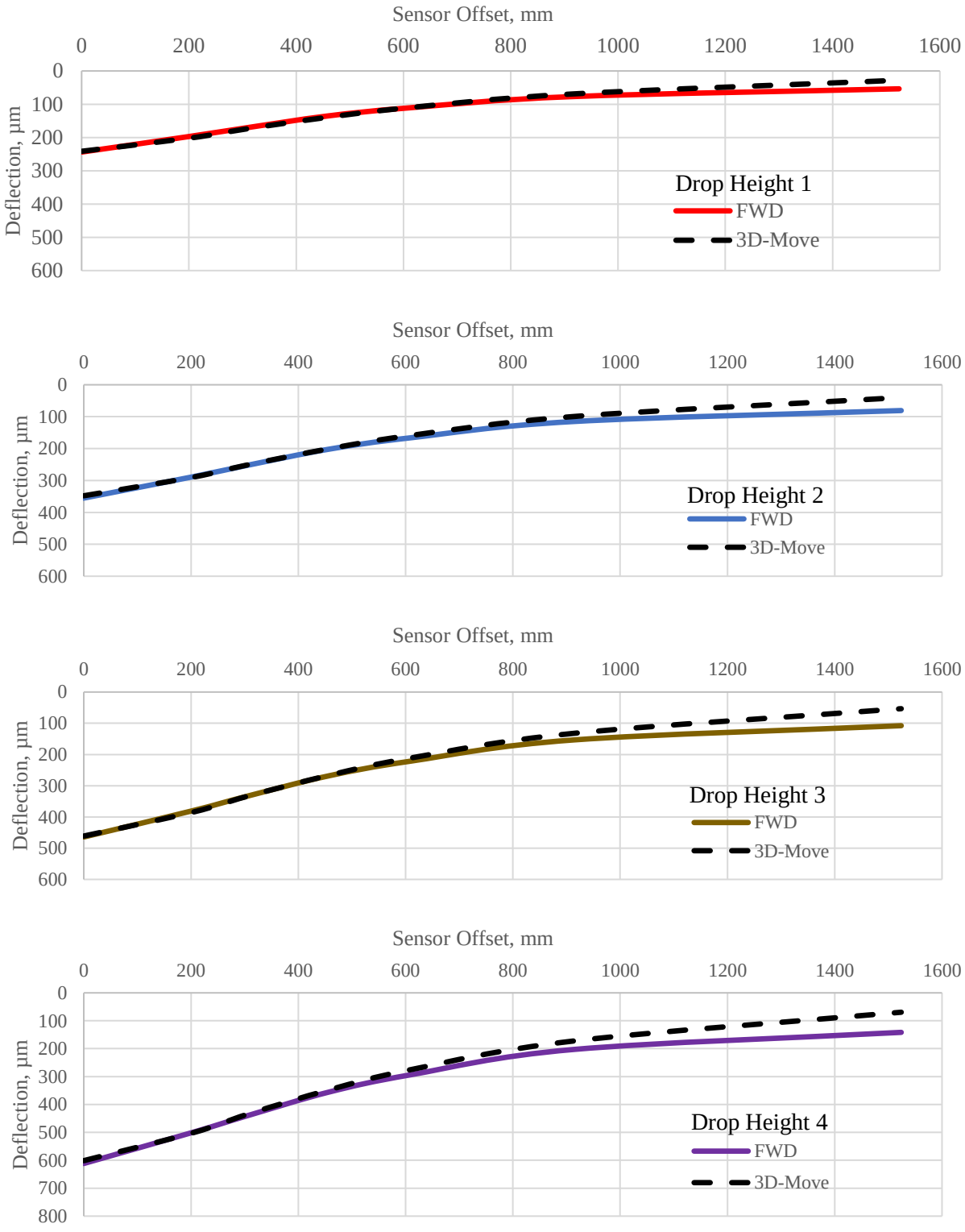

Figure C –31. Simulated Deflection Bowl for the SHRP section 0802.

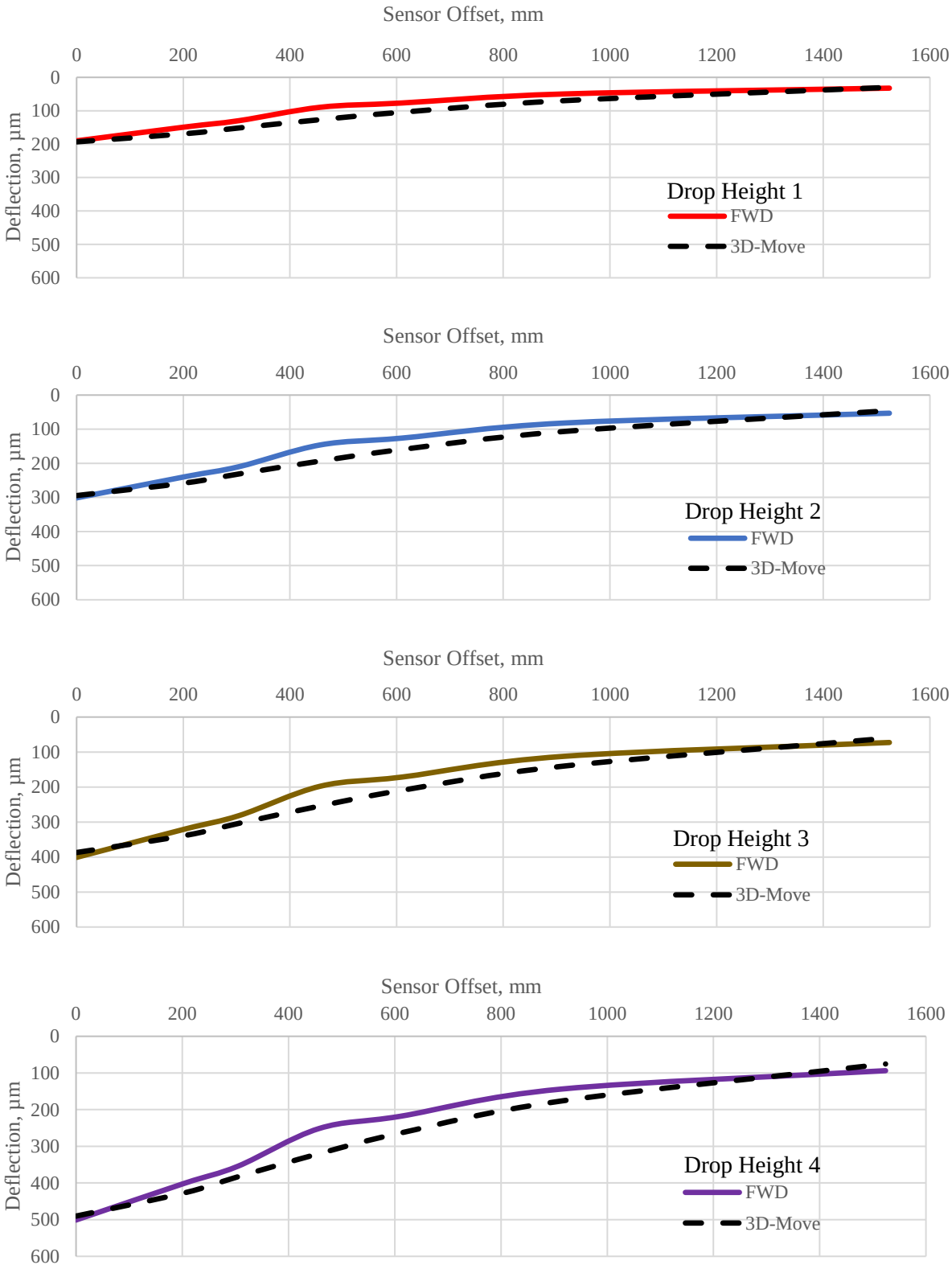

Figure C –32. Simulated Deflection Bowl for the SHRP section 0902.

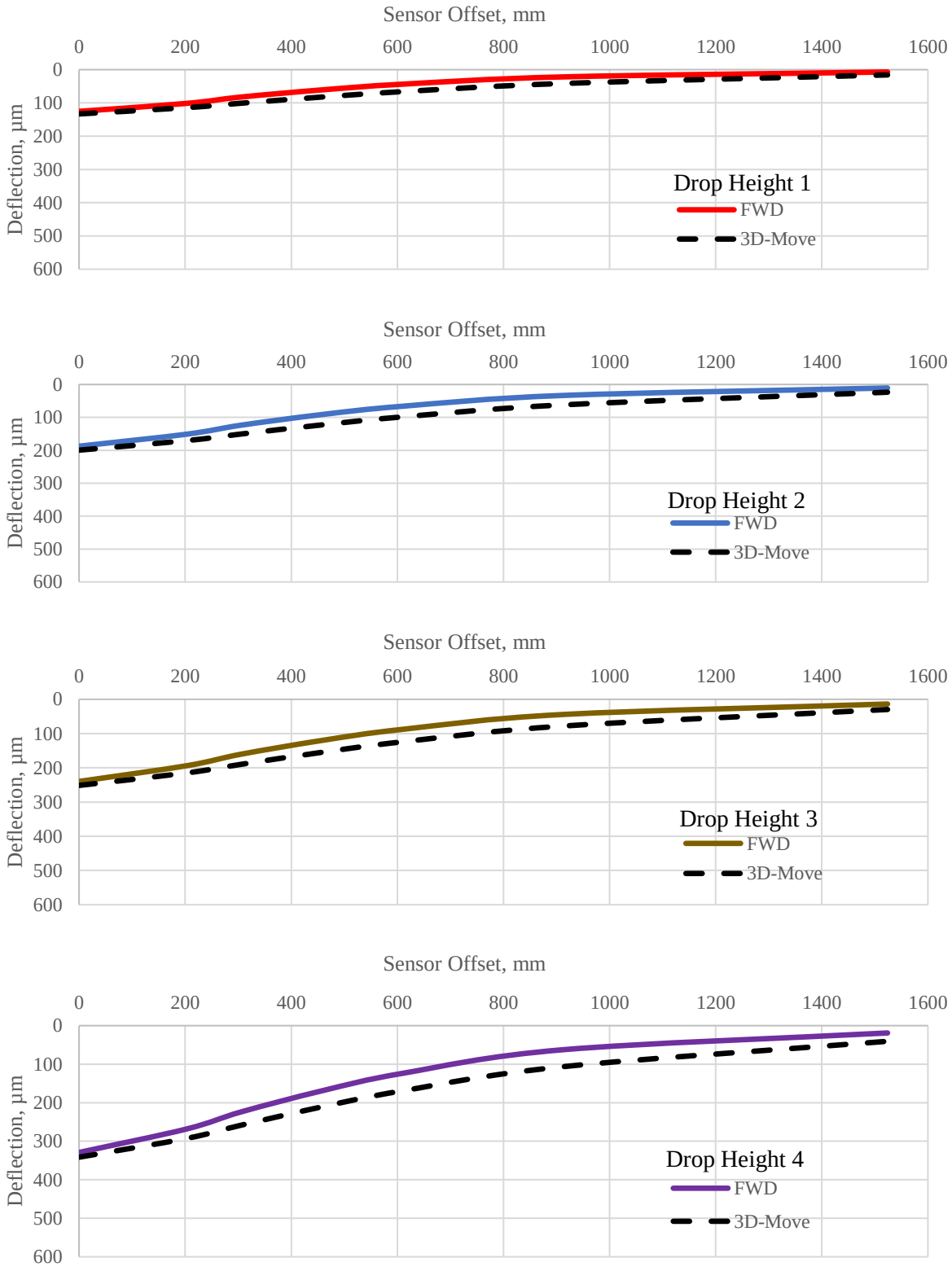

Figure C –33. Simulated Deflection Bowl for the SHRP section 1003.

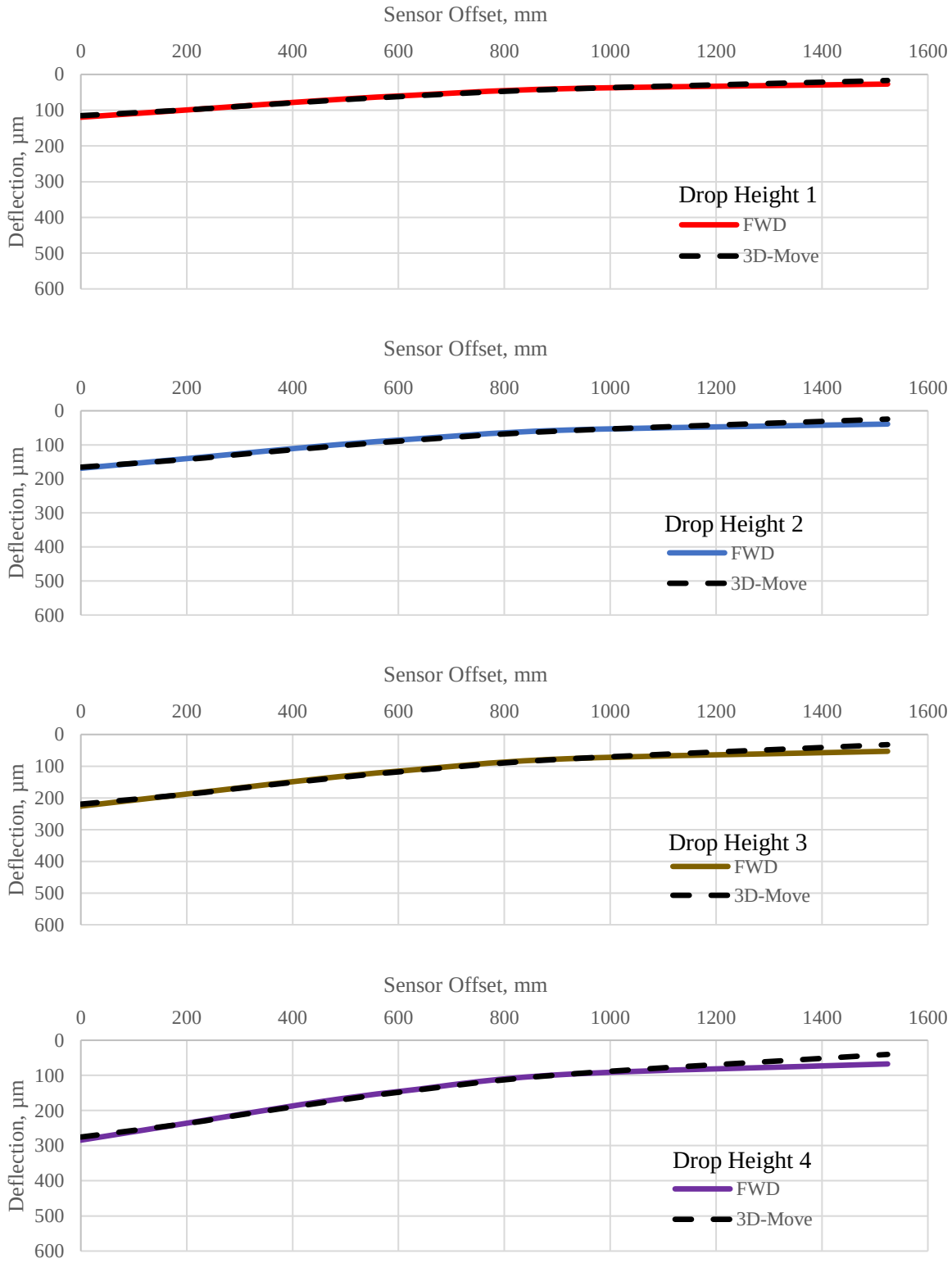

Figure C –34. Simulated Deflection Bowl for the SHRP section 1005.

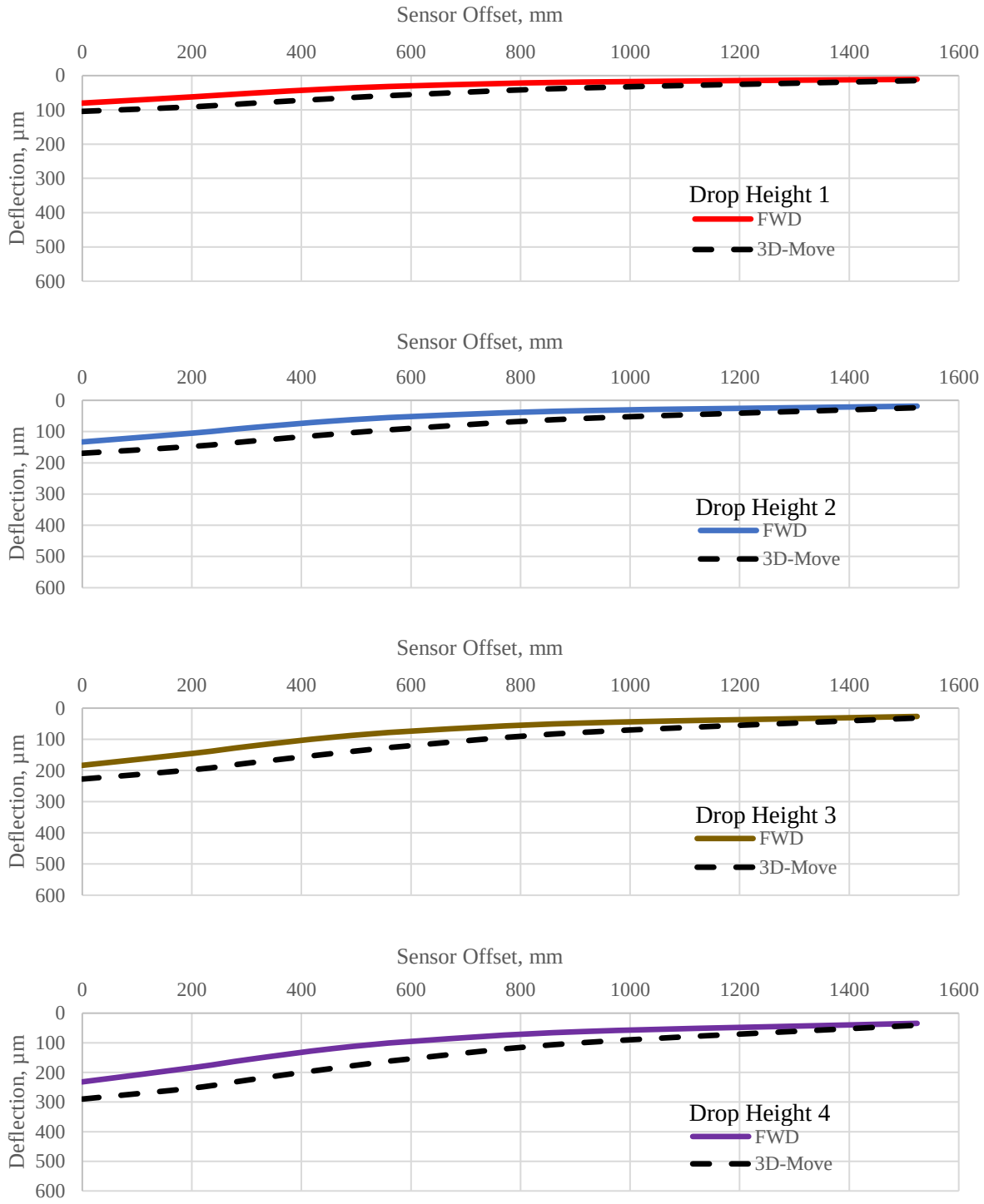

Figure C –35. Simulated Deflection Bowl for the SHRP section 1112.

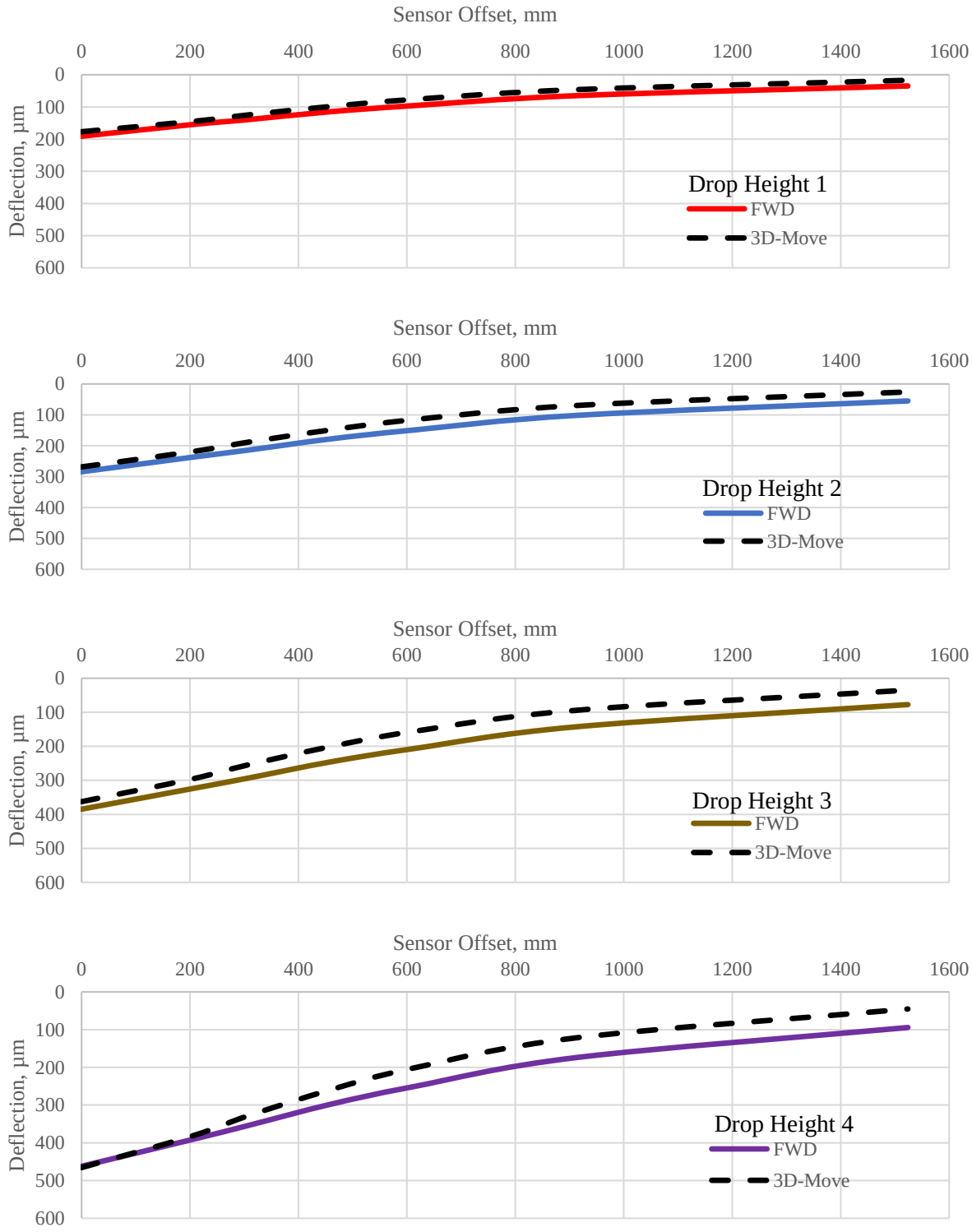

Figure C –36. Simulated Deflection Bowl for the SHRP section 6401.

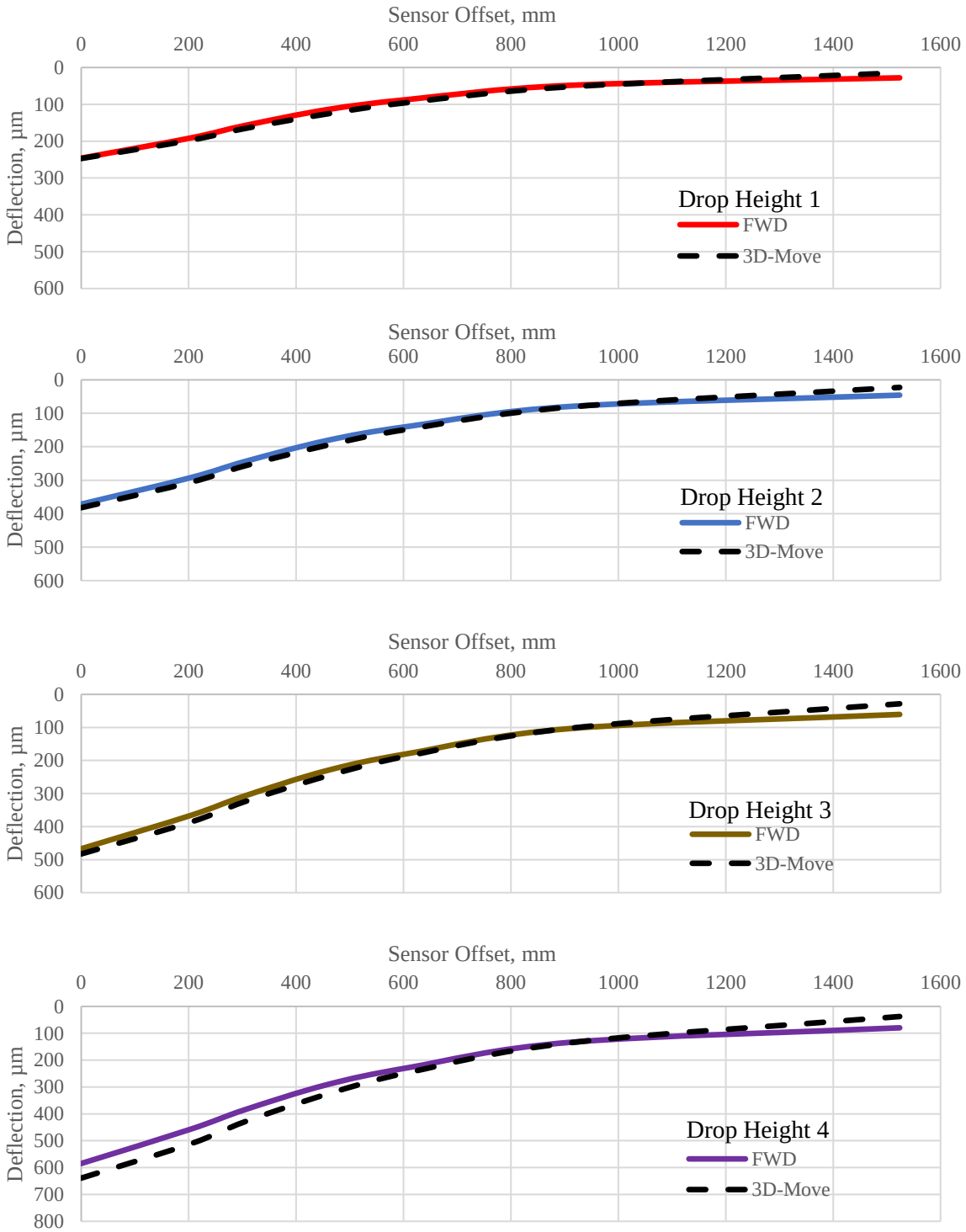

Figure C –37. Simulated Deflection Bowl for the SHRP section 2118.

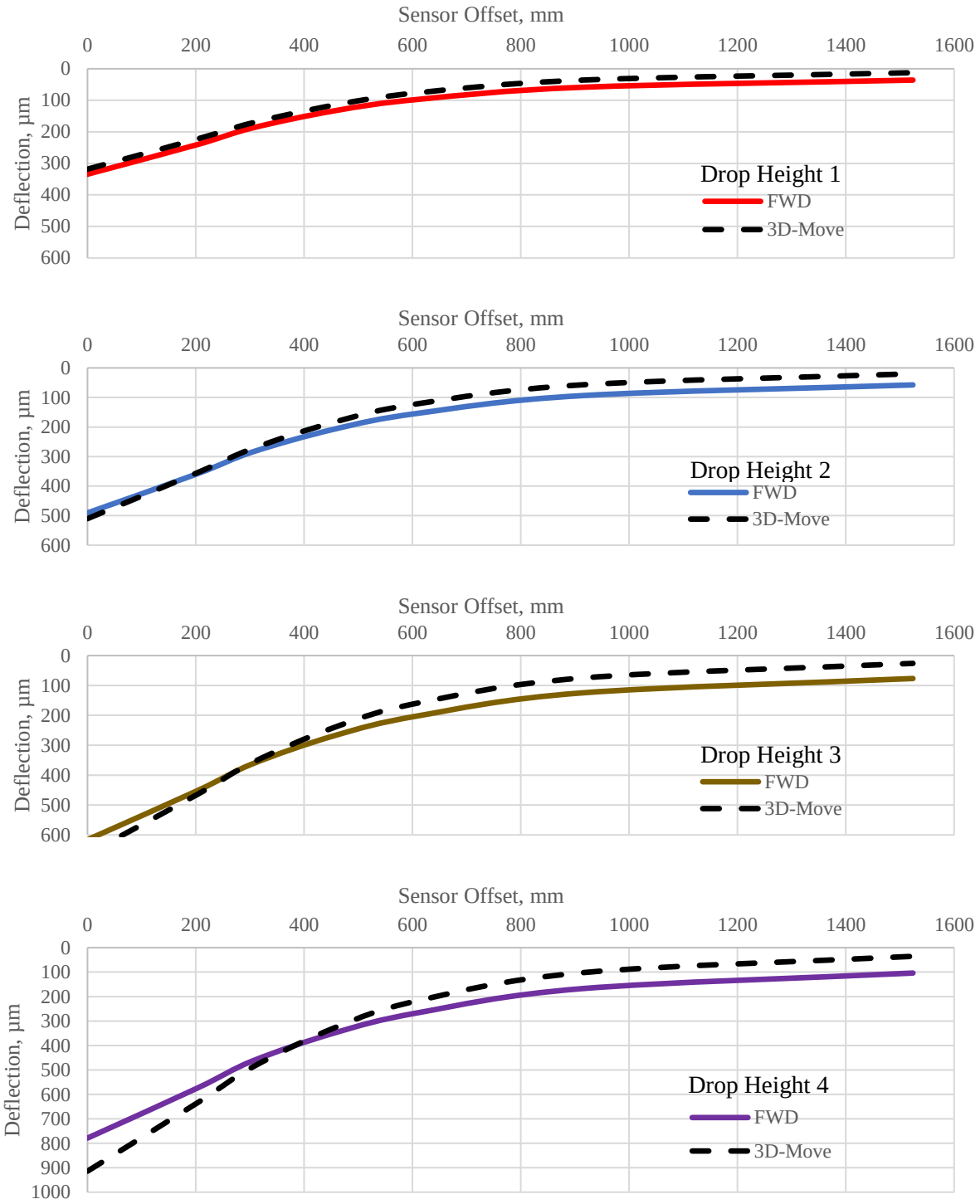

Figure C –38. Simulated Deflection Bowl for the SHRP section 6035.

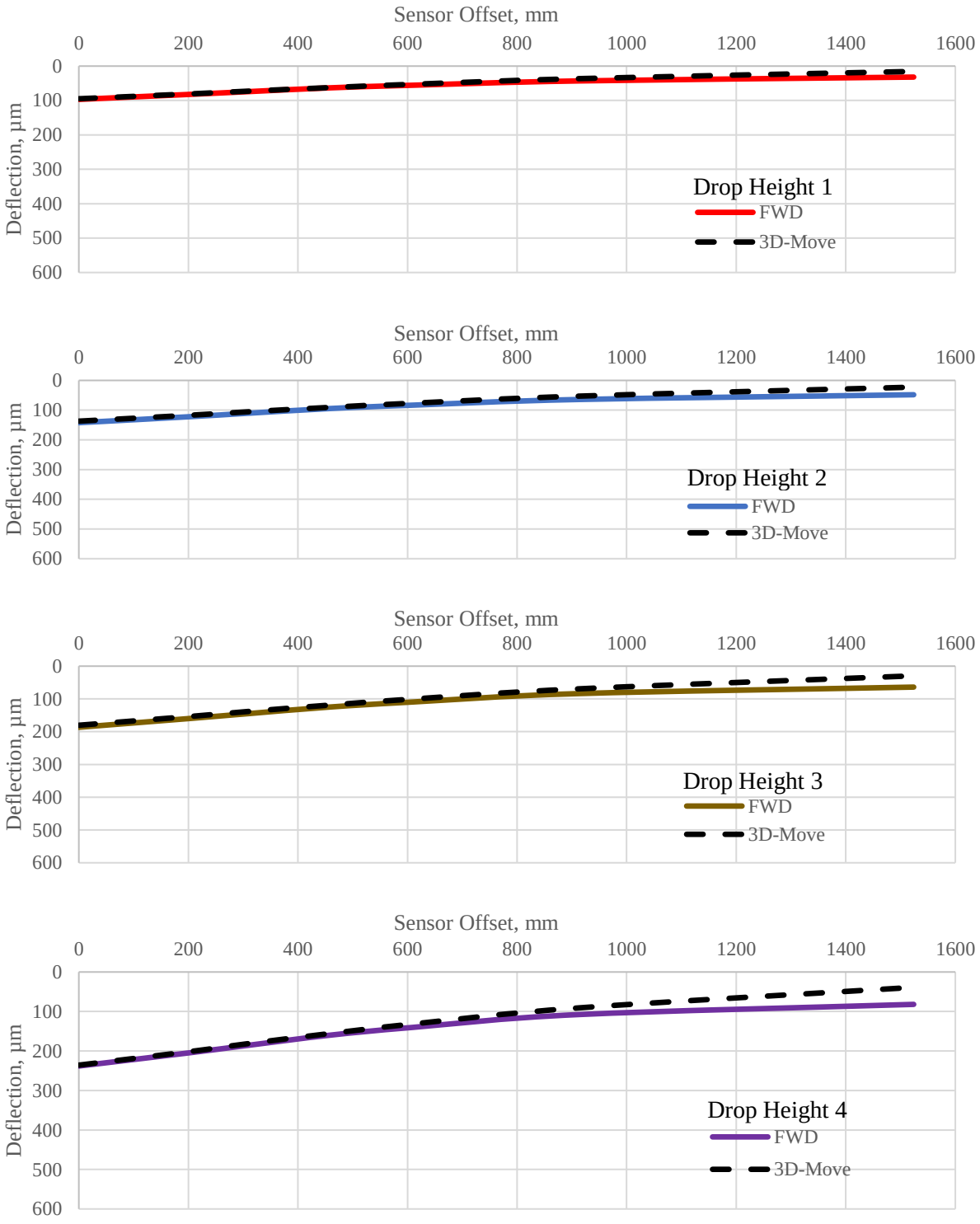

Figure C –39. Simulated Deflection Bowl for the SHRP section AA01

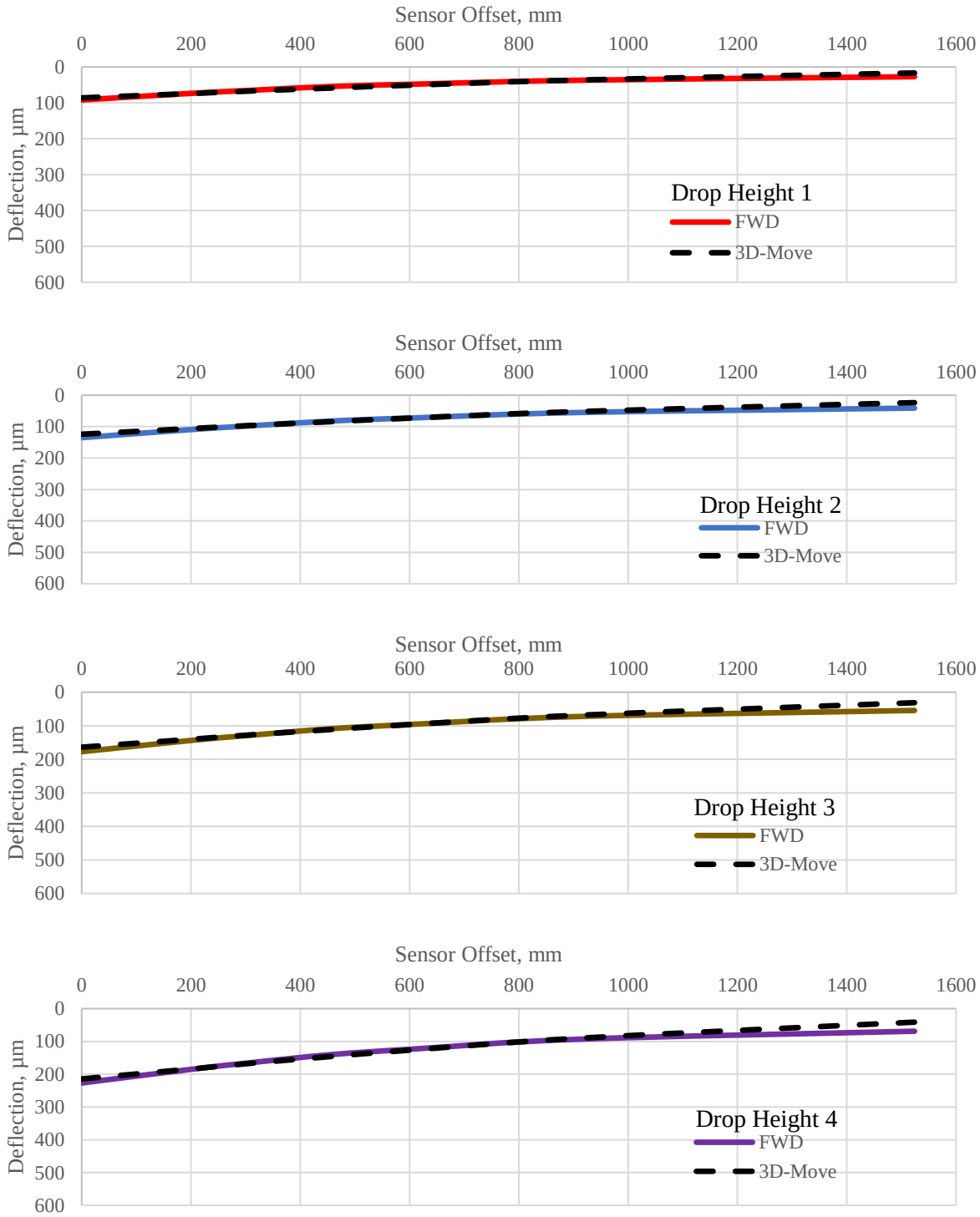

Figure C –40. Simulated Deflection Bowl for the SHRP section AA02.

AA03

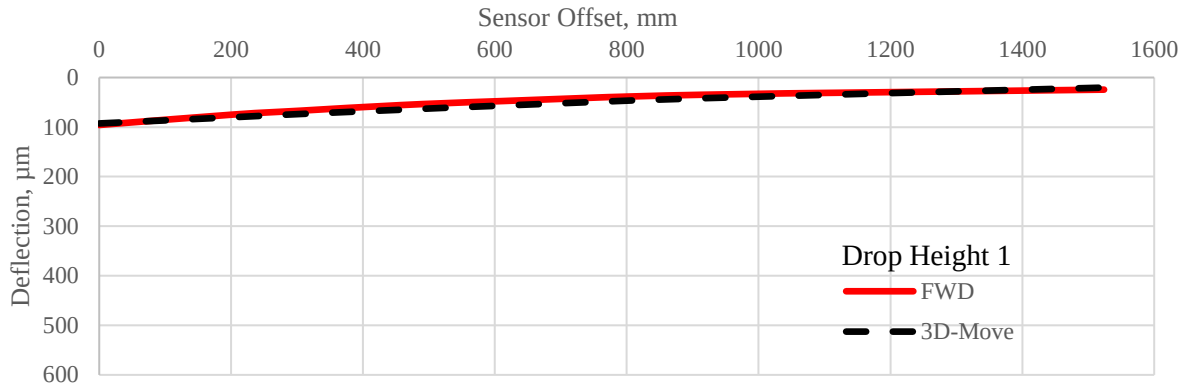

Figure C –41. Simulated Deflection Bowl for the SHRP section AA03.

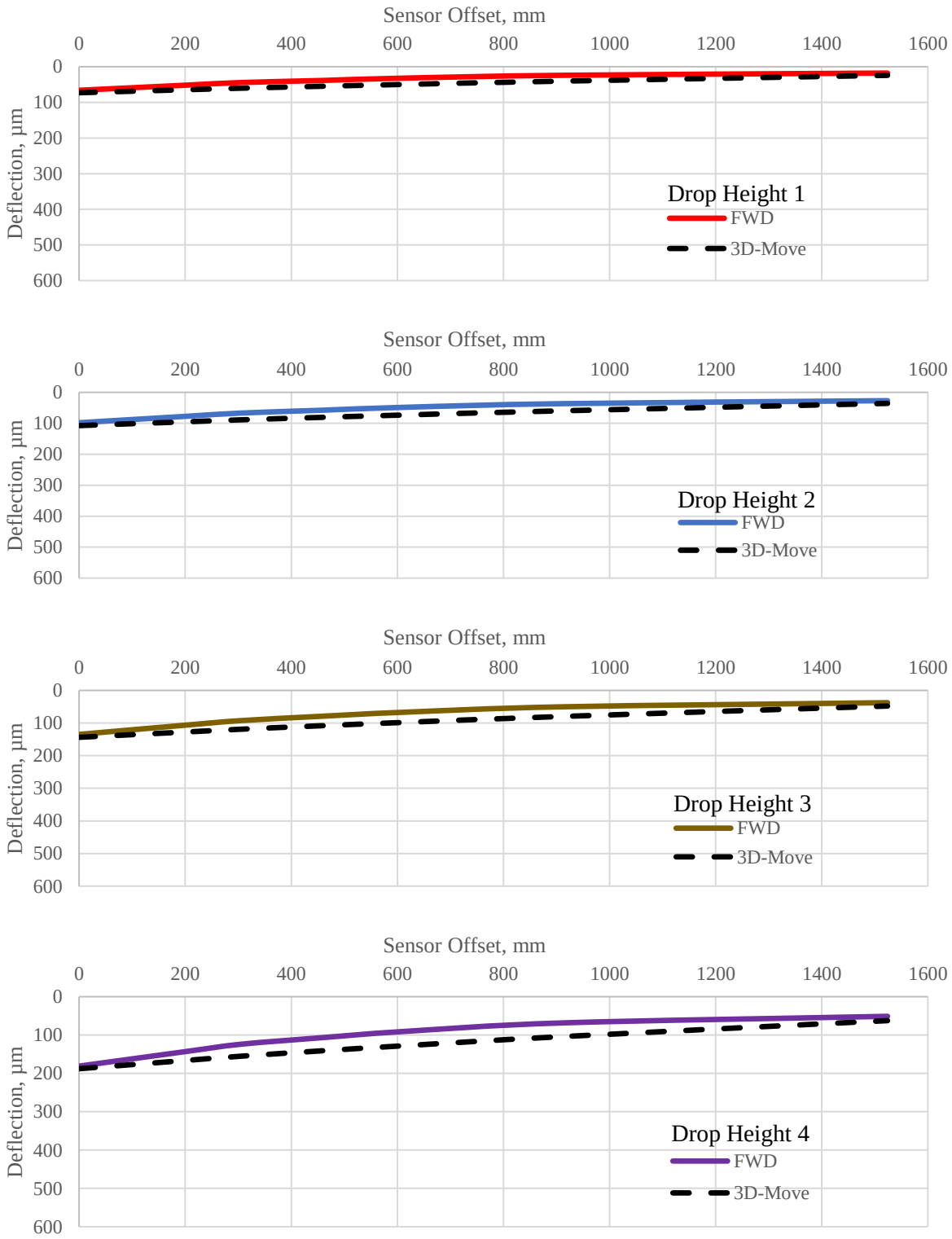

Figure C –42. Simulated Deflection Bowl for the SHRP section 0115.

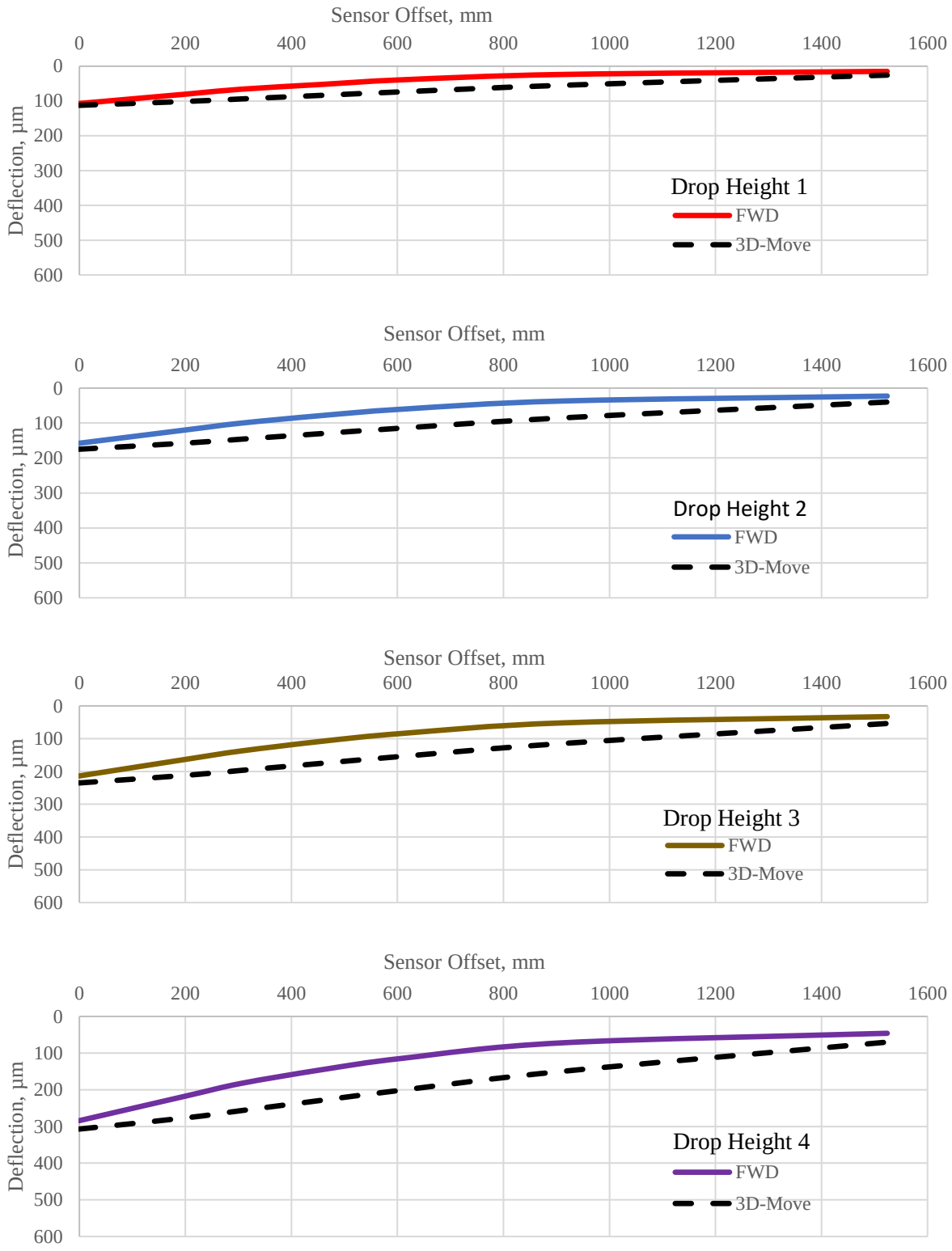

Figure C –43. Simulated Deflection Bowl for the SHRP section 0117.

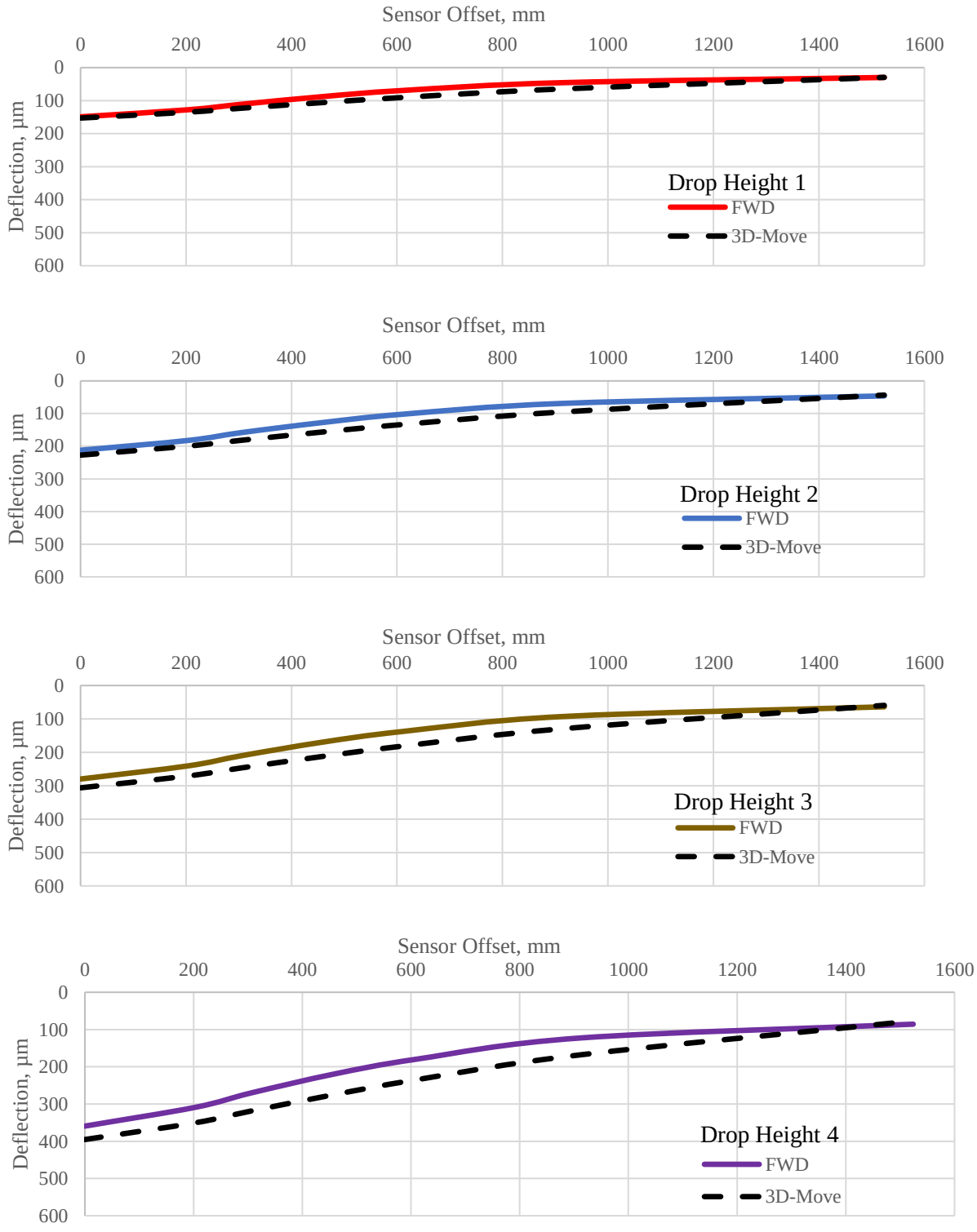

Figure C –44. Simulated Deflection Bowl for the SHRP section 0120.

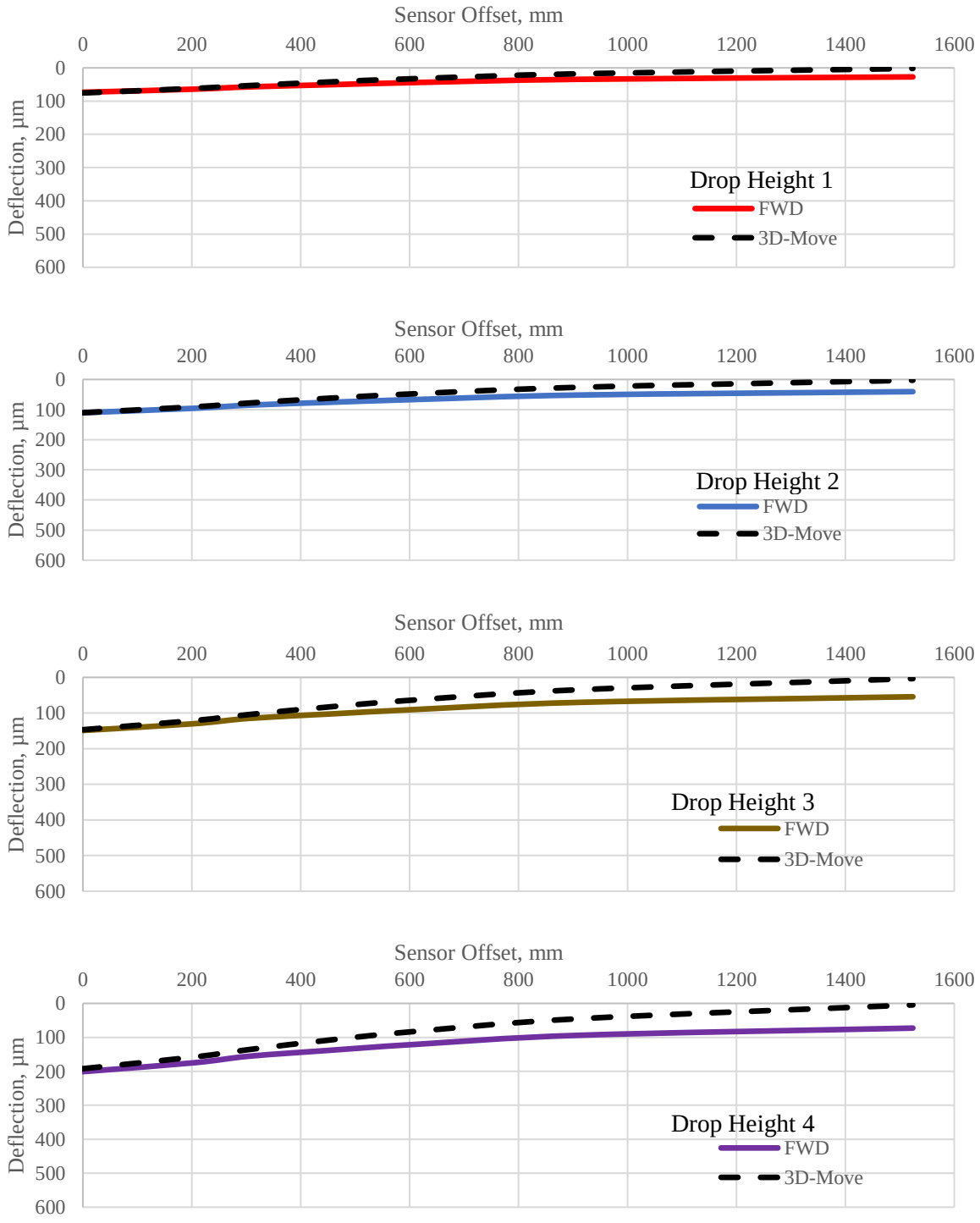

Figure C –45. Simulated Deflection Bowl for the SHRP section 0122.

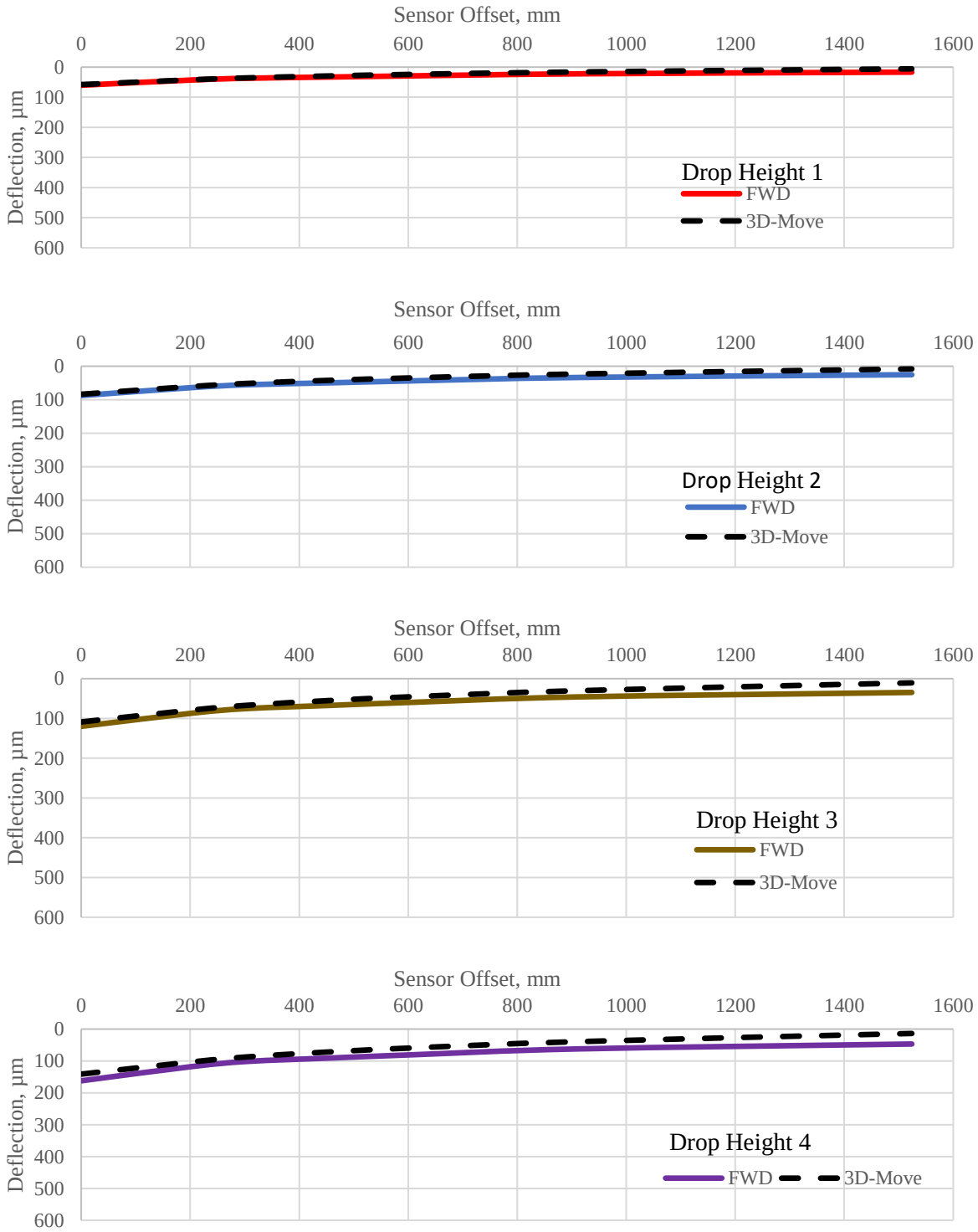

Figure C –46. Simulated Deflection Bowl for the SHRP section 0123.

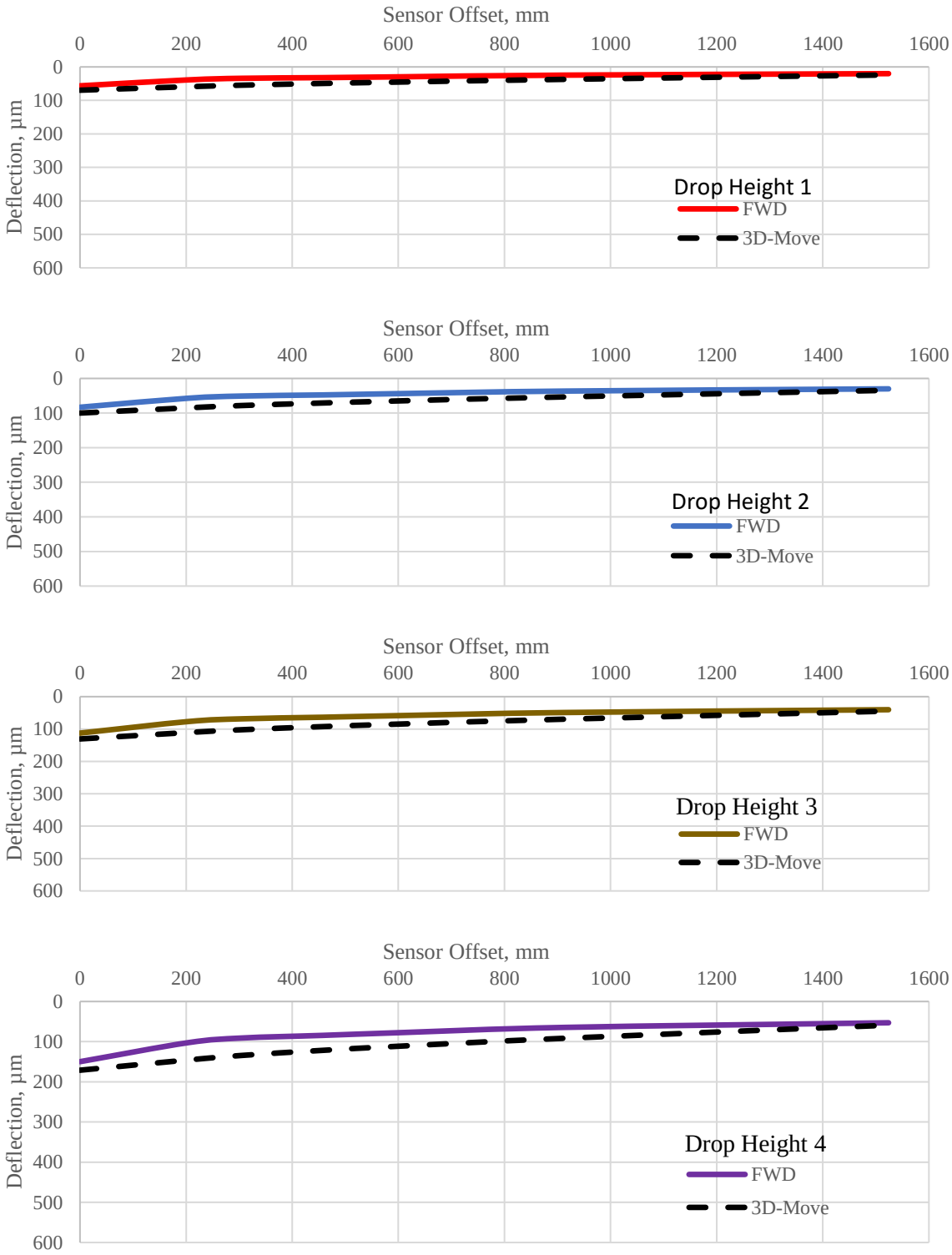

Figure C –47. Simulated Deflection Bowl for the SHRP section 0124.

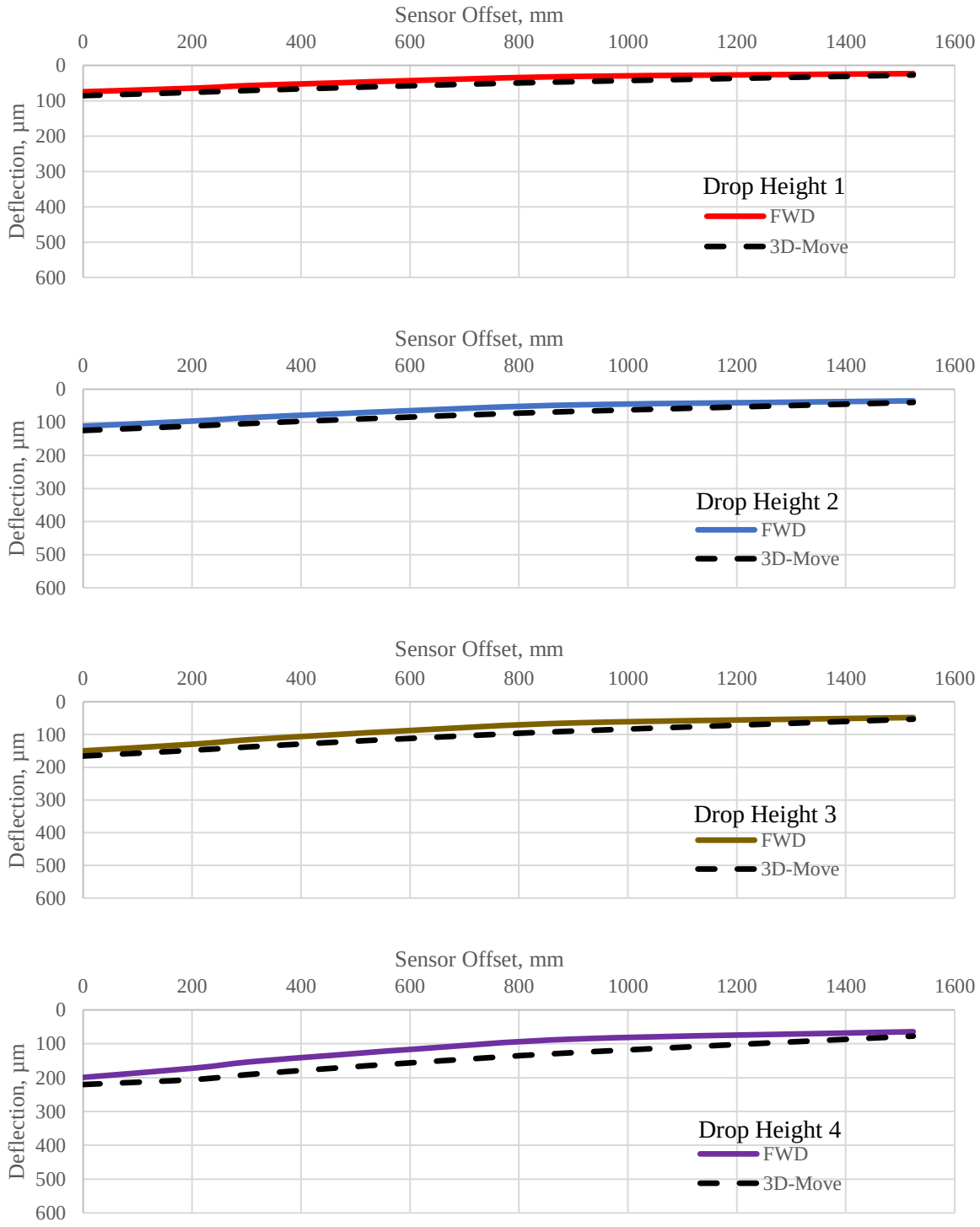

Figure C –48. Simulated Deflection Bowl for the SHRP section 0160.

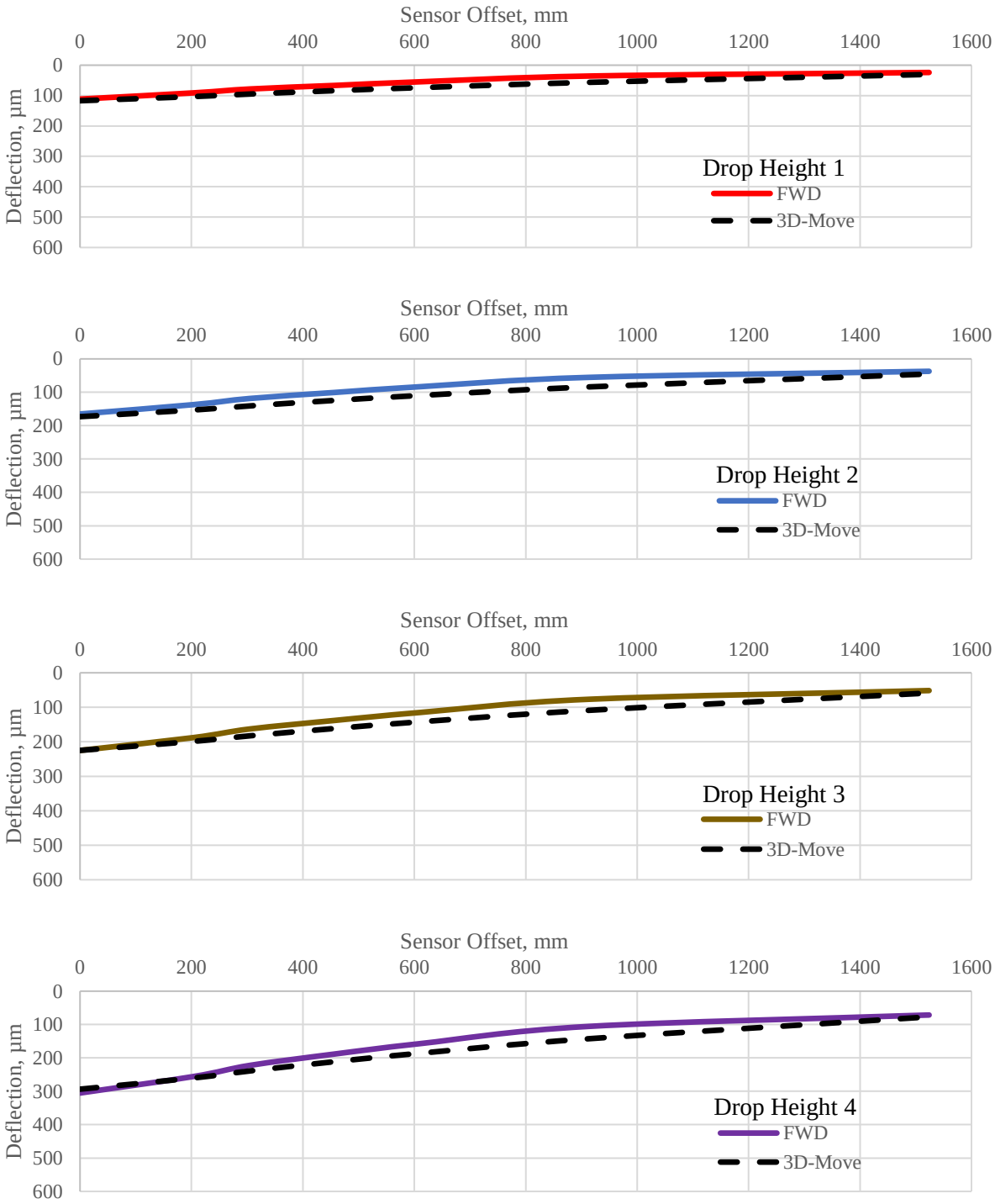

Figure C –49. Simulated Deflection Bowl for the SHRP section 0502.

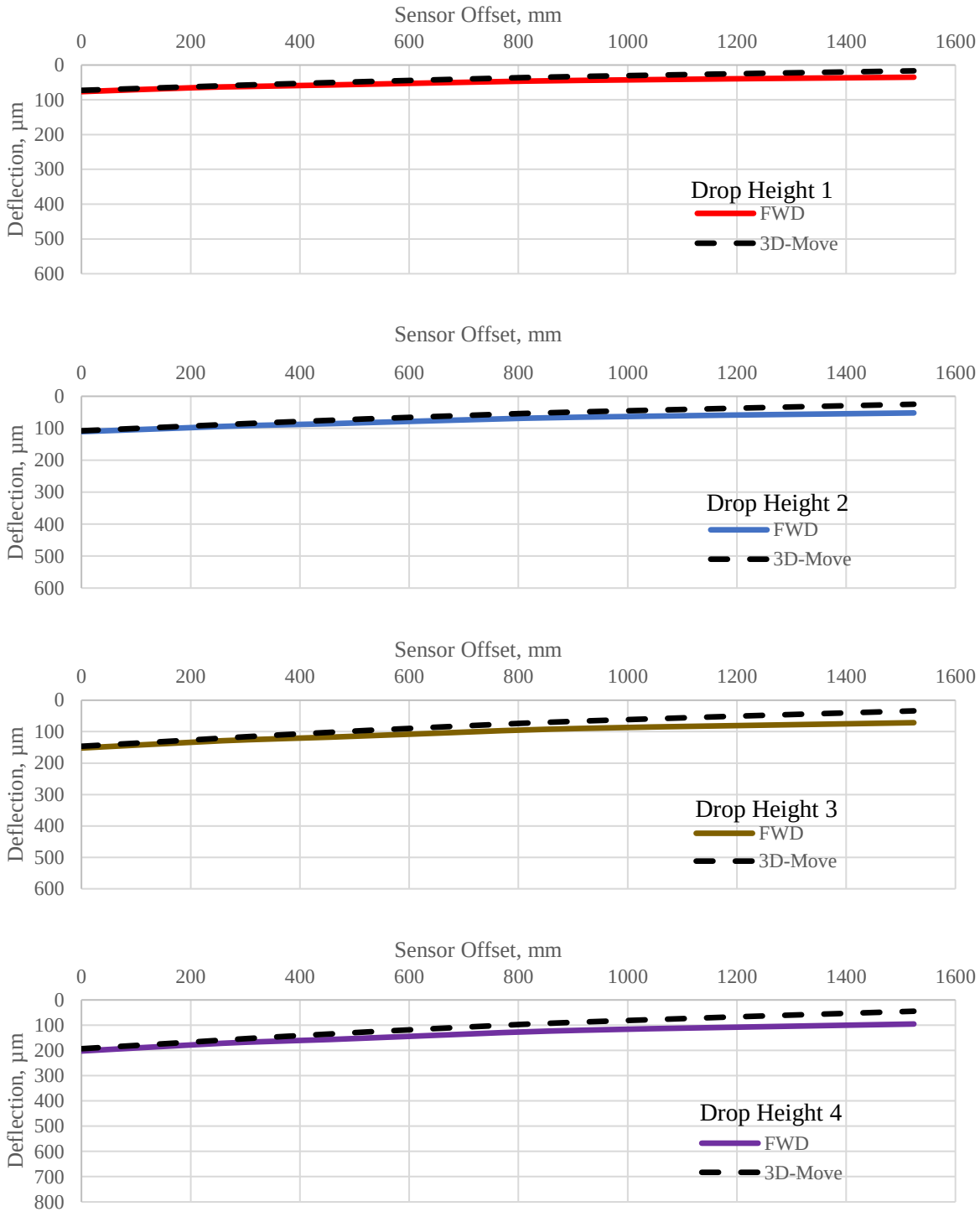

Figure C –50. Simulated Deflection Bowl for the SHRP section 0504.

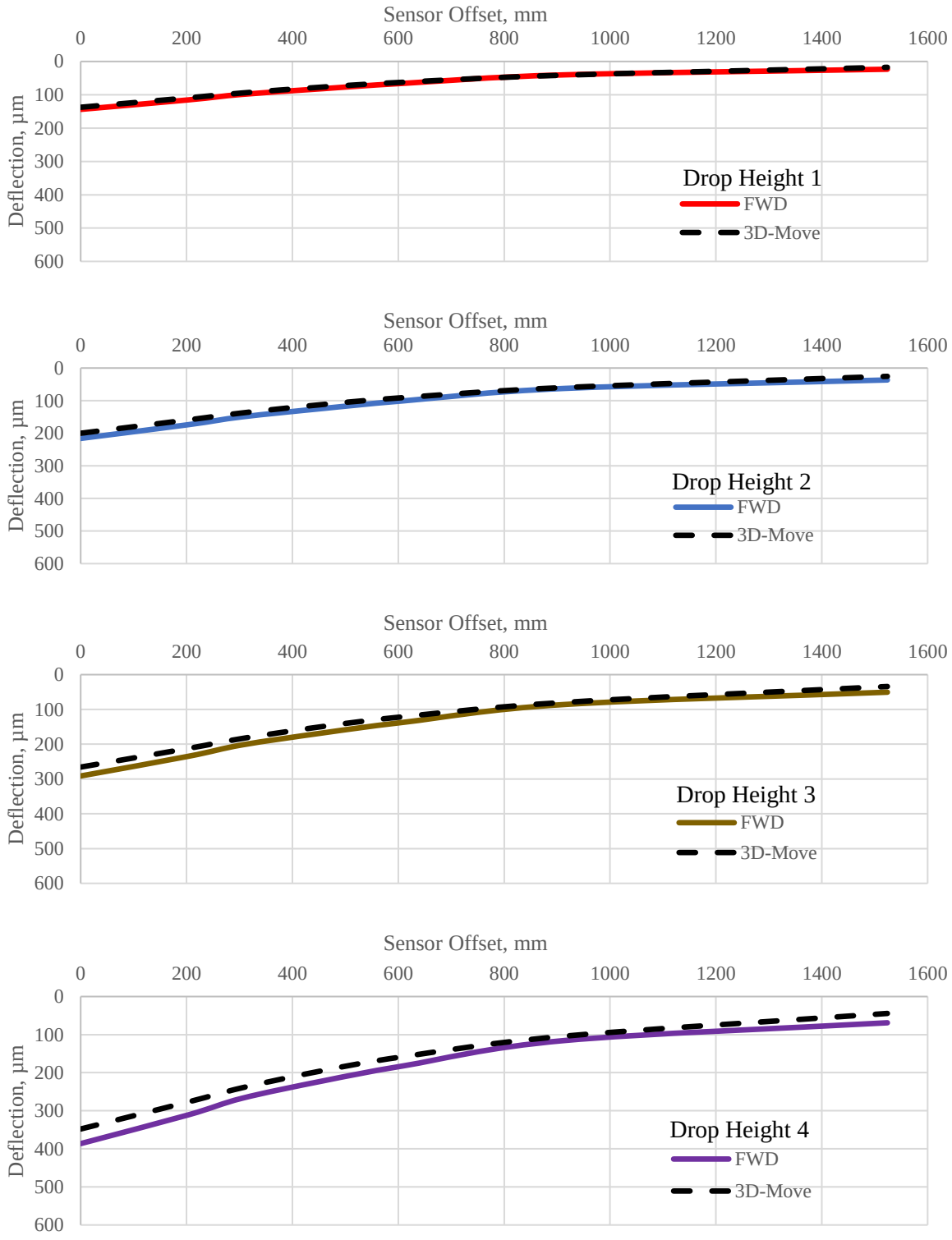

Figure C –51. Simulated Deflection Bowl for the SHRP section 0505.

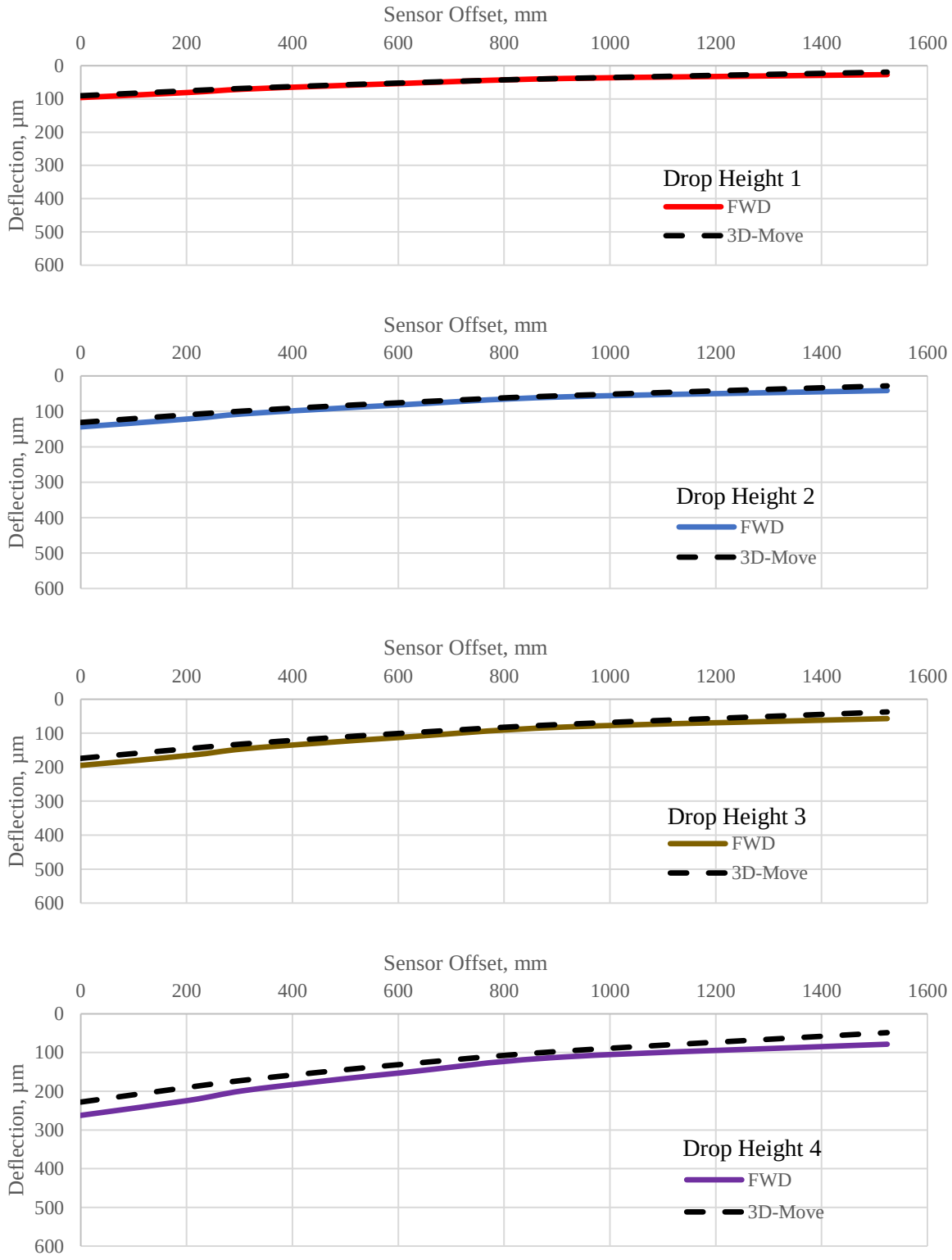

Figure C –52. Simulated Deflection Bowl for the SHRP section 0507.

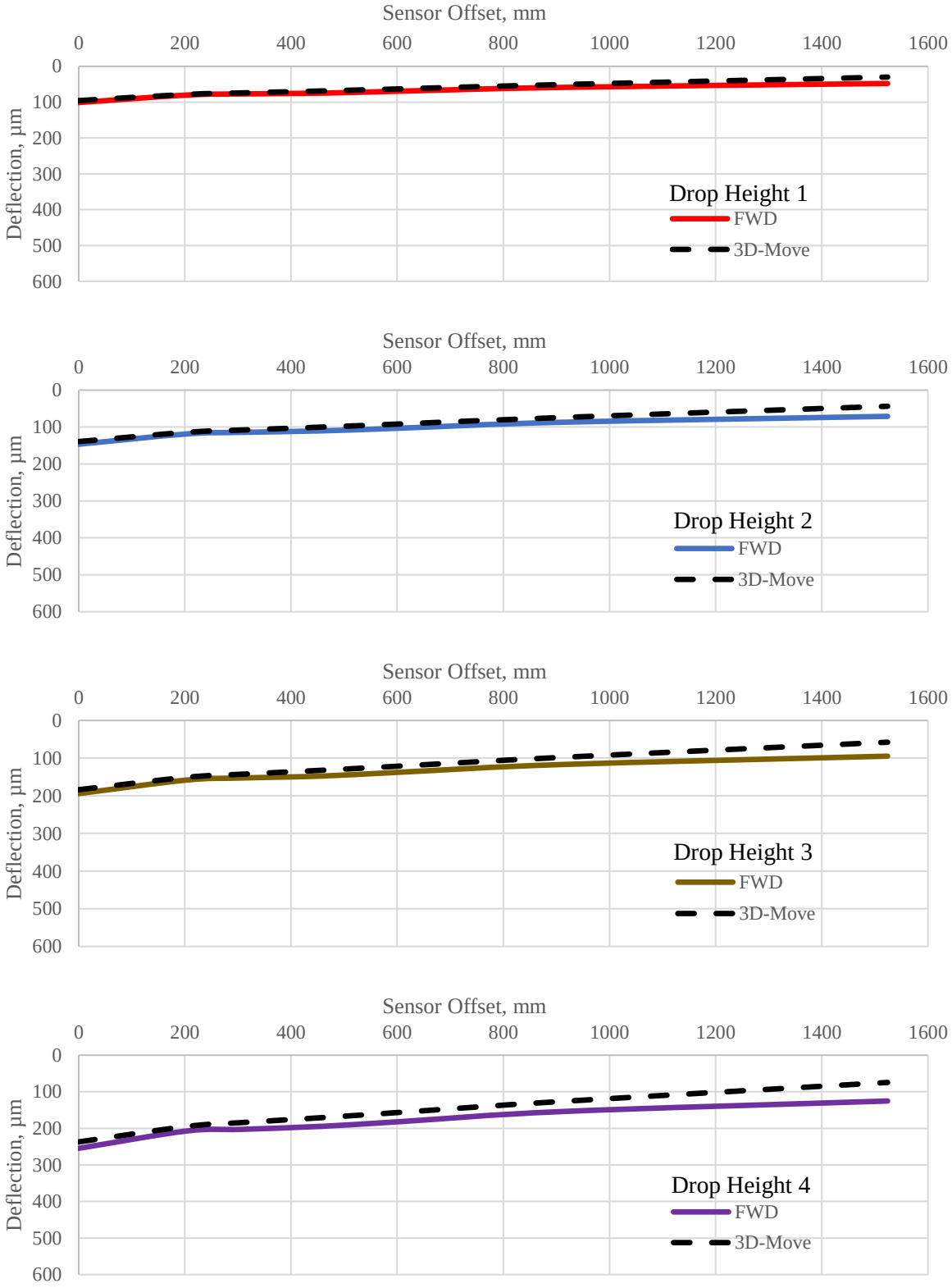

Figure C –53. Simulated Deflection Bowl for the SHRP section 0606.

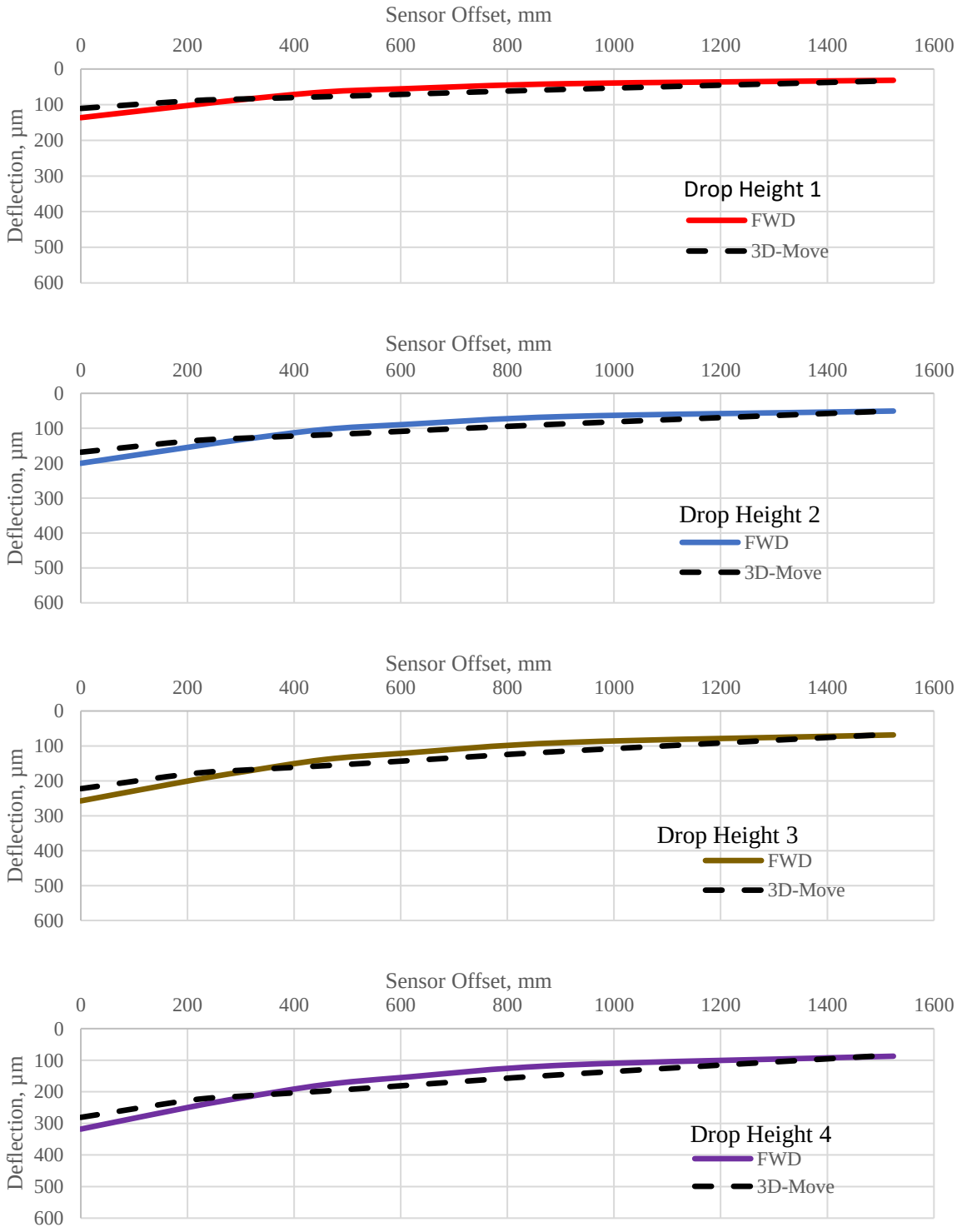

Figure C –54. Simulated Deflection Bowl for the SHRP section 0607.

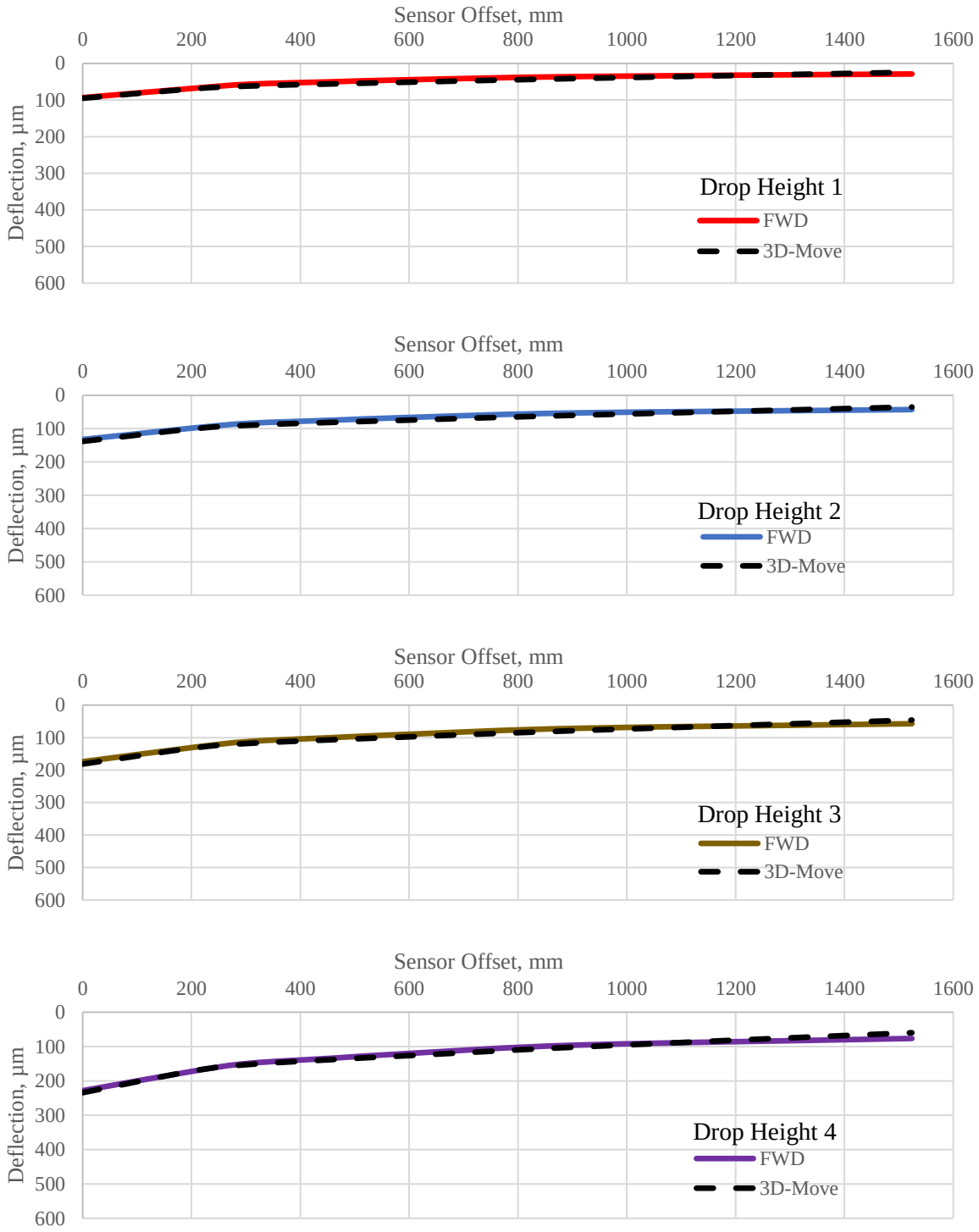

Figure C –55. Simulated Deflection Bowl for the SHRP section 0608.

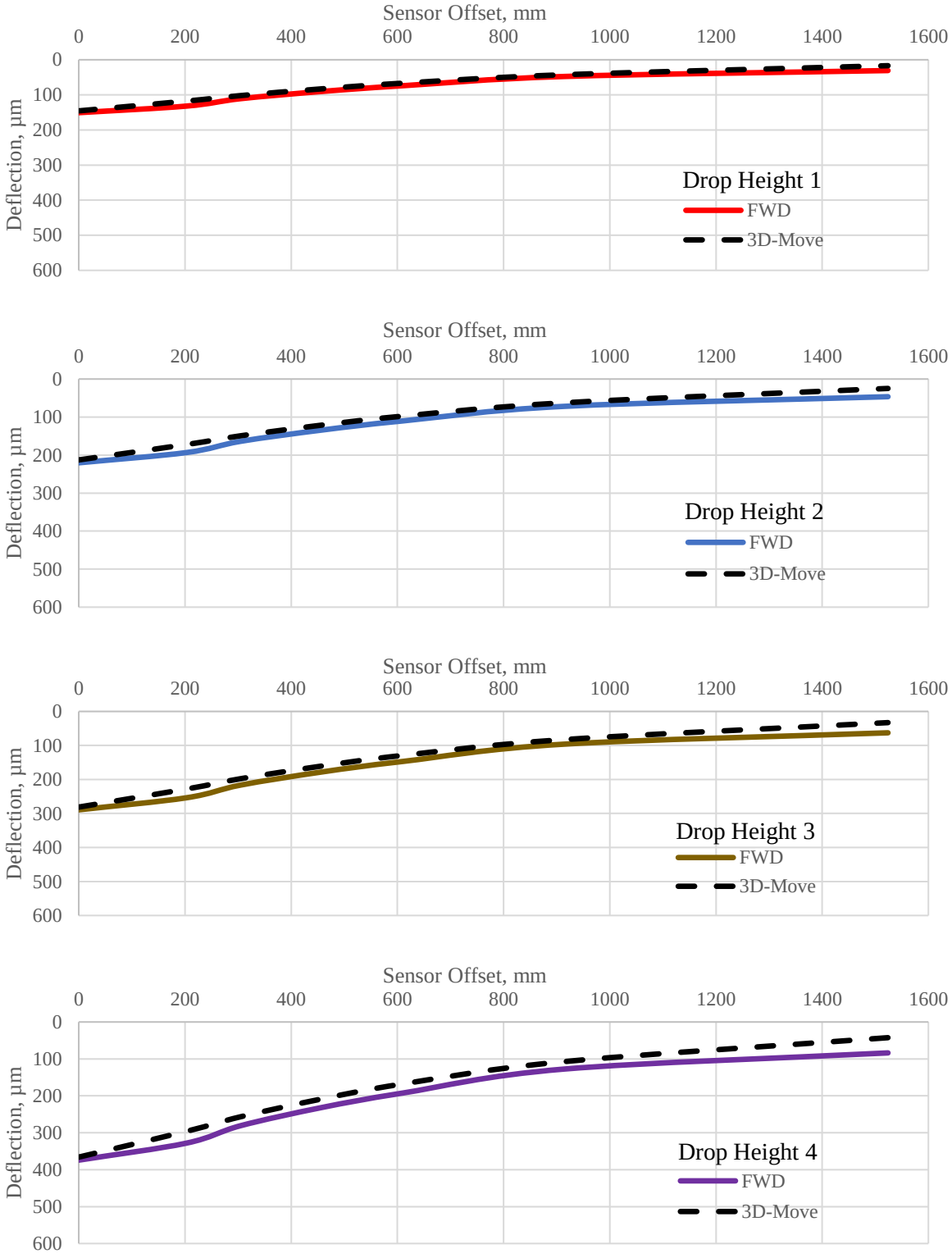

Figure C –56. Simulated Deflection Bowl for the SHRP section 1015.

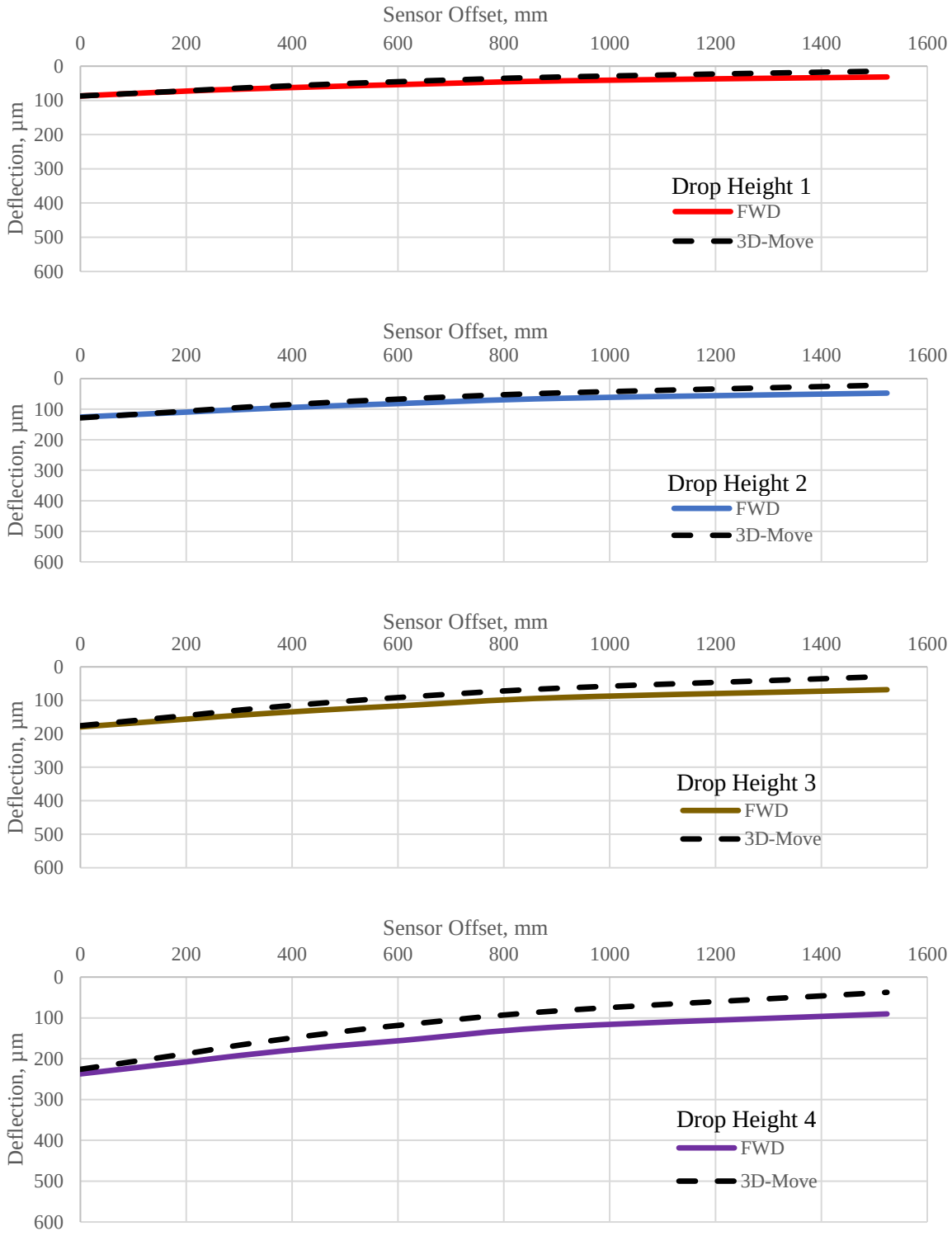

Figure C –57. Simulated Deflection Bowl for the SHRP section 4086.

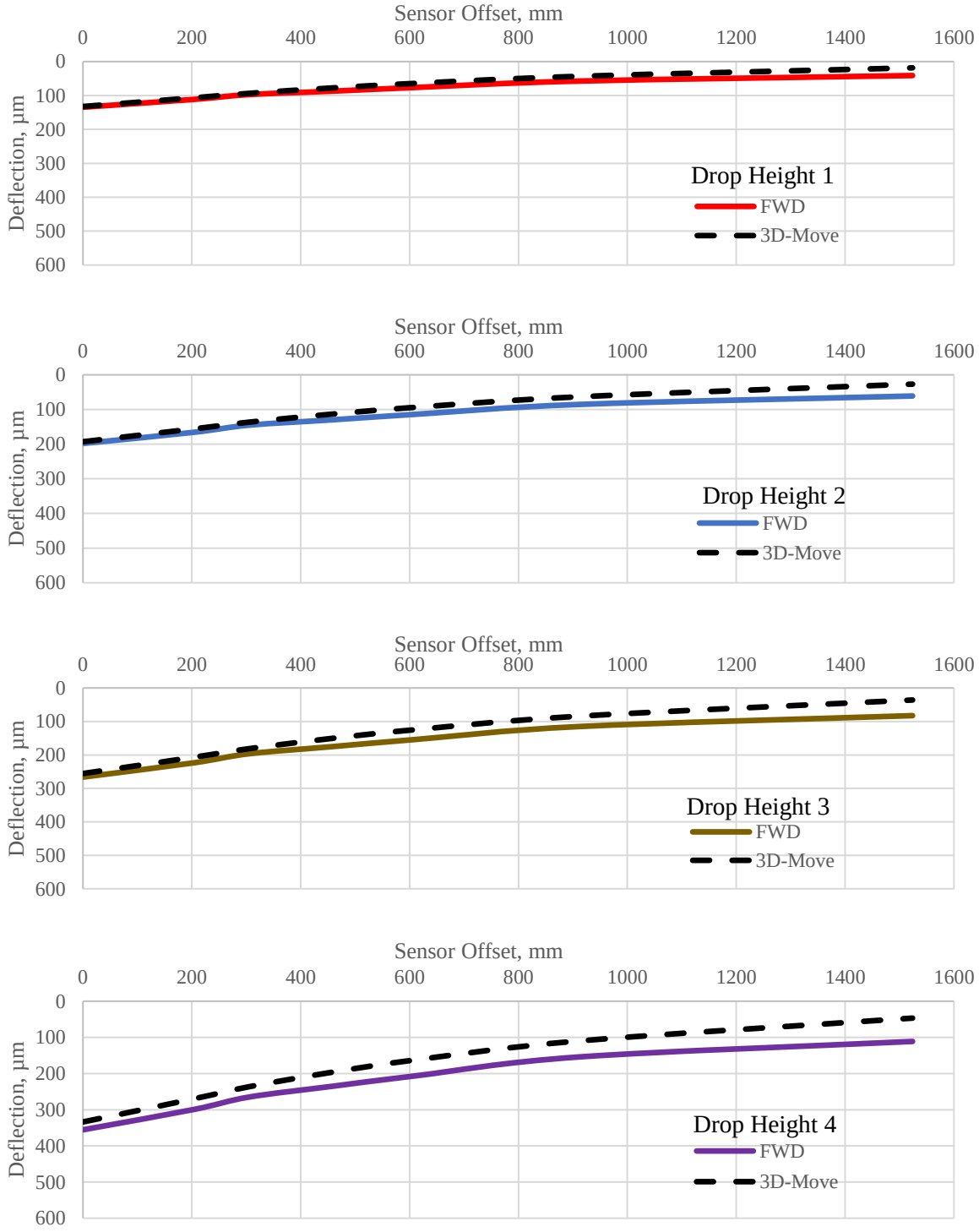

Figure C –58. Simulated Deflection Bowl for the SHRP section 4087.

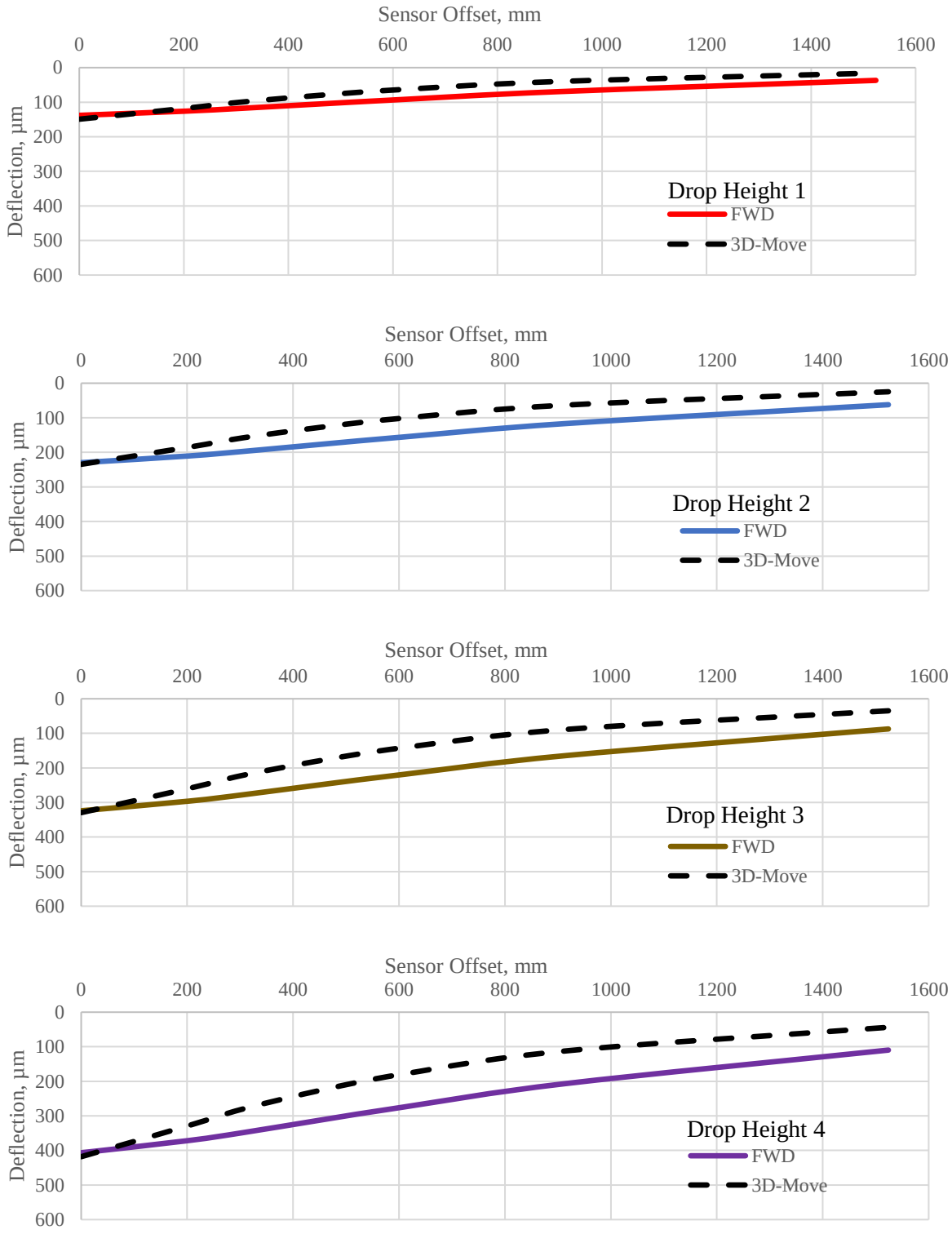

Figure C –59. Simulated Deflection Bowl for the SHRP section 4161.

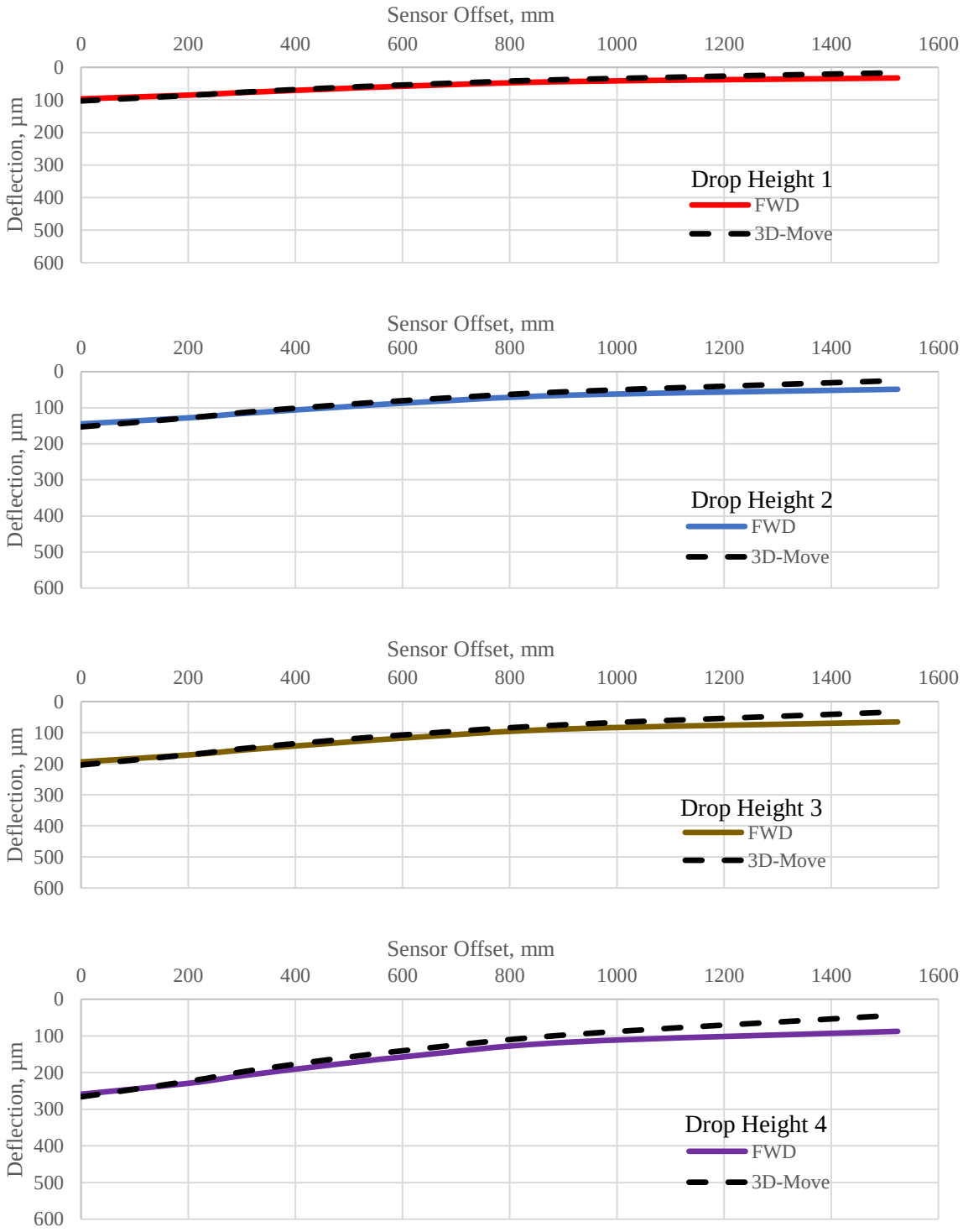

Figure C –60. Simulated Deflection Bowl for the SHRP section 4163.

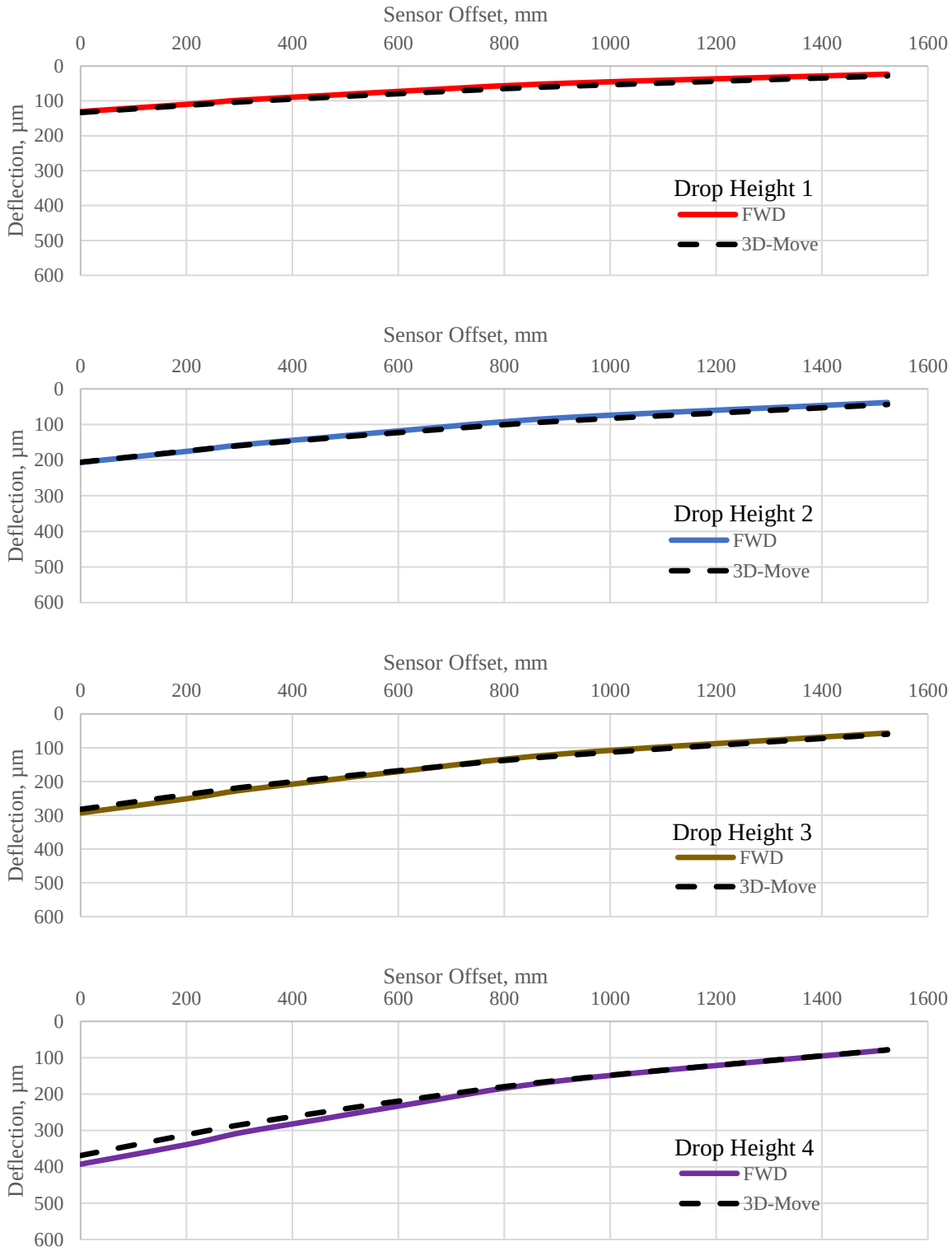

Figure C –61. Simulated Deflection Bowl for the SHRP section 6010.

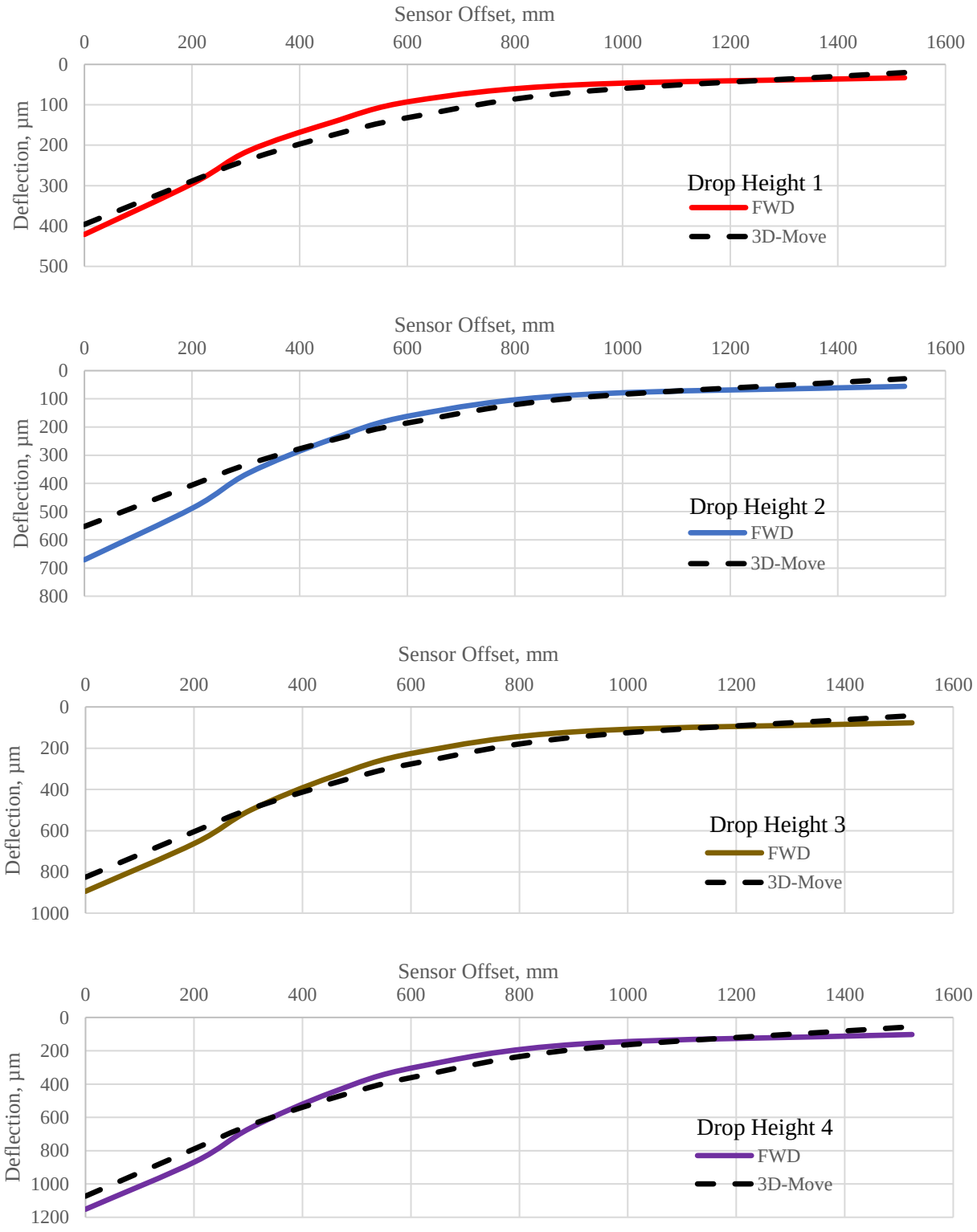

Figure C –62. Simulated Deflection Bowl for the SHRP section AA62.

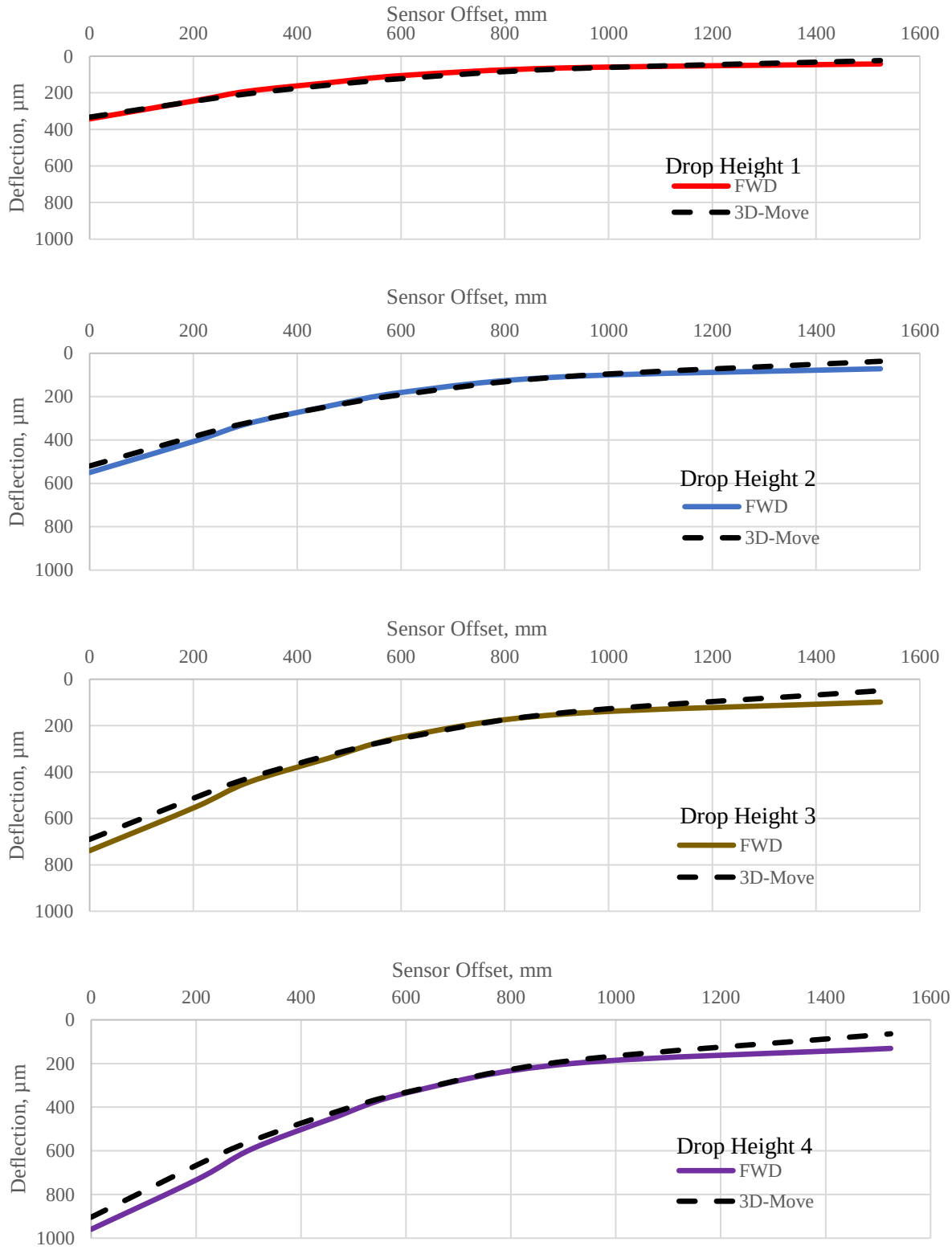

Figure C –63. Simulated Deflection Bowl for the SHRP section AA63.

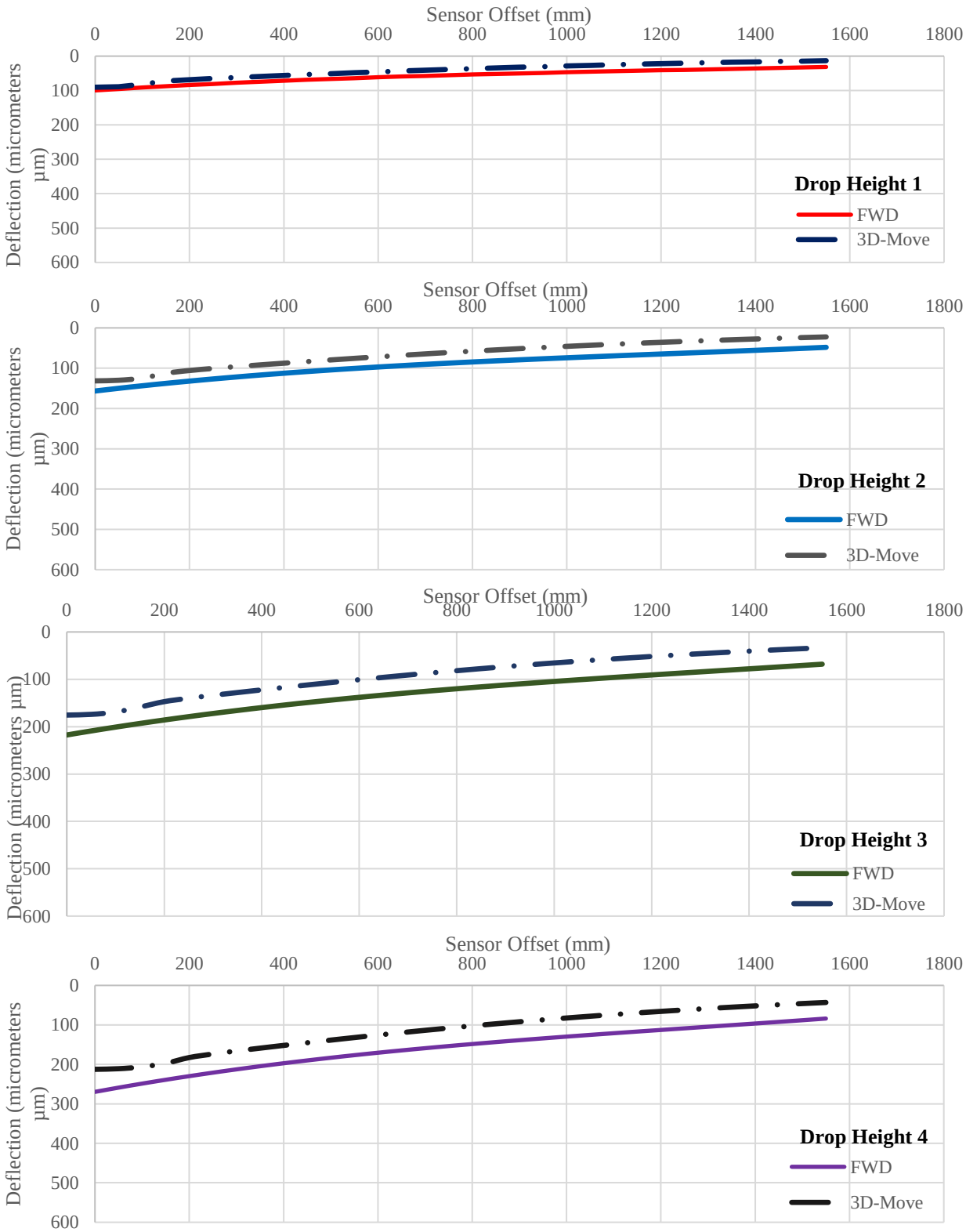

Figure C – 64. Simulated Deflection Bowl for the SHRP section 1046.

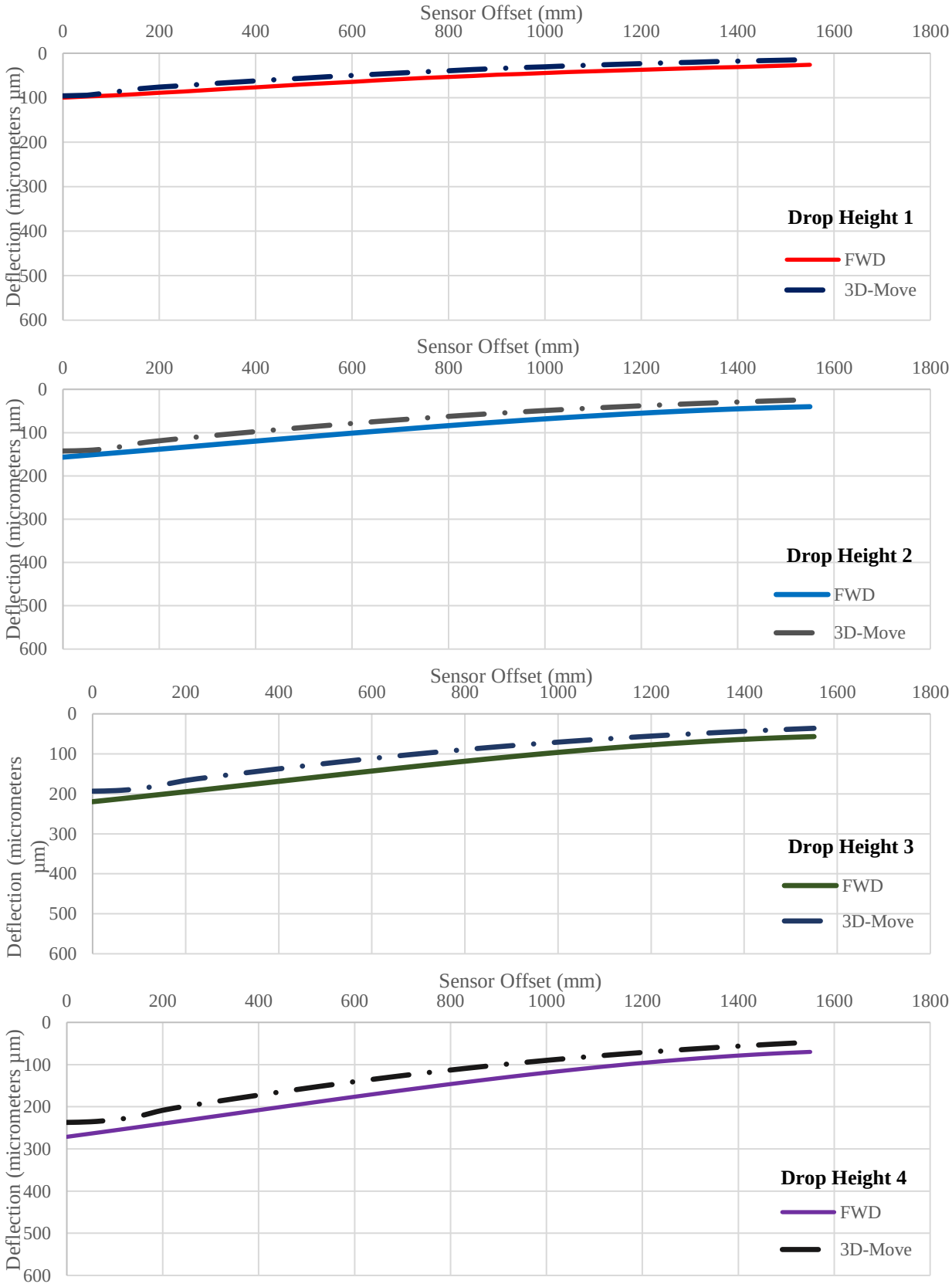

Figure C – 65. Simulated Deflection Bowl for the SHRP section 1047.

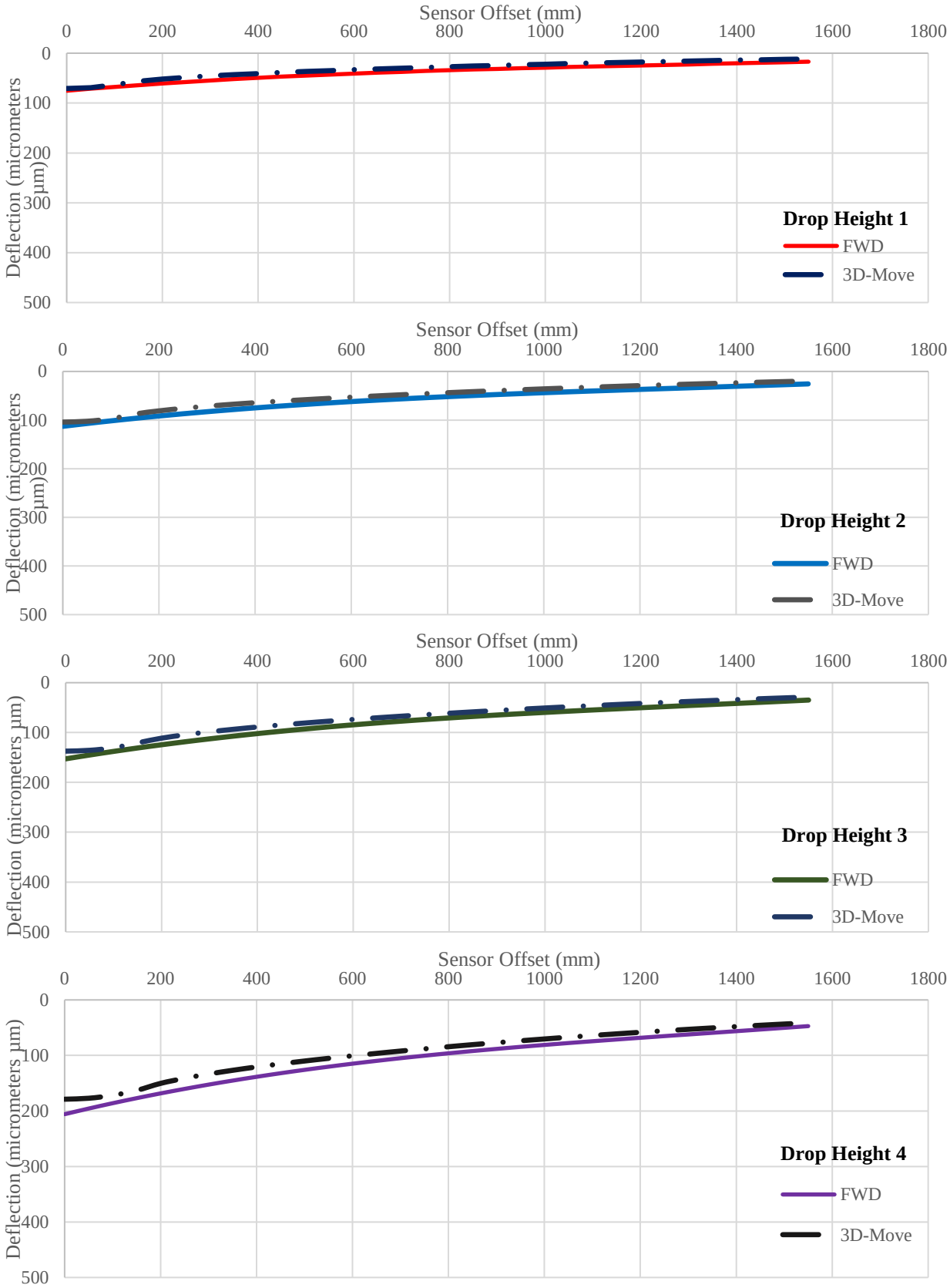

Figure C – 66. Simulated Deflection Bowl for the SHRP section 1049.

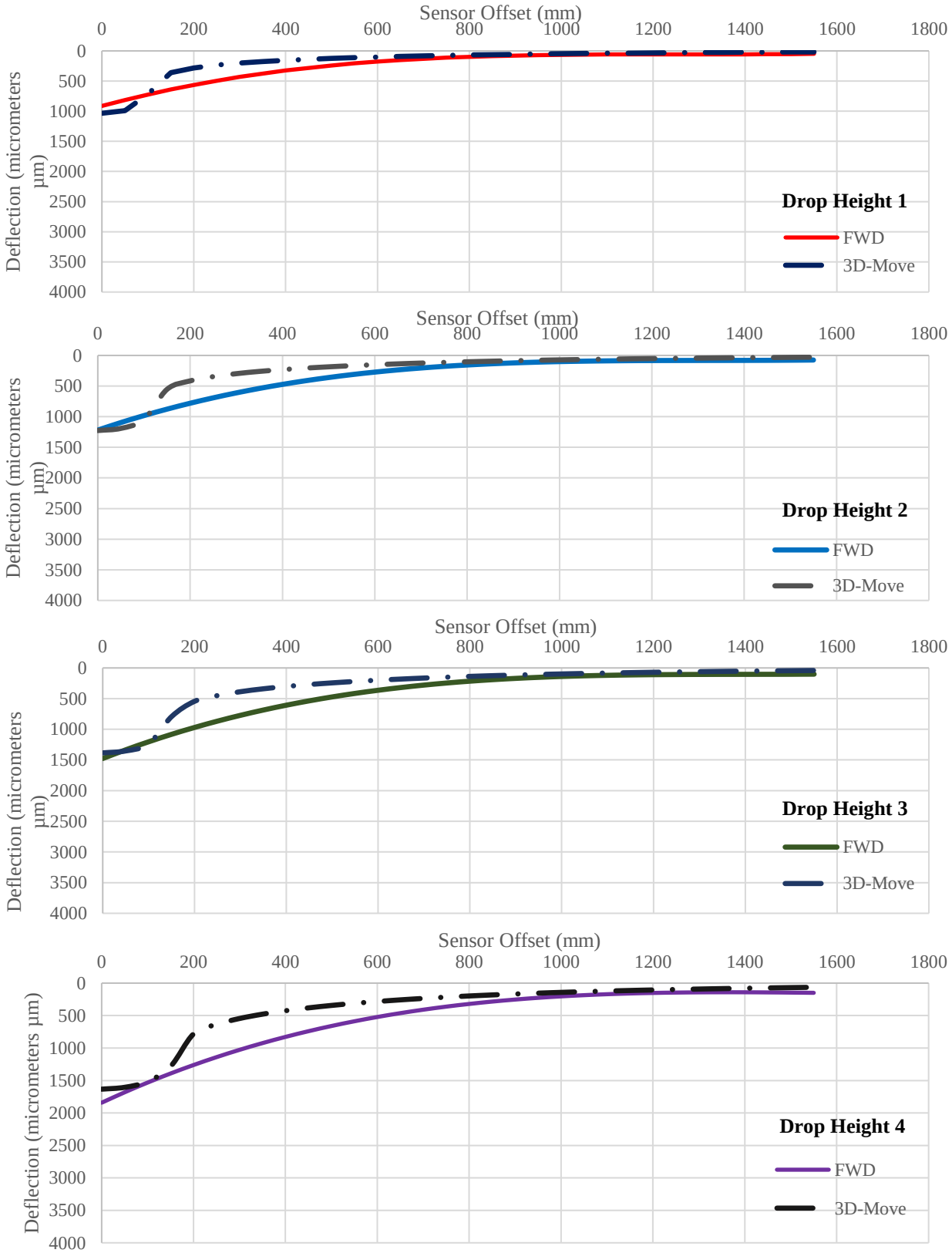

Figure C – 67. Simulated Deflection Bowl for the SHRP section 1056.

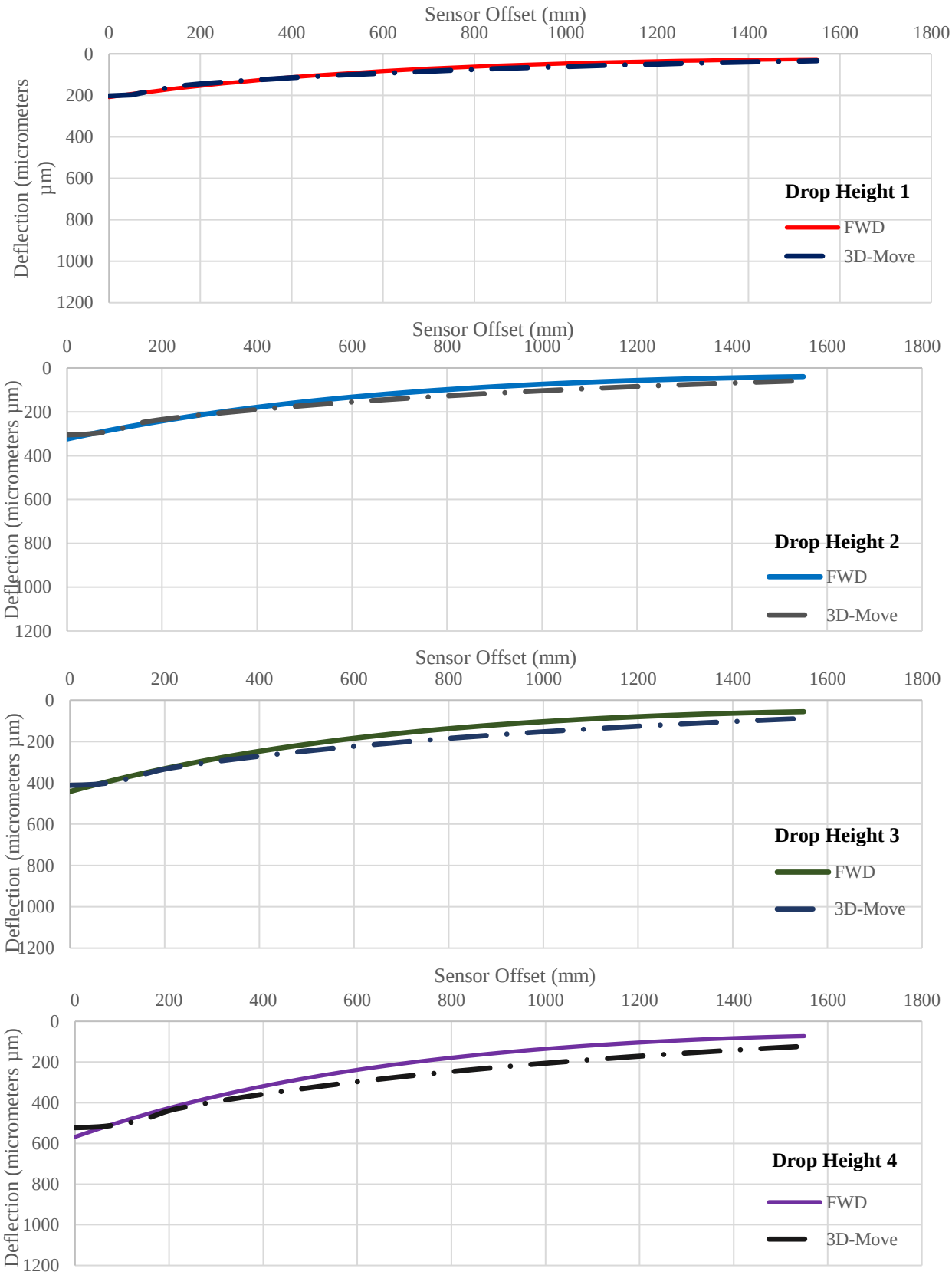

Figure C – 68. Simulated Deflection Bowl for the SHRP section 1068.

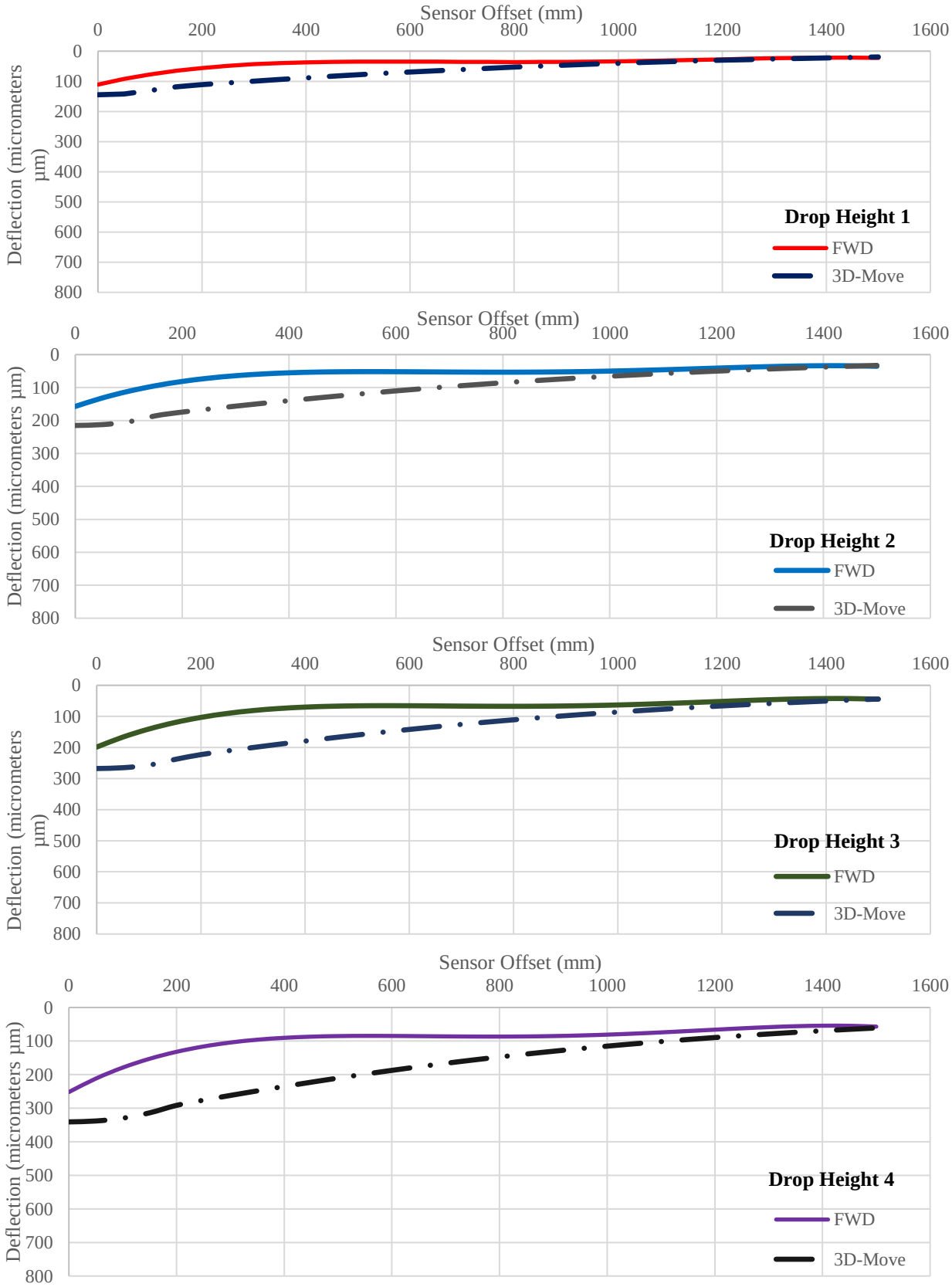

Figure C – 69. Simulated Deflection Bowl for the SHRP section 1069.

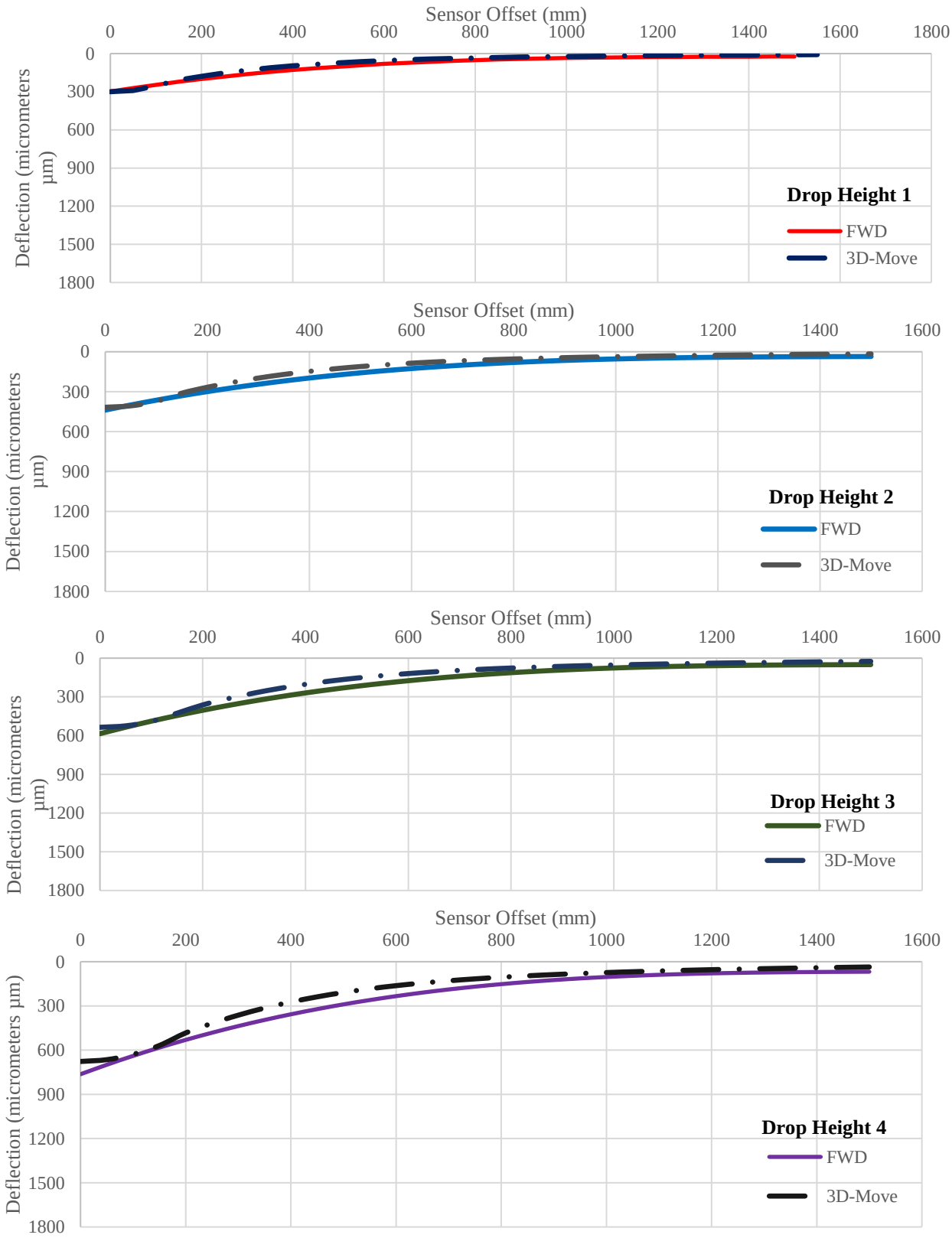

Figure C – 70. Simulated Deflection Bowl for the SHRP section 1076.

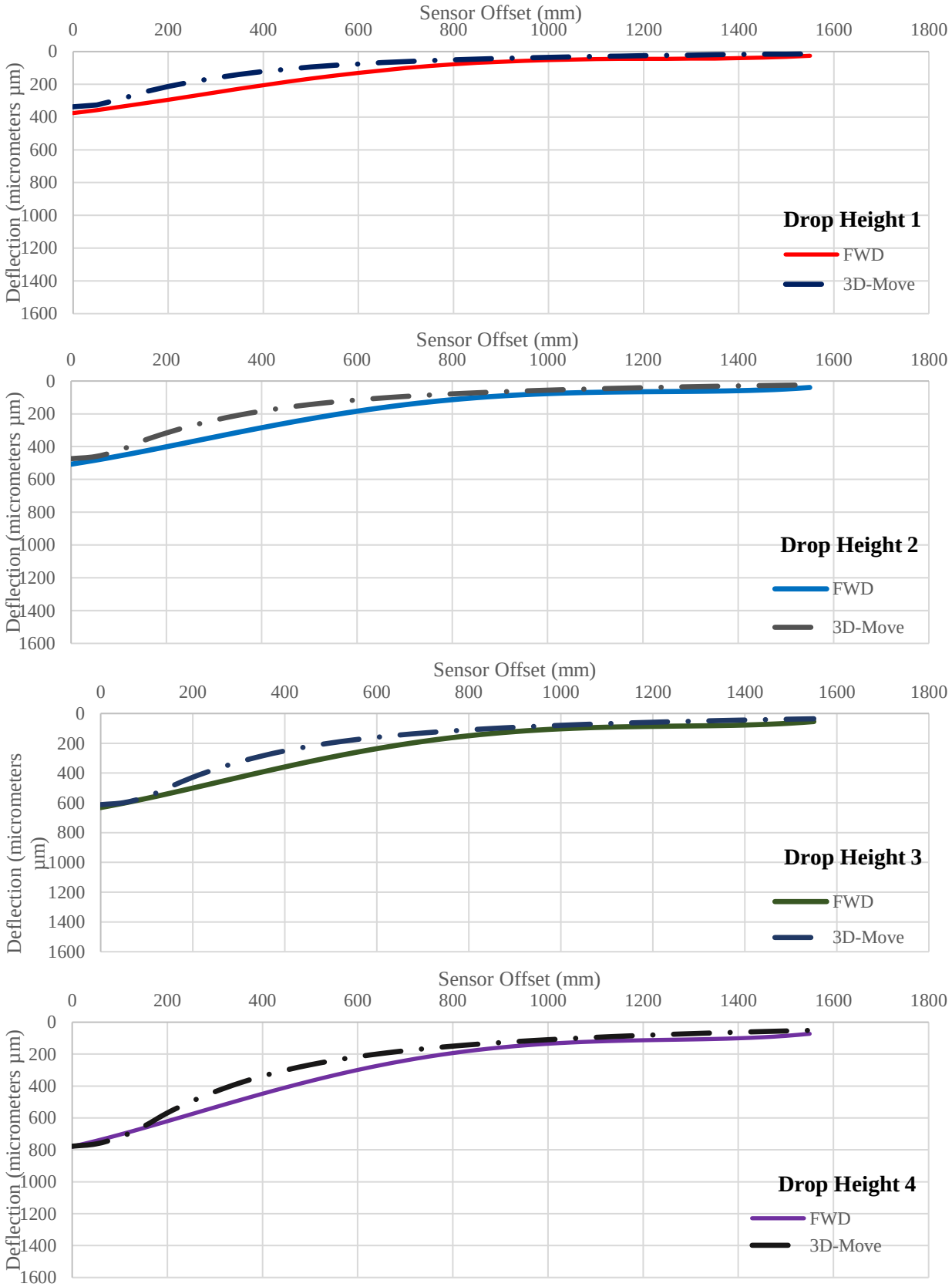

Figure C – 71. Simulated Deflection Bowl for the SHRP section 1093.

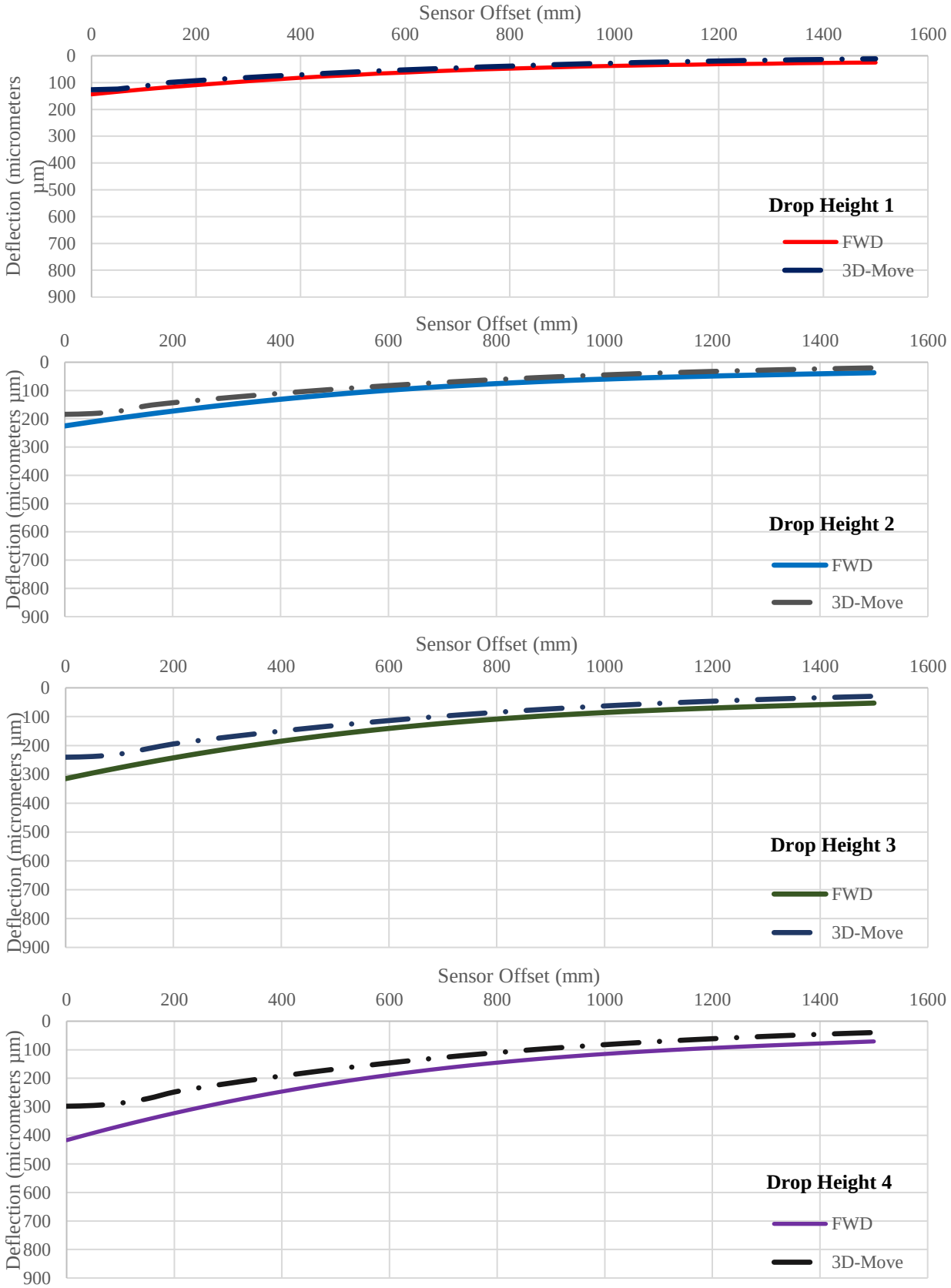

Figure C – 72. Simulated Deflection Bowl for the SHRP section 1111.

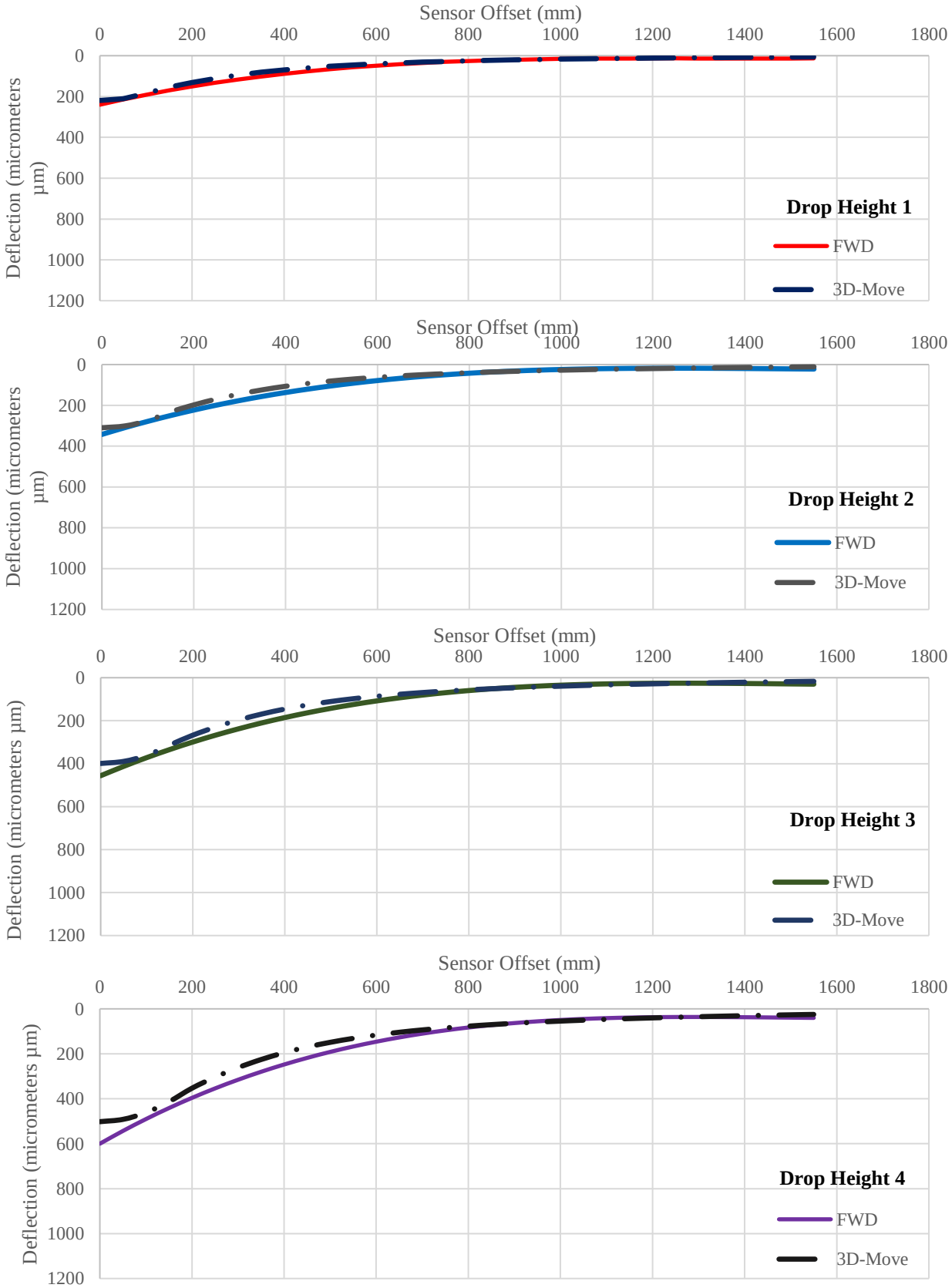

Figure C – 73. Simulated Deflection Bowl for the SHRP section 1113.

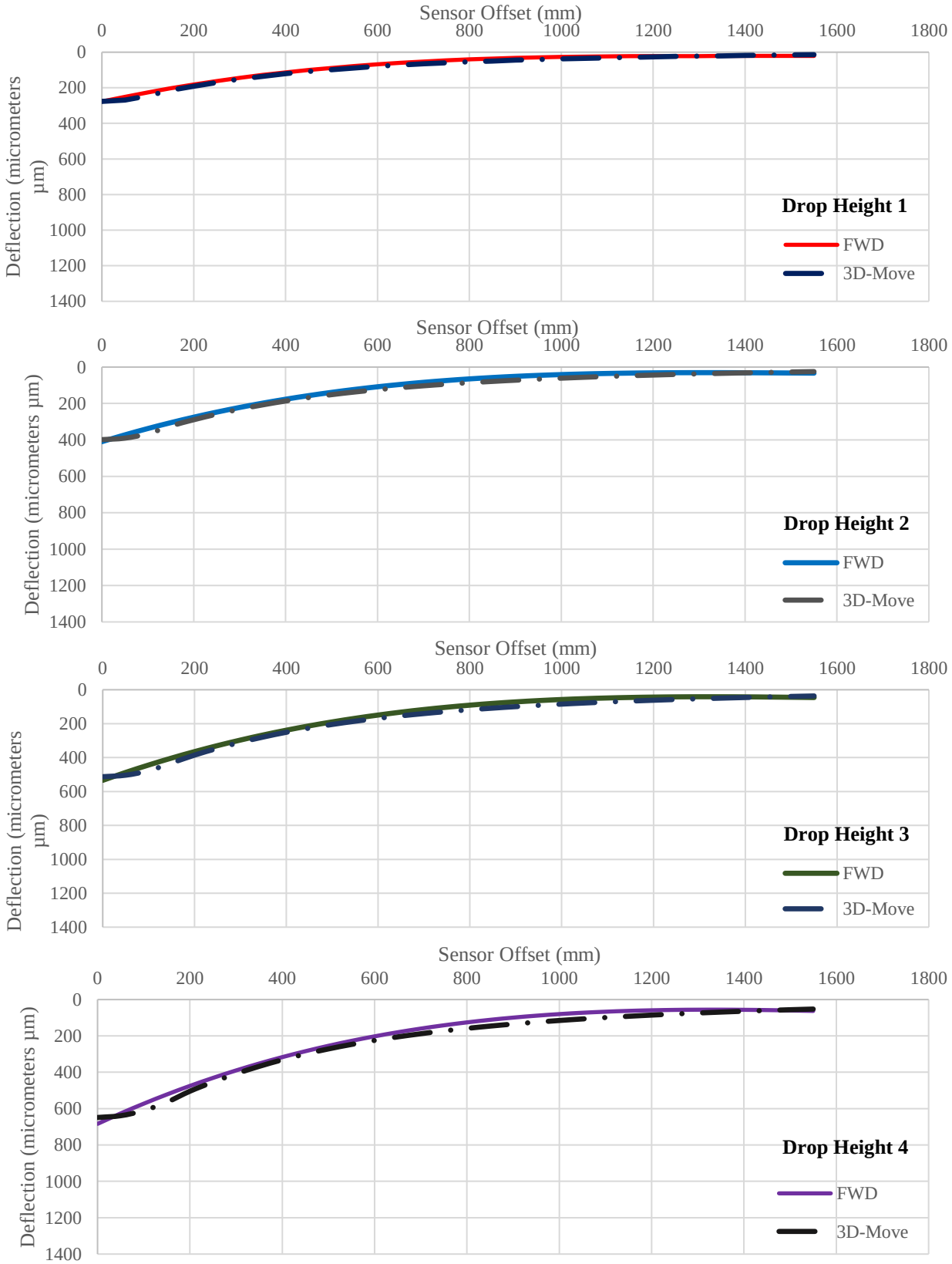

Figure C – 74. Simulated Deflection Bowl for the SHRP section 1116.

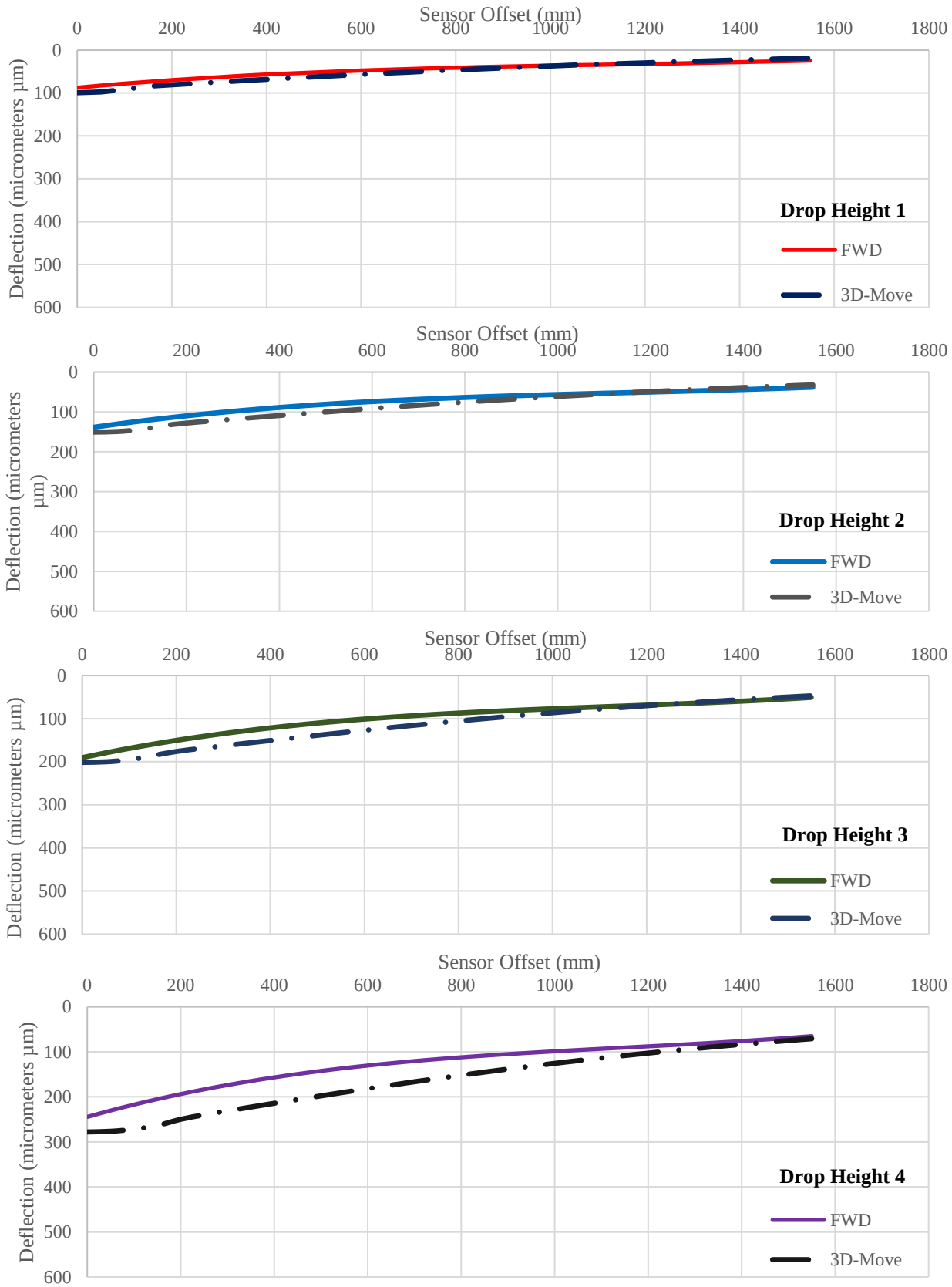

Figure C – 75. Simulated Deflection Bowl for the SHRP section 2172.

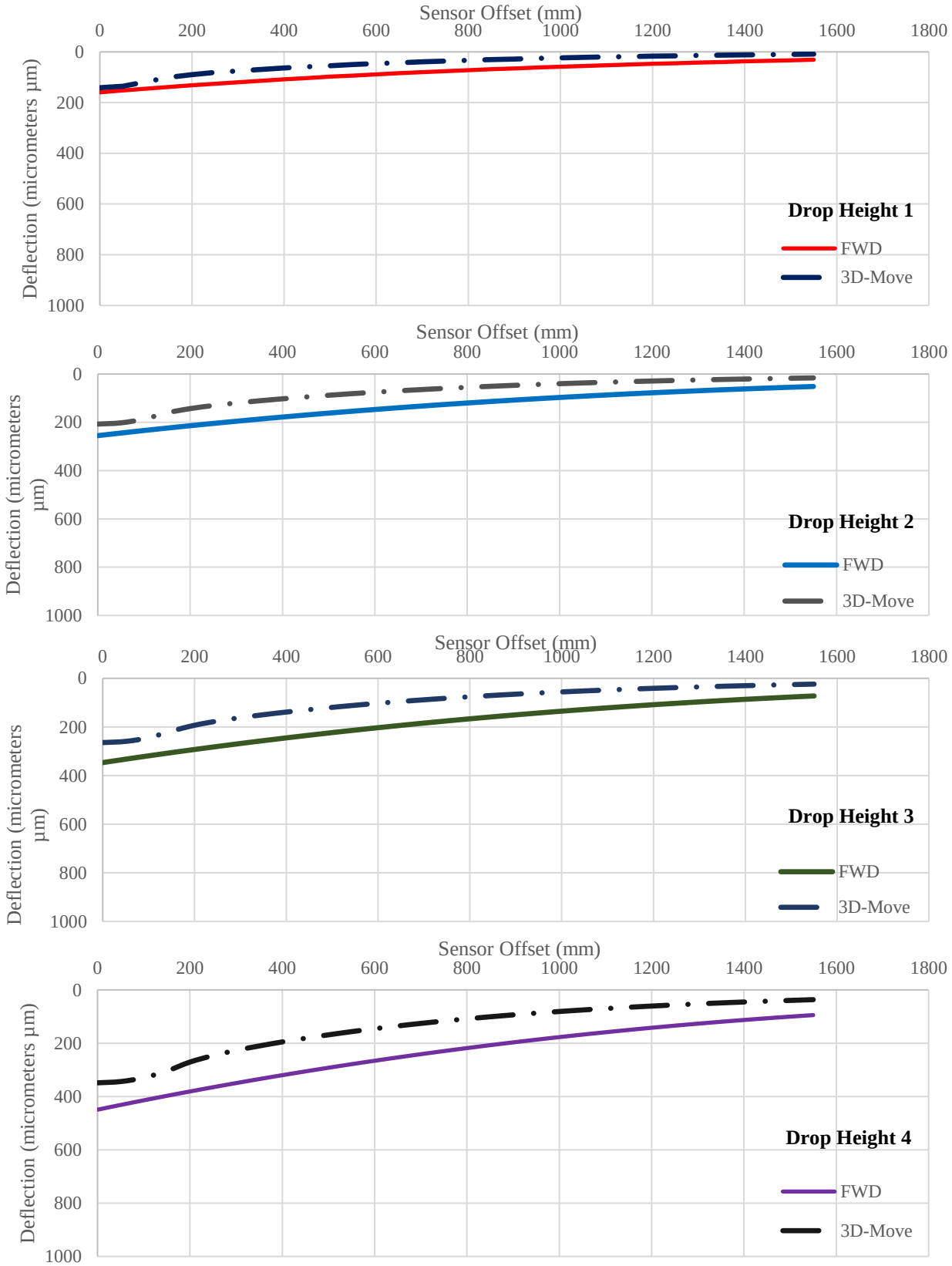

Figure C – 76. Simulated Deflection Bowl for the SHRP section 2176.

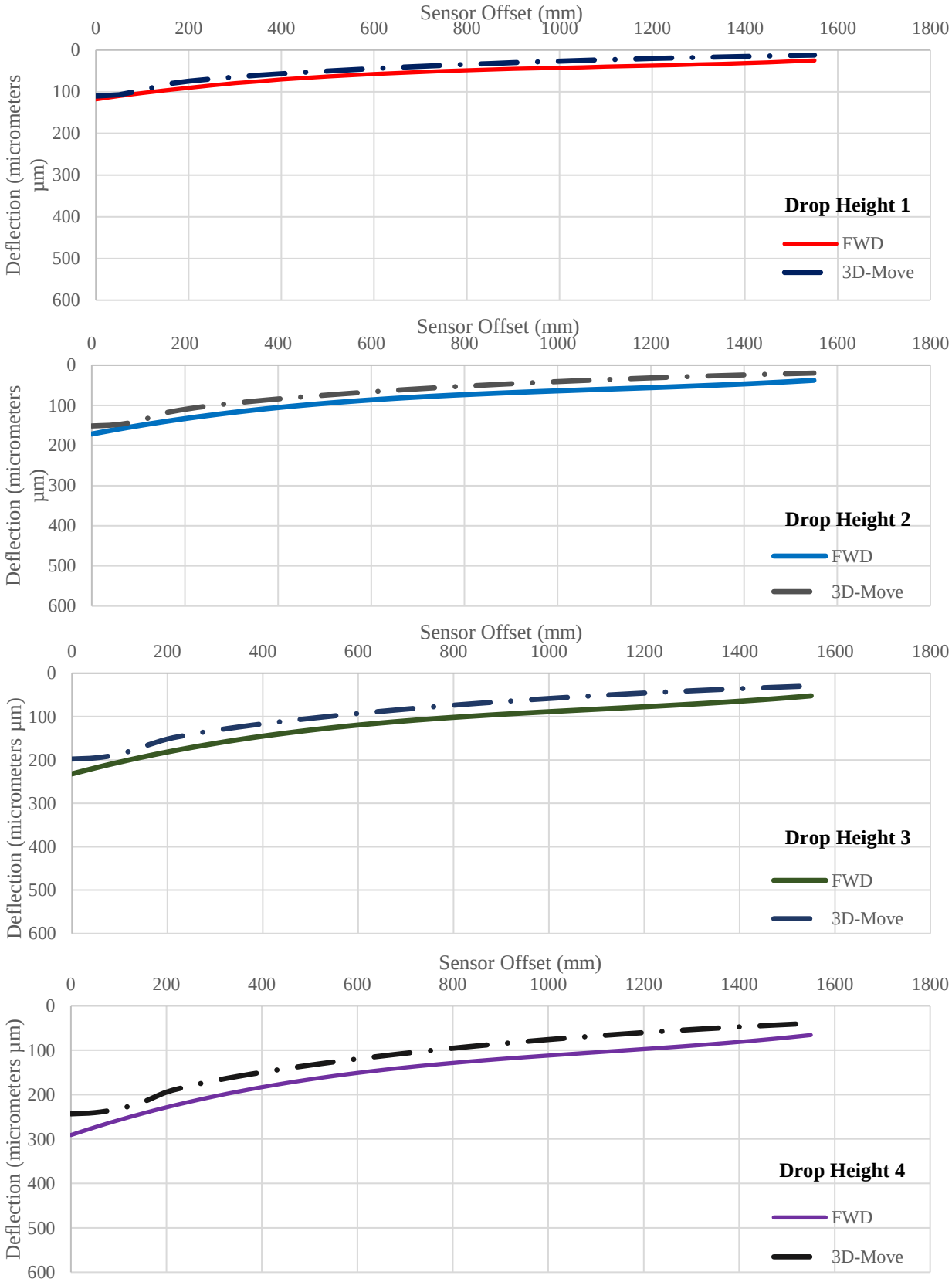

Figure C – 77. Simulated Deflection Bowl for the SHRP section 3669.

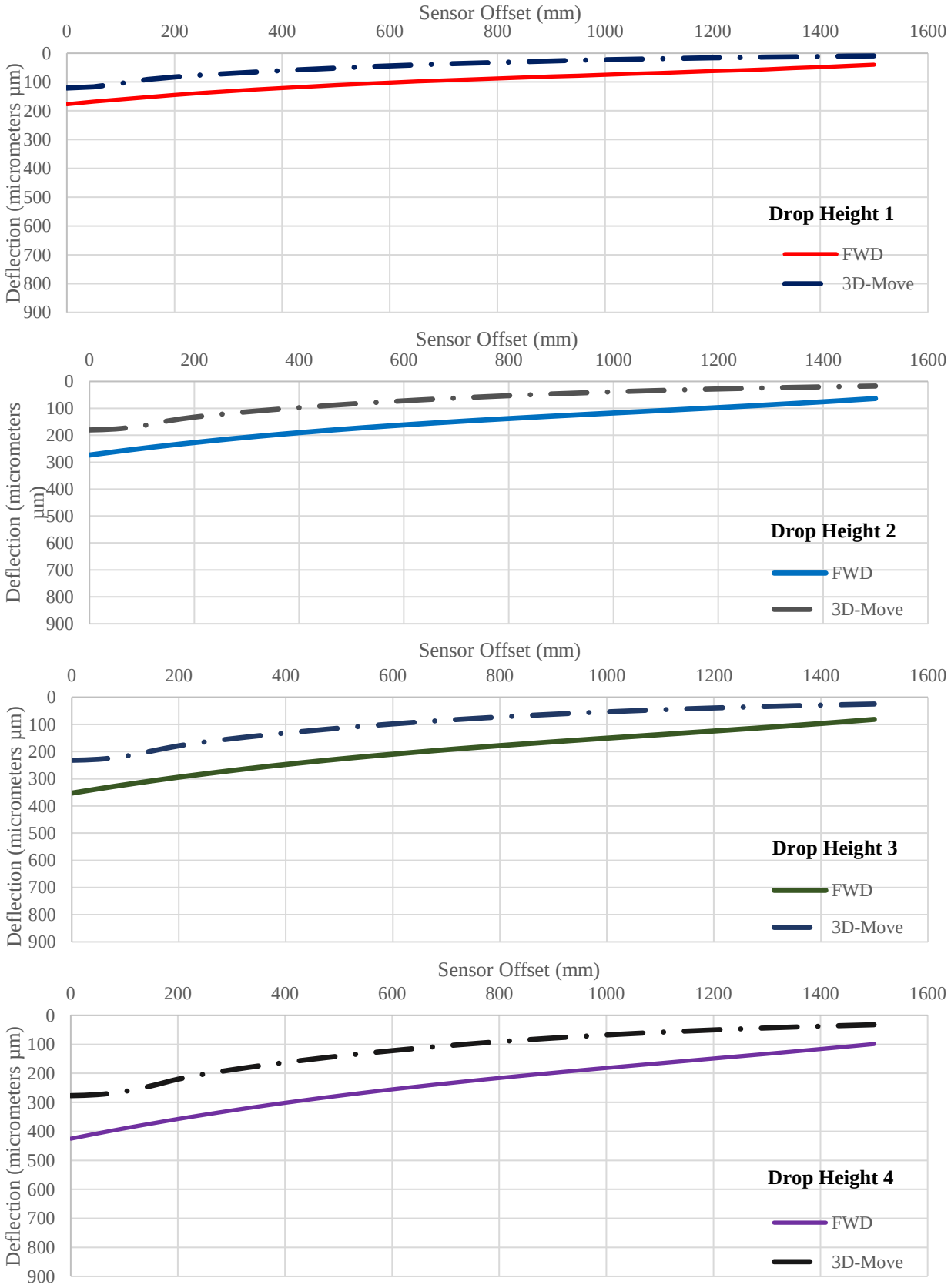

Figure C – 78. Simulated Deflection Bowl for the SHRP section 3679.

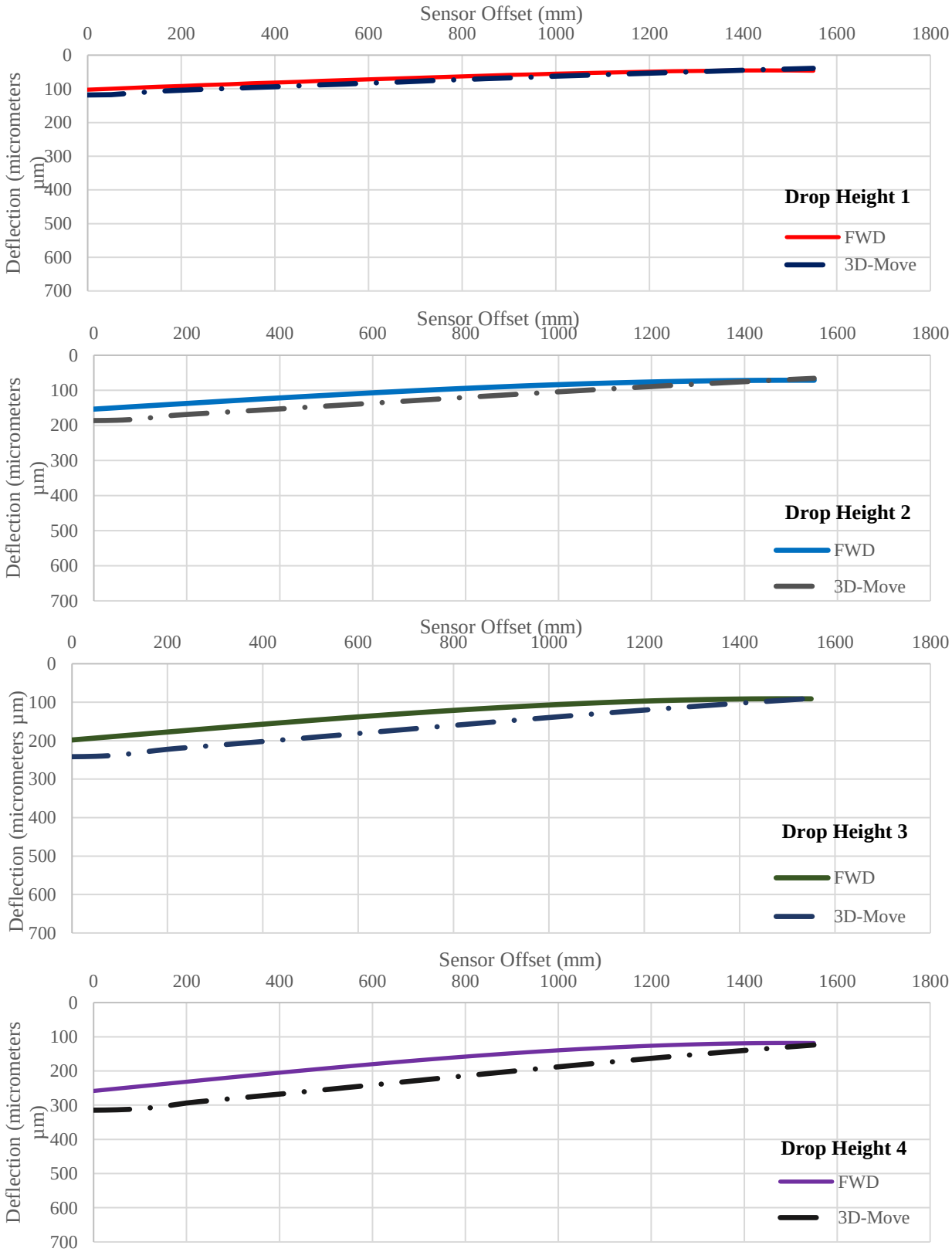

Figure C – 79. Simulated Deflection Bowl for the SHRP section 3729.

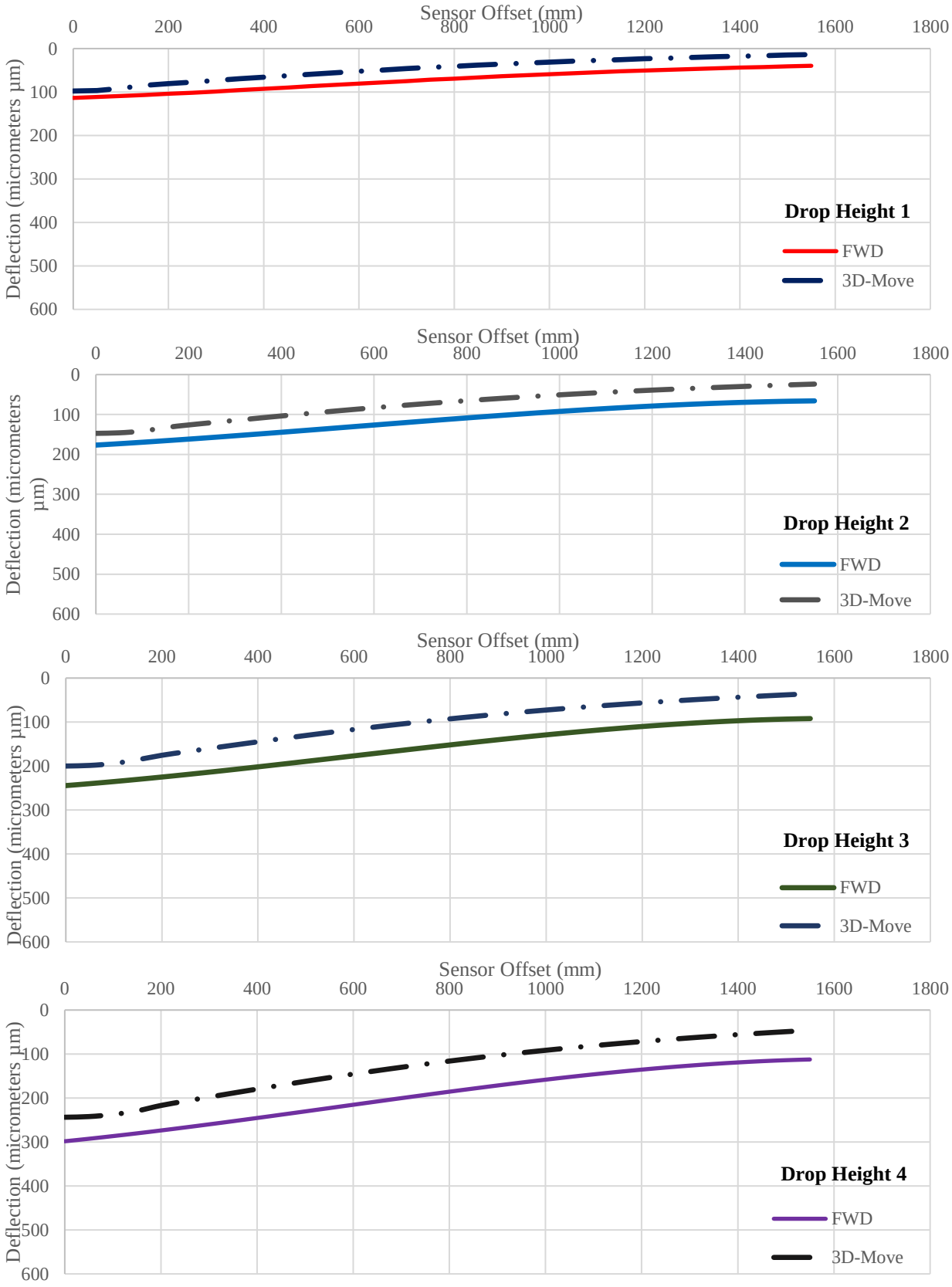

Figure C – 80. Simulated Deflection Bowl for the SHRP section 3835.

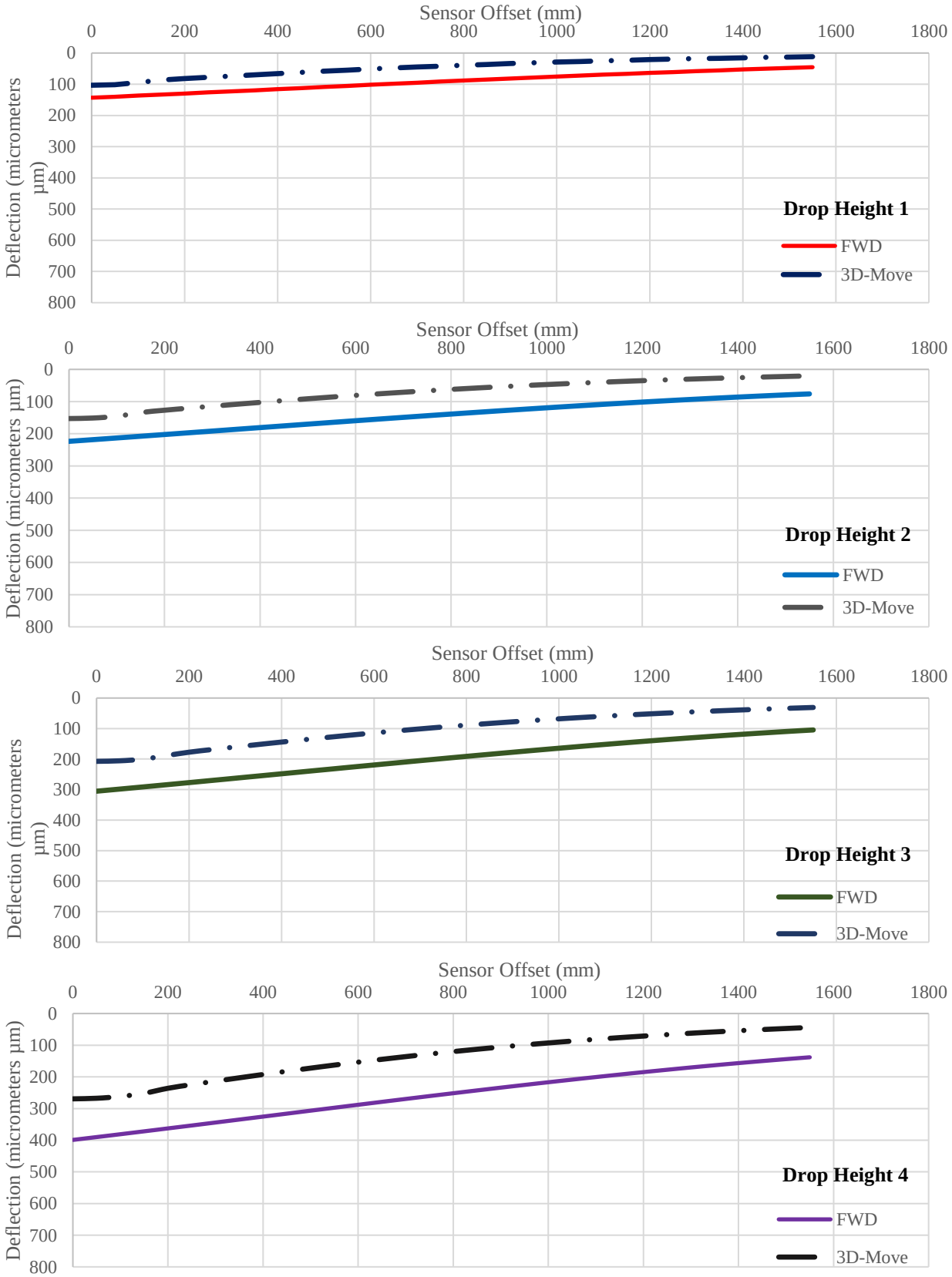

Figure C – 81. Simulated Deflection Bowl for the SHRP section 6079.

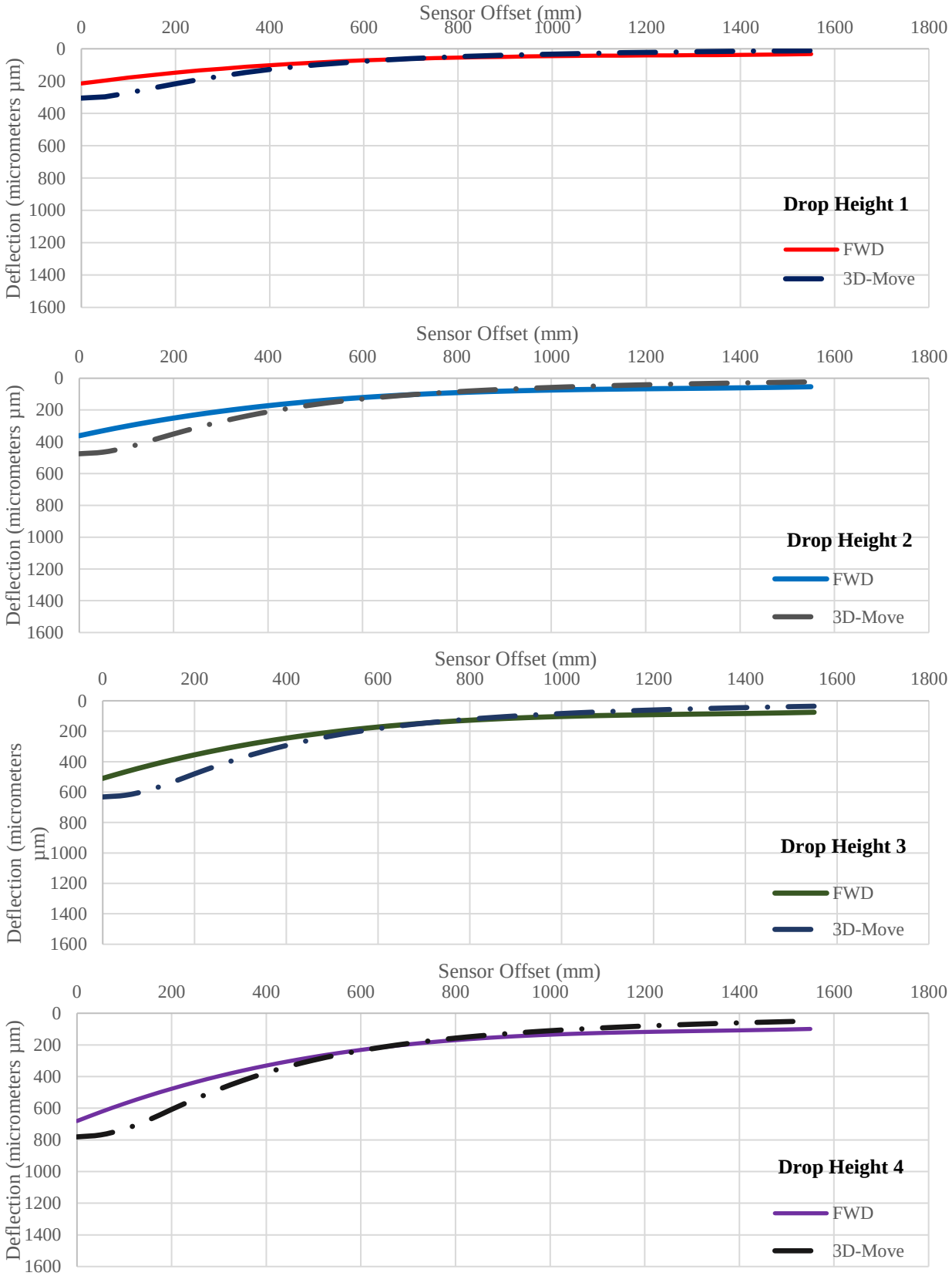

Figure C – 82. Simulated Deflection Bowl for the SHRP section 9005.

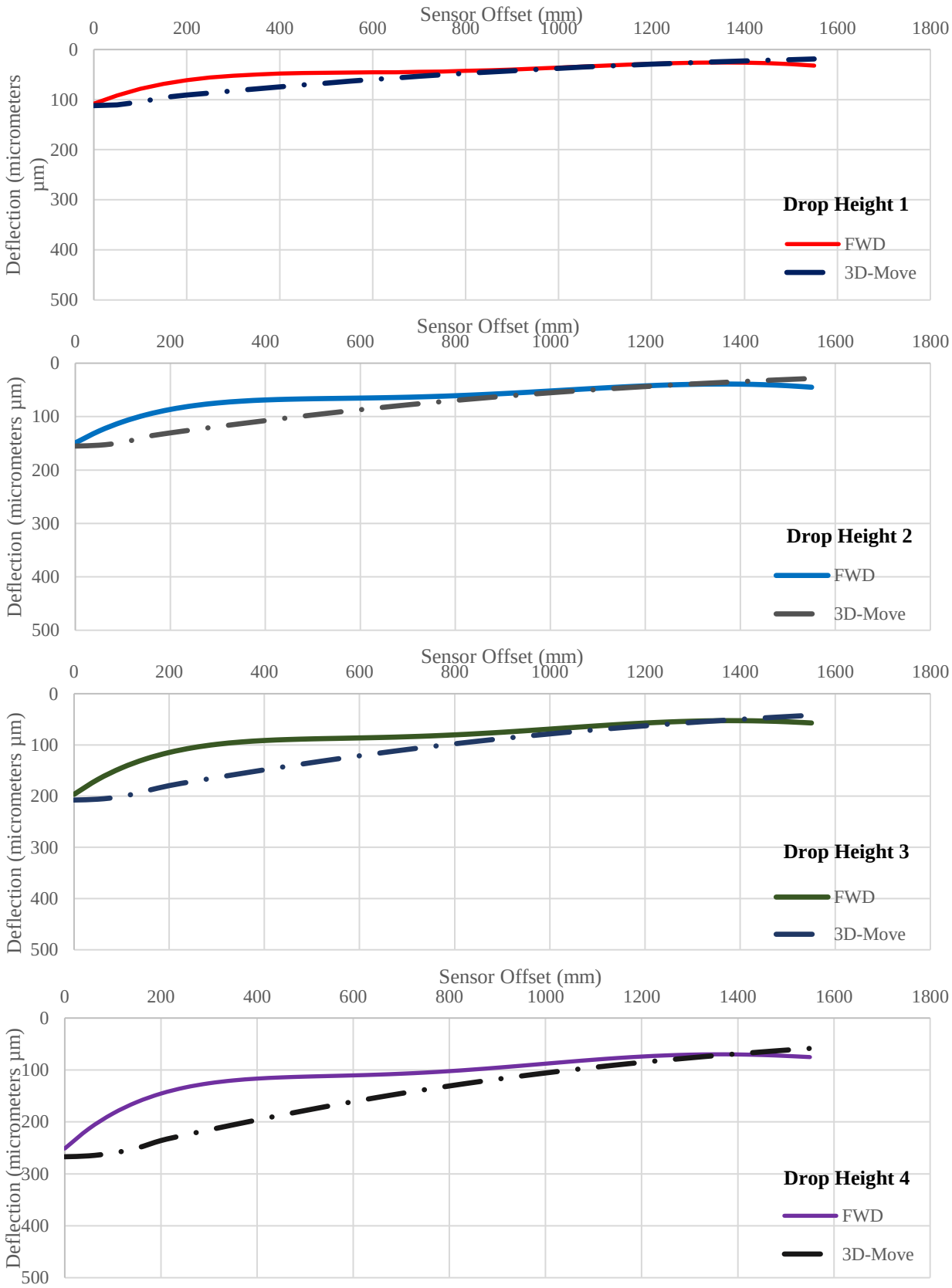

Figure C – 83. Simulated Deflection Bowl for the SHRP section A502.

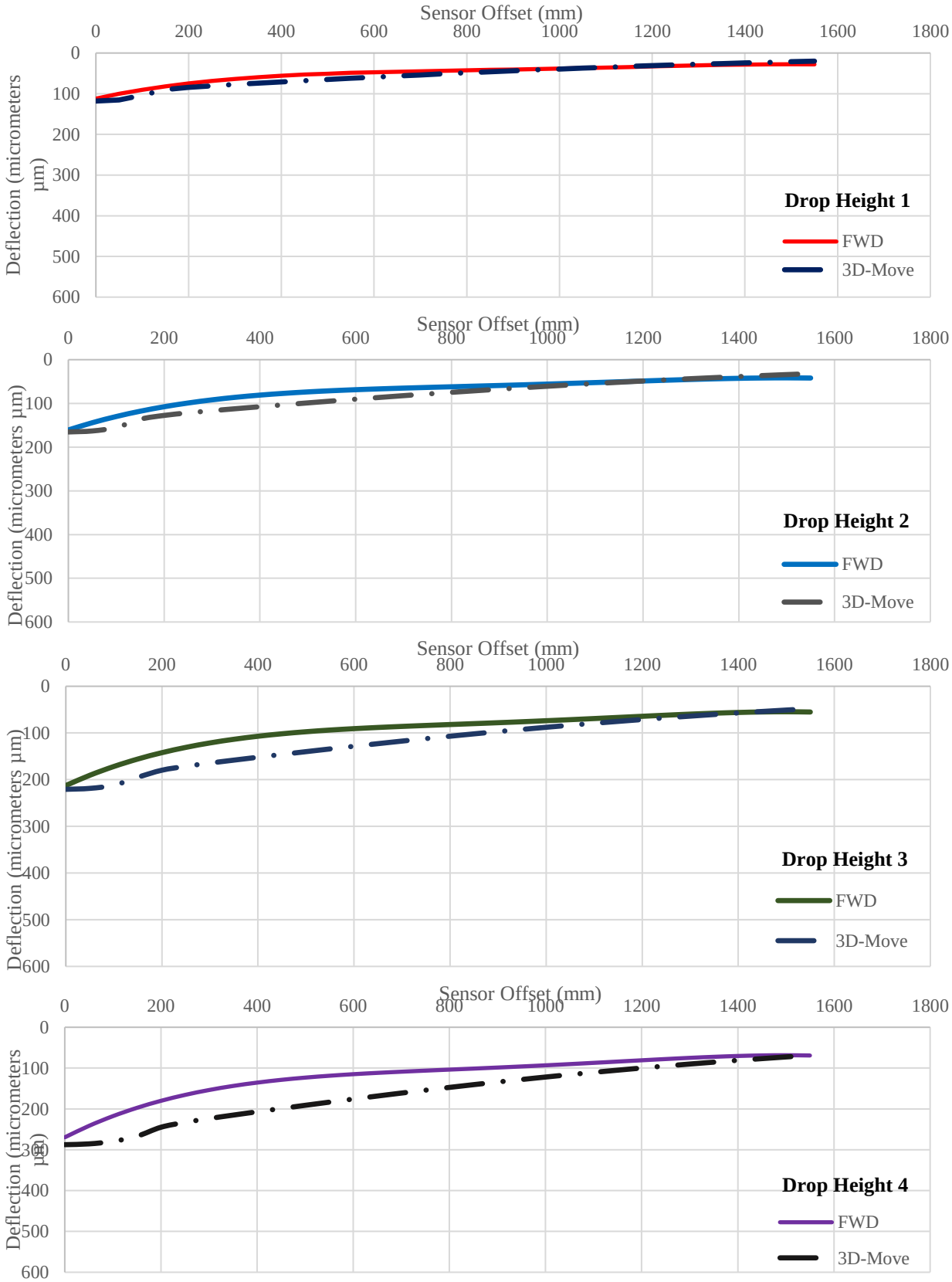

Figure C – 84. Simulated Deflection Bowl for the SHRP section A504.

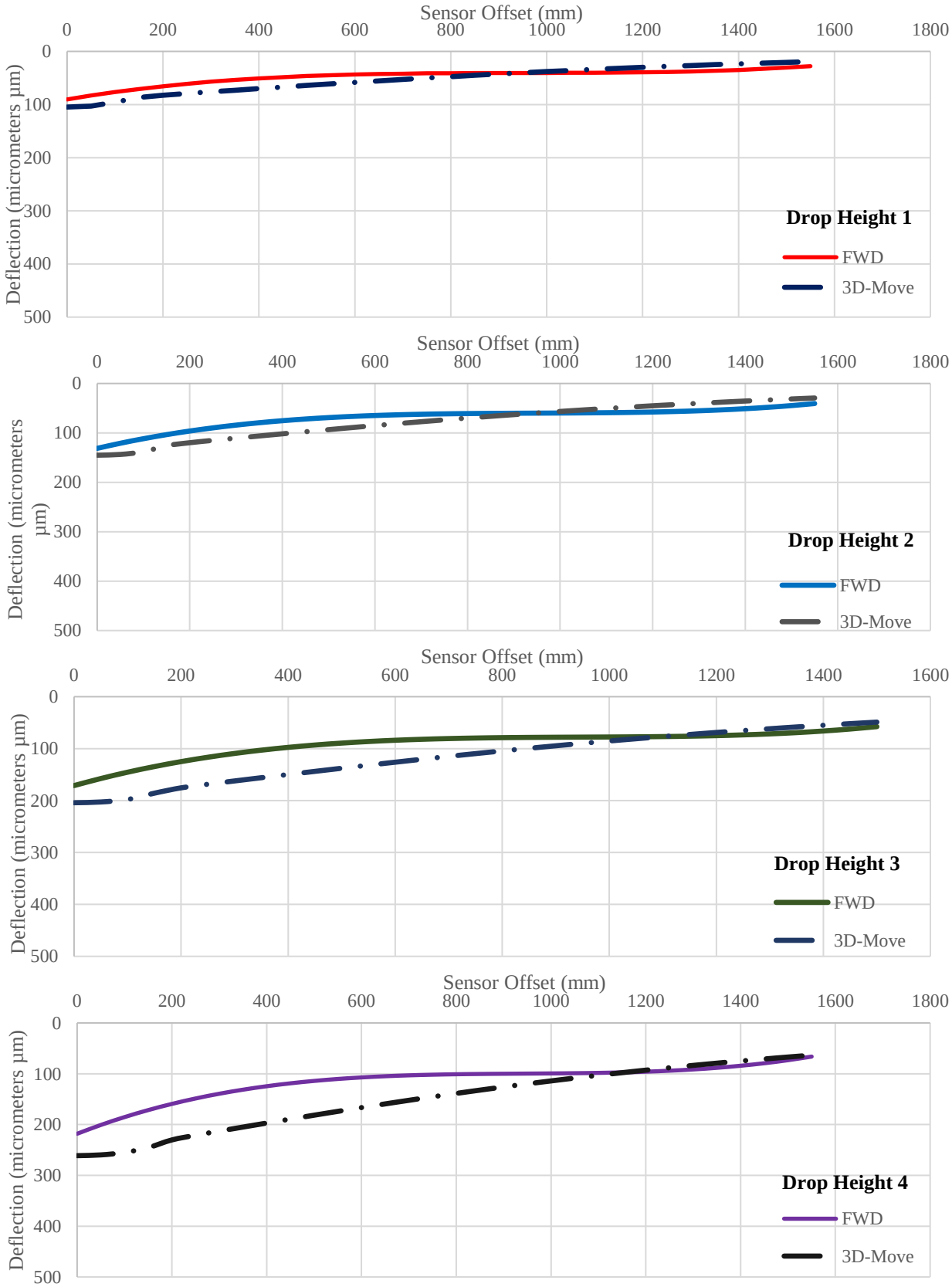

Figure C – 85. Simulated Deflection Bowl for the SHRP section A505.

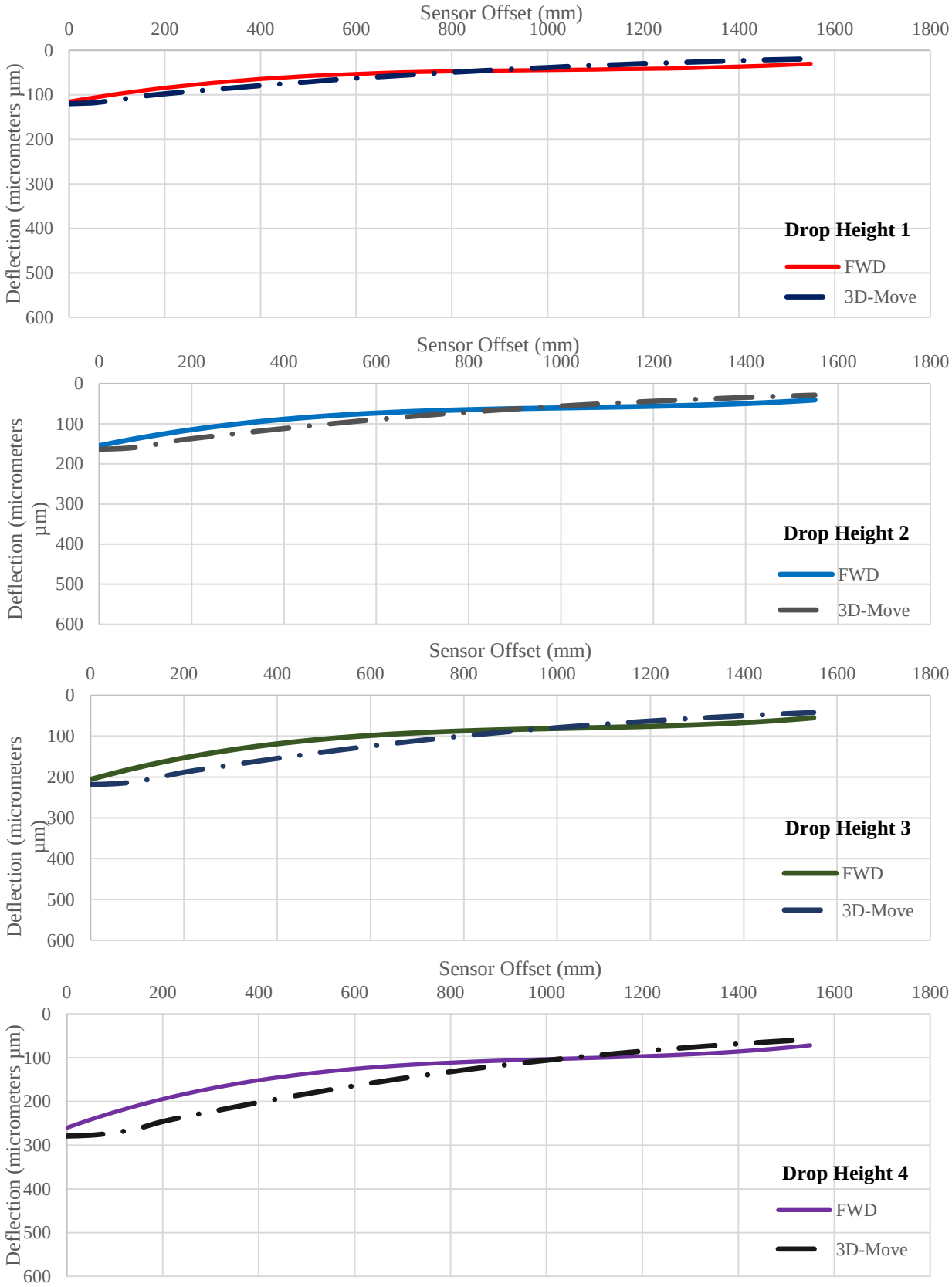

Figure C – 86. Simulated Deflection Bowl for the SHRP section A507.

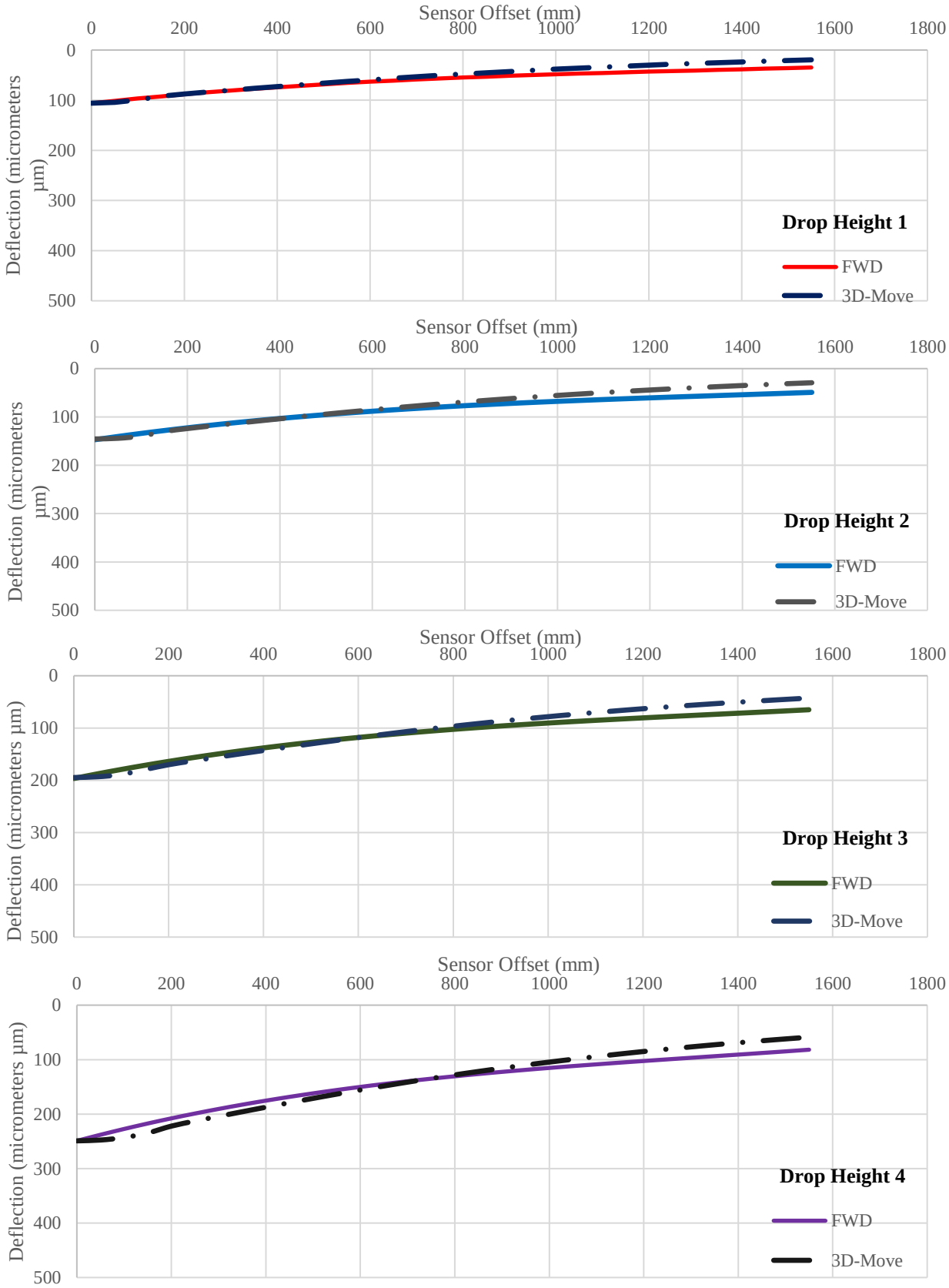

Figure C – 87. Simulated Deflection Bowl for the SHRP section A508.

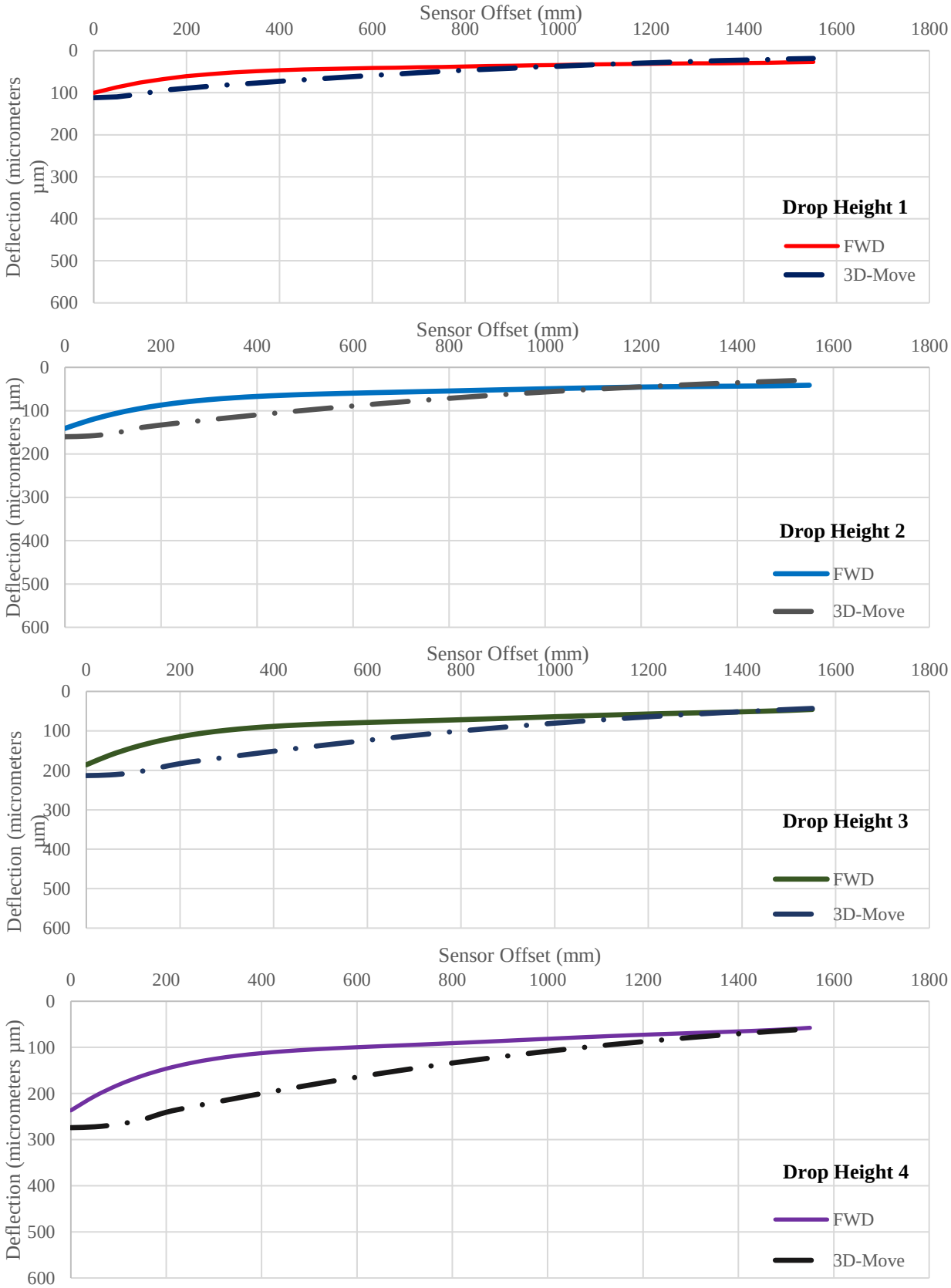

Figure C – 88. Simulated Deflection Bowl for the SHRP section B310.

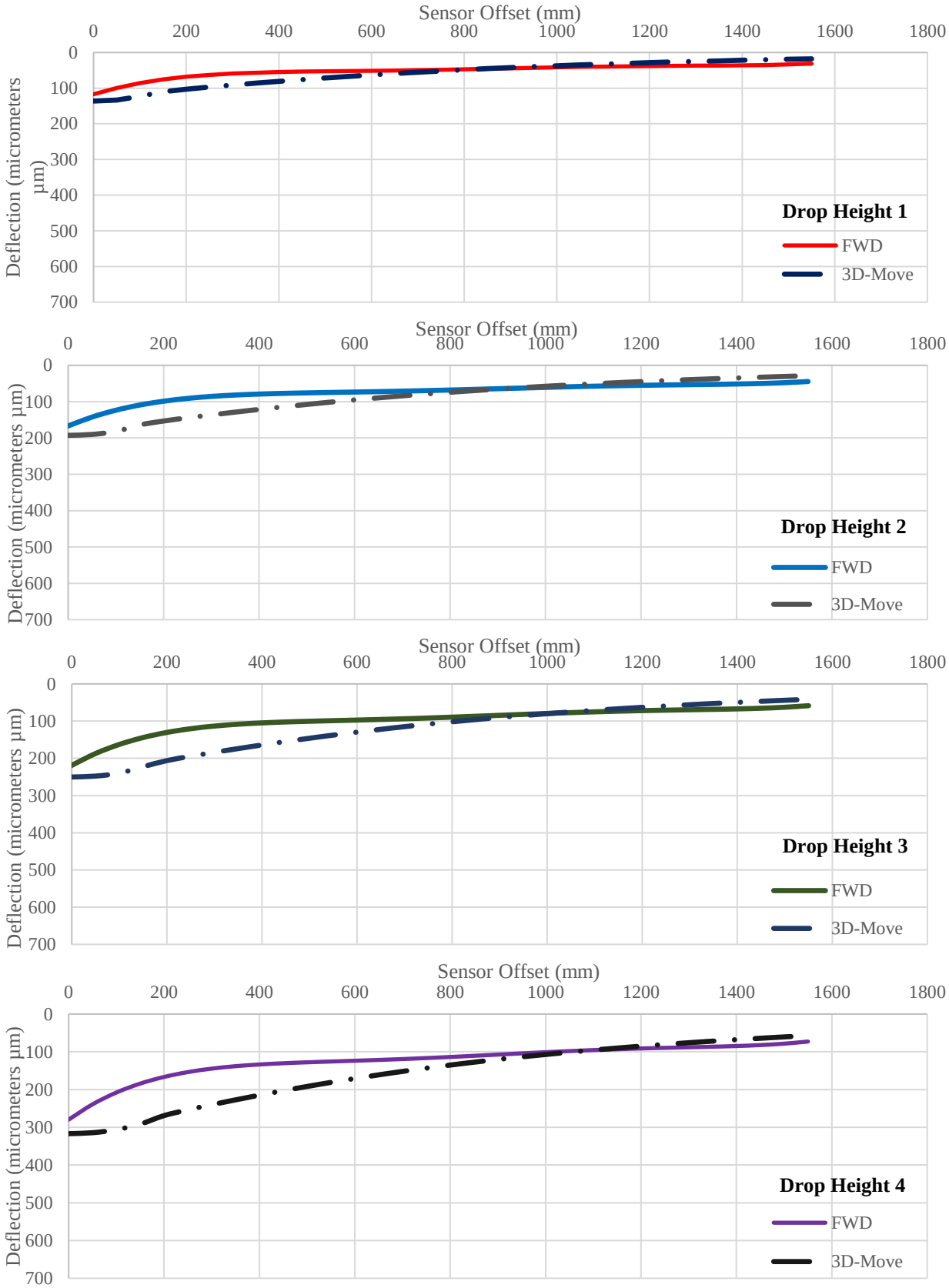

Figure C – 89. Simulated Deflection Bowl for the SHRP section B320.

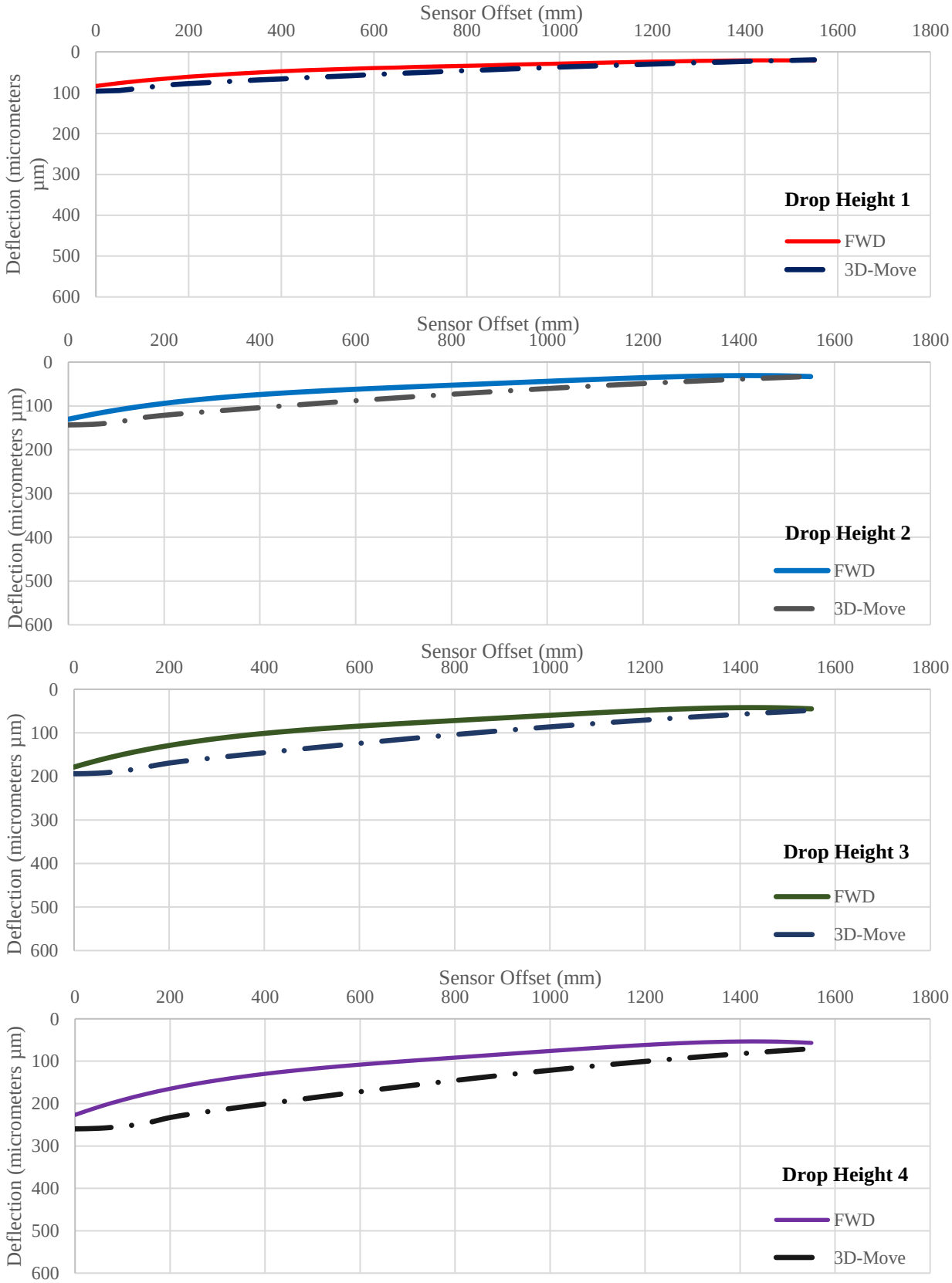

Figure C – 90. Simulated Deflection Bowl for the SHRP section D310.

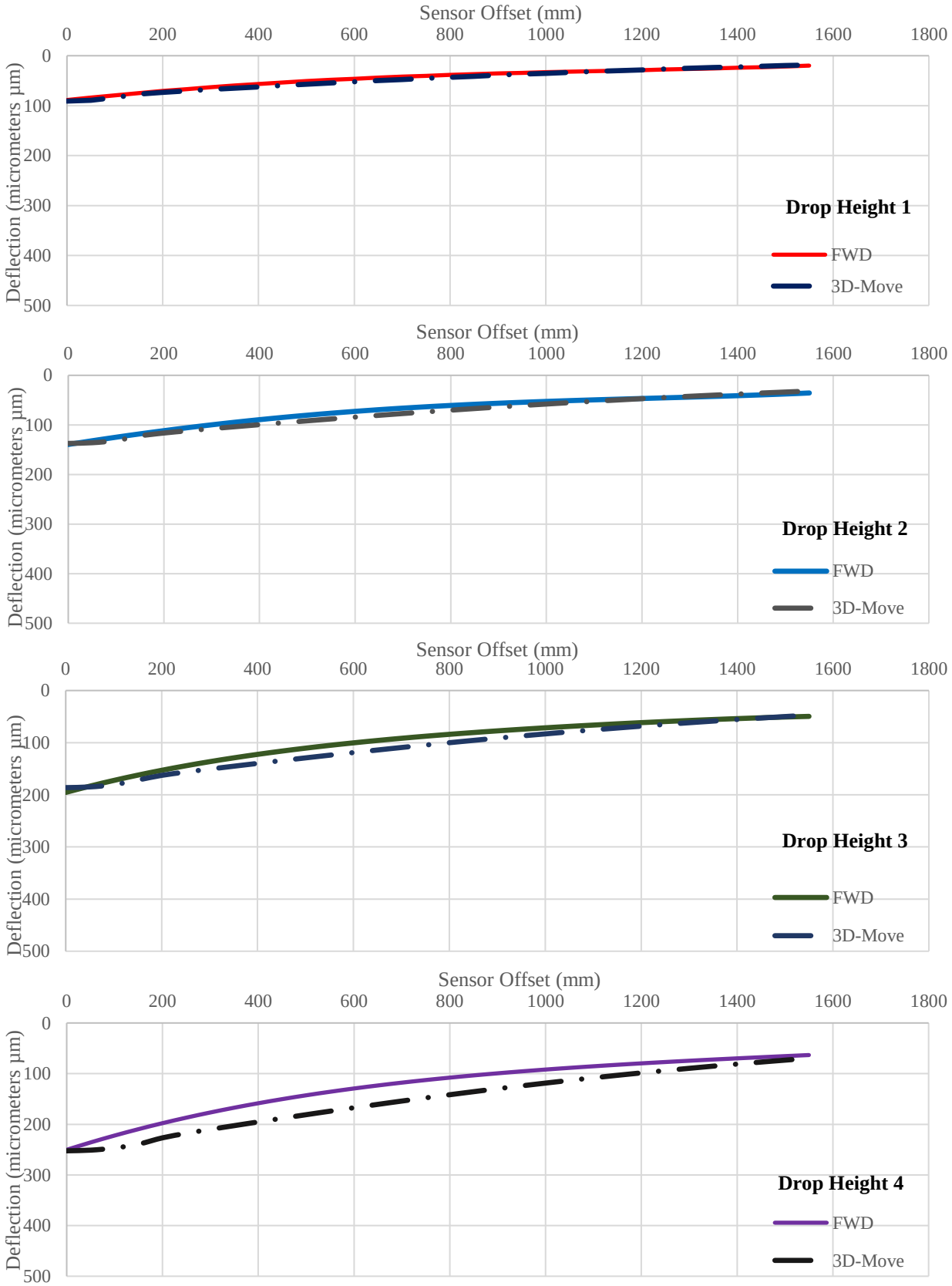

Figure C – 91. Simulated Deflection Bowl for the SHRP section D320.

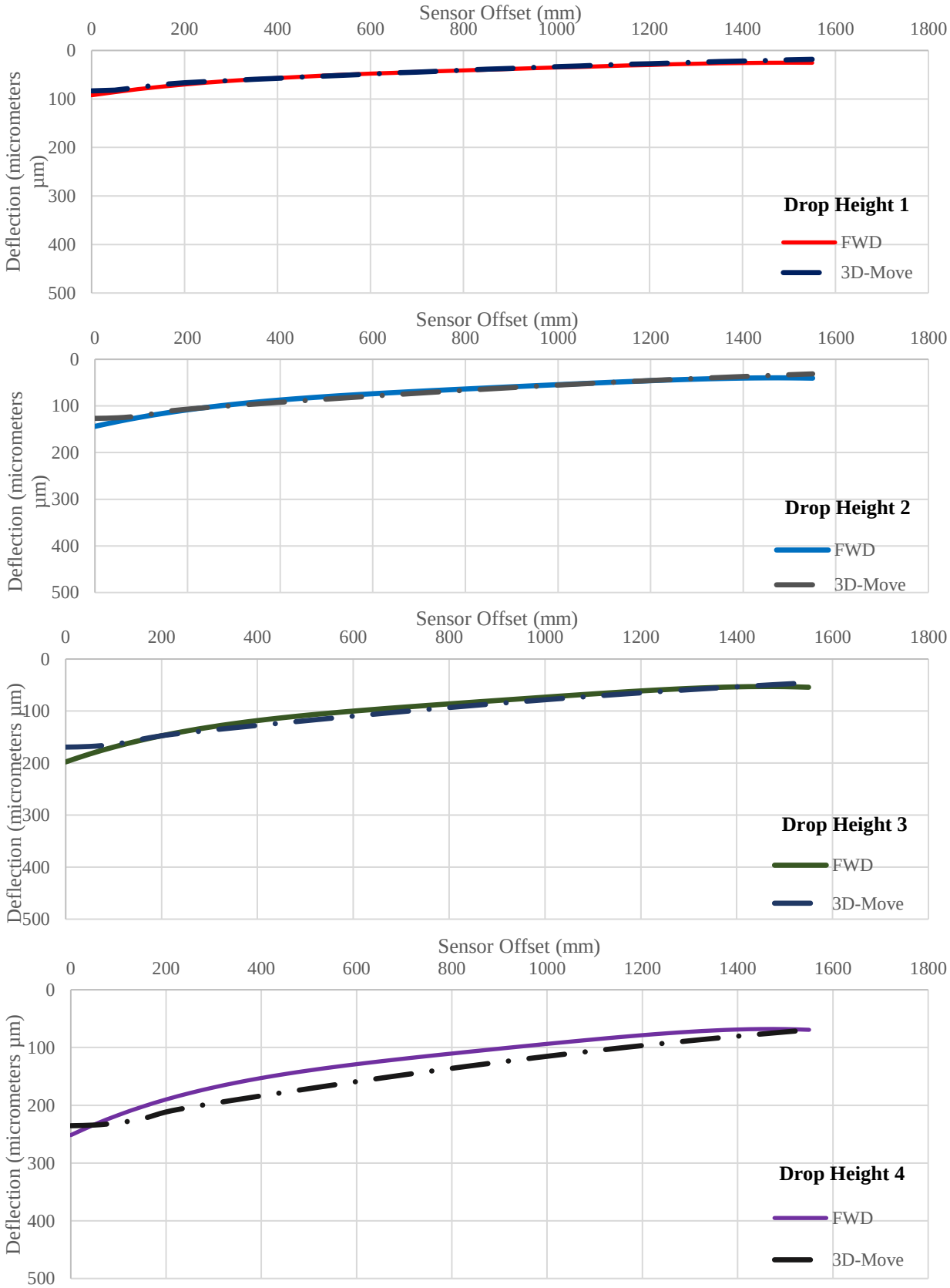

Figure C – 92. Simulated Deflection Bowl for the SHRP section D330.

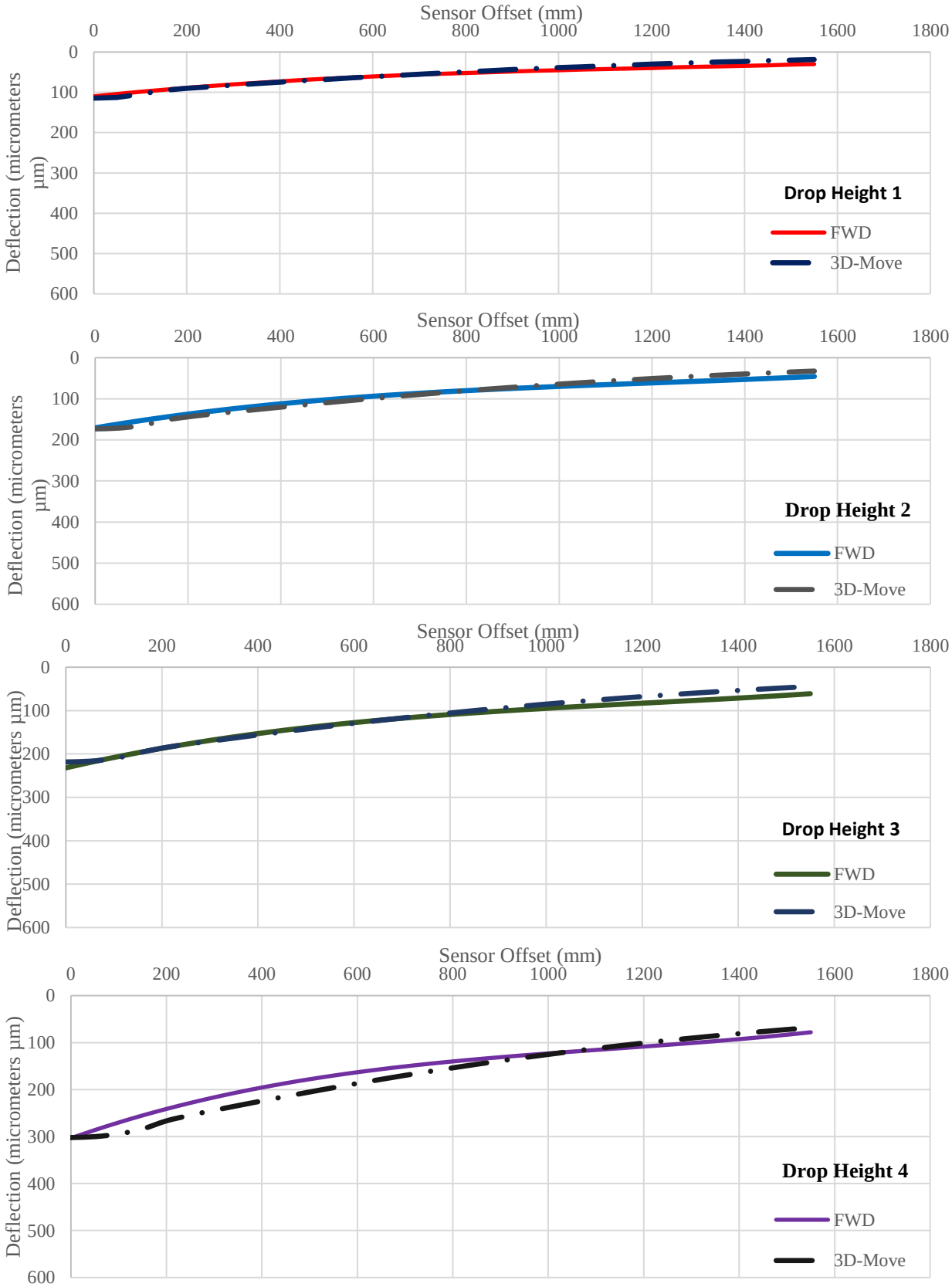

Figure C –93. Simulated Deflection Bowl for the SHRP section D350.

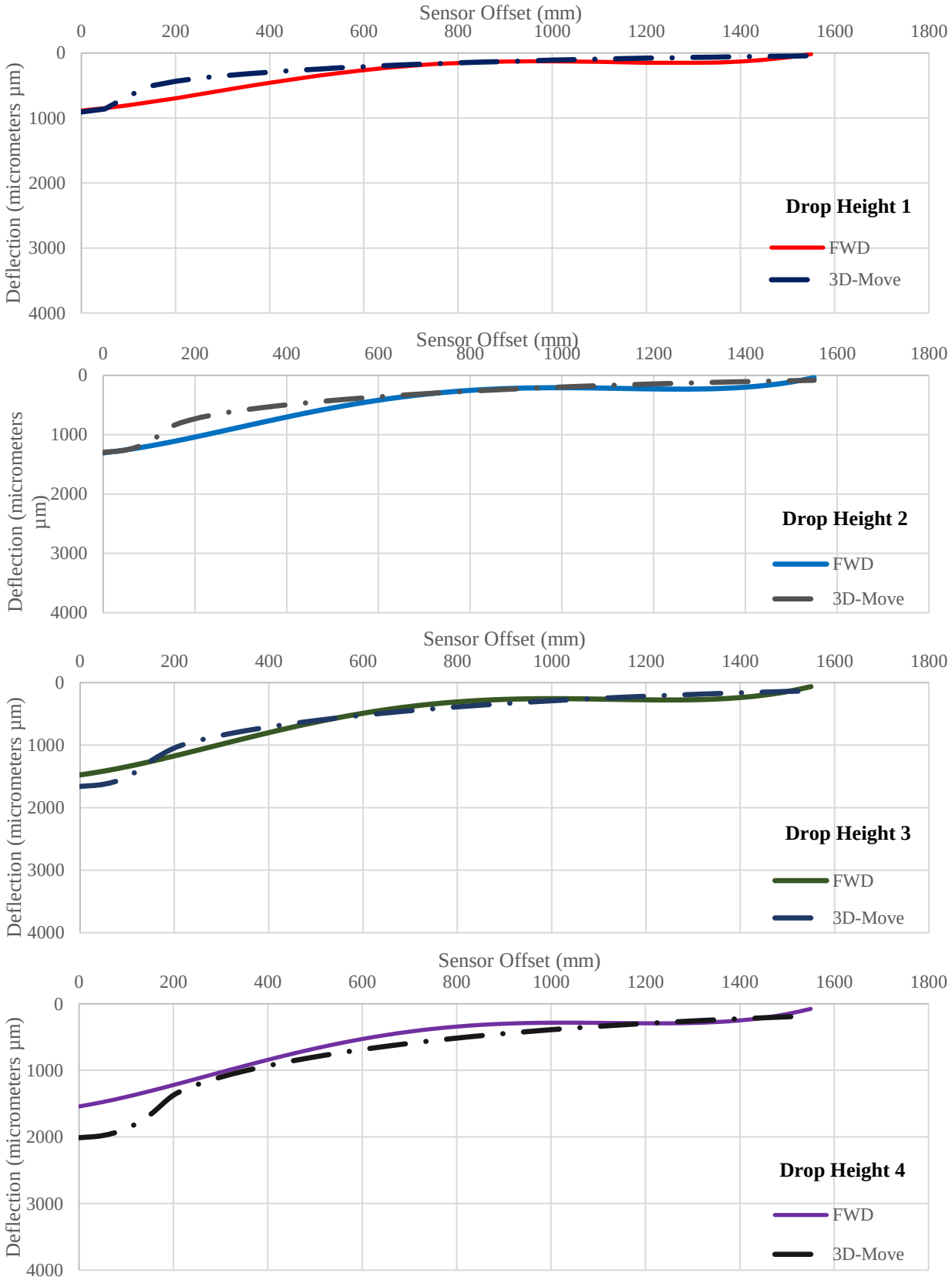

Figure C –94. Simulated Deflection Bowl for the SHRP section M310.

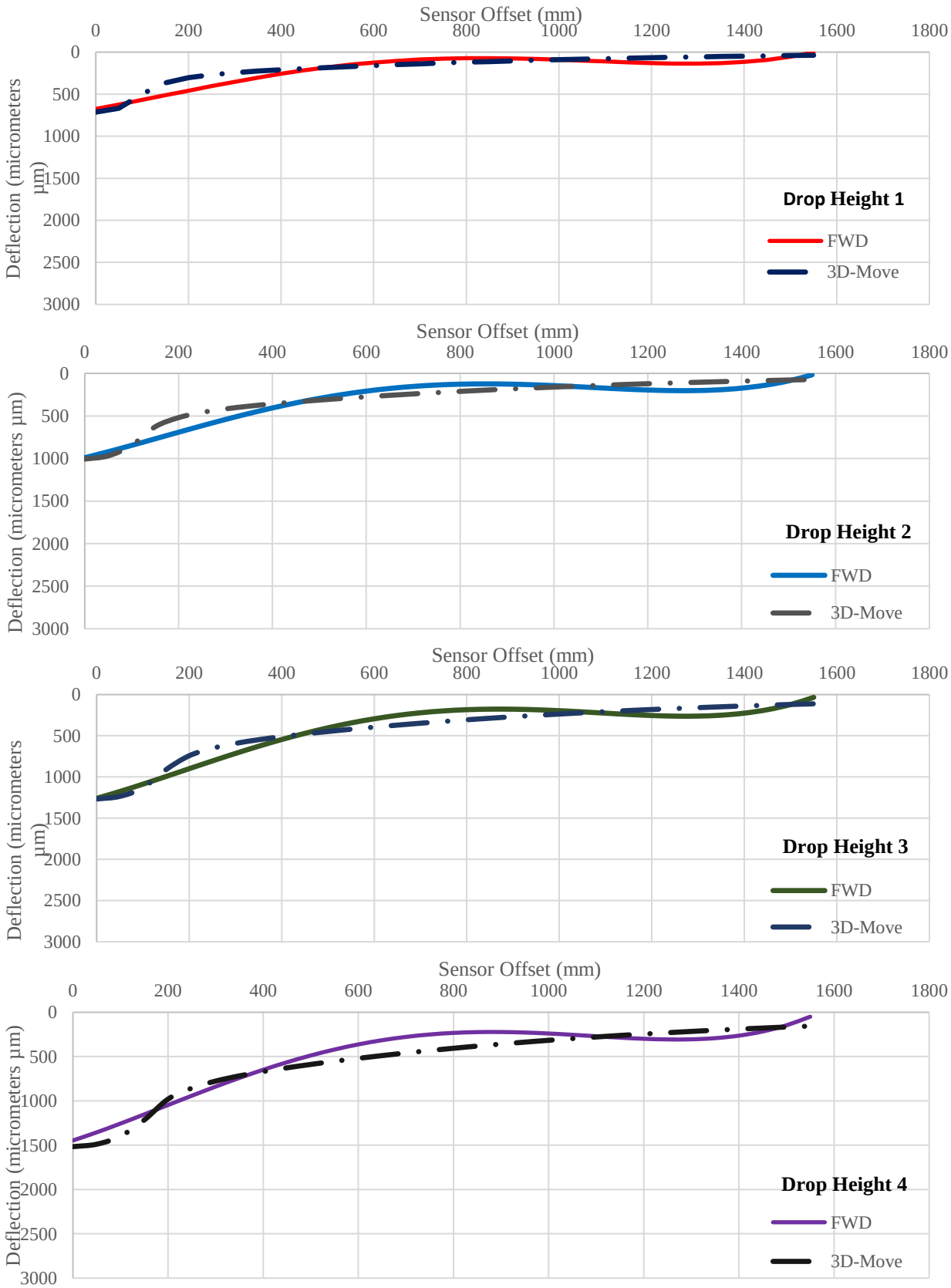

Figure C –95. Simulated Deflection Bowl for the SHRP section M320.

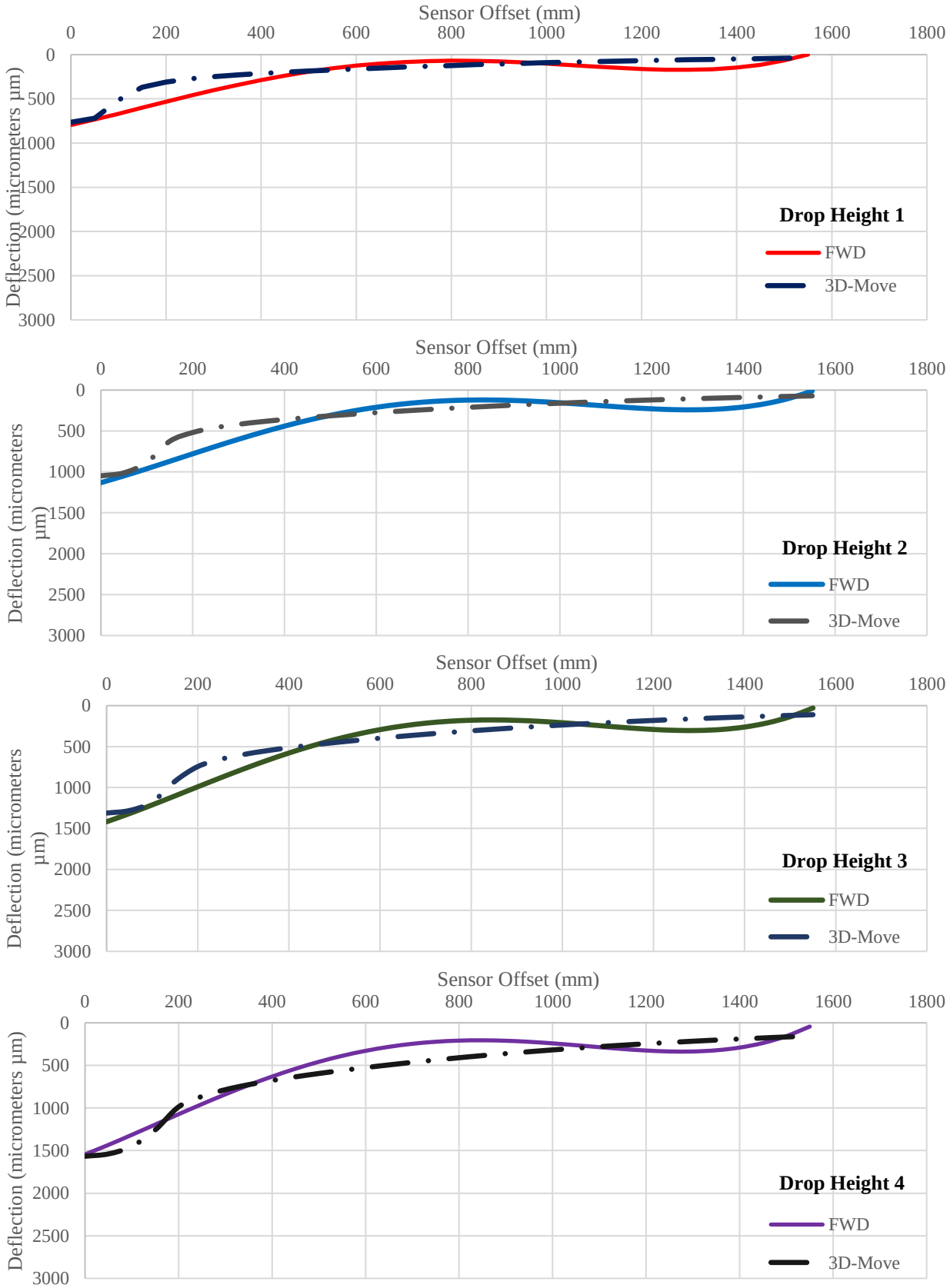

Figure C –96. Simulated Deflection Bowl for the SHRP section M330.

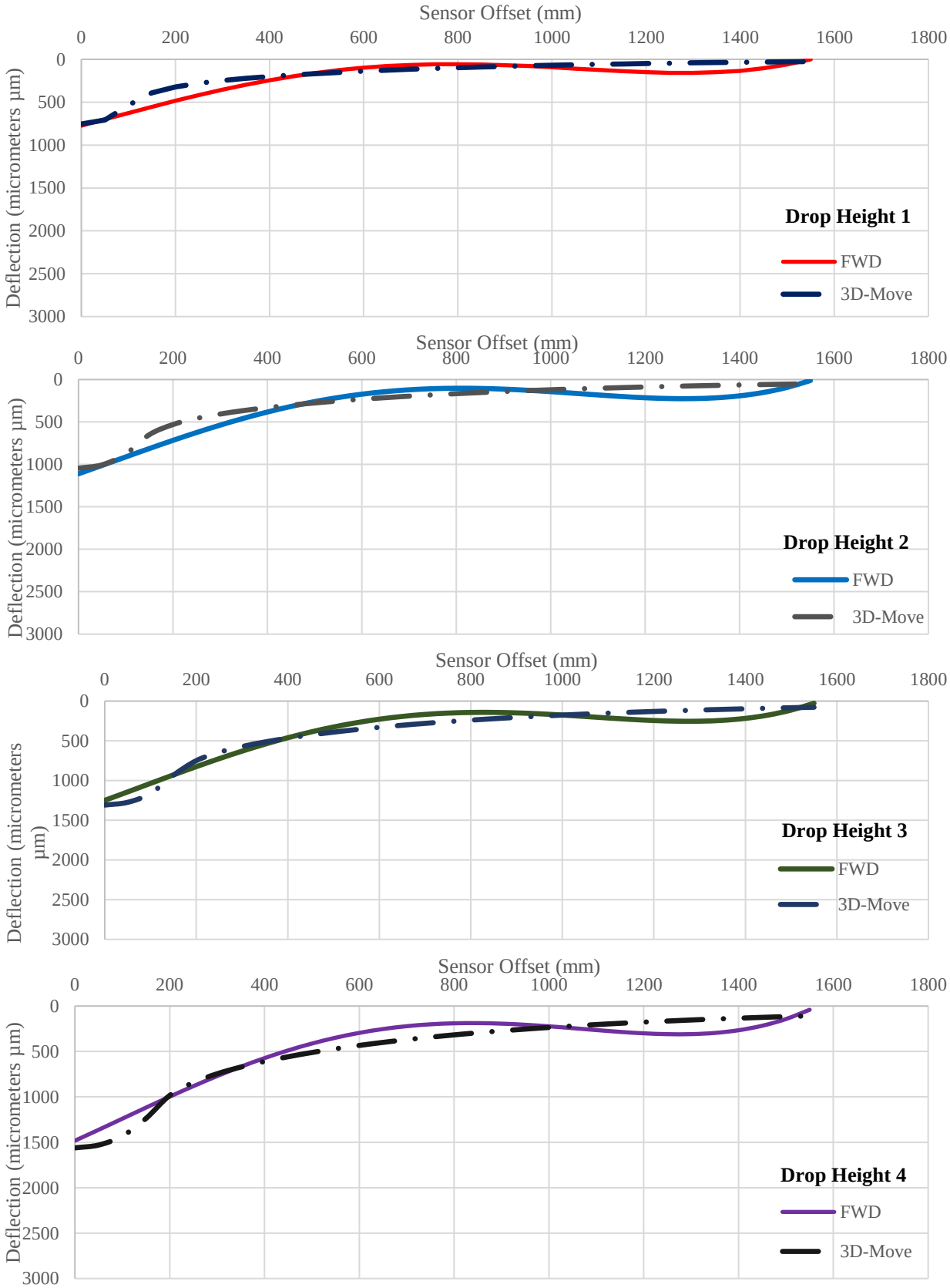

Figure C –97. Simulated Deflection Bowl for the SHRP section M340.

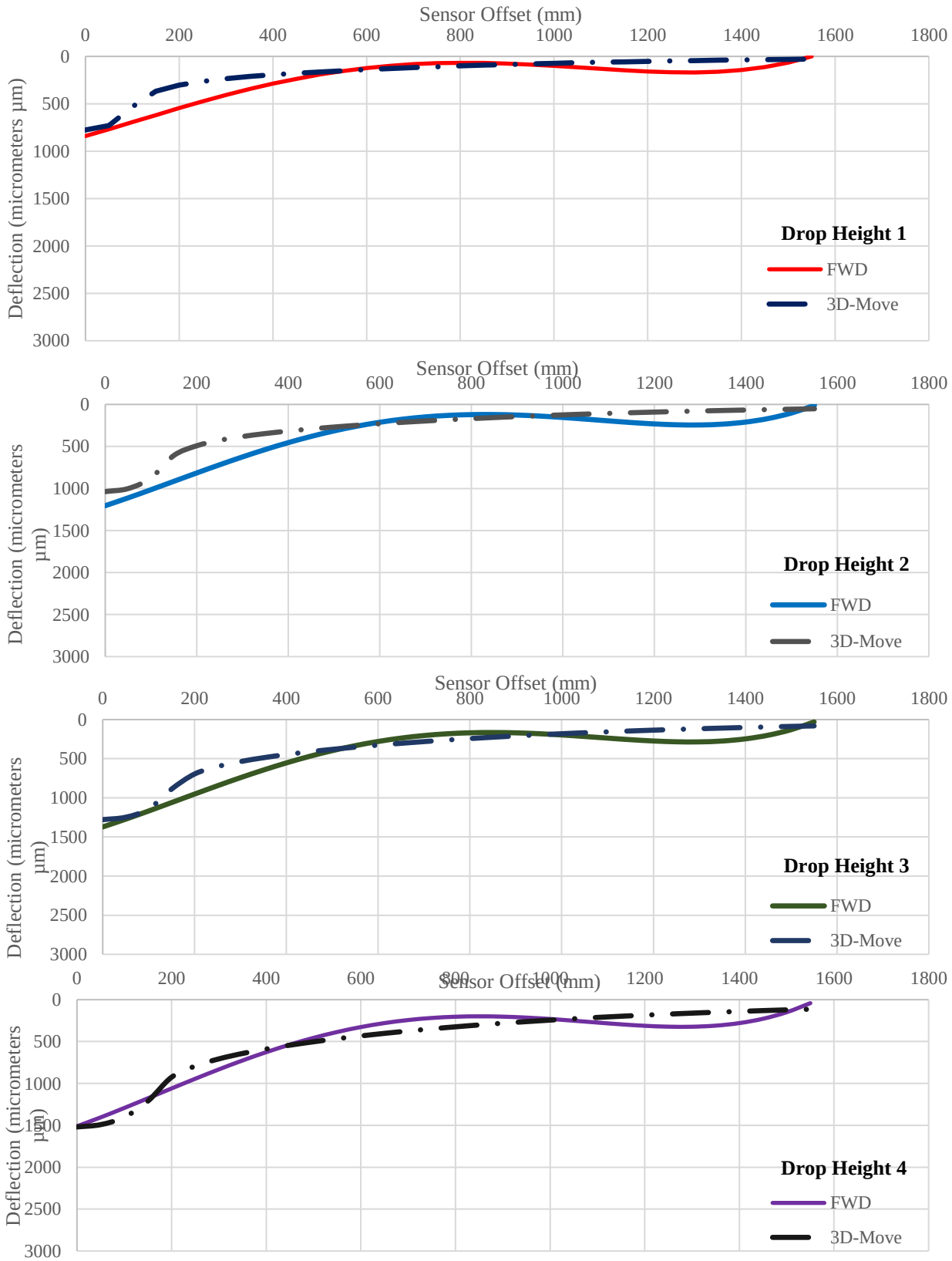

Figure C –98. Simulated Deflection Bowl for the SHRP section M350.

APPENDIX C: FWD TEST, 3D-MOVEANALYSIS, AND ANSYS DEFLECTION BOWL SIMULATIONS

State of Arkansas

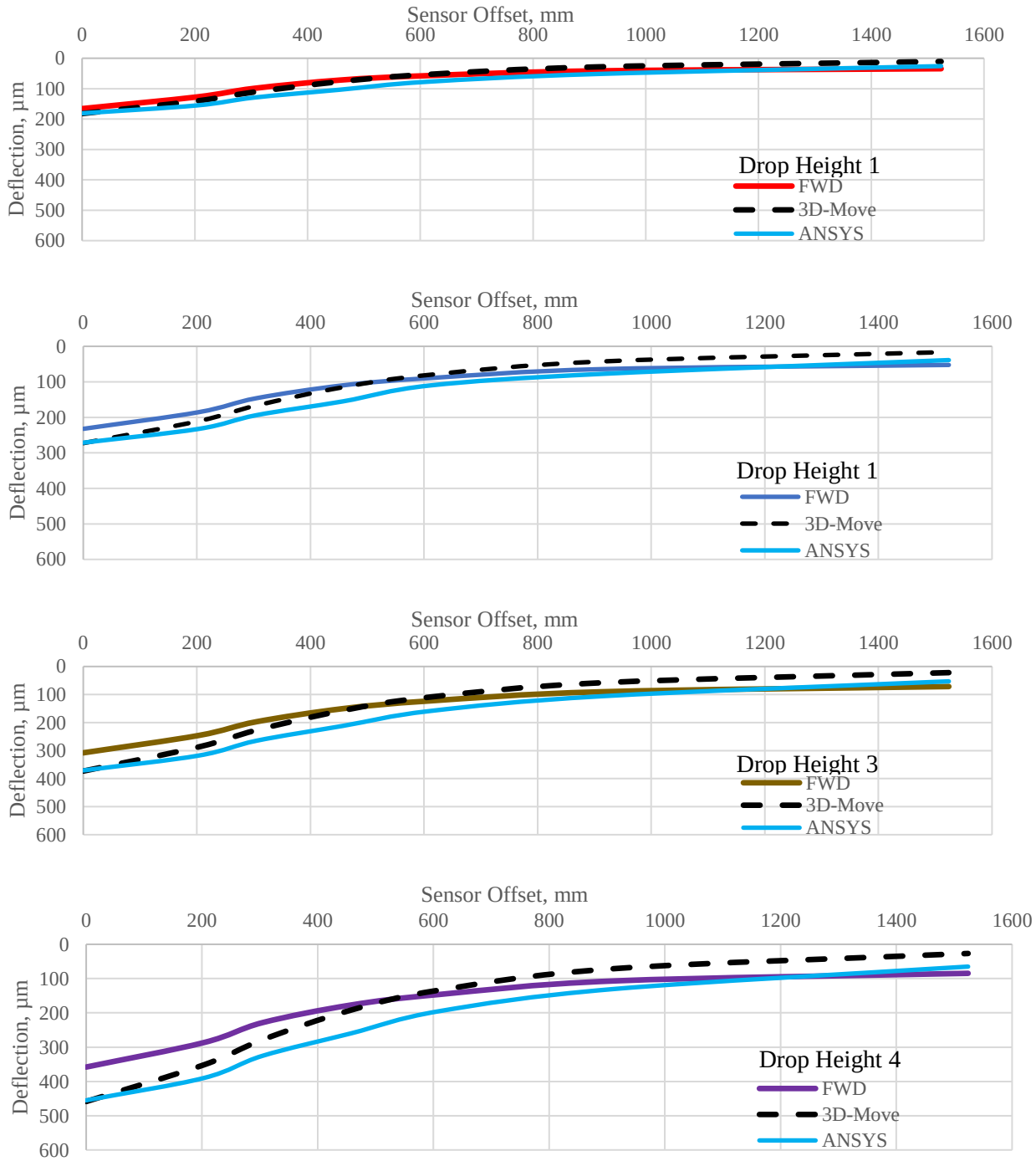

Figure D–1. Simulated Deflection Bowl for the SHRP section 0113.

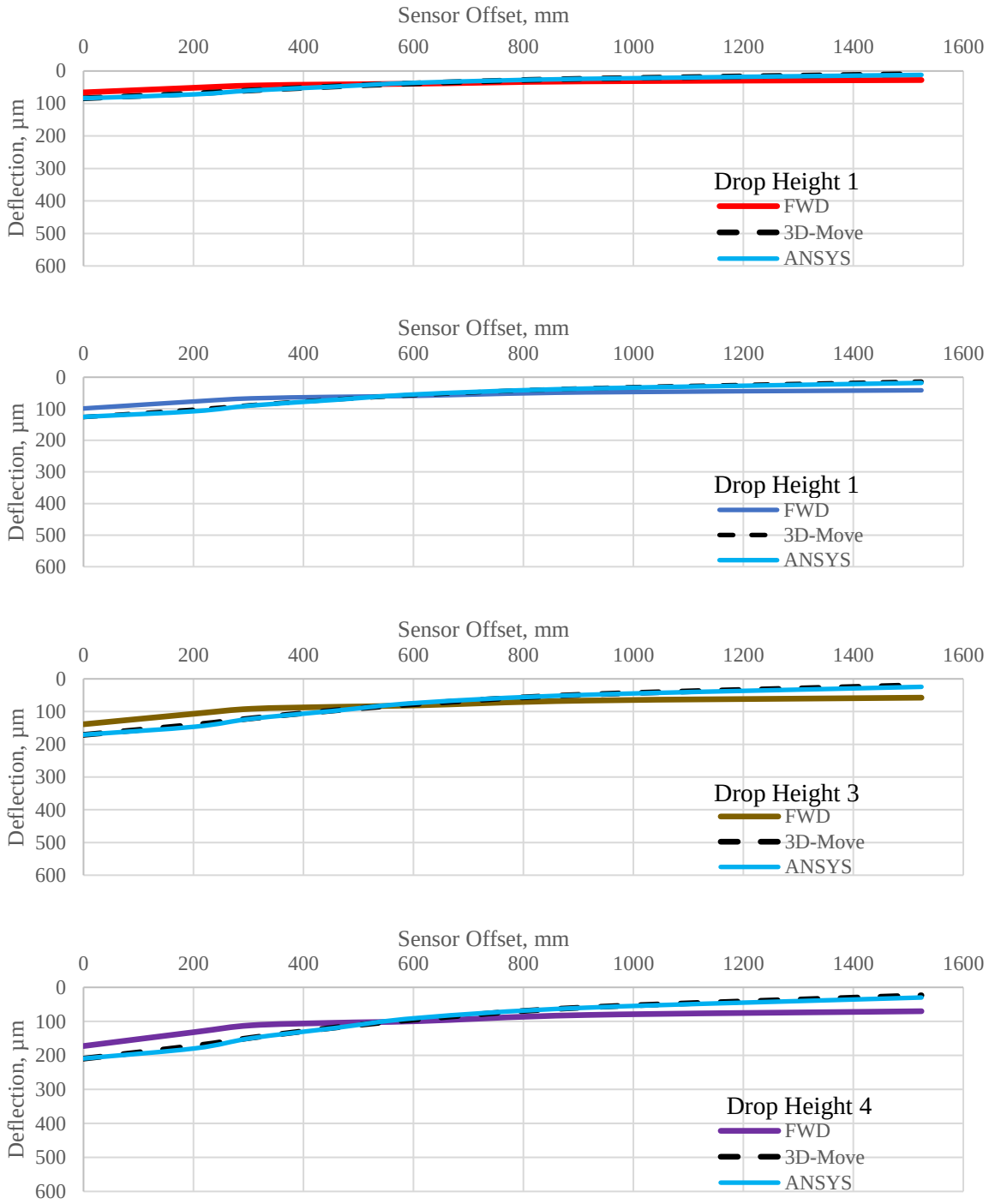

Figure D–2. Simulated Deflection Bowl for the SHRP section 0115.

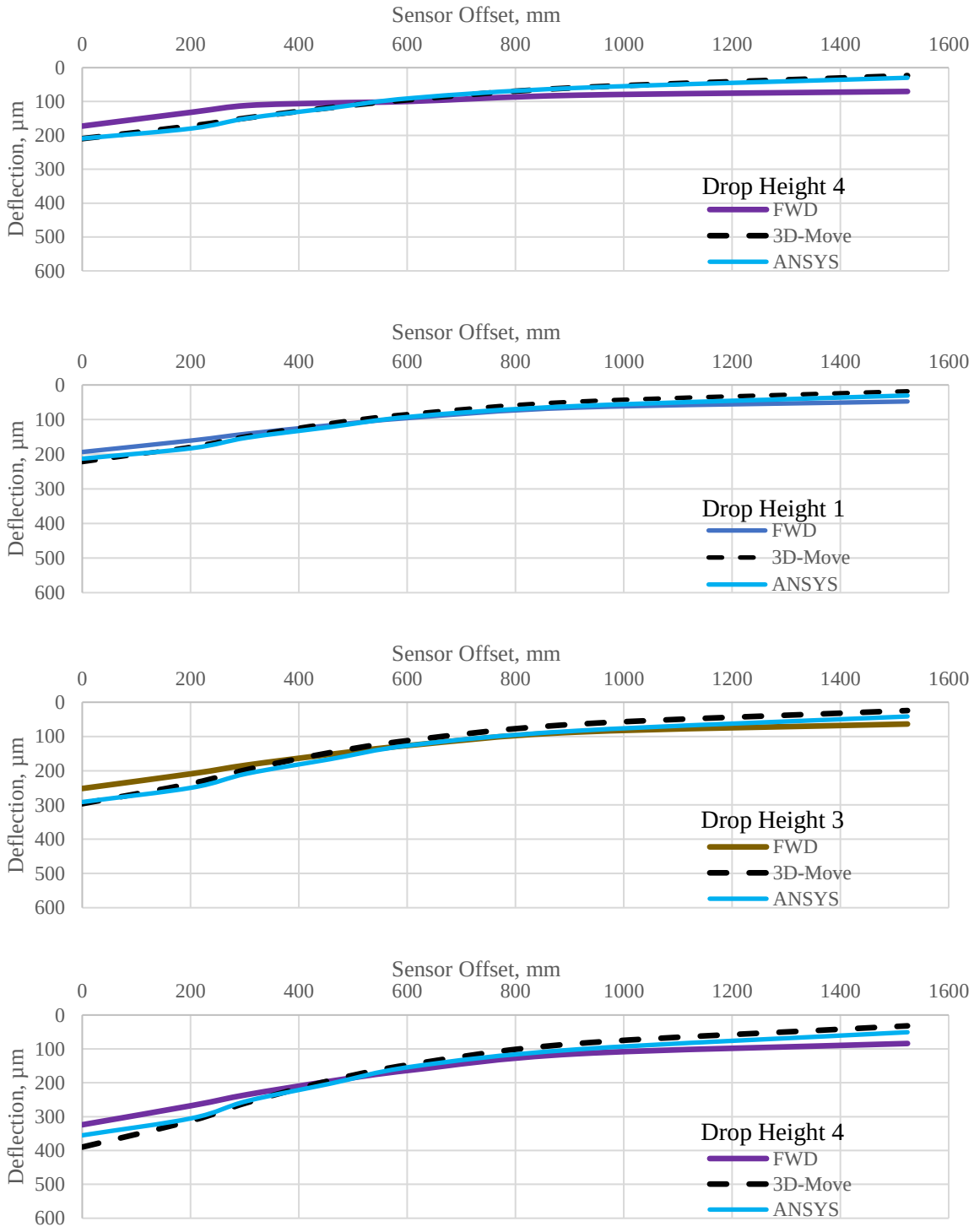

Figure D–3. Simulated Deflection Bowl for the SHRP section 0120.

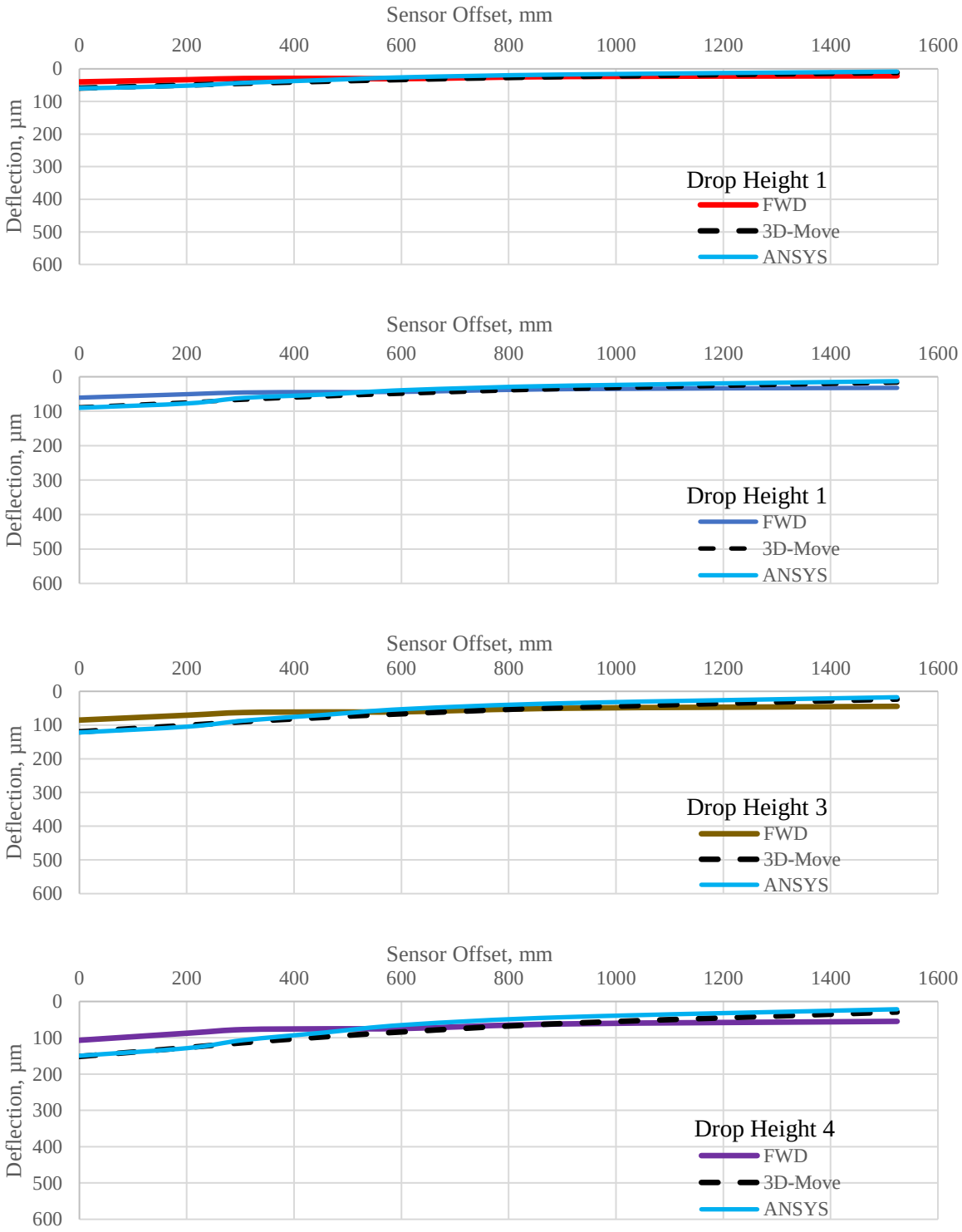

Figure D–4. Simulated Deflection Bowl for the SHRP section 0123.

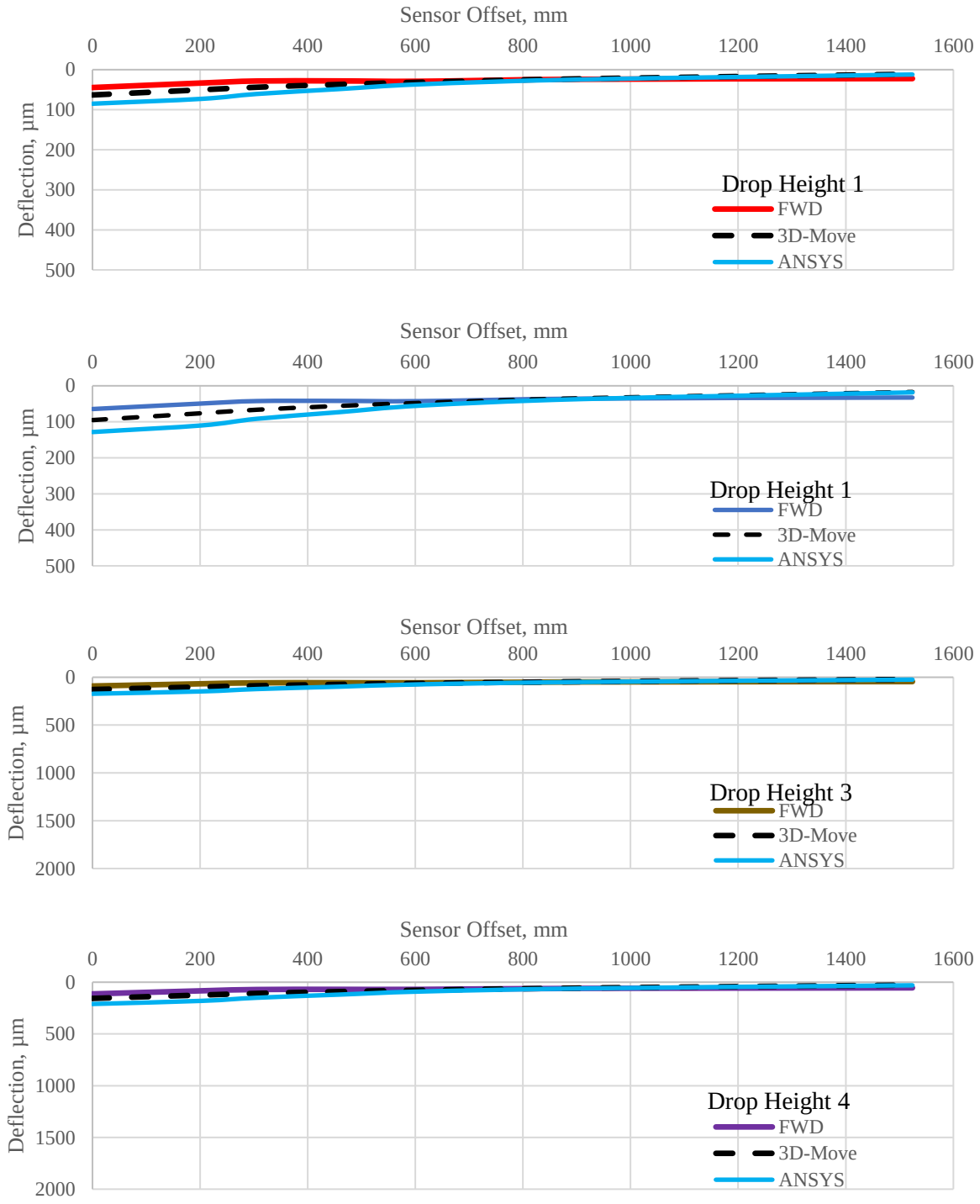

Figure D–5. Simulated Deflection Bowl for the SHRP section 0124.

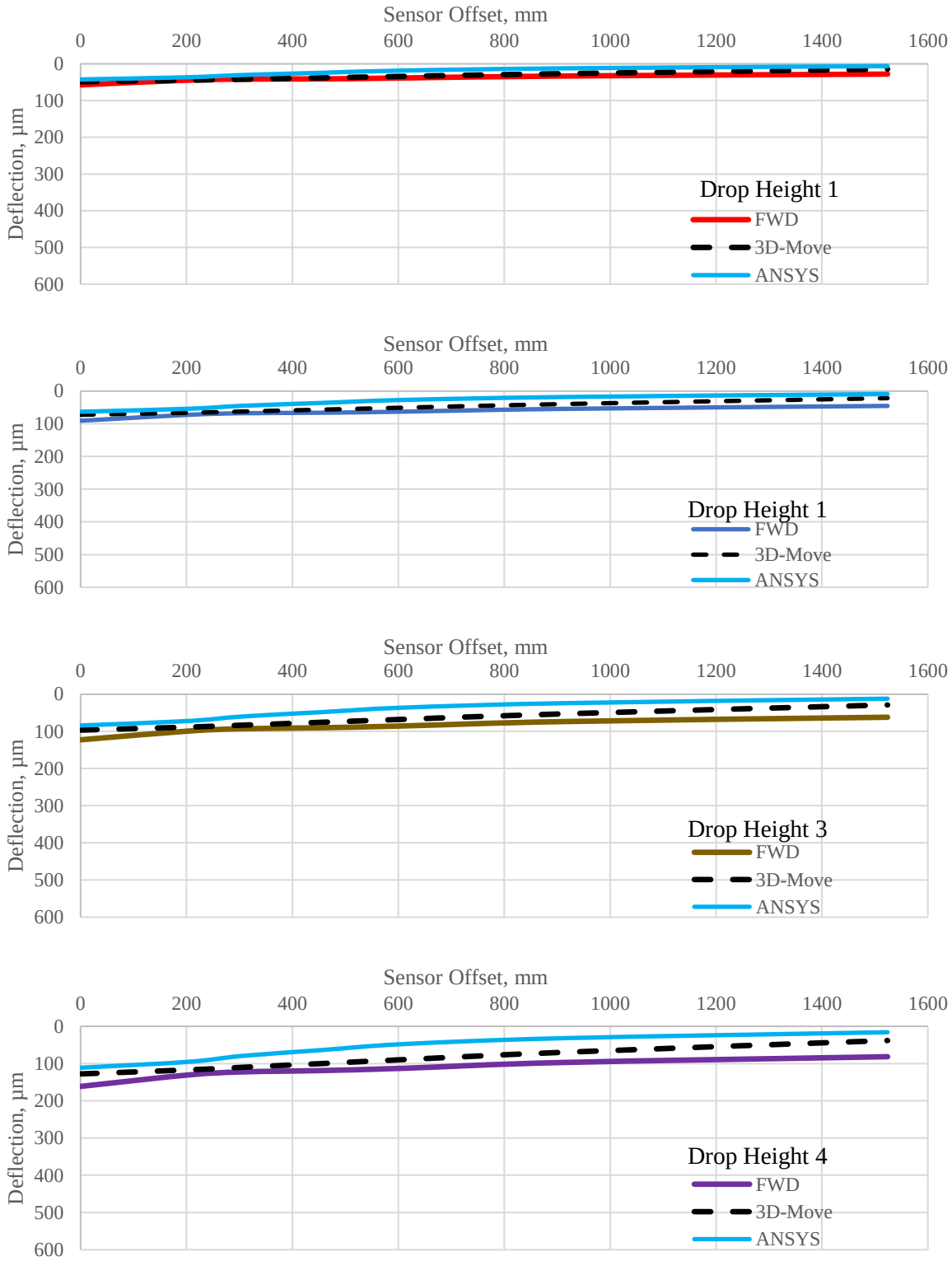

Figure D–6. Simulated Deflection Bowl for the SHRP section 0116.

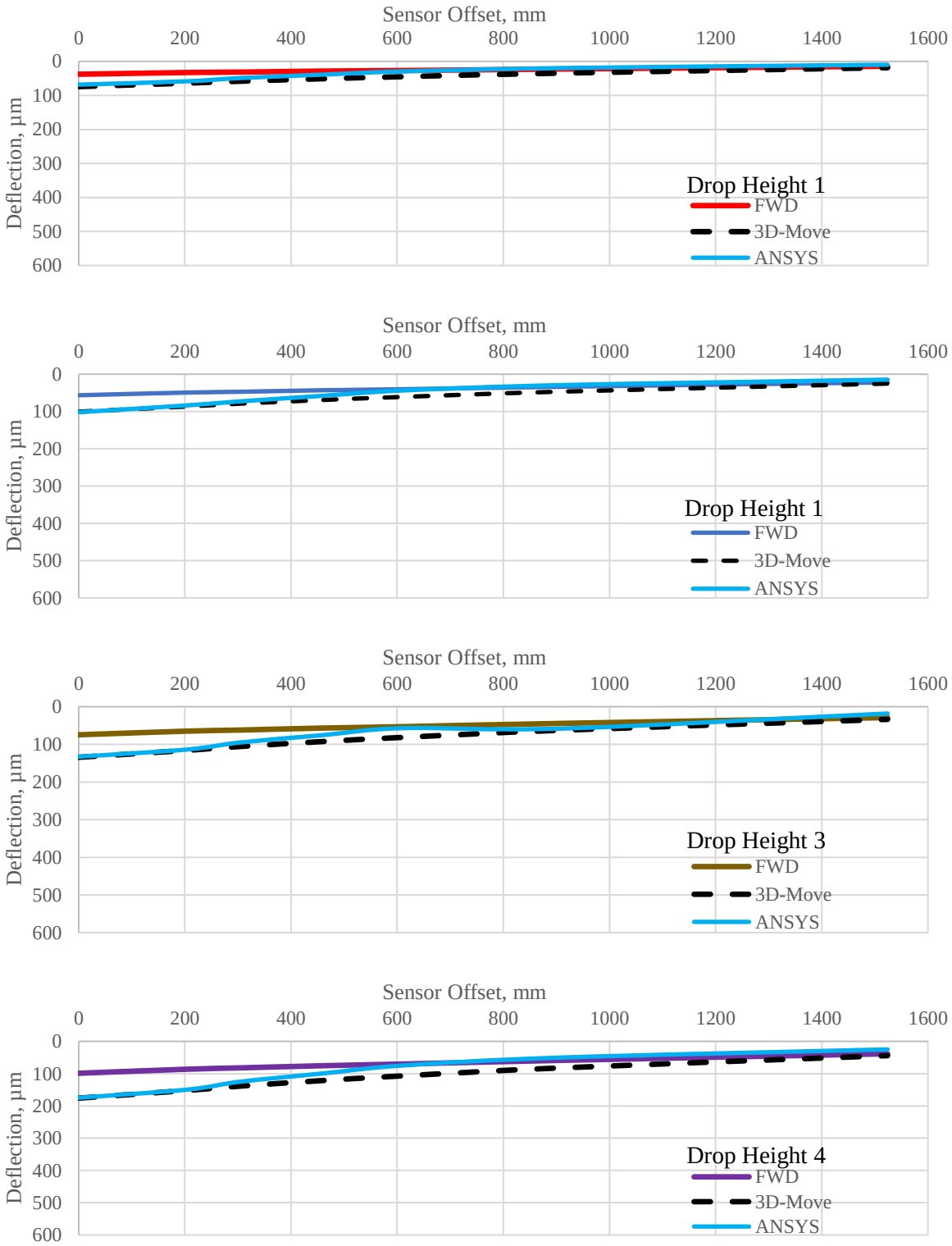

Figure D–7. Simulated Deflection Bowl for the SHRP section 3071.

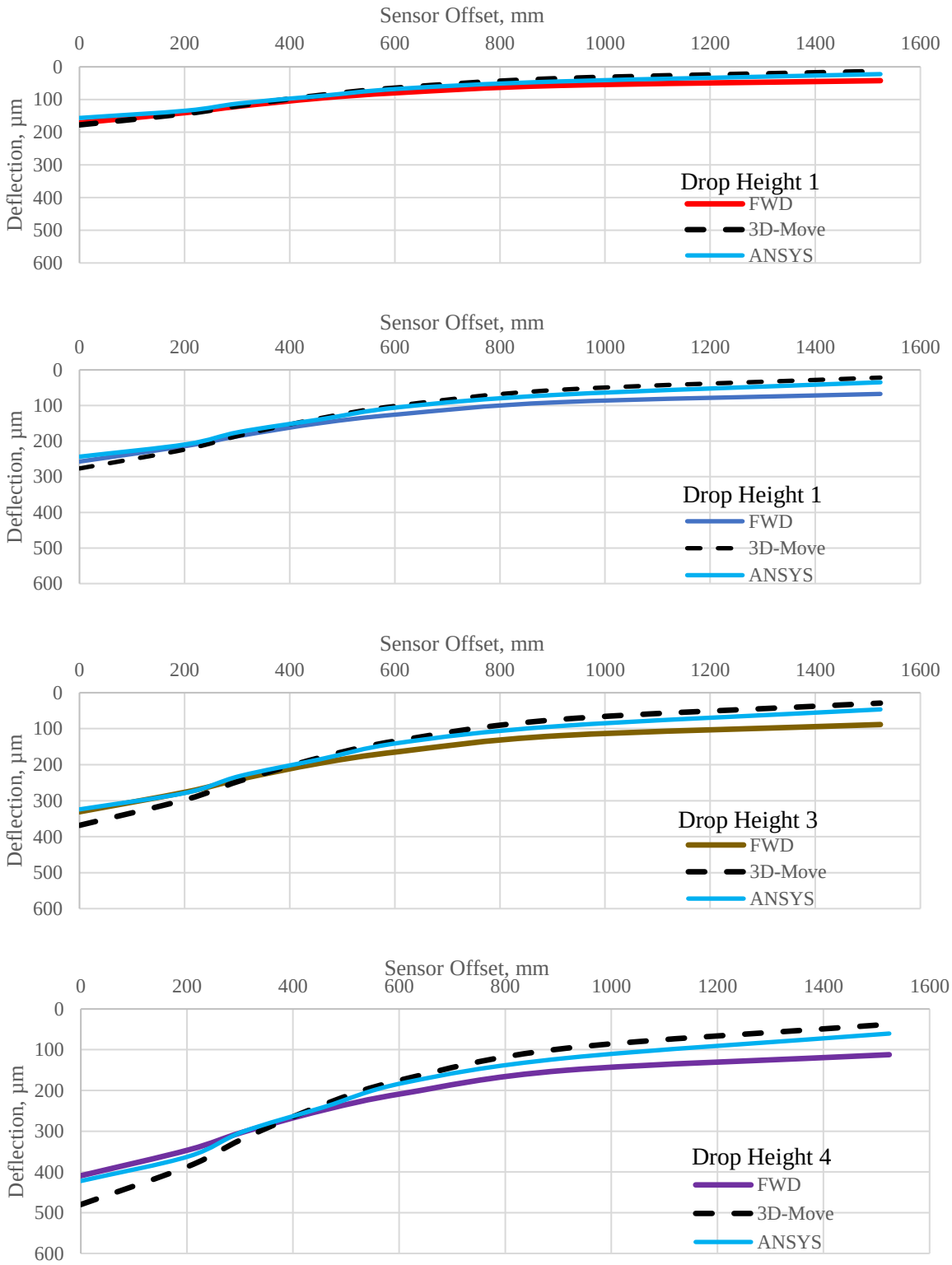

Figure D–8. Simulated Deflection Bowl for the SHRP section 0113.

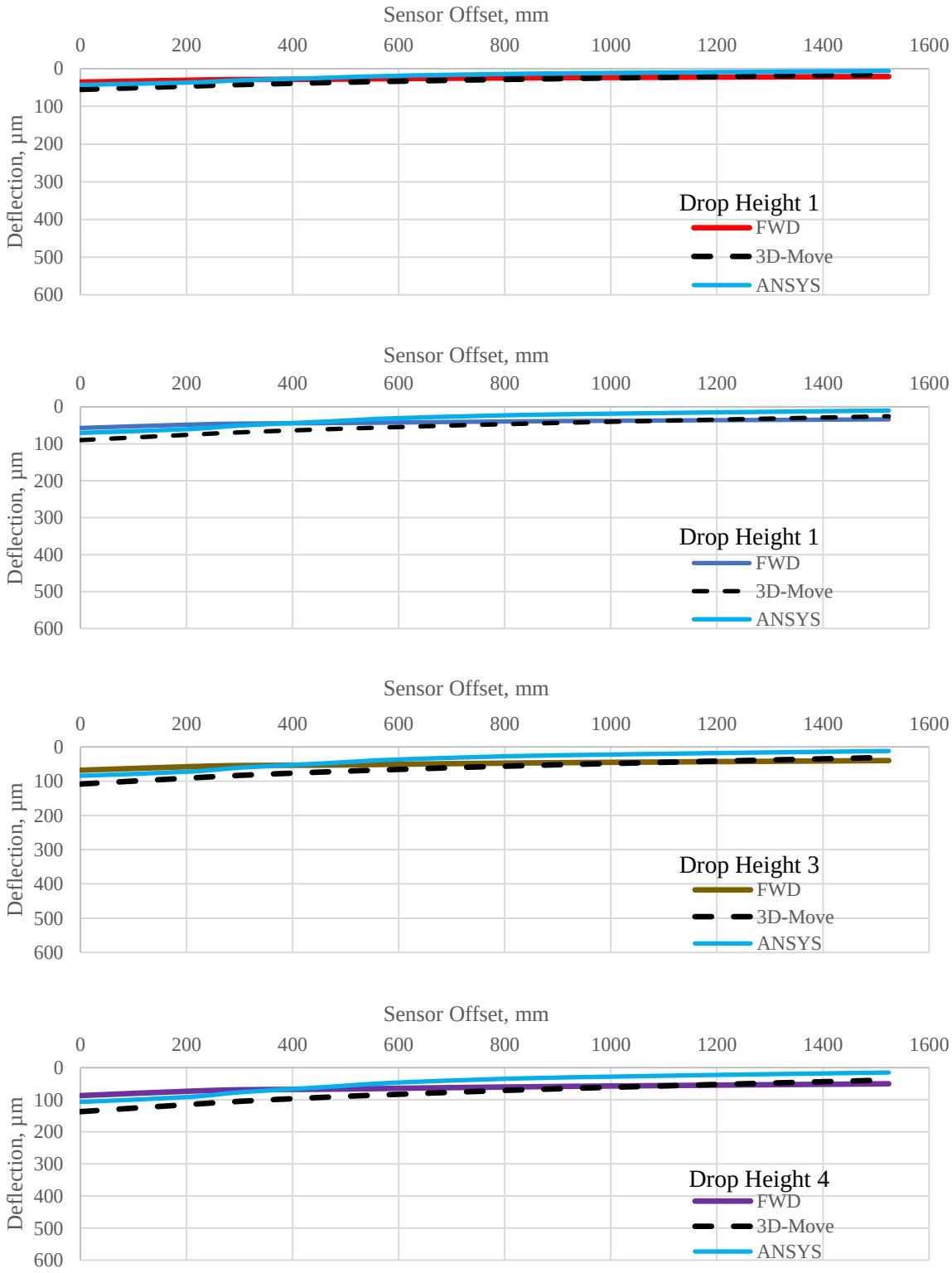

Figure D–9. Simulated Deflection Bowl for the SHRP section 0115.

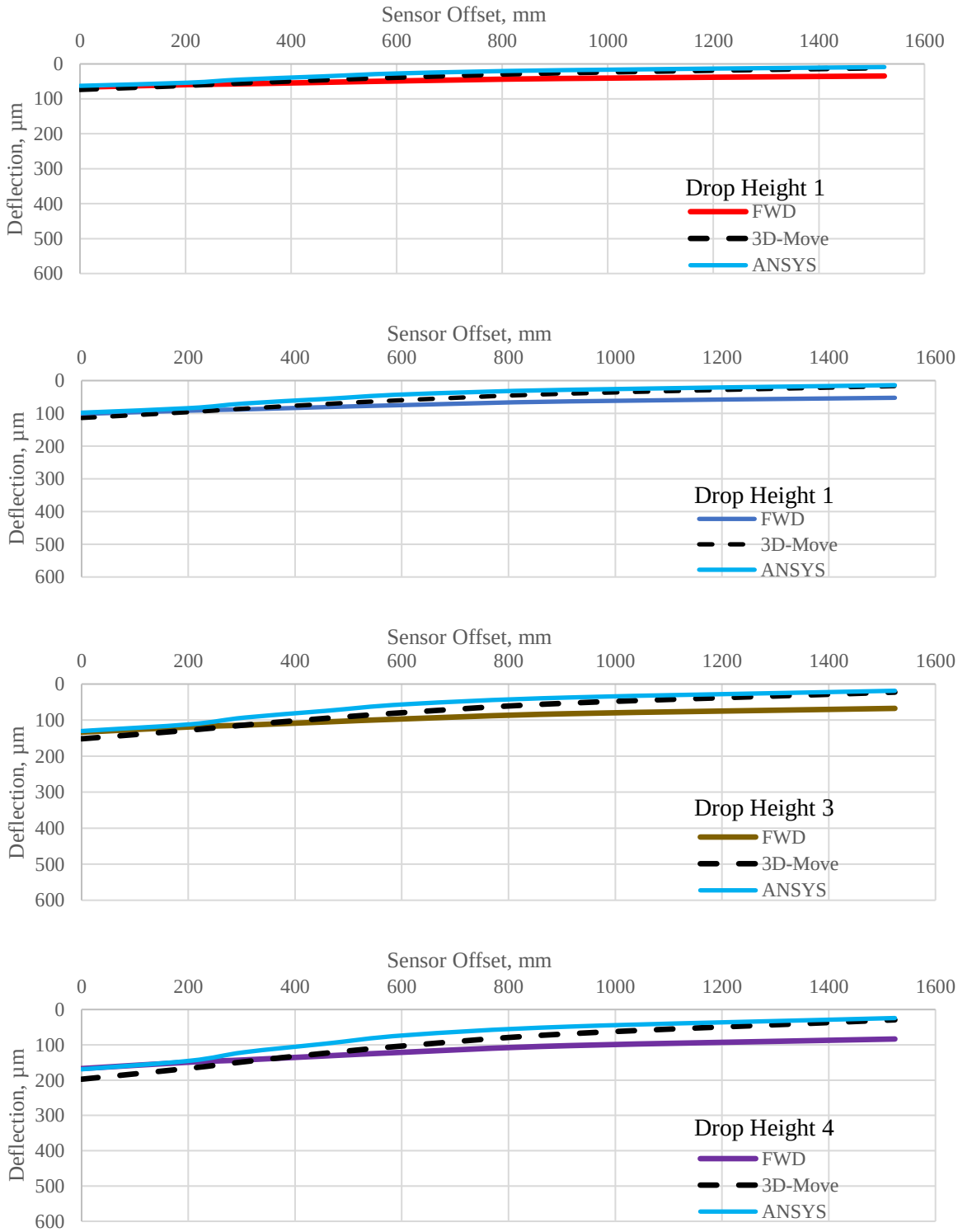

Figure D–10. Simulated Deflection Bowl for the SHRP section 0117.

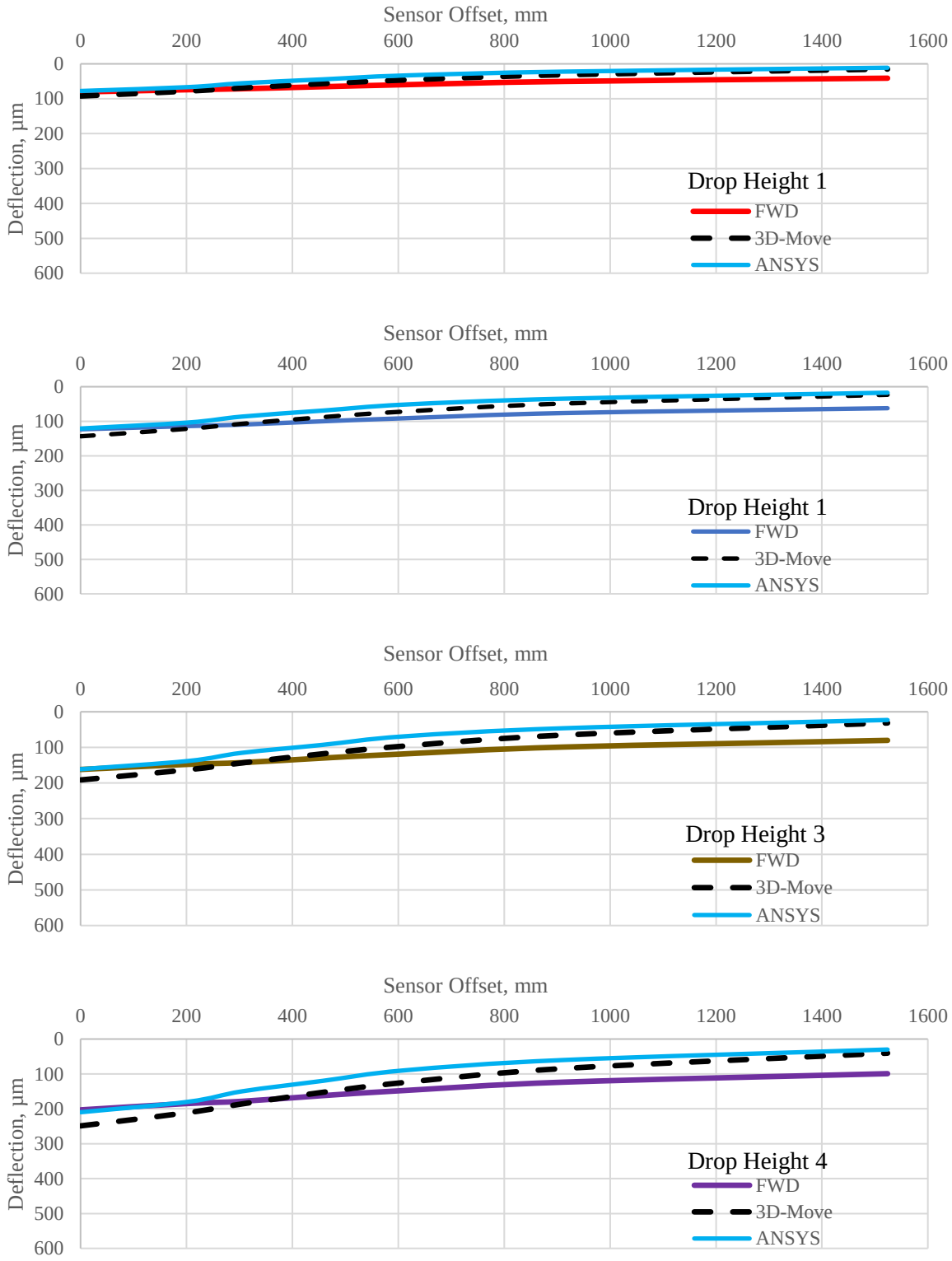

Figure D–11. Simulated Deflection Bowl for the SHRP section 0119.

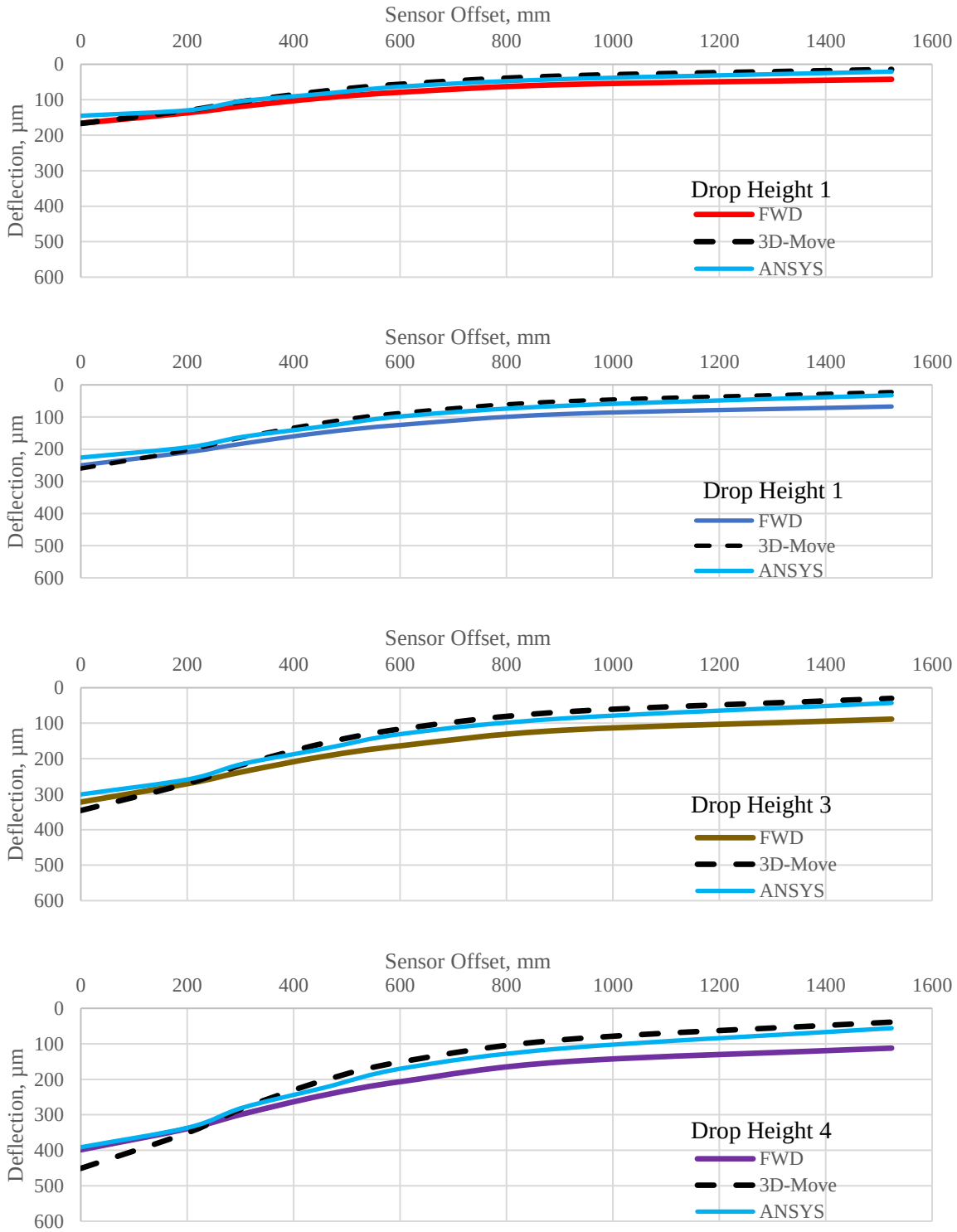

Figure D–12. Simulated Deflection Bowl for the SHRP section 0121.

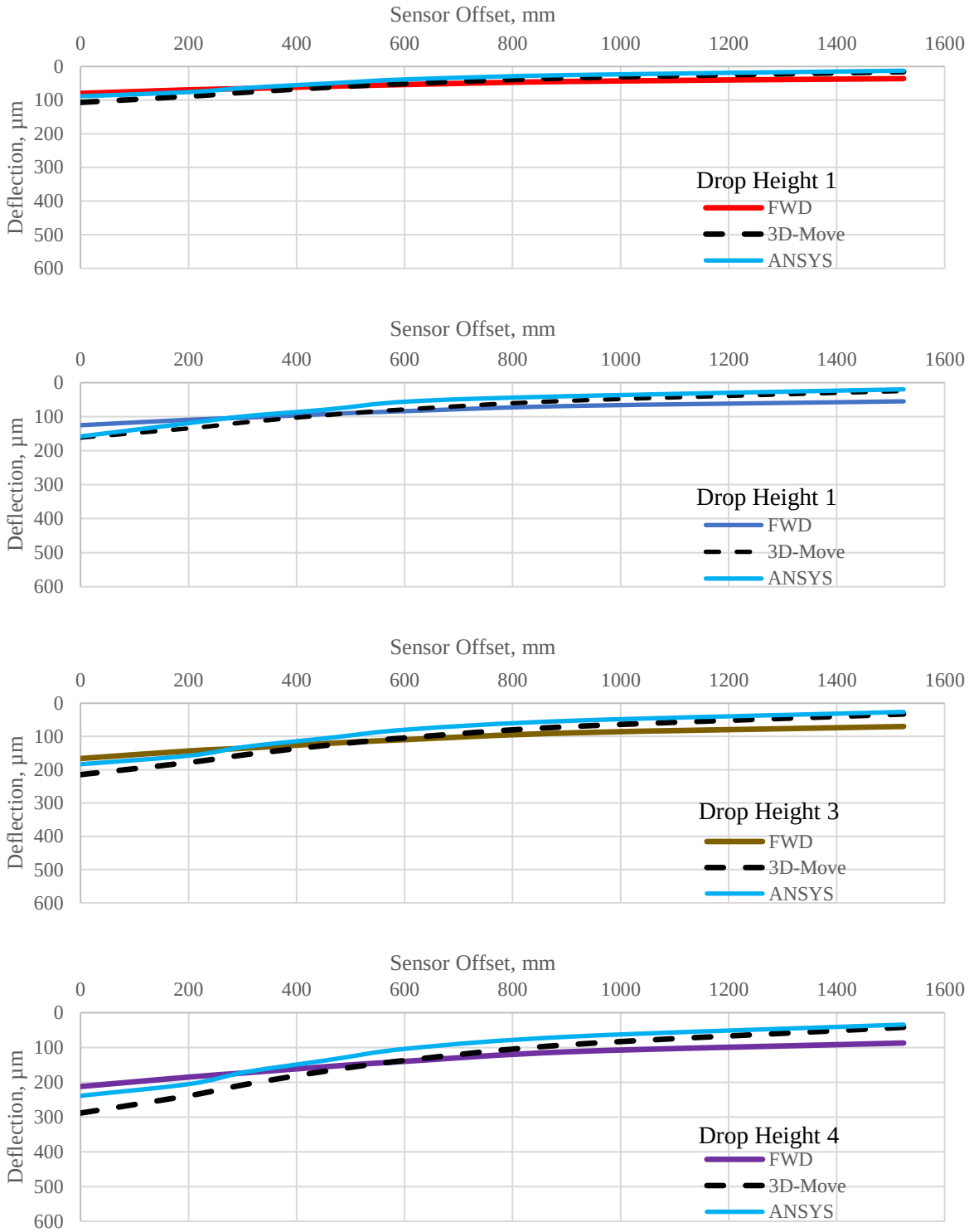

Figure D–13. Simulated Deflection Bowl for the SHRP section 0122.

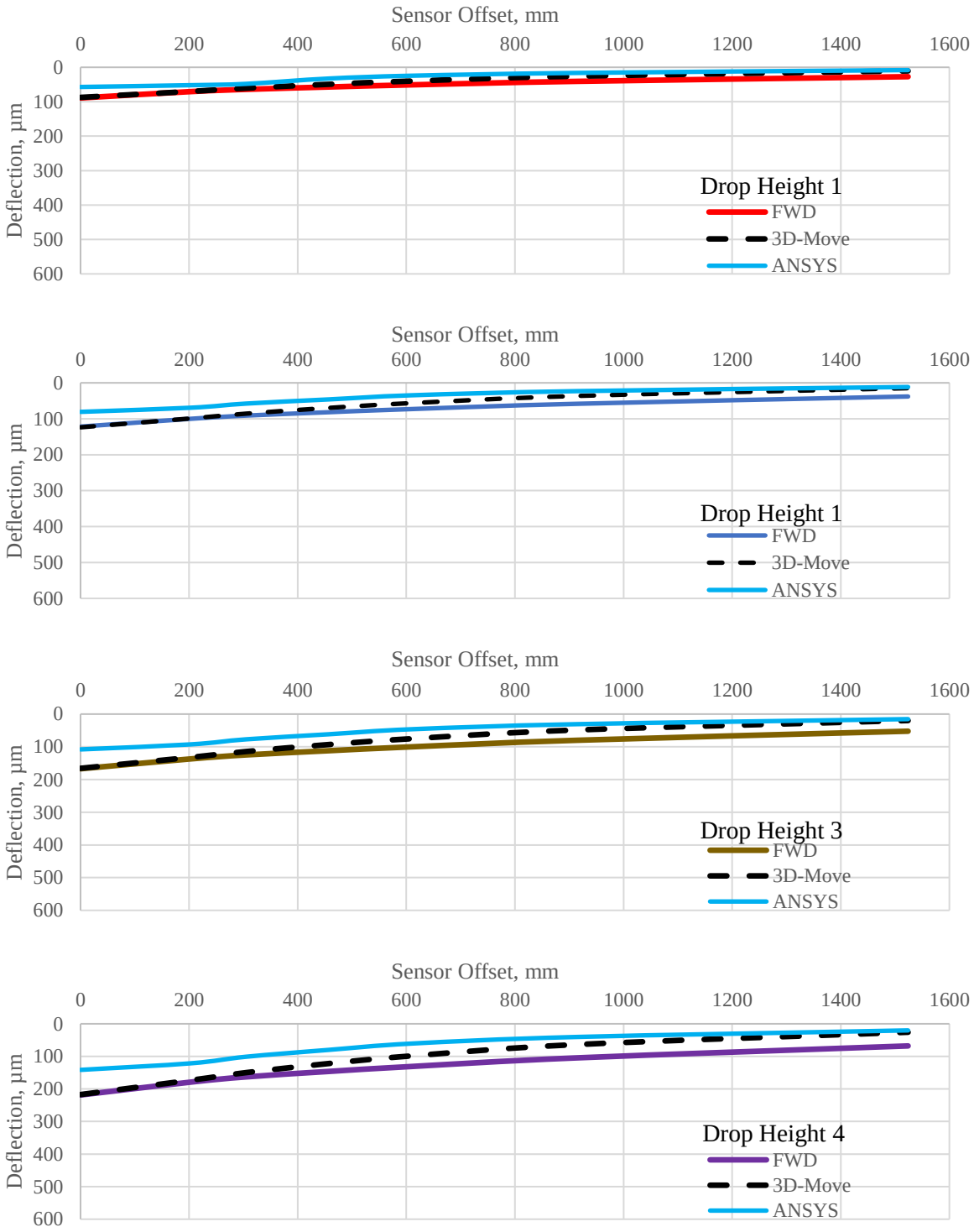

Figure D–14. Simulated Deflection Bowl for the SHRP section 3056.

State of New Mexico

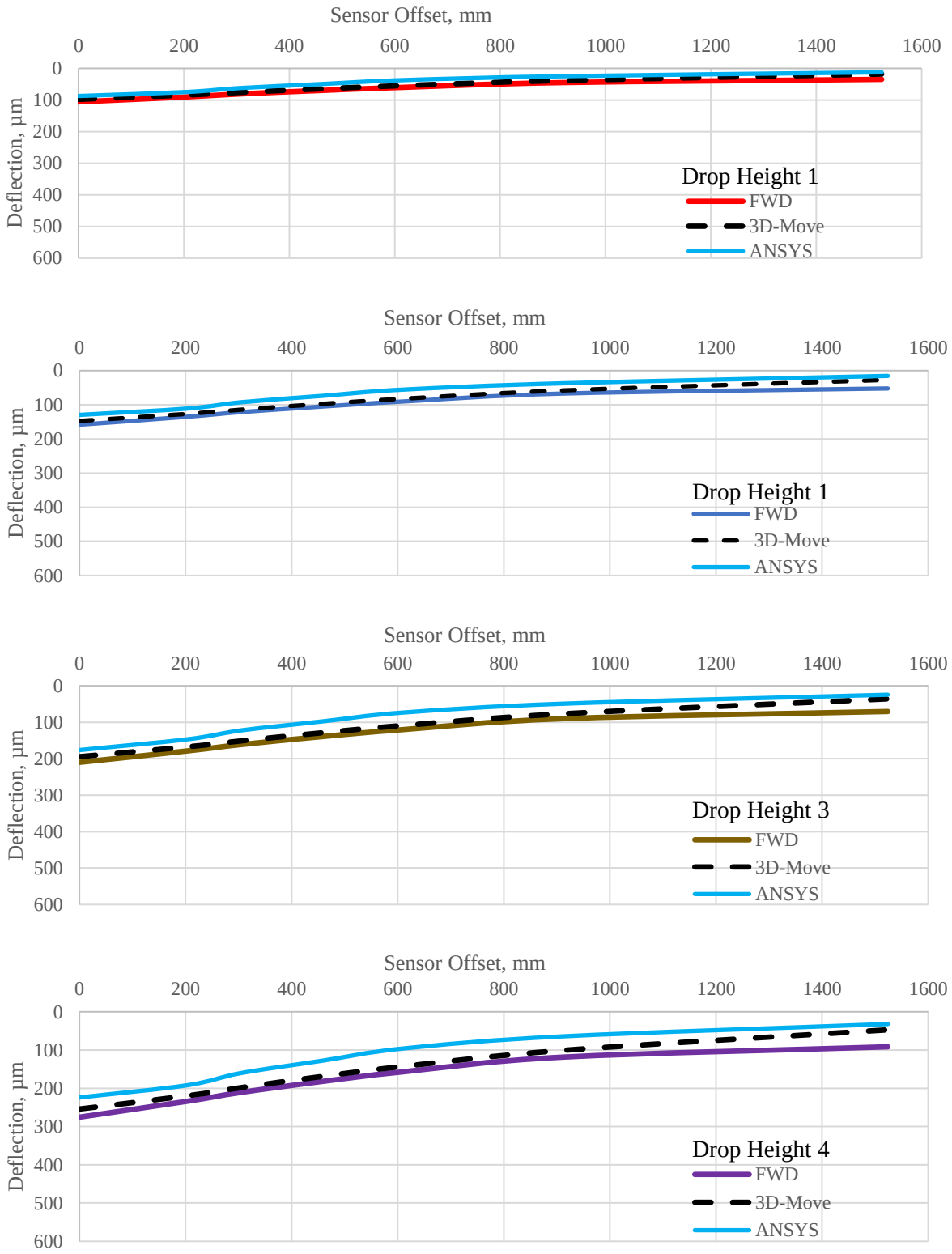

Figure D–15. Simulated Deflection Bowl for the SHRP section 0108.

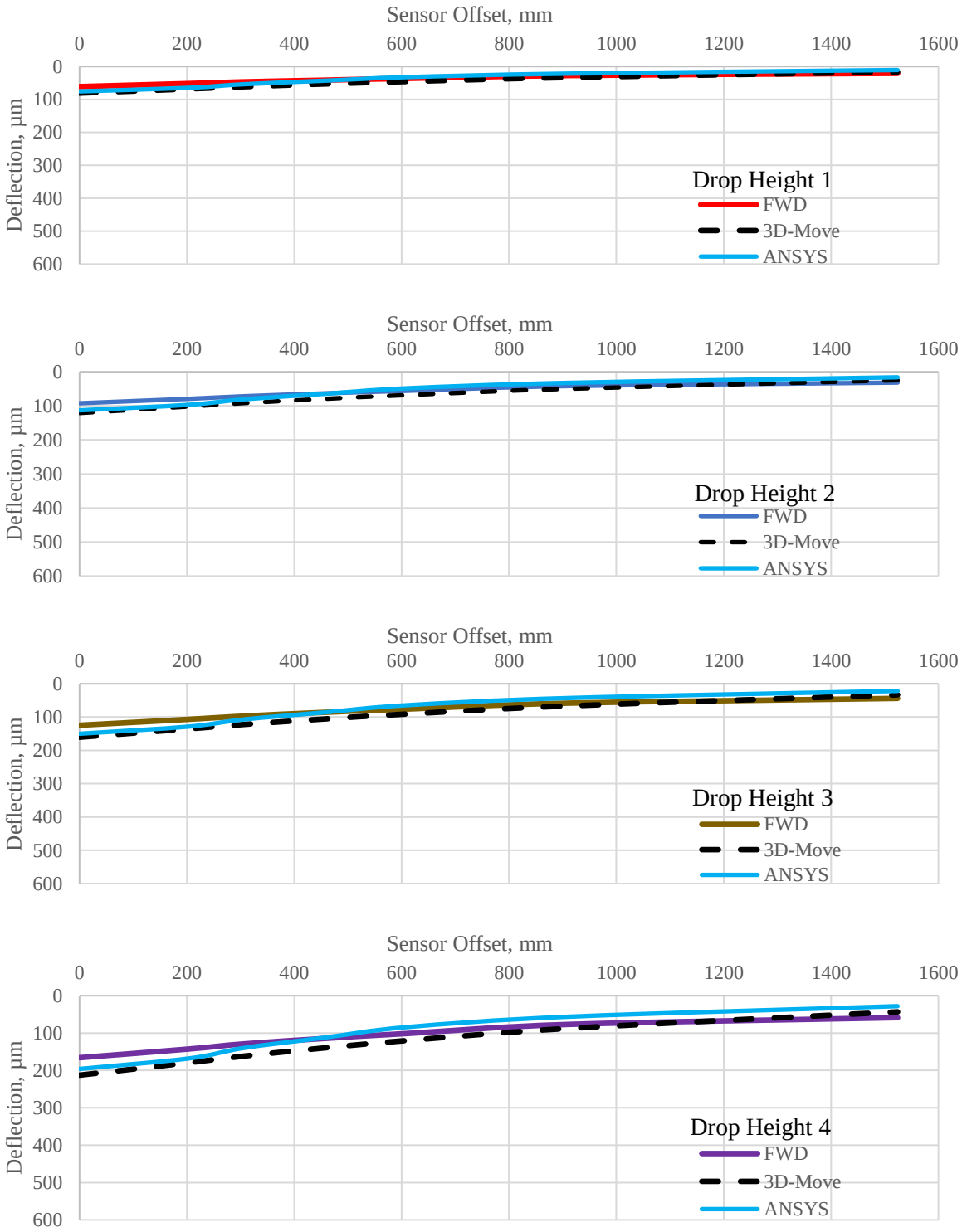

Figure D–16. Simulated Deflection Bowl for the SHRP section 0110.

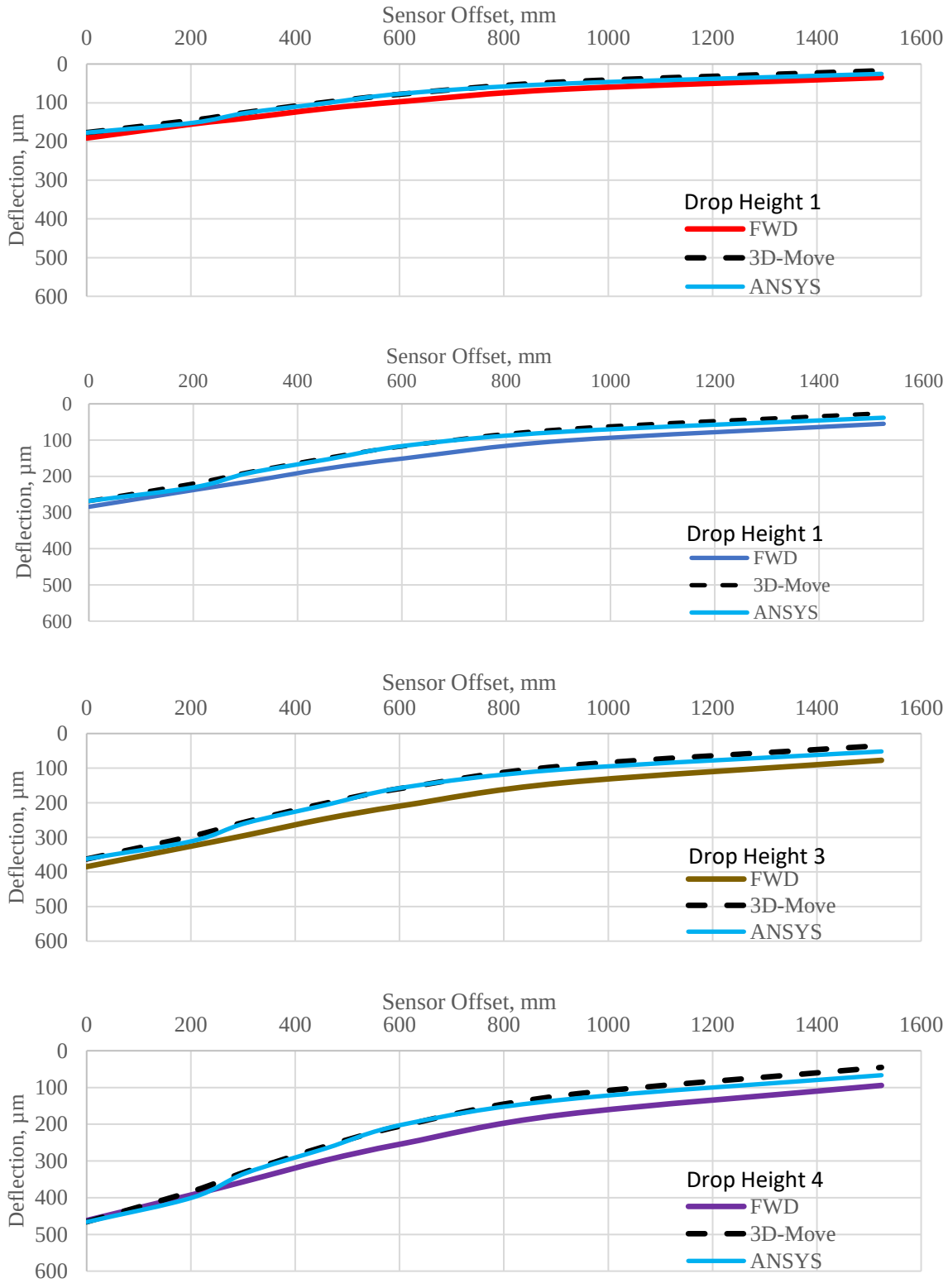

Figure D–17. Simulated Deflection Bowl for the SHRP section 6401.

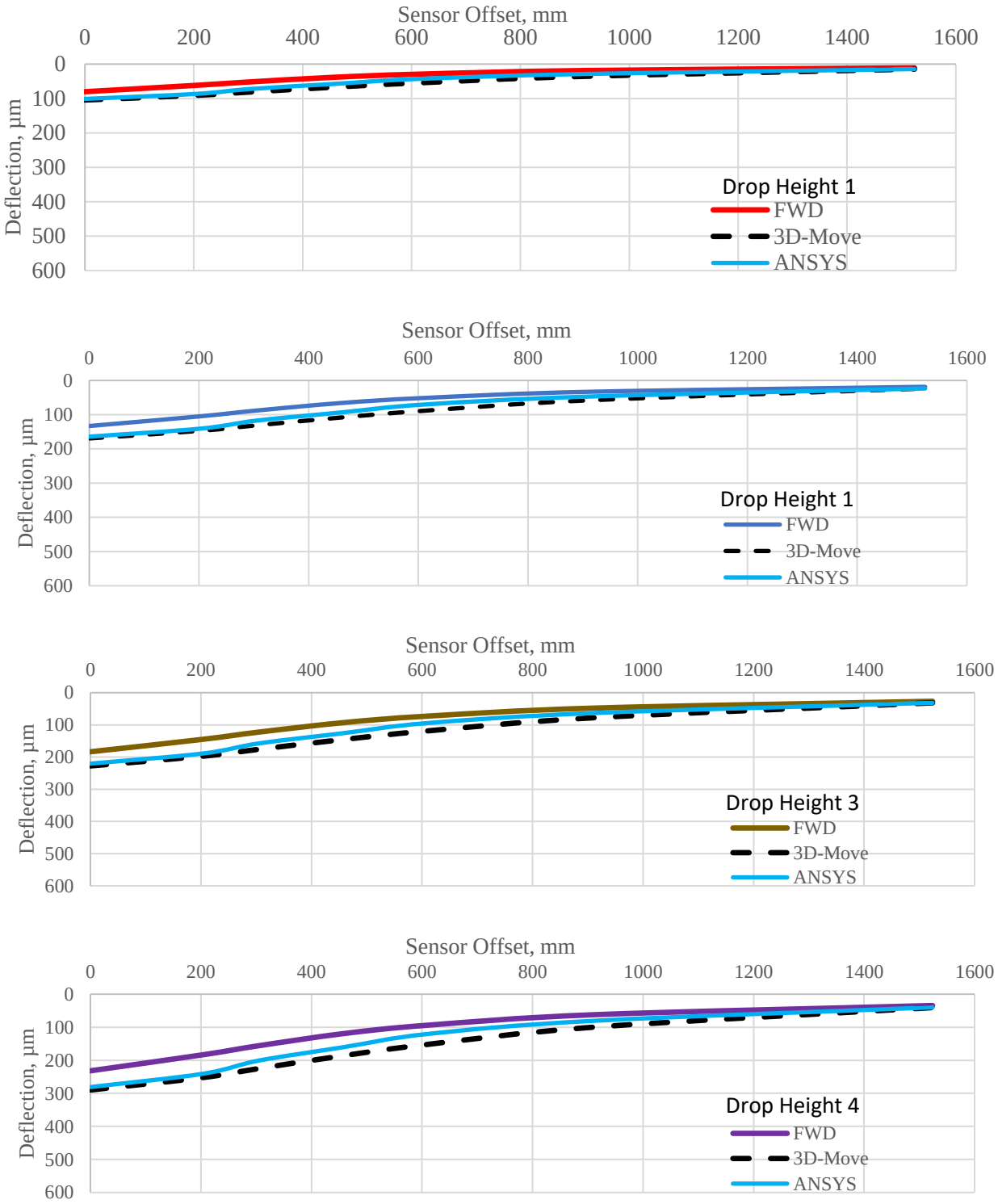

Figure D–18. Simulated Deflection Bowl for the SHRP section 1112.

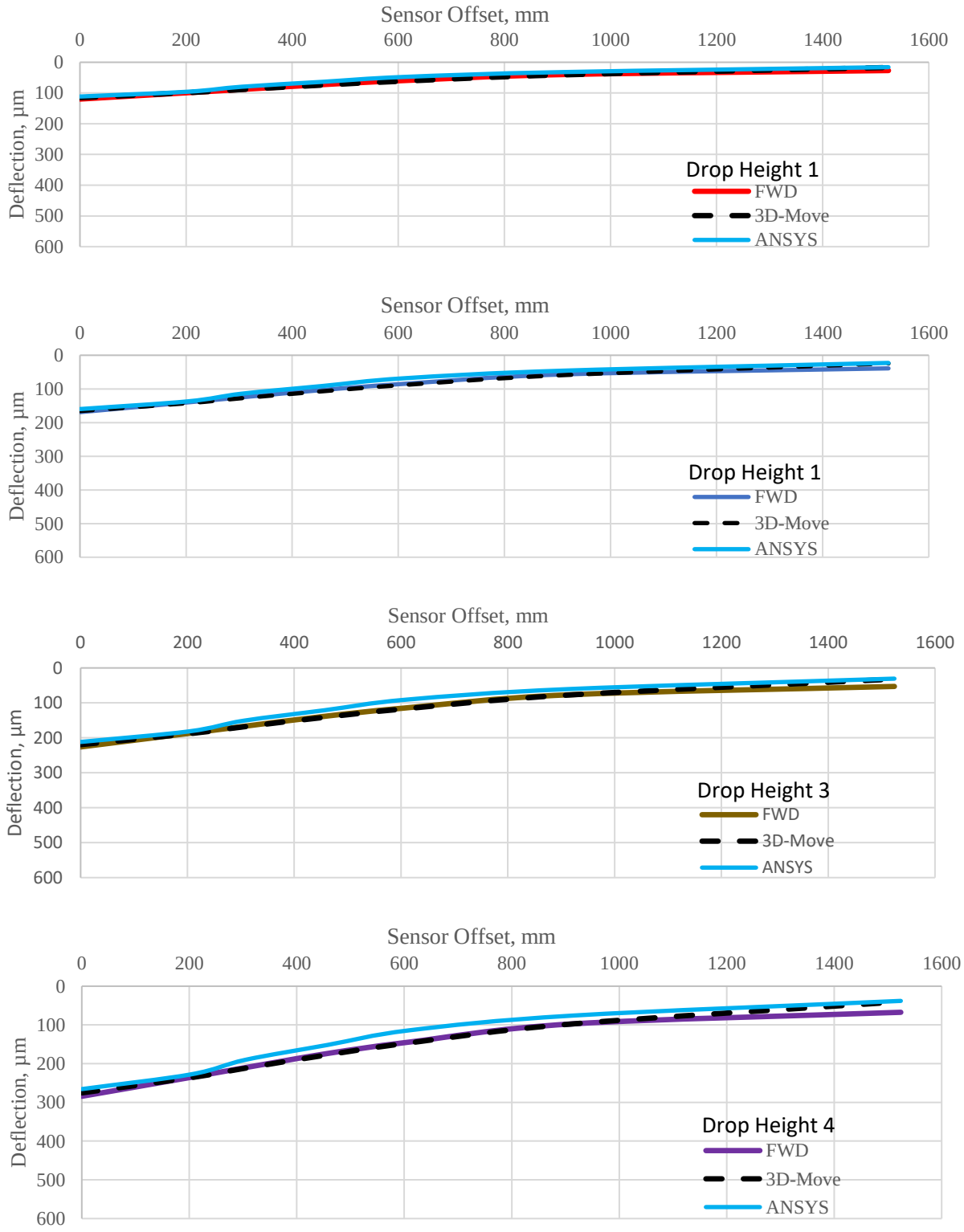

Figure D–19. Simulated Deflection Bowl for the SHRP section 1005.

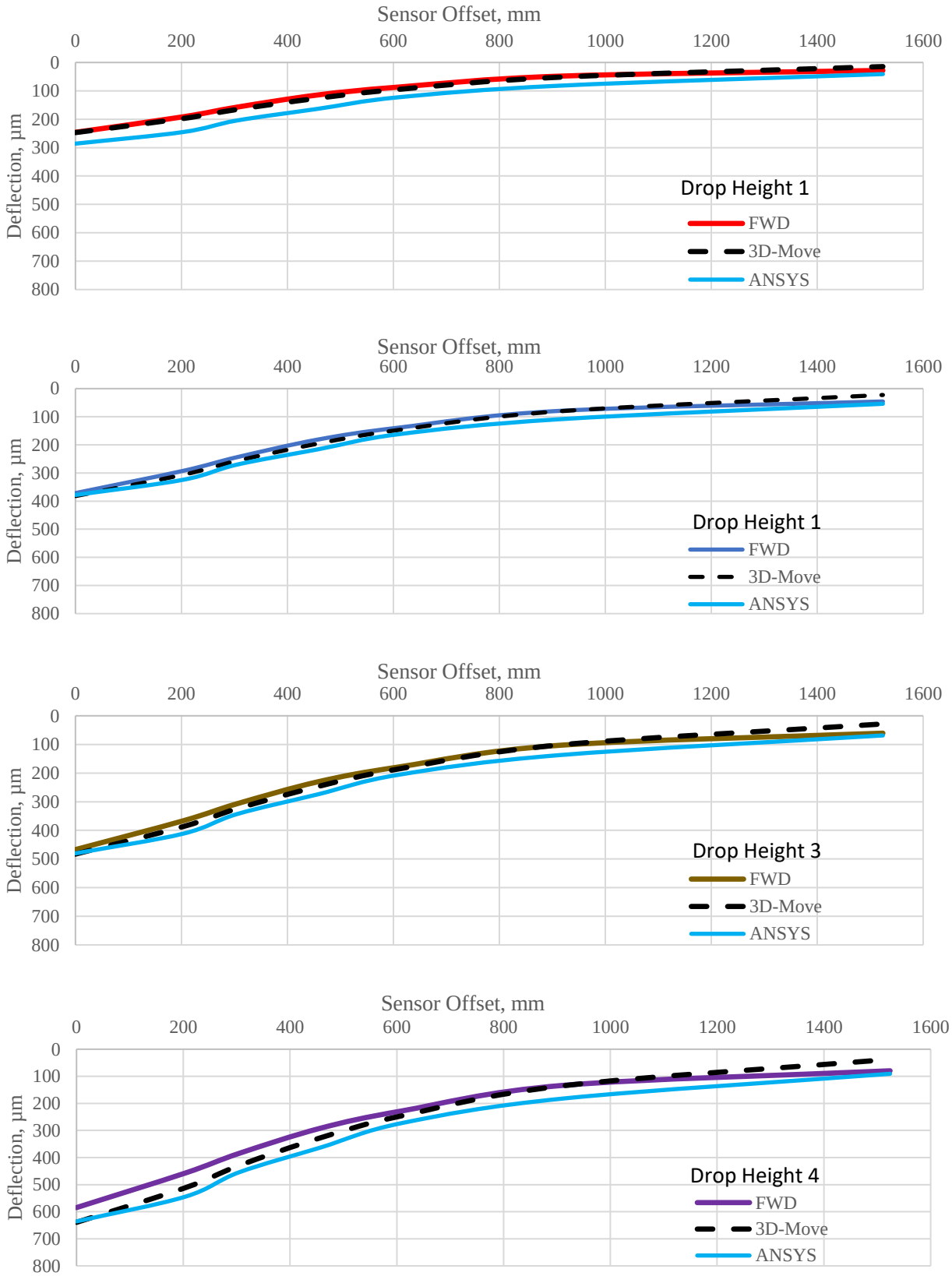

Figure D–20. Simulated Deflection Bowl for the SHRP section 2118.

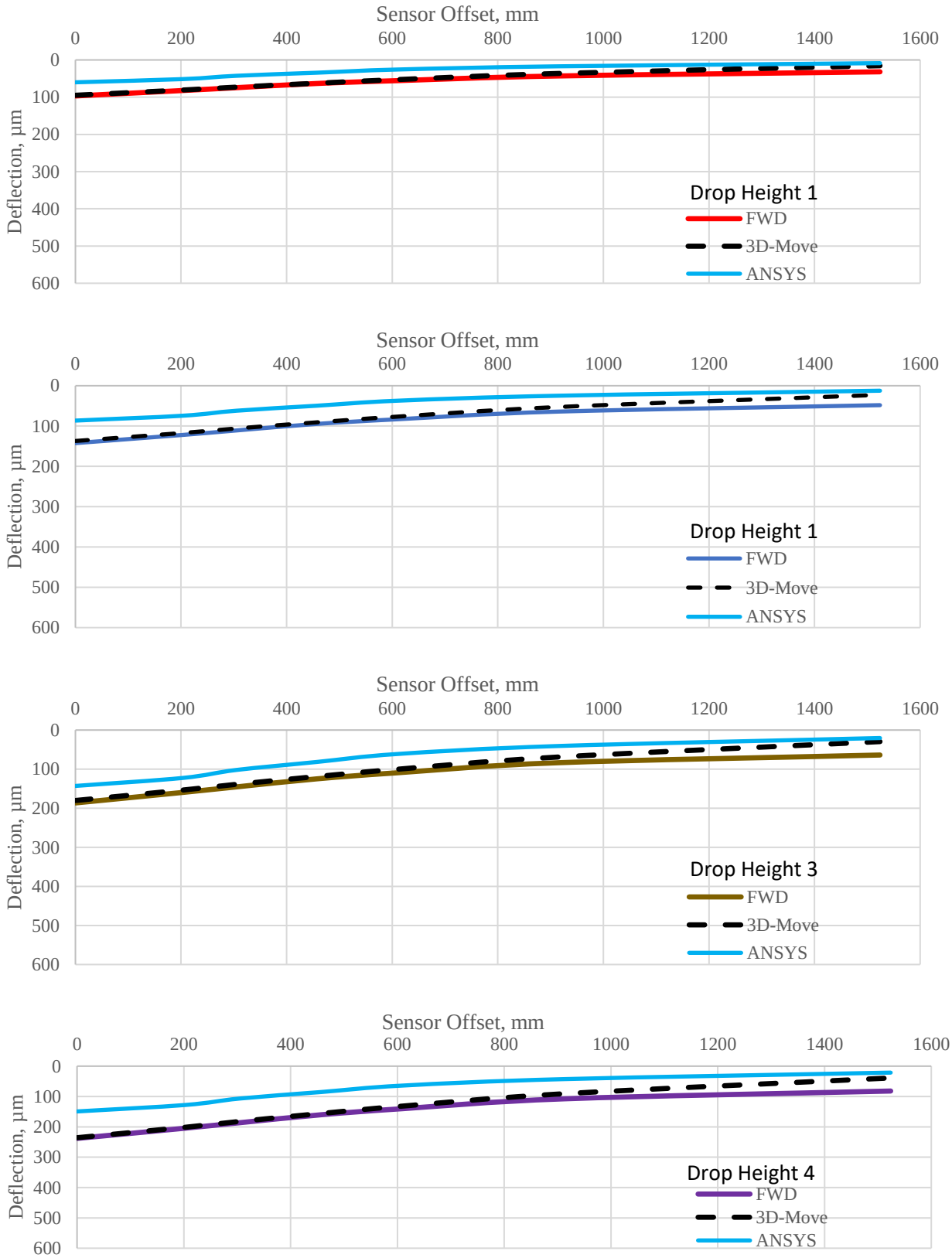

Figure D–21. Simulated Deflection Bowl for the SHRP section AA01.

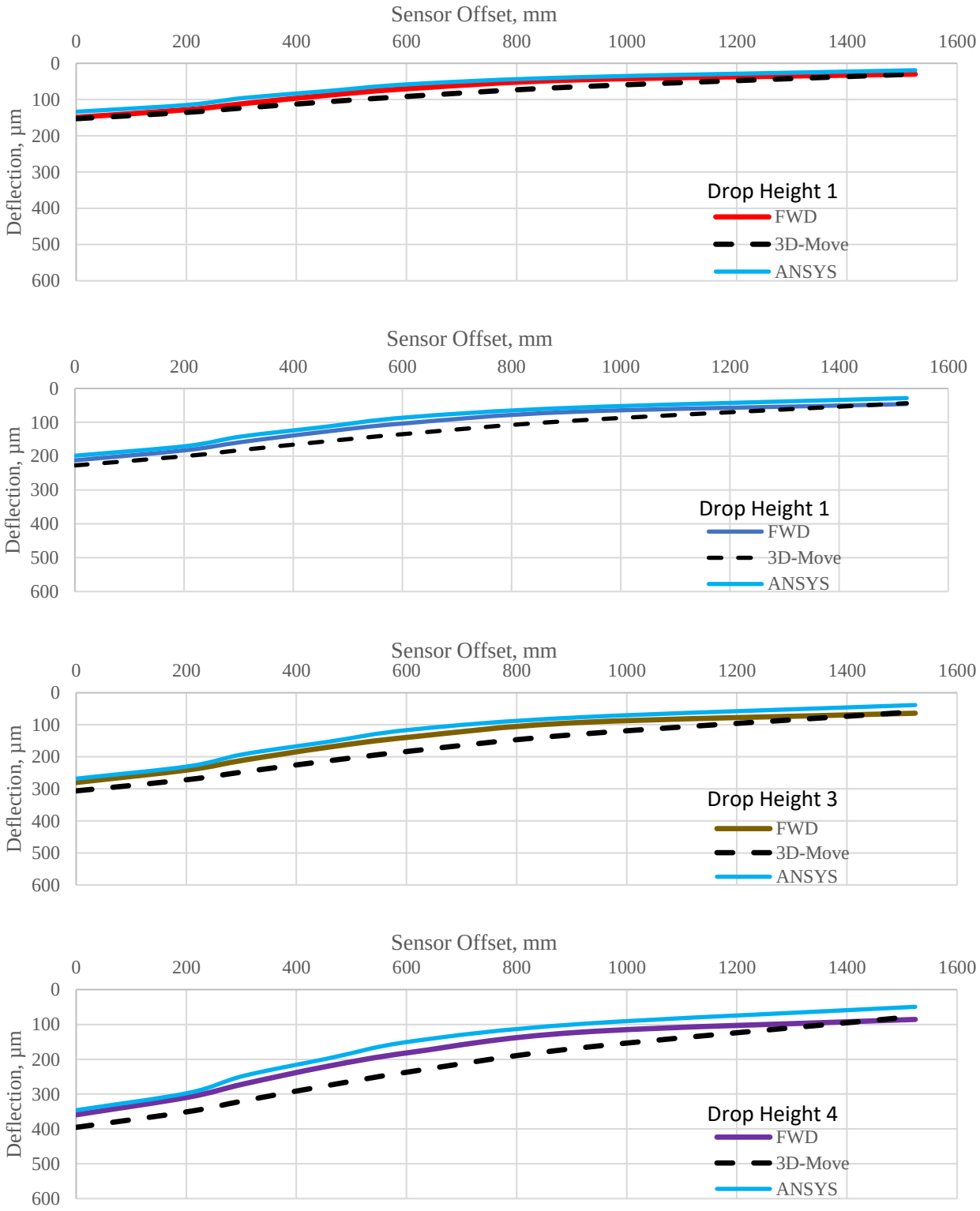

Figure D–22. Simulated Deflection Bowl for the SHRP section 0120.

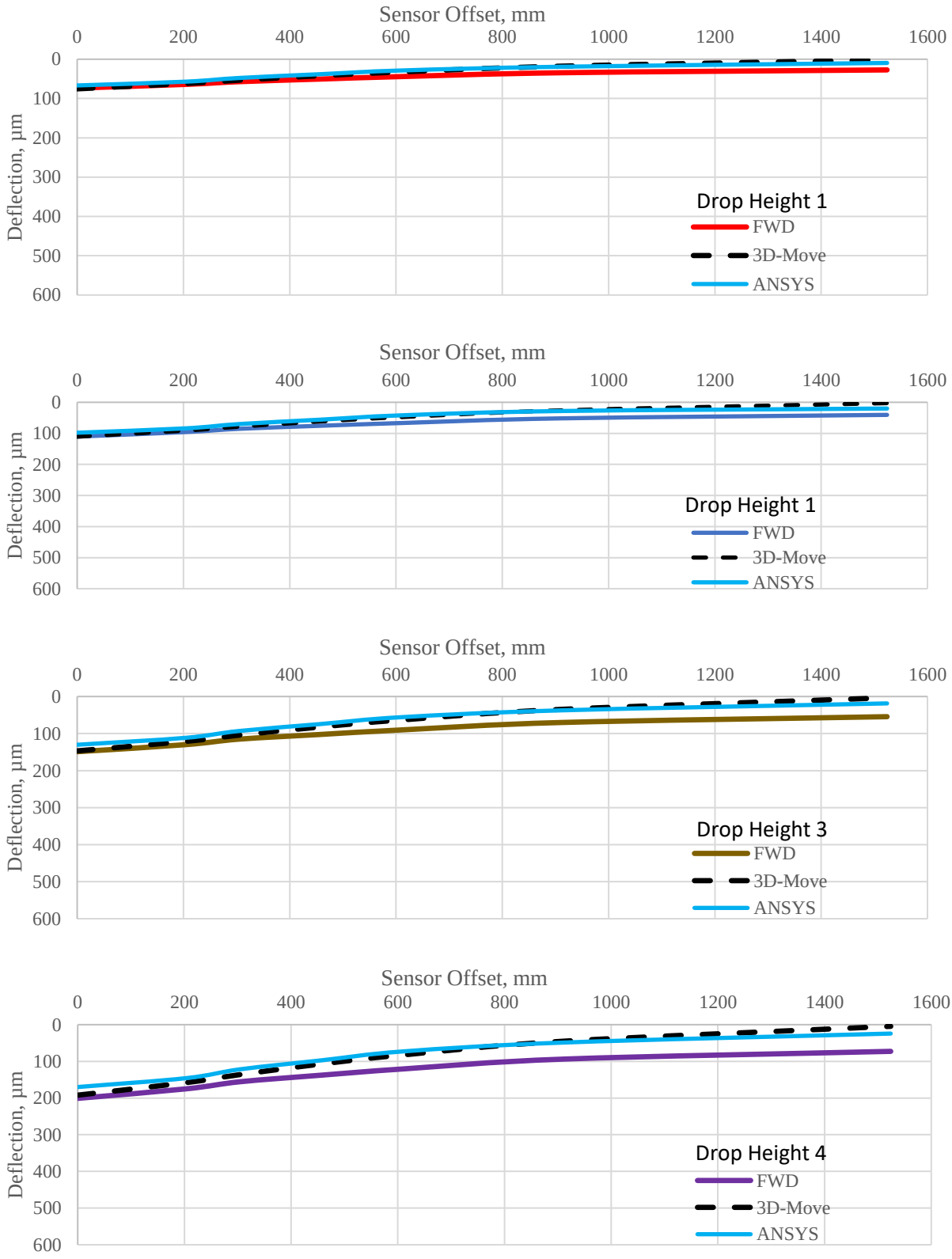

Figure D–23. Simulated Deflection Bowl for the SHRP section 0122.

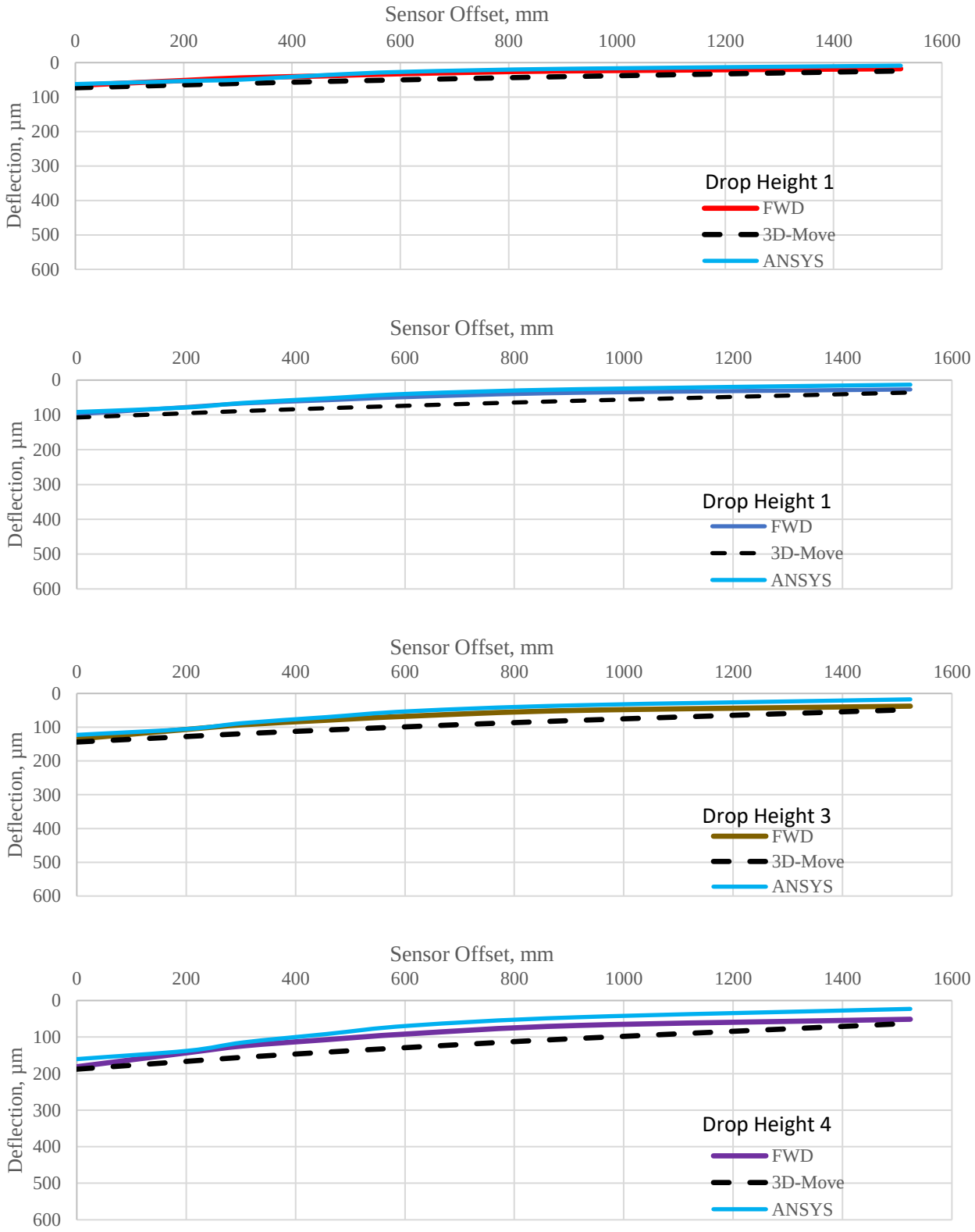

Figure D–24. Simulated Deflection Bowl for the SHRP section 0115.

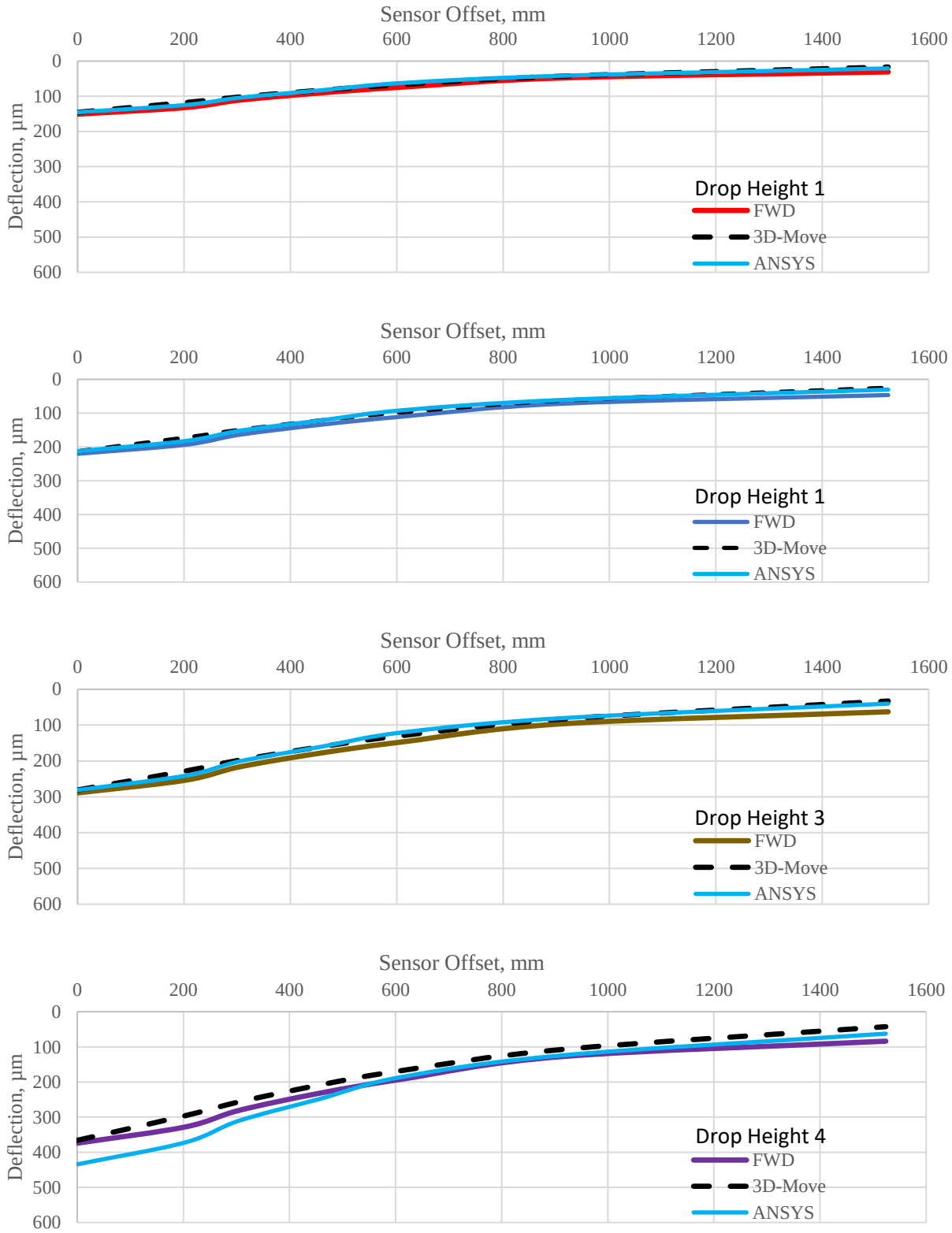

Figure D–25. Simulated Deflection Bowl for the SHRP section 1015.

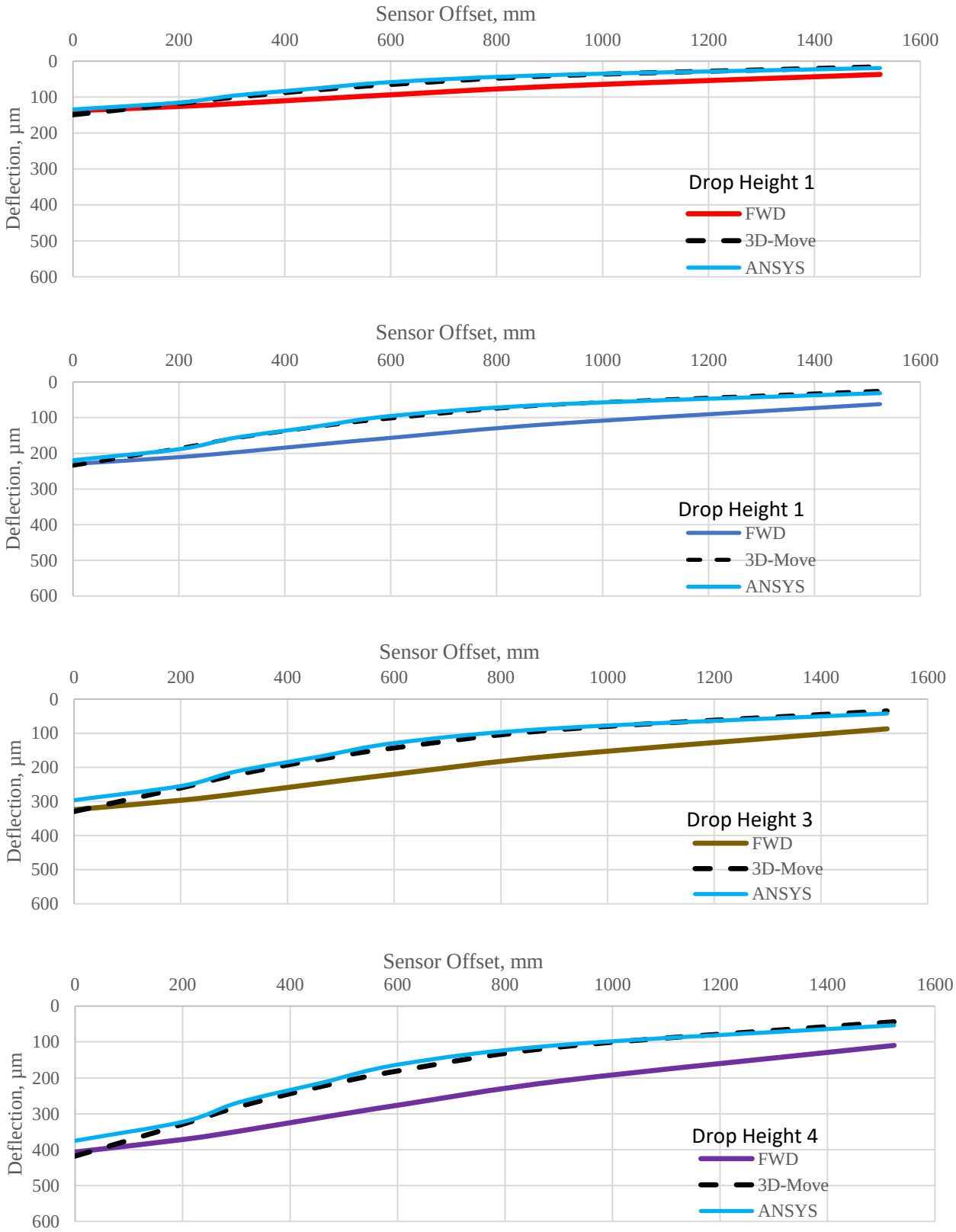

Figure D–26. Simulated Deflection Bowl for the SHRP section 4161.

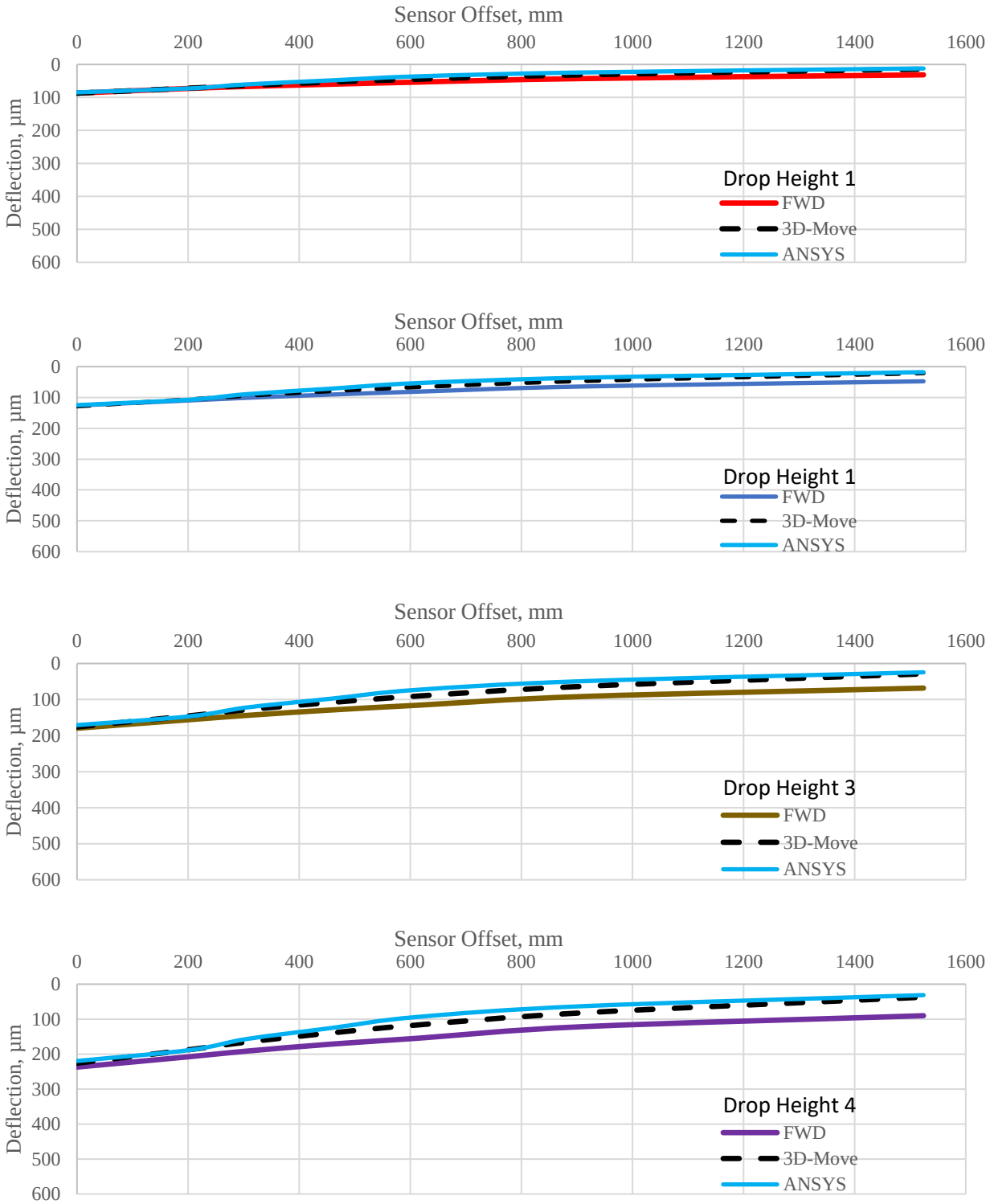

Figure D–27. Simulated Deflection Bowl for the SHRP section 4086.

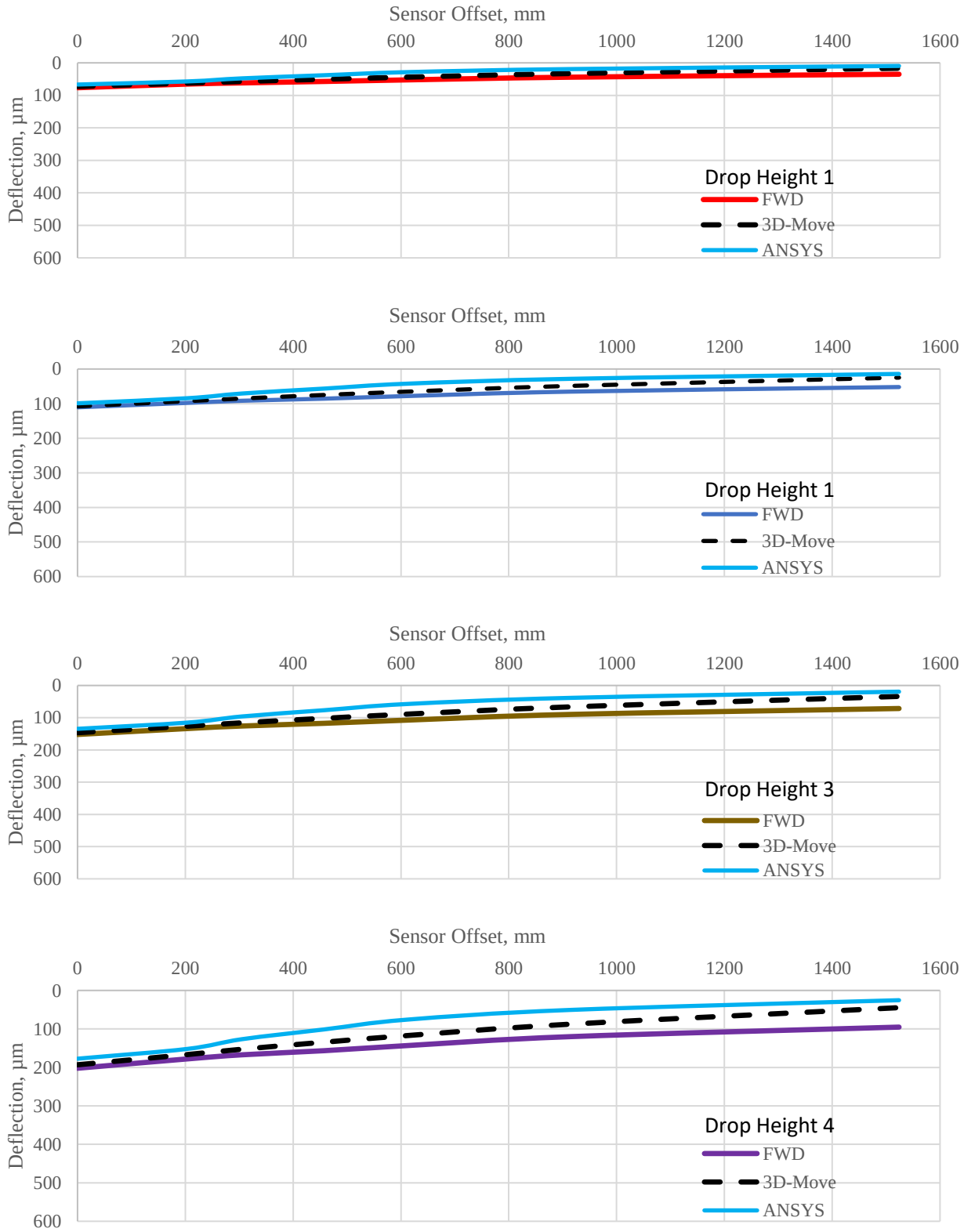

Figure D–28. Simulated Deflection Bowl for the SHRP section 0504.

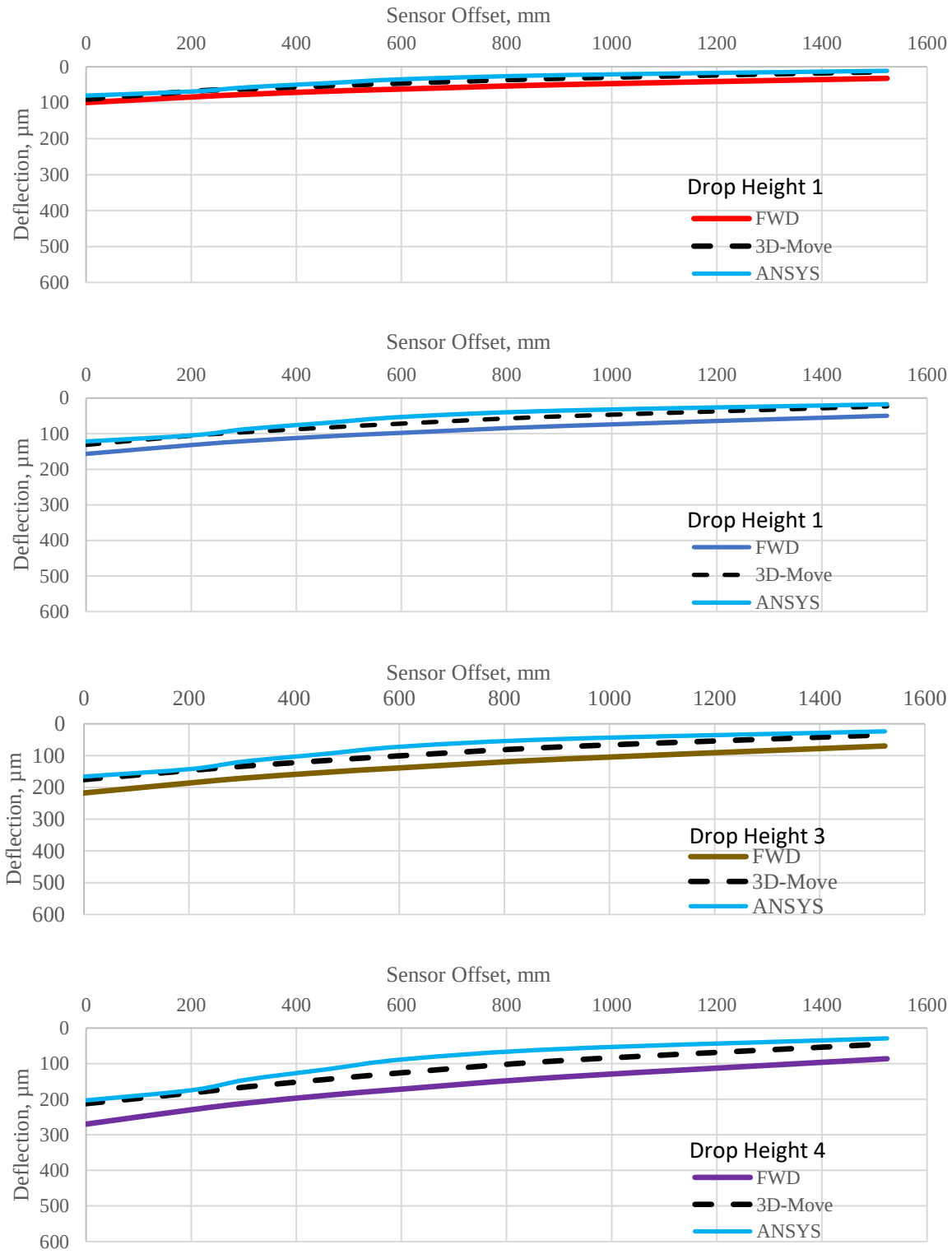

Figure D–29. Simulated Deflection Bowl for the SHRP section 1046.

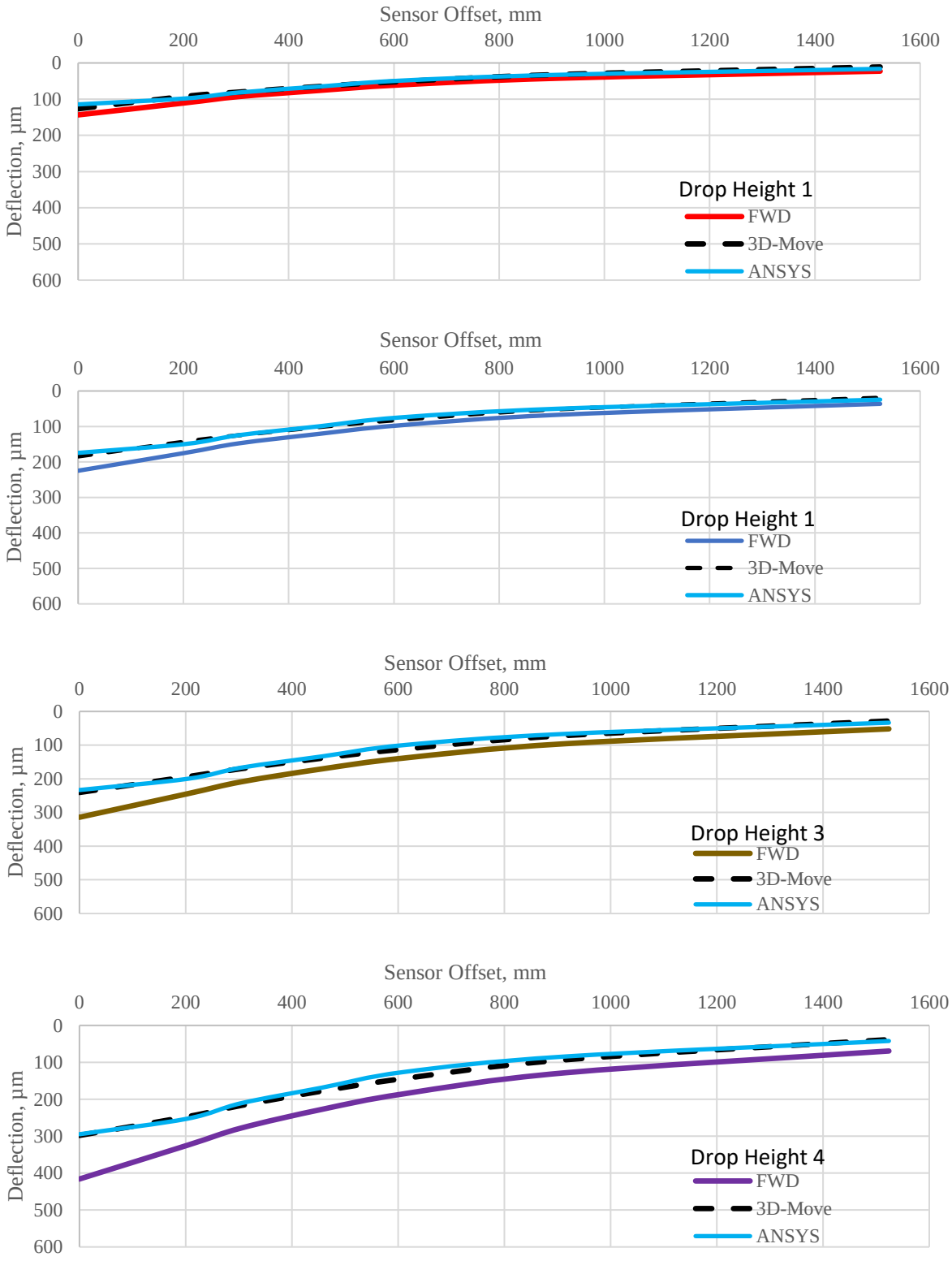

Figure D–30. Simulated Deflection Bowl for the SHRP section 1111.

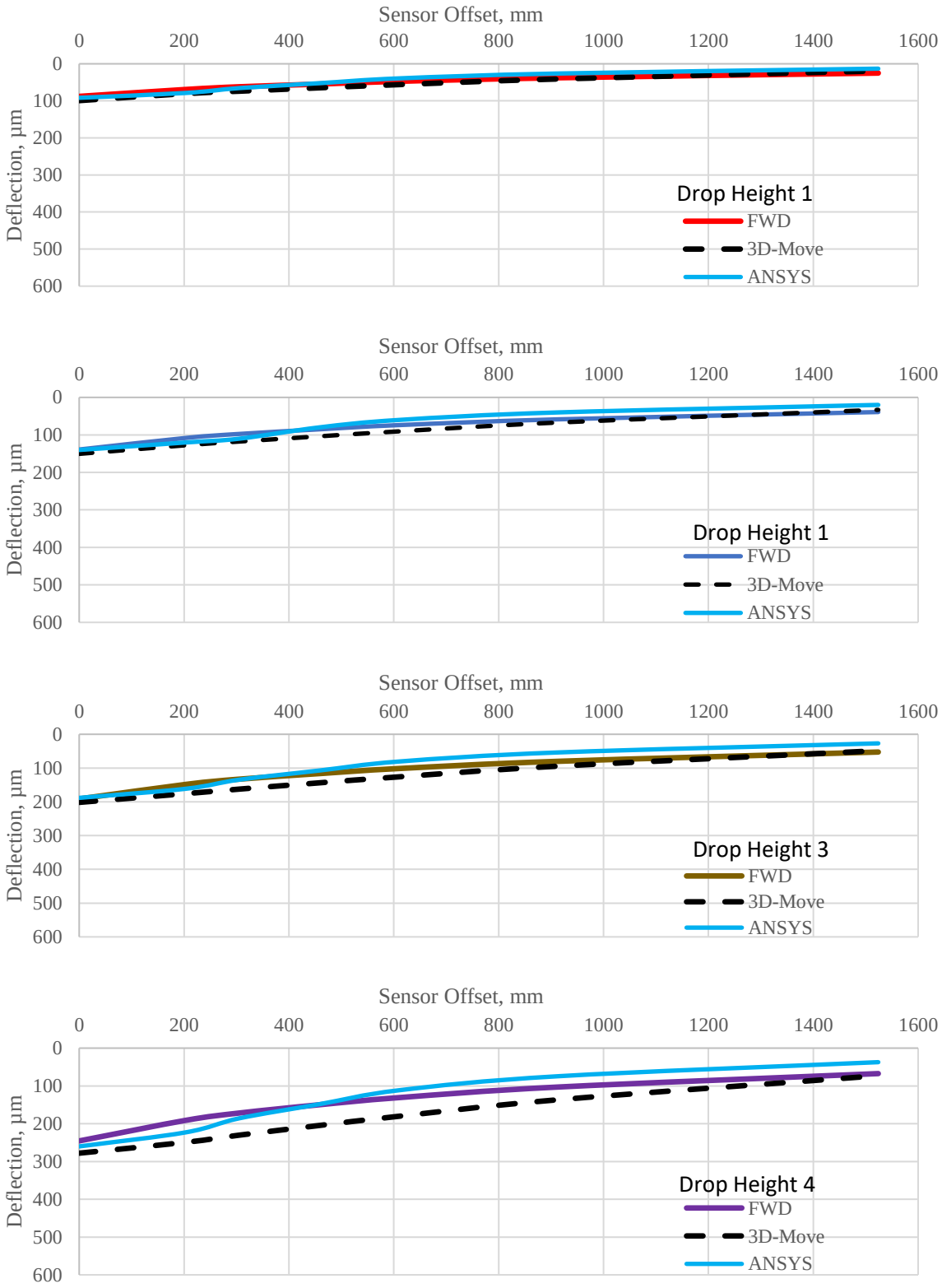

Figure D–31. Simulated Deflection Bowl for the SHRP section 2172.

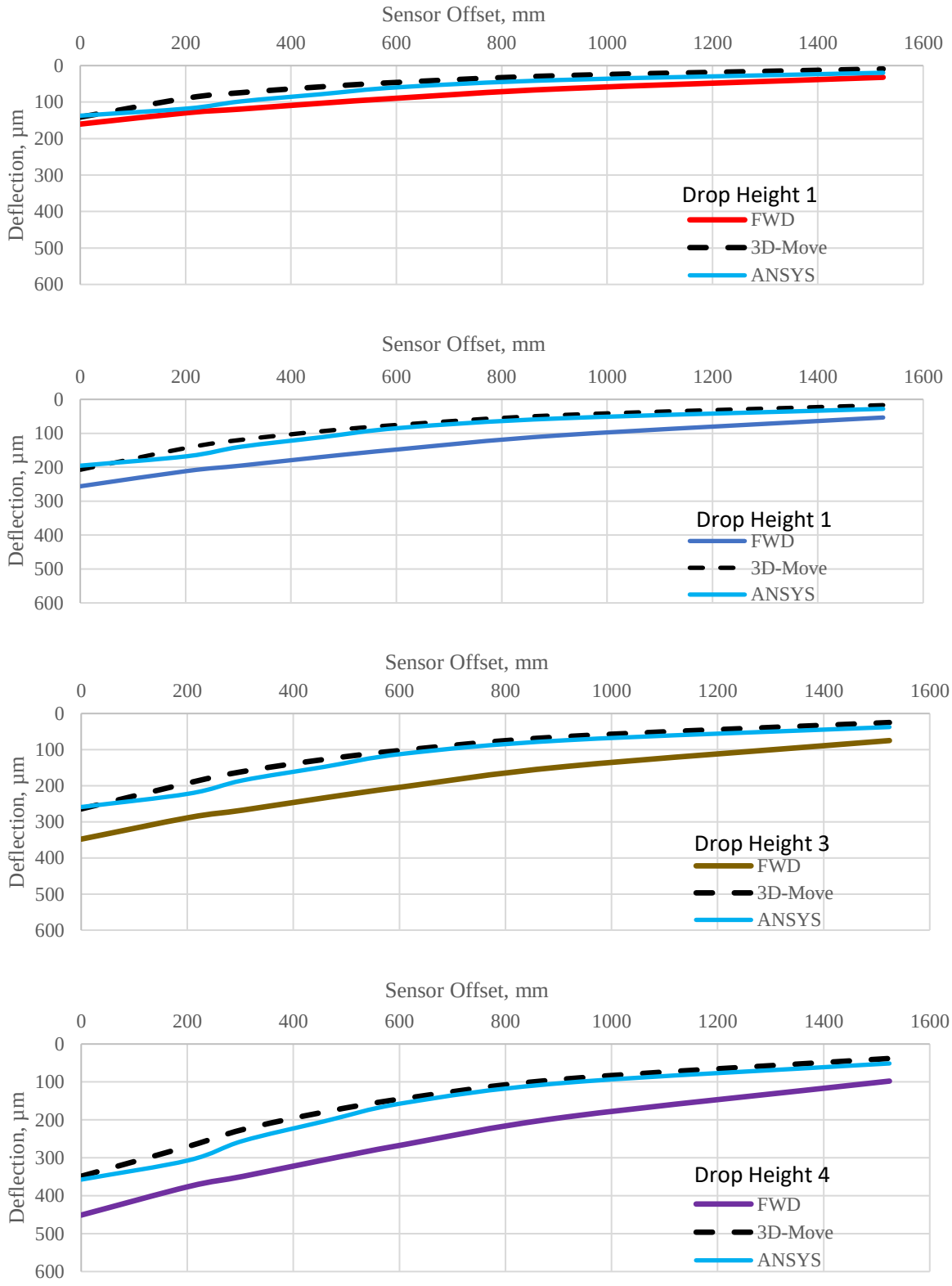

Figure D–32. Simulated Deflection Bowl for the SHRP section 2176.

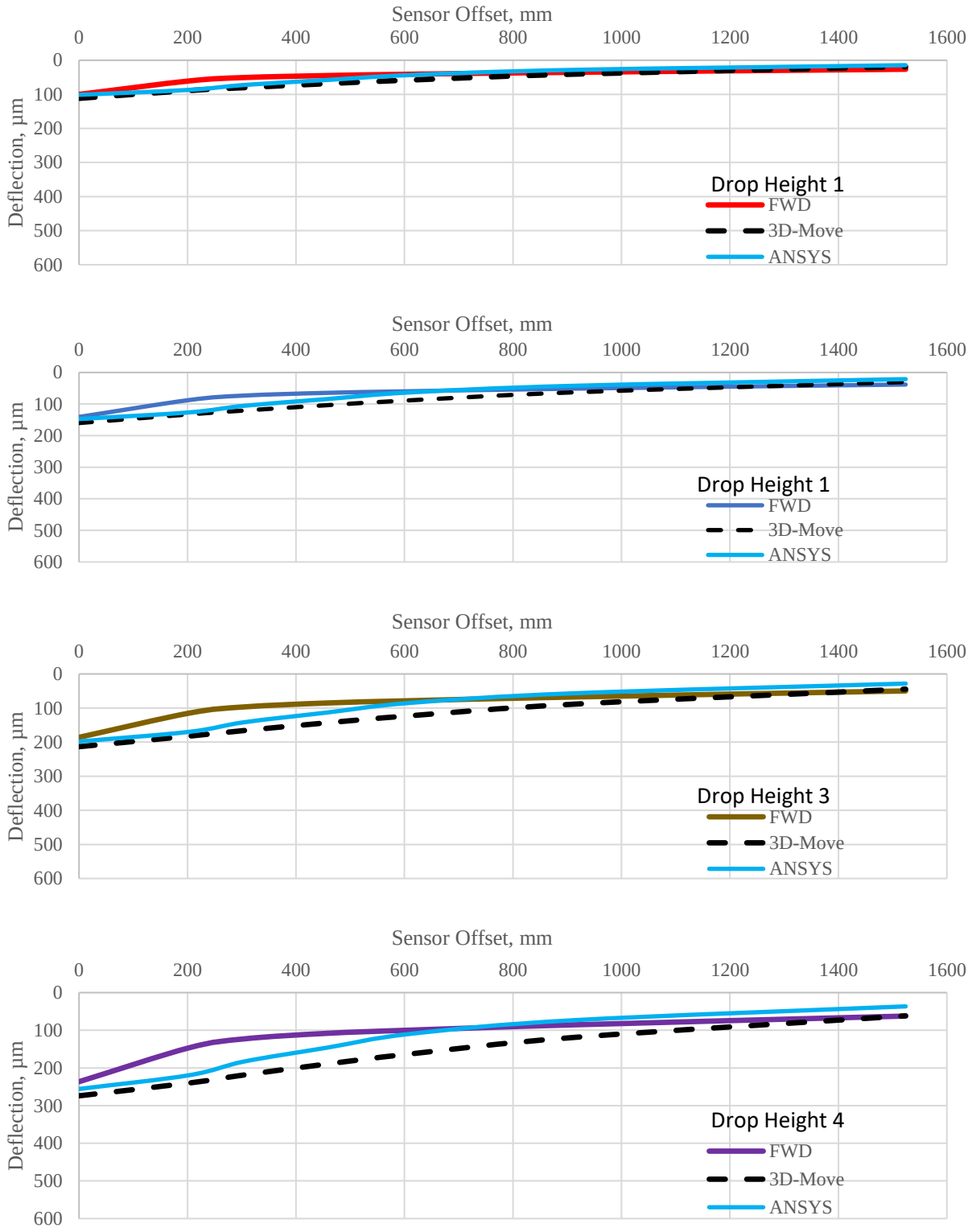

Figure D–33. Simulated Deflection Bowl for the SHRP section B310.

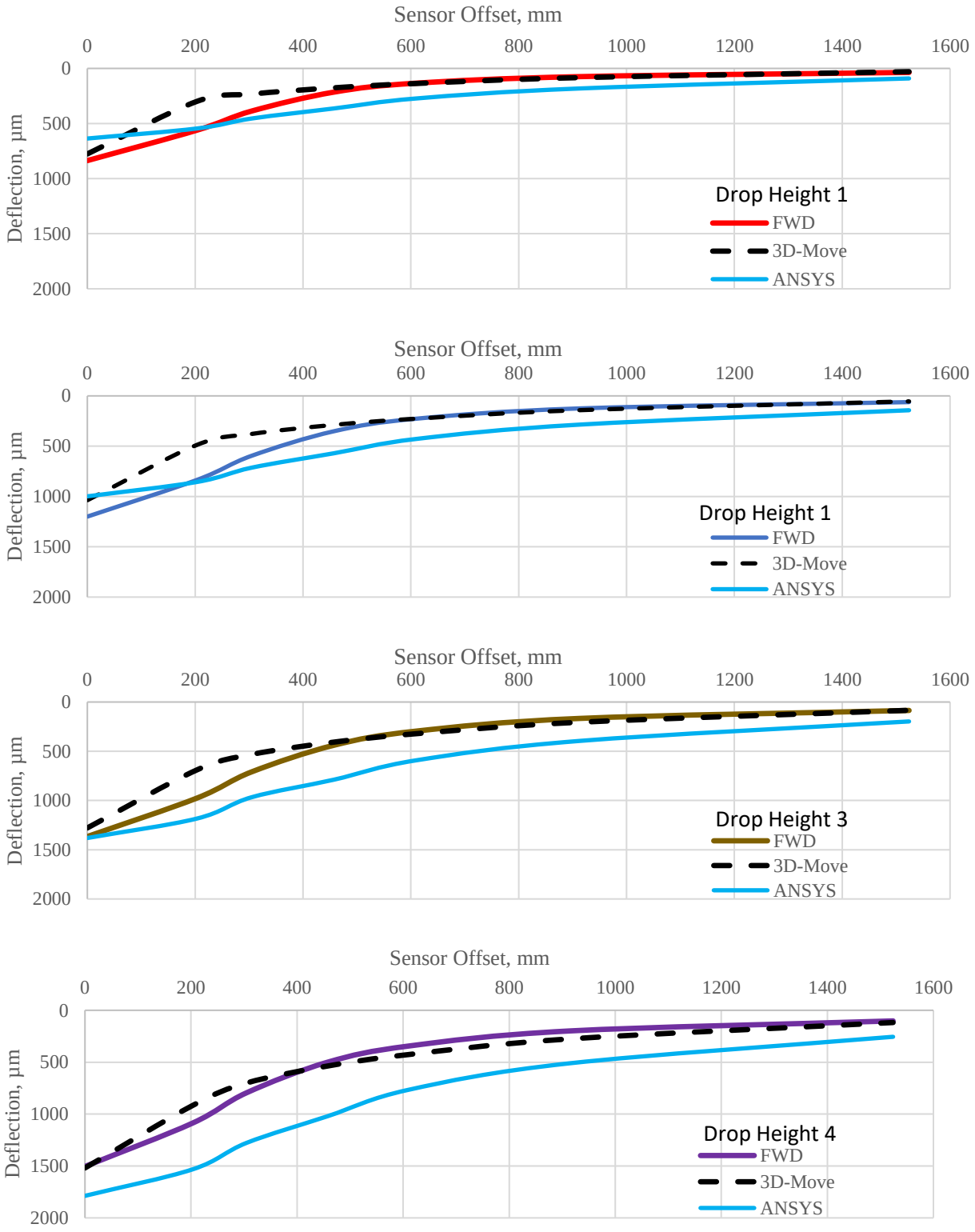

Figure D–34. Simulated Deflection Bowl for the SHRP section M350.

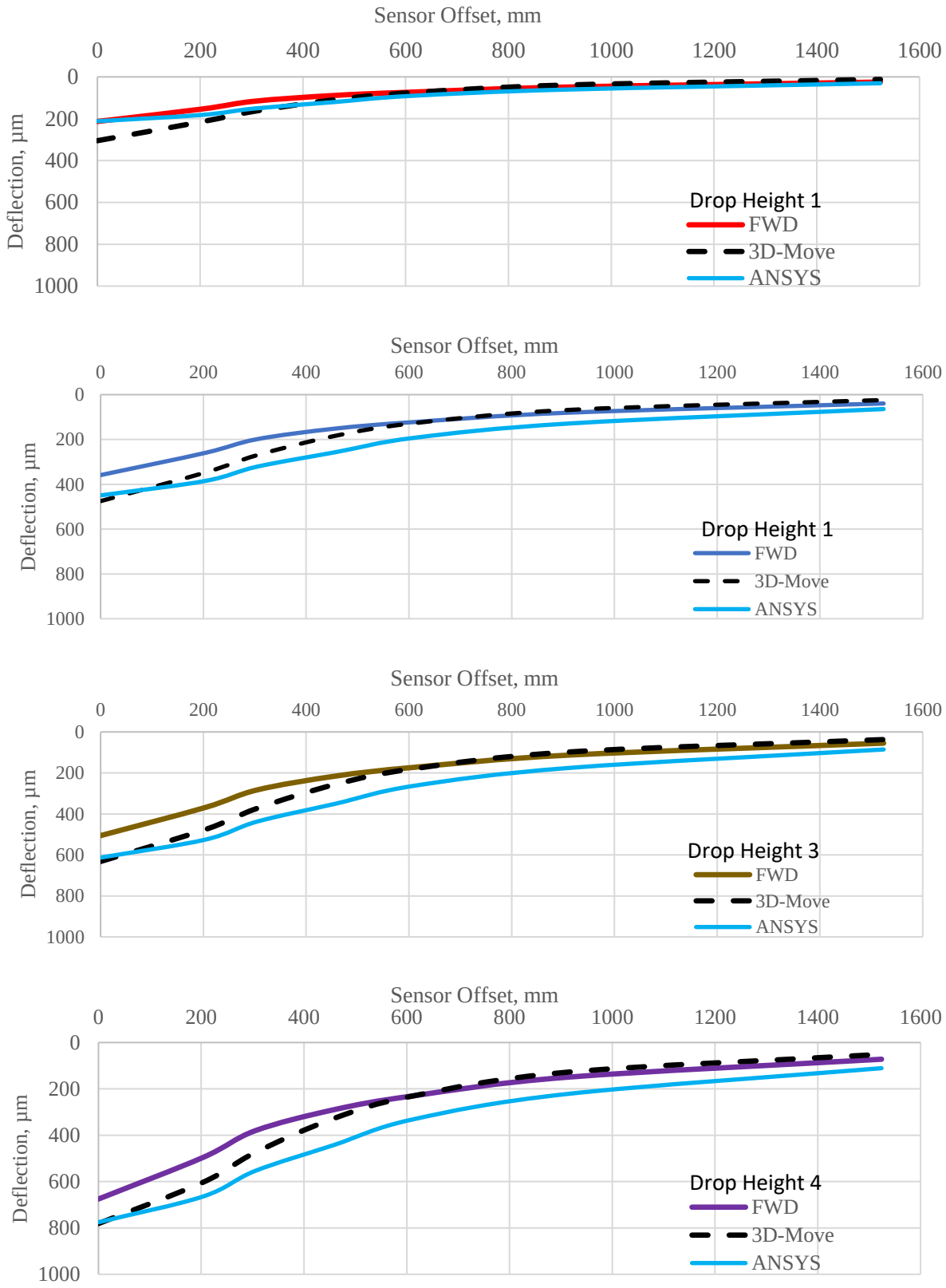

Figure D–35. Simulated Deflection Bowl for the SHRP section 9005